UTS
UNIVERSITY OF TECHNOLOGY SYDNEY

Characterisation of an immune-modulating peptide secreted by a helminth worm

A thesis submitted for the degree of

Doctor of Philosophy

by

Akane Tanaka BSc. (Hons)

School of Life Sciences

Faculty of Science

University of Technology Sydney

2018

Certificate of Authorship/ Originality

I certify that the work in this thesis has not previously been submitted for a degree nor has it been submitted as part of requirements for a degree except as part of the collaborative doctoral degree and/or fully acknowledged within the text.

I also certify that the thesis has been written by me. Any help that I have received in my research work and the preparation of the thesis itself has been acknowledged. In addition, I certify that all information sources and literature used are indicated in the thesis.

Production Note:
Signature removed
prior to publication.

Akane Tanaka Date: 16/02/2018

This research is supported by an Australian Government Research Training Program Scholarship.

Acknowledgements

I would like to start by thanking my supervisors, Associate Professor Bronwyn O'Brien and Associate Professor Sheila Donnelly. It is their undivided attention and immeasurable support that has allowed me to accomplish this remarkable achievement. The countless opportunities they have provided me over the last five years, has allowed me to develop, not only as a critical-thinking, creative and confident research scientist, but overall as a better person, and I cannot express my gratitude enough for that. I would like to carry on their enthusiasm for science, and the ability to persevere during demanding times, towards my career as a scientist and my life onwards.

I would like to thank Dr Valery Combes and Dr Natalia Tiberti for their expertise and assistance in using the IPA analysis software. It is through this predictive analysis, I was able to generate the basis of my numerous hypothesised mechanisms of action of FhHDM-1. I would also like to acknowledge Dr Michael Johnson, Kun Xiao and Dr Lynne Turnbull, for their assistance in training and running flow cytometry and confocal microscopy experiments. I would also like to acknowledge Dr Nham Tran for sharing his knowledge and expertise on RNA based work. Thank you to Dr Maria Sukkar and Venkata Allam for their collaborative work in testing FhHDM-1 in the murine asthma model. To Fiona Ryan and Lalit Overlunde, thank you for the tremendous amount of support in allowing me to become a competent and highly confident animal handling researcher.

To the laboratory team, Joyce To, Maria Lund, Raquel Alvarado, Monique Merino, Susel Mayra Loli Quinteros, Inah Camaya and Alison Ricafrante, thank you for sharing your scientific knowledge and providing such a welcoming and supportive environment throughout the years. Again, to Joyce, I am so lucky to have had you helping me by my side. I want to thank you so much for everything you have done for me. A special thankyou to Maria and Raquel, as my role models- I hope I have been able to follow your footsteps, and inspire the younger students, as you have both done so for me. Monique and Mayra, thank you both for your assistance in obtaining the valuable data towards the work involving the peptide derivatives and PPAR-γ. To all the other postgraduate students, it has been a great experience working alongside such young and vibrant people, and I wish you all the best in your research careers.

To my family, close friends and Clemson, who have been there for me throughout the many years, thank you for supporting me behind the scenes. I am so grateful for the continued encouragement and patience, especially during the practise presentations. I hope to share many more exciting scientific achievements in the future.

I would also like to thank the markers for taking their time to review this thesis, and to thank the Australian Commonwealth Government Department of Industry for the Australian Postgraduate Award Scholarship I received throughout my PhD candidature.

Publications in peer-reviewed journals arising from PhD research

Selection of reliable reference genes for the normalisation of gene expression levels following time course LPS-stimulation of murine bone marrow derived macrophages.

Tanaka, A., To, J., O'Brien, B., Donnelly, S., & Lund, M., 2017, *BMC Immunology*

The Parasitic 68-mer Peptide FhHDM-1 inhibits mixed granulocytic inflammation and airway hyperreactivity in experimental asthma

Tanaka, A., Allam, V. S. R. R., Simpson, J., Tiberti, N., Sheils, J., To, J., Lund, M., Combes, V., Weldon, S., Taggart, C., Dalton, J. P., Phipps, S., Sukkar, M. B., & Donnelly, S., *Journal of Allergy and Clinical Immunology*

Associated publications in peer-reviewed journals

A parasite-derived 68-mer peptide ameliorates autoimmune disease in murine models of Type 1 diabetes and multiple sclerosis.

Lund, M. E., Greer, J., Dixit, A., Alvarado, R., McCauley-Winter, P., To, J., Tanaka, A., Hutchinson, A. T., Robinson, M. W., Simpson, A. M., O'Brien, B., Dalton, J. P., & Donnelly, S., 2016, *Scientific Reports*, 6:37789

A parasitic helminth-derived peptide that targets the macrophage lysosome is a novel therapeutic option for autoimmune disease.

Alvarado, R., O'Brien, B., Tanaka, A., Dalton, J. P., & Donnelly, S., 2015, *Immunobiology*, 220:262-269

Novel Therapeutics for Multiple Sclerosis Designed by Parasitic Worms

Dixit, A., Tanaka, A., Greer, J. M., & Donnelly, S., 2017, *International Journal of Molecular Sciences*, 18, 2141

Scientific presentations arising from PhD Research

Transcriptional Profiling of Macrophages Predicts a Therapeutic Application for a Parasite-Derived Peptide.

Akane Tanaka, Venkata S. R. R. Allam, Natalia Tiberti, Joyce To, Maria E. Lund, Bronwyn O'Brien, Valery Combes, John P. Dalton., Maria B. Sukkar, & Sheila Donnelly. Oral presentation. The New Horizon Conference (33rd Combined Health Science Conference) 2016.

Helminth parasites; should we reunite with our old friends?

Akane Tanaka, Venkata S. R. R. Allam, Natalia Tiberti, Joyce To, Maria E. Lund, Bronwyn O'Brien, Valery Combes, John P. Dalton., Maria B. Sukkar, & Sheila Donnelly. Oral presentation. St George Hospital (St George and Sutherland Clinical School Research in Progress Meetings) 2017.

A helminth derived peptide induces the expression of SerpinB2 in macrophages to regulate Th1 immune responses.

Akane Tanaka, Maria E. Lund, Joyce To, John P. Dalton, Bronwyn O'Brien, Sheila Donnelly. Poster presentation. European Macrophage and Dendritic Cell Society Conference (31st Annual Conference) 2017.

Table of Contents

List of Figures

List of Tables

-	Negative
+	Positive/ plus
±	Plus/minus
↑	Increase
↓	Decrease
^{o}C	Degrees celsius
α	Alpha/anti
β	Beta
δ/Δ	Delta
κ	Kappa
γ	Gamma
µg	Microgram
µl	Microlitre
µm	Micrometre
µM	Micromolar
BHK	Baby hamster kidney cells
BMDM	Bone marrow derived macrophage
CD	Cluster of differentiation
CDAI	Crohn's disease activity index
cDNA	Complementary deoxyribonucleic acid
CEMA	Cationic alpha helical peptide
ChIP	Chromatin immunoprecipitation
CIA	Collagen-induced arthritis
CNS	Central nervous system
CPP	Cell-penetrating peptide
C_t	Cycle threshold value
CXCL	C-X-C-motif chemokine ligand
DAPI	4',6-Diamidine-2'-phenylindole dihydrochloride
DC	Dendritic cell
DMSO	Dimethyl sulfoxide
DNA	Deoxyribonucleic acid
DNAse	Deoxyribonuclease
DNBS	Dinitrobenzene sulfonic acid

dNTP	Deoxynucleotide triphosphate
DSS	Dextran sodium sulfate
EAE	Experimental autoimmune encephalomyelitis
EC50	Half maximal effective concentration
EGFR	Epidermal growth factor receptor
ELISA	Enzyme-linked immunosorbent assay
ES	Excretory/Secretory (products)
FACS	Fluorescence activated cell sorting
FDR	False discovery rate
FhCL1	*Fasciola hepatica* cathepsin L1
FhES	*Fasciola hepatica* excretory/secretory (products)
FhHDM-1	*Fasciola hepatica* helminth defence molecule-1
FhPrx	*Fasciola hepatica* peroxiredoxin
FSC-A	Forward scatter profile
FSC-H	Forward scatter height profile
FSW	Flow cytometry staining wash
GM-CSF	Granulocyte macrophage colony stimulating factor
h	hours
HDP	Host defence peptide
IBD	Inflammatory bowel disease
ICD	Idiopathic chronic diarrhoea
IDR	Innate defence regulator
IFN	Interferon
Ig	Immunoglobulin
IL	Interleukin
IMP	Investigational medicinal product
i.p.	Intraperitoneal
IPA	Ingenuity pathway analysis
kDa	Kilodalton
LDH	Lactate dehydrogenase
LPS	Lipopolysaccharide
LXR	Liver X receptor
M1	Pro-inflammatory macrophage
M2	Anti-inflammatory macrophage
MCP-1	Monocyte chemotactic protein-1

M-CSF	Macrophage colony stimulating factor
MFI	Mean fluorescence intensity
MHC	Major histocompatibility complex
mer	Amino acid residues
min	Minutes
MIP	Macrophage inflammatory protein
ml	Mililitre
MLDS	Multiple-low dose streptozotocin
Mphi	Macrophages
MPO	Myeloperoxidase
MRI	Magnetic resonance imaging
mRNA	Messenger ribonucleic acid
MS	Multiple sclerosis
msec	Milliseconds
NEJ	Newly excysted juvenile
NET	Neutrophil extracellular trap
ng	Nanograms
NK	Natural killer cells
nm	Nanometre
NOD	Non-obese diabetic (mice)
OD	Optical density
O/N	Overnight
Ova	Ovalbumin
Ov-HDM	*Opisthorchis viverrini* helminth defence molecule
PI	Peak I
PII	Peak II
PC	Phosphorylcholine
PMA	Phorbol myristate acetate
Poly (I:C)	Polyinosinic:polycytidylic acid
PPAR	Peroxisome proliferator activated receptor
PSMβ1	Proteasome subunit, beta type1
qRT-PCR	Quantitative reverse transcriptase polymerase chain reaction
RA	Rhematoid arthritis
Relm-α	Resistin-like molecule alpha
RNA	Ribonucleic acid

ROS	Reactive oxygen species
RRMS	Relapsing-remitting multiple sclerosis
RT	Room temperature
RXR	Retinoid X receptor
SEA	Soluble egg antigens
sec	Seconds
SEM	Standard error of mean
SLE	Systemic lupus erythematous
SNP	Single nucleotide polymorphisms
SUMO	Small ubiquitin-like modifier proteins
SPMS	Secondary progressive multiple sclerosis
sup	Supernatant
SSC-A	Side scatter profile
TGF-β	Transforming growth factor-beta
Th1	T-helper 1
Th2	T-helper 2
Th17	T-helper 17
TID	Type 1 diabetes
TIM-3	T cell immunoglobulin domain and mucin domain-3
TLR	Toll-like receptor
TNBS	Trinitrobenzene sulfonic acid
TNF	Tumour necrosis factor
Treg	T-regulatory
uPA	urokinase-type plasminogen activator
vATPase	Vacuolar ATPase
v/v	Volume/volume
x g	Relative centrifugal force

Abstract

Parasitic worms (helminths) have evolved mechanisms to potently modulate the mammalian immune response to ensure their long-term survival, while concomitantly preventing excessive tissue pathology within the host. The outcome of this activity is a potent suppression of mammalian pro-inflammatory Th1 and Th17 immune responses. This immune-modulatory phenomenon is attributable to the molecules excreted/secreted by helminths as they migrate through their human hosts. The identification of these molecules has the potential to contribute to the development of novel therapeutics for the treatment of autoimmune diseases as these diseases are mediated by pro-inflammatory Th1 and Th17 immune responses.

It has previously been shown that the delivery of a single peptide, FhHDM-1, which is excreted/secreted from the helminth, *Fasciola hepatica*, prevented the development of murine type 1 diabetes and multiple sclerosis. The aetiological similarity between these two diseases, is the establishment of the pro-inflammatory environment by macrophages and neutrophils. Therefore, it was hypothesised that FhHDM-1 likely mediated its protective effect through anti-inflammatory mechanisms directed at these cells. In this study, it was confirmed that FhHDM-1, specifically interacted with both murine and human neutrophils and macrophages. Furthermore, it was demonstrated that FhHDM-1 modulated the activity of these cells, by inhibiting the secretion of pro-inflammatory cytokines/chemokines, which, in turn, prevented further activation of pro-inflammatory T cells and dendritic cells.

The use of transcriptional profiling revealed that, of the 41,436 genes analysed in macrophages, treatment with FhHDM-1 altered the expression levels of only 6 of these. Of these, only the expression level of *SerpinB2* was increased, and this was shown to subsequently mediate the suppression of pro-inflammatory cytokine secretion by T cells. In the context of an inflammatory stimulus, FhHDM-1 regulated the expression of numerous pro-inflammatory genes in macrophages. Pathway analysis predicted that this anti-inflammatory activity was mediated through the activation of PPAR-γ pathways. This is the first report of a PPAR-γ agonist being secreted by a helminth parasite as a mechanism of modulating mammalian innate immune responses.

Importantly, a homologous parasite peptide from a related trematode parasite demonstrated the same activity suggesting a conserved mechanism of action among parasite helminths.

Analysis of the sequence of the FhHDM-1 peptide, combined with immunological assays of peptide derivatives, supported the discovery of the minimally active sequence, FhHDM-1.C2. This peptide contained both the amphipathic C-terminus region, previously identified as functional, and a sequence of 5 amino acids (KARDR), which was newly identified as essential for the binding and internal localisation of FhHDM-1. This C2 derivative mimicked the activity of the full length peptide in every way, such as the ability to bind and be internalised by macrophages, to increase macrophage lysosomal pH, to induce the expression of *SerpinB2*, and to inhibit the production of pro-inflammatory cytokines.

In summary, this thesis has newly identified the binding and active domains of the parasite immune-modulatory peptide, FhHDM-1, and discovered the novel mechanisms by which the peptide regulates pro-inflammatory innate immune responses. Combined, these findings have significantly advanced the progress towards translation of the FhHDM-1 peptide for therapeutic use in immune-mediated diseases.

Chapter 1: Introduction

1.1 Helminth parasites are potent immune-modulators

The first evidence of parasite infections appear in the writings of the Egyptians and the Greeks, dating back to 3000 BC [1], with eggs of intestinal parasites found within prehistoric human coprolites (1250 AD) [2]. However, the interaction between humans and the major helminth groups began hundreds of millions of years ago, coincident with the evolution of the mammalian adaptive immune system [3, 4]. Over millennia of shared evolution, helminth parasites have developed elaborate mechanisms to modulate the human immune system to minimise the physical and immunological pathology to the host. These same immune-modulatory mechanisms also prevent parasite expulsion from the host to ensure long-term survival, and thus successful reproduction [5, 6]. The effectiveness of this adaptation is proven by the continued prevalence of endemic helminth infections in up to a third of the world's population, which equates to over 2 billion people being currently infected [7].

Generally, the mammalian immune response to an invading pathogen, such as bacteria or viruses, is a pro-inflammatory, T-helper 1 (Th1) and Th17 (Th1/Th17) type response [8] (Fig. 1.1). This response is characterised by the functions of innate immune cells, notably pro-inflammatory macrophages (termed M1) and dendritic cells (DCs), that secrete cytokines, such as interleukin (IL)-1, IL-6, IL-12, and tumour necrosis factor (TNF). This pro-inflammatory cytokine milieu activates the expansion of Th1 $CD4^+$ T cell populations, that exacerbate the pro-inflammatory response through the secretion of additional cytokines, such as interferon gamma (IFN-γ) and IL-6, which, in turn, activate other immune cells [8]. The net result is the elimination of the pathogen, and subsequent resolution of the pro-inflammatory immune response.

In contrast, when challenged with helminth parasites, the development of the Th1 immune response is inhibited, and instead an anti-inflammatory T-helper 2 (Th2) and T-regulatory (Treg) immune response predominates (Th2/Treg) [9, 10] (Fig. 1.1). This response is characterised by the activation of eosinophils, basophils, mast cells, and regulatory B cells [5, 8, 11]. The switch towards a Th2 immune response during a helminth parasite infection is controlled at the level of the innate immune response, characterised by the inhibition of pro-inflammatory M1 macrophages and DCs [12, 13],

and the induction of an immature phenotype of dendritic cells (DC2s), and an anti-inflammatory phenotype of macrophages (termed helminth-M2 macrophages) [14, 15]. The phenotype of these 'helminth-induced' M2 macrophages is characterised by increased gene expression levels of Arg-1, Ym1 and Resistin-like molecule (Relm)-α [16, 17]; and surface receptors, including Programmed Death-Ligand 1 (PDL1) [18, 19]. This profile is characteristic of murine macrophages, but not human macrophages, as Ym1 is not expressed in human macrophages [20], and there is debate as to whether Arg-1 is also expressed by human anti-inflammatory macrophages [21]. There are, however, many other characteristics shared by both helminth-induced M2 macrophages in mice and humans, such as the induced differentiation of T cells into a Th2 phenotype, due to macrophage secretion of anti-inflammatory cytokines, such as IL-4, IL-5, IL-9 and IL-13 [22, 23], and the concomitant suppression of Th1 cellular proliferation [13, 18]. Therefore, the overall result of M2 macrophage activity is the inhibition of pro-inflammatory Th1 immune responses, which would be ineffective against large multicellular helminths, and, if activated, would instead result in significant collateral damage to tissues and organs. In addition, the generation of helminth-induced M2 and Th2 cells mediate wound repair mechanisms to repair tissue damaged due to parasite migration [5, 24, 25]. Deficiency of helminth-M2 macrophages in mice has led to mortality by sepsis due to intestinal damage caused by parasite migration, and subsequent release of bacteria [26], which highlights the importance of helminth-M2 macrophages in prolonging the parasite's survival within a host, while simultaneously minimising tissue damage.

As the parasite infection reaches chronicity, the differentiation of Treg populations is initiated. These cells secrete regulatory cytokines, such as IL-10 and transforming growth factor-β (TGF-β) [27, 28], which further inhibit the development of Th1 responses, and also regulate Th2 responses. This prevents the generation of extensive tissue fibrosis, which would result from sustained wound healing activity mediated by helminth-M2 macrophages, and their products [24].

In contrast to the immune response profile elicited by parasites (i.e. Th2 and Treg), are the immune reactions involved in the pathogenesis of autoimmune diseases (Fig. 1.1), which are typically characterised by a combination of Th1 and Th17 pro-inflammatory responses. Examples of autoimmune disorders include rheumatoid arthritis (RA), type

1 diabetes (T1D), inflammatory bowel disease (IBD), and multiple sclerosis (MS). These diseases are characterised by dysregulated and exacerbated pro-inflammatory immune responses directed against auto-antigens, resulting in tissue destruction [29]. In some syndromes, such as T1D, in which the pancreatic insulin-secreting beta (β) cells are destroyed, a single organ is affected, whilst in other instances, the destruction is systemic dependent upon the auto-antigen(s) against which immune responses are elicited.

The pathogenesis of autoimmune disease is multifactorial, involving a complex interplay between genetic, environmental and immunological factors, and these contribute to the varied pathologies and clinical symptoms. Despite such etiological differences, many autoimmune diseases exhibit commonalities in the pathological immune responses; namely the production of pro-inflammatory cytokines (IL-1β, IL-6, IL-12, TNF and IFN-γ, and IL-17) by DCs and M1 macrophages [15]. Pro-inflammatory macrophages are among the first immune cells to infiltrate target tissues in several autoimmune diseases [30]. Due to the secretion of pro-inflammatory cytokines (the quantity of which often correlates positively with disease severity [31-33]), they are the primary drivers of tissue destruction and disease development [34]. Tissue damage occurs both directly, via the release of pro-inflammatory mediators, and, indirectly through the activation and expansion of Th1/Th17 immune cell populations. For example, in mouse models of MS and T1D, M1 macrophages predominate and their elimination, via the use of liposome-encapsulated dichlormethylene diphosphonate [35, 36] or silica [37], prevented the clinical symptoms of MS and stopped the development of T1D, respectively. Observations that the elimination of M1 macrophages attenuates disease progression, confirms their central role in the development of the Th1/Th17 responses that dominate during the development of autoimmunity.

As one of the other most abundant innate immune cell types, neutrophils have recently been ascribed a critical role in the initiation and perpetuation of autoimmunity [38, 39]. They are recruited very early to the tissue site [40] where they establish a pro-inflammatory environment, which serves to recruit other pro-inflammatory innate cells [41, 42]. For example, in mouse models of T1D, neutrophils from the pancreas have been shown to activate DCs, which, in turn, release the pro-inflammatory cytokine,

IFN-α. This creates the pro-inflammatory environment necessary for the initiation of autoimmunity in T1D [41]. In fact, the appearance of neutrophils within the pancreatic islets precedes that of macrophages. There is also a correlation between increased neutrophil infiltration and increased inflammation, implying their importance as one of the principal immunological players in animal models of systemic lupus erythematosus (SLE) [43-45] and RA [46-49]. Furthermore, in mouse models of MS, depletion of neutrophils delayed the onset of disease, by impairing the priming and maturation of DCs and macrophages [42]. All such evidence highlights the significance of neutrophils in the pathogenesis of autoimmune diseases.

The pro-inflammatory environment, established by M1 macrophages and neutrophils, facilitates the generation and expansion of Th1 cells and, in turn, $CD8^+$ T cell populations, which destroy cells expressing auto-antigens, such as the insulin-producing β cells in the case of T1D [50]. It was initially thought that these Th1 cells, particularly $CD4^+$ T cells that produce IFN-γ, were the cause of autoimmunity development [32], however, murine studies using anti-IFN-γ antibodies [51] or mice deficient in IFN-γ, have shown no protection against MS [52] or RA [53] development, but rather disease symptoms were exacerbated. This was similarly observed after the administration of anti-TNF antibodies, where only half of the mice were prevented from T1D development [54]. This was shown to be an age-dependent phenomenon, as mice treated with anti-TNF antibodies from 2 weeks of age, as opposed to 4 weeks of age (when only 50% efficacy was observed), were completely protected [54]. Studies such as these, in which the elimination of a single pro-inflammatory cytokine failed to prevent autoimmunity, indicate that complex mechanisms determine the development of autoimmune disease. The IL-17 producing $CD4^+$ effector cell lineage (Th17 cells) are now also recognised as inducers of inflammation and autoimmune disease, which operate in concert with Th1 cells to amplify pro-inflammatory immune responses. Th17 cells are initially recruited by IL-6 and TGF-β [55, 56], and then maintained by IL-23 [57], which subsequently leads to the production of IL-17 by these T cells, that contributes to the progression of autoimmunity [58].

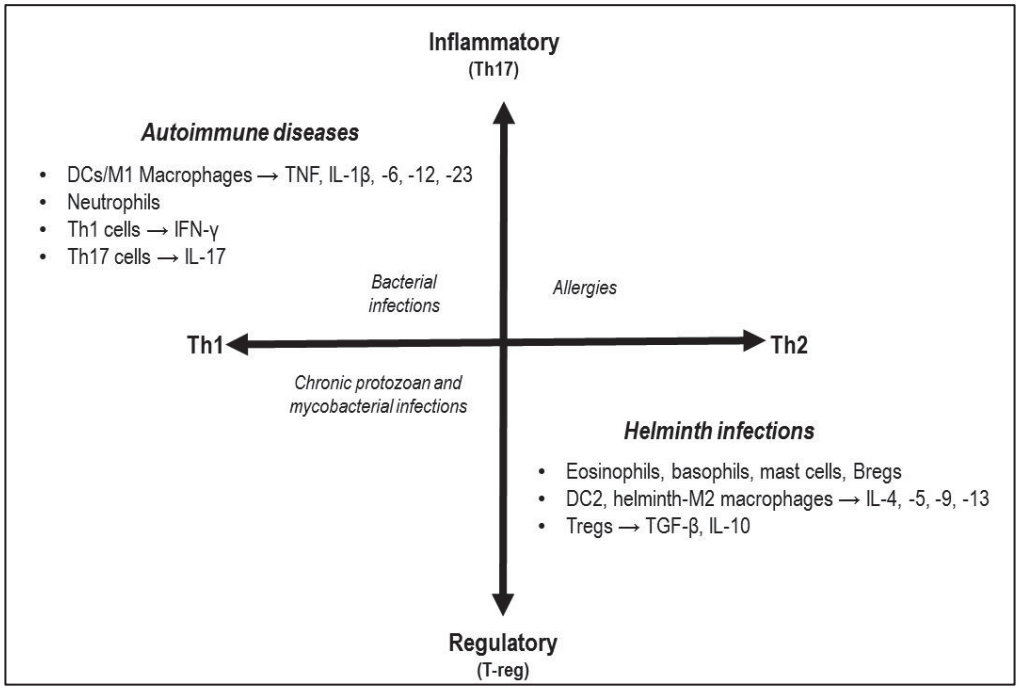

Figure 1.1 Axes of the immunological response profiles for activated CD4$^+$ T cells. CD4$^+$ T cell populations can be functionally separated into four major phenotypes: T-helper 1 (Th1), T-helper 17 (Th17), T-helper 2 (Th2), and T-regulatory (Treg). Each population is associated with the induction of immunity against pathogens, and/or development of pathologies (notably autoimmune disease and allergy) that lie between the arms. Th1/Th17 (pro-inflammatory responses) precipitate autoimmune disease, characterised by pro-inflammatory dendritic cells (DCs) and macrophages (M1), neutrophils, and Th1/Th17 cells that produce pro-inflammatory cytokines. The Th1/Th17 immune responses inhibit the Th2/Treg responses (and *vice versa*) that are dominant in helminth infections, characterised by eosinophils, basophils, mast cells, regulatory B cells, anti-inflammatory/regulatory DC2s, helminth-induced anti-inflammatory (M2) macrophages, and Tregs that produce Th2/Treg cytokines. Arrows indicate the respective cytokines produced by each immune cell type. Adapted from [8].

The mutually antagonistic effects of the Th2/Treg and Th1/Th17 responses [8] (Fig. 1.1), explains, in part, the inverse correlation between the decreased prevalence of helminth parasite infections in given populations, and the increasing incidence of autoimmune diseases over recent decades [59, 60]. The rise in the incidence of autoimmune disease over the last 50 years has predominantly occurred in Westernised populations, such as Europe [61, 62] and Australia [63, 64], but remains low (to negligible) in developing countries in which levels of sanitation are low, and concomitant exposure to parasites is still relatively high. For example, the prevalence of MS was significantly reduced once a critical threshold of helminth infection rates (10%) was exceeded in any given population [65, 66]. Furthermore, MS patients, who were infected with helminths experienced remissions of clinical symptoms, and significantly fewer neurological lesions were observed. In these helminth-infected patients, the cytokine profile (as measured in peripheral blood) was skewed towards a Th2/Treg phenotype, with increased levels of IL-10 and TGF-β, whilst IL-12 and IFN-γ levels were decreased [67, 68]. This evidence further supports the premise that the historically ubiquitous presence of helminths in the human population has strongly influenced the development of the human immune system. Indeed, analysis of 91 cytokine genes within 52 human populations revealed that the highest frequencies of single nucleotide polymorphisms (SNP) within interleukin genes were among inhabitants of geographical areas exhibiting the highest incidence of endemic helminth infections [69]. It has been suggested that polymorphisms in immune-related genes have arisen due to selective pressure exerted by the immune-modulatory ability of helminth parasites. However, in populations where helminth infections are not endemic, and consequently their immune-modulatory effects are absent, there is an increased likelihood of dysregulated pro-inflammatory responses towards self-antigens, and the development of autoimmune diseases [70].

The observed geo-epidemiological distribution of helminths and autoimmune disease implies that the presence of helminth parasites likely constitutes a significant protective environmental factor against the development of autoimmune disease. Conversely, the absence of helminths confers an increased risk for the development of autoimmune disease [71, 72]. This phenomenon, known as the ‘Hygiene Hypothesis’, was first established by David Strachan in 1989 [73], and has since been re-termed the ‘Old Friend Hypothesis’ by Rook [74]. Although the premise behind these hypotheses is

similar, the ‘Hygiene Hypothesis’ states that the increased levels of sanitisation in human societies have decreased exposure to pathogens, thereby causing an increased prevalence of autoimmunity [73]. The ‘Old Friend Hypothesis’ asserts that humans have ‘lost touch’ with the pathogens with which we have evolved, and hence re-establishing the exposure to these ‘old friend’ organisms could facilitate the prevention of autoimmune diseases [74]. In support of these proposals, the Th2 and Treg responses initiated in response to infection with helminth parasites are sufficiently potent to prevent the establishment of bacterial-specific Th1 responses in co-infection studies [75]. In addition, in mammalian populations where helminth parasites are endemic, the induction of the protective Th1 immune responses to vaccination is compromised [76, 77]. Further, this ‘immunologic hypo-responsiveness’ can be reverted by the administration of anti-helminthic drugs, which further supports the notion that helminth parasites are causing this type of immune-modulation [11].

1.2 Helminth parasites as "worm therapy"

It has been suggested that the potent immune-modulatory ability of helminths can be exploited therapeutically [78, 79]. Initial studies focused on the concept of "worm therapy", based on the premise that the re-introduction of live helminth worms would induce anti-inflammatory/regulatory immune responses, and thus suppress the pro-inflammatory (Th1 and Th17) responses, which mediate autoimmune disease ('Old Friend Hypothesis').

Experimentally, proof-of-concept has been widely demonstrated using animal models with a wide variety of helminths (Table 1.1). Most cases have shown either delayed onset and/or alleviated symptoms of disease when helminth infection was used as a prophylactic treatment. Generally, disease protection induced by helminth infection in these animal models was associated with a reduction in auto-antigen specific Th1 and Th17 responses, characterised by reduced secretion of TNF [80-83], IFN-γ [82-86] and IL-12 [84], and increased differentiation/expansion of Tregs [86, 87]. Furthermore, the presence of M2 macrophages, and increased levels of IL-10, contributed to the protection of mice from autoimmune diseases [80, 88-90], as the depletion of M2 macrophage populations [88, 91], or reduced IL-10 [92] production, abrogated the protective effects. Interestingly, some mice were protected from colitis [91, 93-95] and T1D [96] even in the absence of IL-10 production. This demonstrates the complex mechanisms by which helminth therapy prevent autoimmunity. Indeed, contrary to the therapeutic benefits observed with helminth infections, exacerbation of colitis was observed with the use of *Trichuris muris* [97] and *Hymenolepis diminuta* [98, 99]. Thus, not all worms may be efficacious as therapeutic agents to prevent/treat autoimmune disease.

In humans, a number of small clinical trials (17 in total) using helminth infection to treat autoimmune disease have been completed (Table 1.2). To date, only two parasites, *Necator americanus* and *Trichuris suis*, have been used in human clinical trials. *T. suis* is a porcine whipworm, and, accordingly, is unable to colonise the human gut. Therefore, its administration to humans has been predicted to not cause disease or extensive pathology [100]. However, after ingestion of the eggs, the juvenile worms,

which hatch in the human intestine, are quickly expelled because humans are not a natural host for *T. suis*. Accordingly, the treatment regime consists of 2,500 eggs, taken orally every two weeks. In contrast, *N. americanus* is a human parasitic worm. Therapeutically, the patient is infected with 20 larvae, applied to the skin. Although the burrowing of *N. americanus* through the skin reportedly causes a mild itch, the use of a low number (20-25) of infecting worms presumes that minimal pathology will result. Both of these parasites typically reside in the intestine and can remain viable for 1-2 years for *T. suis* [101] and up to 5 years for *N. americanus* [102, 103]. Both worm species have gained approval as an Investigational Medicinal Product (IMP) by the Food and Drug Administration (FDA) agency in the US [104].

The outcomes of the reported human clinical trials using helminths to treat autoimmune diseases are summarised in Table 1.2. In general, the majority of patients showed improved clinical symptoms, with no severe adverse short or long-term side effects (although some individuals experienced symptoms of mild itching, rashes and intestinal enteropathy) [105]. Although such clinical outcomes are encouraging, the small sample sizes and the short monitoring periods mean that results must be interpreted with caution. A series of phase II clinical trials have been completed over the past five years, which had increased sample sizes and improved experimental design (double-blinded, placebo-controlled). However, many studies did not produce the desired results. For example, the TRUST-2 study (clinical trial identification number: NCT01279577) for Crohn's disease was terminated due to a lack of treatment efficacy [106]. Another study (NCT01953354) was terminated due to the manufacturer's decision to discontinue the production of *T. suis* eggs [107]. The MUCUS study (NCT01433471) for ulcerative colitis had insufficient numbers of participants to draw any significant clinical conclusions [108]. The WIRMS (NCT01470521) study for MS [109, 110] was completed in early 2016, and outcomes are yet to be reported.

There are likely numerous reasons for the failure of these human clinical trials. Firstly, there is frequently a disjunction between the translations of successful animal studies to human trials. This is attributable, in part, to the majority of animal studies establishing that helminths prevent the development of autoimmunity, rather than ameliorating established autoimmune disease (Table 1.1). The anatomical locality of the helminth infection may also be an issue for parasites that do not induce systemic

immune-modulatory effects. For example, *T. suis* only resides in the intestine, and, therefore, may not be efficacious for the neurological sequelae of MS. Other factors contributing to the lack of efficacy may include the duration and/or dosage of the helminth infection, and the host's genetics [111]. For example, different strains of mice are known to have varying susceptibility to helminth infections [112, 113]. Therefore, an individual's genetic make-up may also modulate susceptibility to helminth infection, thereby introducing a confounding factor for clinical trials. Nonetheless, collectively the results of human and rodent studies, along with the established epidemiological inverse relationship between helminth infection and autoimmunity, indicate that helminths, and their products, are potent immune-modulators with significant therapeutic potential.

Table 1.1 Use of helminth infections, and their products, to prevent or treat autoimmune disease in animal models

Rodent model	Human equivalent	Parasite	Prophylactic/ Therapeutic	Clinical Outcomes	Ref
EAE	MS	*H. polygyrus*	Prophylactic	Adoptive transfer of B cells from infected mice alleviated symptom severity	[63]
		S. mansoni	Prophylactic	Delayed onset of clinical symptoms with treatment 2 weeks and 4 days prior to the induction of EAE Reduced recruitment of inflammatory cells to CNS	[114]
			Therapeutic	Delayed onset of clinical symptoms with treatment applied on 2 days from EAE initiation but not in effector days (days 7, 10 and14 from induction of EAE)	
			Prophylactic	Delayed onset of clinical symptoms and inflammation of EAE	[115]
		T. crassiceps	Prophylactic	Reduced the symptoms of EAE in half of the mice infected	[116]
		T. pseudospiralis	Prophylactic	Reduced CNS inflammation and delayed onset of EAE	[117]
		T. spiralis	Prophylactic	Reduced the severity of EAE development in rats	[85]
NOD	T1D	*H. polygyrus*	Prophylactic	Reduced onset of T1D Inhibition of pancreatic insulitis T1D prevented up to 36 weeks [118] and 40 weeks of age [87, 119]	[87, 118, 119]
		L. sigmodontis	Prophylactic	Prevented the onset of T1D	[120]

Cont'

		S. mansoni	Prophylactic	Reduced onset of T1D	[121]
		T. pseudospiralis	Prophylactic	Free of T1D symptoms up to 36-37 weeks of age	[118]
MLDS-induction	T1D	*H. polygyrus*	Prophylactic	Reduced the severity of MLDS-induced T1D but not in single high-dose induced T1D. Prevented decrease in pancreatic islet size	[96]
		S. mansoni	Prophylactic	Reduced induction of T1D and prevented pancreatic degeneration	[122]
		T. crassiceps	Prophylactic	Reduced induction of T1D (40% of infected mice developed T1D, as opposed to 100% of uninfected mice) Decreased pancreatic insulitis	[80]
TNBS-induction	IBD	*H. polygyrus*	Prophylactic	Inhibited the onset of colitis	[123, 124]
		S. japonicum	Prophylactic	Reduced symptoms of colitis and mortality of mice	[125, 126]
		S. mansoni	Prophylactic	Protected mice from TNBS-induced inflammation and hence attenuated colitis Concurrent infection reduced the duration of TNBS-induced colitis from 4 weeks (uninfected) to 2 weeks in rats	[84] [127]
DNBS-induction	IBD	*H. diminuta*	Prophylactic	Reduced clinical symptoms of colitis and hence protected mice from colitis	[92, 128]

Cont’

		T. pseudospiralis	Prophylactic	Reduced severity of colitis symptoms and decreased mortality of mice	[129, 130]
DSS-induction	IBD	*H. polygyrus*	Prophylactic	Inhibited the onset of DSS-induced colitis and inflammation	[131]
		S. mansoni	Prophylactic	Inhibited the onset of DSS-induced colitis, with prevention of weight loss and colon length shortening Adoptive transfer of colon lamina propria macrophages from infected mice protected mice from colitis	[81, 91]
		T. crassiceps	Prophylactic	Reduced DSS-induced colitis Adoptive transfer of alternatively activated macrophages from infected mice reduced severity of colon inflammation	[132]
		T. papuae	Prophylactic	Reduced DSS-induced colitis and prevented weight loss, shortening of colon length	[133]
		T. spiralis	Prophylactic	Inhibited the onset of colitis and prevented weight loss and shortening of colon length	[134]
IL-10$^{-/-}$	IBD	*H. polygyrus*	Prophylactic	Inhibited the onset of colitis and inhibited intestinal inflammation	[93-95]
		T. muris	Prophylactic	Exacerbated colitis and intestinal inflammation	[97]
Oxazolone-induction		*H. diminuta*	Prophylactic	Exacerbated colitis and intestinal inflammation	[98, 99]
CIA	RA	*S. japonicum*	Prophylactic	Reduced the severity and incidence of type II collagen-induced arthritis at the pre-established acute stage of infection	[83, 135]

Cont'

		S. mansoni	Prophylactic	Reduced the severity of type II collagen-induced arthritis with decreased systemic and local inflammation	[82]

Other models	Human equivalent	Parasite	Prophylactic/ Therapeutic	Clinical outcomes	Reference
Idiopathic chronic diarrhoea in macaques monkeys	IBD	*T. trichiura*	Therapeutic	Improved clinical symptoms (increase in weight gain) of 4 out of 5 monkeys with established idiopathic chronic diarrhoea	[86]

EAE: Experimental Autoimmune Encephalomyelitis; MS: Multiple Sclerosis; *H. polygyrus*: *Heligmosomoides polygyrus*; Tregs: T-regulatory cells; *S. mansoni*: *Schistosoma mansoni*; CNS: Central nervous system; *T. crassiceps*: *Taenia crassiceps*; *T. pseudospiralis*: *Trichinella pseudospiralis*; *T. spiralis*: *Trichinella spiralis*; NOD: Non-obese diabetic mice; T1D: Type-1 diabetes; *L. sigmodontis*: *Litomosoides sigmodontis*; MLDS: Multiple-low dose streptozotocin; TNBS: Trinitrobenzesulfonic acid-induced mice; IBD: Inflammatory bowel disease; *S. japonicum*: *Schistosoma japonicum*; DNBS: Dinitrobenzene sulfonic acid; *H. diminuta*: *Hymenolepis diminuta*; DSS: Dextran sodium sulfate; *T. papuae*: *Trichinella papuae*; IL-10: Interleukin-10; *T. muris: Trichuris muris*; CIA: Collagen-induced arthritis; RA: Rheumatoid Arthritis; *T. trichiura*: *Trichuris trichiura.*

Table 1.2 Use of helminth infections and products to treat autoimmune disease in humans

Autoimmune disease	Study outline and number of subjects	Clinical outcomes	Ref
IBD (Crohn's disease)	Single dose of 2500 *T. suis* eggs given to 2 patients, who were monitored every 2 weeks for 12 weeks Repeated dose of 2500 *T. suis* eggs given to 2 patients, who were monitored every 3 weeks for 28 weeks	No adverse effects Single dose outcome: 75% of patients achieved remission and 67% of these relapsed within 12 weeks Repeated dose outcome: 100% of patients achieved remission, with 50% maintaining remission for ≥ 1year	[136]
	Repeated dose of 2500 *T. suis* eggs given to 29 patients, who were monitored every 3 weeks for 12 weeks	No adverse effects 79% of patients responded to treatment at 12 weeks 72% of patients achieved remission for 12 weeks	[101]
	Single dose of 25–50 *N. americans* larvae given to 4 patients and recorded CDAI at 3 week intervals Repeated dose of 25-50 *N. americanus* larvae given at week 0 and week 27 or 30 given to 5 patients with recorded CDAI at 3 week intervals	Presence of adverse effects for both dose groups, such as mild itching (lasting a few initial days), rash, transient enteropathy Achievement in remission with improvement in average CDAI of 165 at week 0 to 64 at week 20 (for single dose group) and 75 at week 45 (for repeated dose group), where <150 CDAI equates to remission	[105]
	Single dose of 500, 2500 and 7500 *T. suis* eggs were given to 3 groups of 12 patients (where 9 patients of each group were given the eggs, whilst 3 of each group were given a placebo) with monitoring days 1, 3, 5, 7, 9, 11 and 14, and months 1, 2 and 6. (Randomized, double-blind, placebo-controlled study; ClinicalTrials.gov identifier: NCT01576461)	No short or long-term side effects were observed. Overall, 26% of infected patients and 33% of placebo-patients reported gastrointestinal issues, however this was not a dose-dependent effect	[137]

Cont'

	(Named TRUST-1): Repeated dose of 7500 *T. suis* eggs or placebo given to 250 patients every 2 weeks for 12 weeks. (Randomized, double-blind, placebo-controlled Phase II study; ClinicalTrials.gov identifier: NCT01576471)	Did not meet primary endpoint of improved response, of a decrease of 100 CDAI points nor secondary endpoint of remission (defined as <150 CDAI) Non-significant improvement in patients with > 290 CDAI patients	[106]
	(Named TRUST-2): Low, medium and high doses of (250, 2500 or 7500) *T. suis* eggs or placebo given to 252 patients every 2 weeks, for 12 weeks and CDAI observed over 12 weeks (Double-blind, randomised, placebo-controlled, Phase II study; ClinicalTrials.gov identifier: NCT01279577)	No significant adverse effects observed Clinical remission seen in 38.5%, 35.2%, and 47.2% of patients receiving 250, 2500, or 7500 eggs, respectively and in 42.9% of placebo-patients No advantage of treatment over placebo group Trial terminated	[138]
IBD (Ulcerative colitis)	Single dose of 2500 *T. suis* eggs given to 1 patient and monitored every 2 weeks until 12 weeks Repeated dose of 2,500 *T. suis* eggs given to 2 patients and monitored every 3 weeks until 28 weeks	No adverse effects Single dose outcome: 100% of patients achieved remission and 33% relapsed within 12 weeks Repeated dose outcome: 100% of patients achieved remission and maintained remission for a year (or over)	[136]
	Repeated dose of 2500 *T. suis* eggs or a placebo given to 54 patients and monitored every 2 weeks until 12 weeks	43% of infected patients and 17% of patients given the placebo responded to treatment at 12 weeks 10% of infected patients and 4% of patients given the placebo achieved remission at 12 weeks	[139]
	(Named MUCUS): Repeated dose of 2500 *T. suis* eggs given to 2 patients every 2 weeks for 12 weeks, and then crossed over to 12 weeks of placebo; whilst another 2 patients received placebo for 12 weeks and then crossed over to 12 weeks of egg treatment	Study had been completed, however, due to the small sample group, outcome measures were not collected and analysed	[108]

Cont’

	(Double blind, randomised, placebo-controlled study; ClinicalTrials.gov identifier: NCT01433471)		
MS	(Named HINT-1): Repeated dose of 2500 *T. suis* eggs given to 5 RRMS patients every 2 weeks for 12 weeks (ClinicalTrials.gov identifier: NCT00645749)	No significant adverse effects were observed 3 out of 5 patients experienced mild gastrointestinal symptoms Brain MRI scans showed reduced number of lesions with an average of 6.6 at baseline screening to 3 at 12 weeks of treatment	[140]
	(Named HINT-2): Repeated dose of 2500 *T. suis* eggs given to 15 RRMS patients every 2 weeks over 10 months (Phase I study; ClinicalTrials.gov identifier: NCT00645749)	Brain MRI scans showed reduced number of lesions with an average of 3.2 at baseline screening to 2.1 in the last 5 months of treatment Treatment deemed safe and eggs were well-tolerated	[141]
	Repeated dose of 2500 *T. suis* eggs given to 4 SPMS patients every 2 weeks over 3 months (EU clinical trials register identifier: EUCT2009-015319-41)	A decrease in inflammatory immune response and increase in anti-inflammatory response observed Treatment deemed to be safe	[142]
	(Named TRIMS A):Repeated dose of 2500 *T. suis* eggs given to 10 RRMS patients every 2 weeks for 12 weeks (Phase I study; ClinicalTrials.gov identifier: NCT01006941)	Patients reported gastrointestinal issues No beneficial effects reported of the treatment	[143]
	(Named TRIOMS): Repeated dose of 2500 *T. suis* eggs or placebo given to 50 RRMS patients every 2 weeks over 12 months (and continual monitoring with immunological assays and MRI scans during the treatment and post 6 months treatment)	Trial terminated	[144, 145]

Cont'

	(Double blind, randomised, placebo-controlled Phase II study; ClinicalTrials.gov identifier: NCT01413243; EU clinical trials register identifier: EUCTR2009-015319-41-DE)		
	Repeated dose of 7500 *T.suis* eggs or placebo given to 16 patients with left-sided ulcerative colitis every 2 weeks over 10 weeks	Trial terminated due to manufacturer's decision to halt production of *T.suis* eggs	[107]
	(Named WIRMS): Single dose of 25 *N. americanus* larvae or placebo given to 36 patients (total 72 patients) and monitored over 12 months with clinical, immunological and MRI assays (Double blind, randomised, placebo-controlled Phase II study; ClinicalTrials.gov identifier: NCT01470521; EU clinical trials register identifier: EUCT2008-005008ZY-GB)	Outcome data not available	[109, 110]
RA	Repeated dose of 2500 *T.suis* eggs or placebo given to 50 patients every 2 weeks for 24 weeks. An add on-therapy for patients on stable methotrexate treatment (EU clinical trials register identifier: EUCTR2011-006344-71-DE)	Trial terminated	[66]

IBD: Inflammatory bowel disease; *T. suis*: *Trichuris suis*; *N. americanus*: *Necator americanus*; CDAI: Crohn's disease activity index; MS: Multiple sclerosis; RRMS: Relapsing–remitting multiple sclerosis, MRI: Magnetic resonance imaging; SPMS: Secondary-progressive multiple sclerosis; RA: Rheumatoid arthritis

1.3 Limitations and challenges for the use of live worm therapy

Despite the unsuccessful outcomes of the larger clinical trials, the earlier smaller studies, the natural endemic population studies, and the vast majority of the animal studies provide a strong rationale that 'worm therapy' should be pursued for the prophylactic or therapeutic treatment of autoimmune disease. However, the use of live parasites is not optimal. The compliance of patients is predicted to be generally poor, and this is largely attributable to negative attitudes associated with the concept of being infected with live pathogens [146]. Also, the administration of live parasites (and, in some cases, the subsequent infection) has caused adverse side effects, at times even exacerbating pro-inflammatory conditions, due to the parasite's feeding and migratory activities [147, 148]. Additionally, the larval stages, which have been shown to be therapeutically beneficial in trials, must be produced in a mammalian host [6]. This criterion prohibits the mass scale production required for a truly global therapeutic. There is also a significant risk of contamination with other human pathogens. For example, the parasite *N. americanus* is harvested from the faeces of infected individuals. The use of the porcine whipworm, *T. suis*, does not circumvent this problem as there is a transferral risk of hepatitis E virus, which is often found in pigs and is pathogenic to humans [104]. Accordingly, the use of pathogen-free pigs would be required to ensure the absence of such infectious contaminants [101, 104]. Additionally, using *T. suis* as a therapeutic agent requires the frequent intake of 2,500 eggs, a dosing regimen with which many patients fail to comply. Further, the viability of eggs cannot be established prior to delivery to a patient, therefore an effective dose cannot be determined as some eggs fail to produce viable juveniles. Finally, but most importantly, there is a lack of specificity with the use of live parasites. As discussed previously, in populations endemically infected with helminths, protective immunity (i.e. Th1 and/or Th17 responses) is compromised, which prevents the development of appropriate immune responses to bacterial/viral pathogens and vaccination [147, 149]. Thus, the patient is effectively immune-compromised, just as he/she would be if prescribed immunosuppressive drugs. For individuals who are already immune compromised (such as children, the elderly, and pregnant women) [150, 151], treatment regimens using live helminth infections may be of greater risk than benefit [152, 153]. Therefore, the use of live helminth infection is not a realistic treatment for autoimmune disease.

A safer and more realistic alternative to live infection would be to identify the specific immune-modulatory molecules produced by helminth parasites. This approach would allow the precise mechanism(s) of action to be characterized, and their properties to be modified to increase therapeutic efficacy [154]. In addition, synthetic peptides can be easily manufactured to therapeutic standard, and can be modified during synthesis into small molecule analogues to enhance stability, and to reduce undesirable immunogenicity and toxicity. To date, there have been no clinical trials conducted to assess helminth products for the treatment of autoimmune diseases. However, based on the large body of evidence that helminth molecules possess potent immune-modulatory activity, they likely have tremendous therapeutic potential [106].

1.4 Use of excretory/secretory molecules of helminth parasites to prevent autoimmunity

Within their mammalian hosts, helminth parasites secrete and excrete a mixture of molecules. These excretory/secretory (ES) products perform a number of biological functions to support the parasite's growth and reproduction, such as degradation of haemoglobin into essential nutrients [155] and cleavage of collagen to facilitate migration through tissues [156]. However, it has been widely reported that the ES products from many helminths also have the capacity to modulate host immune responses, analogous to live infection *per se* [157-159]. Furthermore, the delivery of ES products has been shown to prevent or ameliorate the clinical symptoms of autoimmune disease in several animal models (Table 1.3). Like infection, protection is typically associated with a reduction in Th1 and Th17 immune responses that are central to disease development, and the induction of Th2/Treg type immune responses. Macrophages have been shown to play a central role in this skewing of immune responses induced by helminth ES products. For example, IL-10-producing macrophages were responsible for reducing colonic inflammation mediated by *Acanthocheilonema vitae* cystatin [160]. Delivery of ES-62 (from *A. vitae*) inhibited Th1 cytokine production by pro-inflammatory macrophages [161, 162]. Collectively, this data suggests that ES products drive macrophages towards the M2 phenotype, and suppress the development of M1 macrophages, and thus the initiation of Th1/Th17 immune responses, in an analogous manner to live helminth infections. Therefore, elucidating the immune-modulatory mechanisms of action of individual ES product components would be highly advantageous in the process of developing novel therapeutics for autoimmune disease [157].

Table 1.3 Use of helminth excretory/secretory (ES) products as therapeutics in animal models of autoimmune disease

Animal model	Human equivalent	Parasite molecule	Clinical outcomes	Ref
CIA in mice	RA	ES-62 (the natural PC-containing glycoprotein) from *A. viteae*	Reduction in severity and progression of arthritis and production of Th1 cytokines	[163]
			Down-regulation of collagen-specific pro-inflammatory, Th1 cytokines	[164]
			Down-regulation of Th1 and Th17 cytokine production	[165]
			Restored regulatory B cell infiltration into the joints	[166]
NOD mice	T1D	DiAg from *D. immitis*	Reduction in pancreatic islet antigen-specific Th1 response and switch to an anti-inflammatory Th2 response Complete prevention of pancreatic insulitis (in 6 out of 7) and diabetes in 6-week old NOD mice	[167]
TNBS-induced mice	IBD	AcES from *A. caninum*	Reduction in Th1 cytokines and an increase in Treg cytokines Decrease in macroscopic inflammation score and MPO activity (indicative of inflammation) of colon and lymph nodes of TNBS-induced mice	[168]
DSS-induced mice			Increased Th2 cytokines and reduced Th1 cytokines in draining lymph nodes and the colon of DSS-induced mice Reduced colon pathology and DSS-mediated weight loss	[169]
		ES products from *A. ceylanicum*	Reduction in Th1 and Th17 cytokine production Minimised clinical and microscopic colonic inflammation scores and MPO activity	[170]

Cont'

		ES products from *T. spiralis*	Reduction in Th1 and Th17 cytokine production and increase in Treg cytokines Reduced macroscopic and microscopic inflammation in the colon, lymph nodes and spleen	[171]
		Av17 (protease inhibitor, cystatin) from *A. viteae*	Decreased colon inflammatory activity, infiltrations and epithelial damage Increase in Treg cytokines	[160]
		ES product (55kDa) from *H. polygyrus*	Reduction in pro-inflammatory cellular infiltration and Th1 cytokine gene expression Reduced colon pathology and DSS-mediated weight loss Increase in Treg cytokine	[172]
DNBS-induced mice		ES product (high molecular weight fraction) from *H. diminuta*	Reduced inflammation with decreased Th1 cytokine production and increase in Th2/Treg cytokines	[173]

CIA: Collagen-Induced Arthritis; RA: Rheumatoid Arthritis; PC: phosphorylcholine; *A. viteae*: *Acathocheilonema viteae;* Th1: T-helper 1; NOD: Non-Obese Diabetic mice; T1D: Type-1-Diabetes; *D. immitis*: *Dirofilaria immitis*; Th2: T-helper 2; DSS: Dextran Sodium Sulphate; IBD: Inflammatory-Bowel Disease; *A. caninum*: *Ancylostoma caninum*; TNBS: Trinitrobenzene Sulfonic acid; Treg: T-regulatory; MPO: Myeloperoxidase; *A. caeylanicum*: *Ancylostoma ceylanicum*; *T. spiralis*: Trichinella *spiralis*; *A. viteae*: *Acanthocheilonema viteae*; DNBS: Dinitrobenzene Sulfonic acid; *H. diminuta*: *Hymenolepis diminuta*

**Cases using the soluble egg antigens (SEA) from S. mansoni and Schistosoma japonicum have also shown efficacy in treating murine T1D [161] and MS [162], respectively, via the induction of a Th2/Treg response. Although results are promising with the use of SEA, the use of egg antigens do not truly reflect the proteins that are actively produced during an infection, as it is more of an experimental preparation. Therefore, the works described here are focusing only on helminth ES products that have shown therapeutic evidence in autoimmunity.*

1.5 *Fasciola hepatica* is a potent immune-modulator

Fasciola hepatica, commonly known as the liver fluke, has adapted to long-term survival within its mammalian hosts, living up to 20 years in some instances [174]. Additionally, *F. hepatica* exhibits a widespread geographical distribution [175], and host range (infecting the greatest variety of mammals, including mice, sheep, cattle, goats, humans, hares, rabbits, and even birds) of all helminth parasites [175-177]. This suggests that *F. hepatica* has evolved efficient mechanisms to invade host tissue and to increase longevity within the host [178]. The ability of *F. hepatica* to infect and complete its life-cycle in newer hosts, such as the kangaroo [179], also implies a superior adaptation, as compared to other helminth parasites, such as *Nippostrongylus brasiliensis* and *Brugia malayi,* which have adapted to only infect a single host [76]. Collectively, these characteristics suggest that *F. hepatica* excretes/secretes molecules that possess considerable immune-modulatory potential.

The infection pathway of *F. hepatica* begins within the host after the ingestion of metacercariae, which are the encysted larval form of the worm (Fig. 1.2). Upon reaching the acidic environment of the gastrointestinal tract, immature flukes hatch, and these newly excysted juvenile (NEJ) flukes migrate through the gut wall to enter the peritoneal cavity (Fig. 1.2). The NEJ flukes continue to burrow through to the liver, reaching the bile ducts 10-12 weeks after ingestion. Within the bile ducts, the NEJ flukes mature into adult forms, which feed on blood by puncturing holes in the bile duct wall, and then reproduce (Fig. 1.2) [174]. In order for *F. hepatica* to survive and successfully reproduce in such an environment, this helminth has developed elegant mechanisms to inhibit the host's protective pro-inflammatory Th1 immune responses [152], and to drive the development of Th2 and Treg immune responses (Table 1.4).

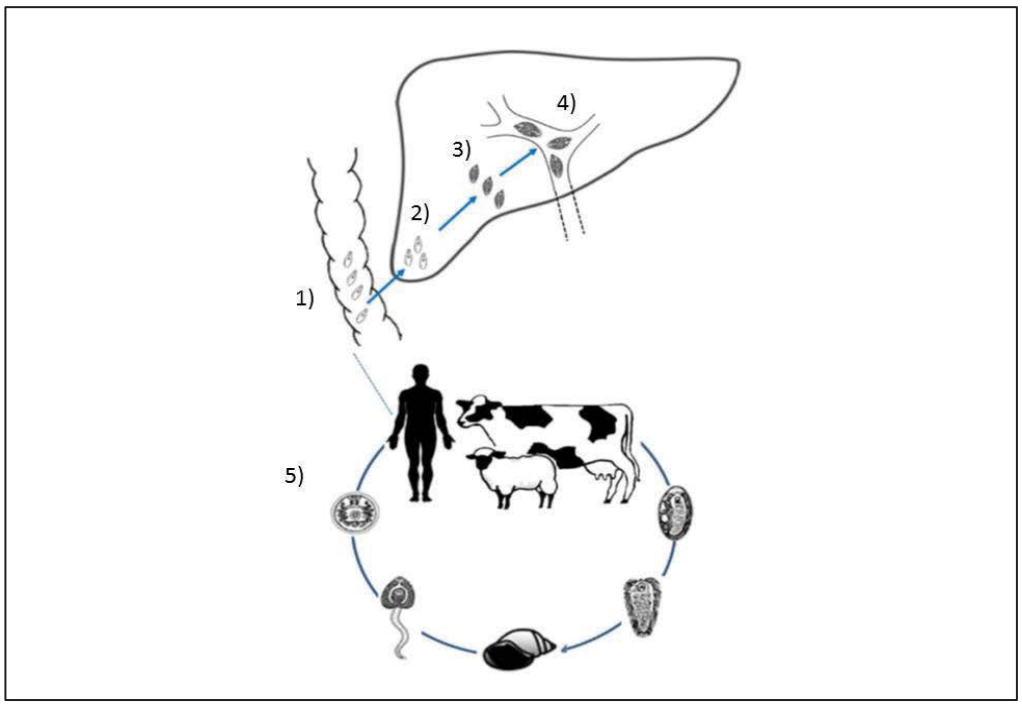

Figure 1.2 Lifecycle of *Fasciola hepatica*. Graphical representation of *F. hepatica* lifecycle. (1) Within the host (varying from humans, cattle and sheep), immature flukes hatch from metacercariae upon reaching the acidic environment of the gastrointestinal tract. These newly excysted juvenile (NEJ) flukes migrate through the gut wall to enter the peritoneal cavity and (2) burrow through the liver. (3) The NEJ flukes continue to burrow through to the liver, (4) reaching the bile ducts to mature into adult forms. (5) The further lifecycle stages of *F. hepatica* after the eggs are released via faeces from the host, into pasture. From the eggs, the miracidium form of *F. hepatica* infects the snail intermediate host, *Galba truncatula*. Within the snail host, the parasite develops through the sporocyst, rediae and cercariae lifecycle stages, and are deposited on vegetation for the dormant metacercariae to be ingested by the host. Adapted from [180].

Within hours after the ingestion of *F. hepatica* metacercariae, the phenotype and function of innate immune cells are altered. Coincident with the penetration of the parasite through the intestinal wall, the expression levels of M1 associated genes in peritoneal macrophages are significantly decreased (Donnelly *et al.,* unpublished data). As the parasite reaches the liver, macrophages express the characteristic markers of a helminth-M2 macrophage phenotype [181-184]. These macrophages promote the expansion of Th2 cells that secrete IL-4 [183, 185, 186] and IL-5 [186], which facilitate the production of the Th2-associated antibody, IgG1 [186-189]. As infection progresses to the chronic phase (6 weeks post-infection in a natural host, such as cattle), the levels of the Treg cytokines, IL-10 and TGF-β, increase [28, 185, 186]. Simultaneously, the levels of Th1-associated IgG2 antibody decrease [187], and T cells no longer produce Th1 type cytokines in response to bacterial challenge [75, 186]. This potent immune-modulatory ability of *F. hepatica* was sufficient to significantly delay the onset and reduce the clinical severity of disease in a mouse model of MS [28]. Disease protection was associated with a suppression of Th1 and Th17 responses, and an increase in the levels of IL-10 and TGF-β secreted by Tregs and M2 macrophages [28]. These data suggest that *F. hepatica* produces potent immune-modulatory molecules capable of polarising the immune system towards anti-inflammatory/regulatory responses.

It has been demonstrated that the immune responses induced by live infection with *F. hepatica* are replicated by use of the ES products (termed FhES) alone. *In vitro*, administration of FhES to bovine macrophages induced increased secretion of IL-4 and IL-10, and a switch to a M2 phenotype [182]. In addition, administration of FhES to mice (via intraperitoneal injection) resulted in a polarised Th2 immune response, and the activation of helminth-M2 macrophages [183, 184]. Similar to observations using live infection, the delivery of FhES to mice also prevented the development of bacterial specific Th1 immune responses in response to co-infection with *Bordetella pertussis*, or in response to immunisation with a whole cell pertussis bacterial vaccine [75]. Given these observations, the potency of immune-modulation by FhES was tested in the non-obese diabetic (NOD) mouse model of T1D. Only 6 intraperitoneal injections of FhES (10μg each) delivered on alternate days was sufficient to prevent autoimmune diabetes when delivered at a time-point coincident with the infiltration of macrophages into islets and the initiation of diabetogenic T cell priming events (4 weeks of age) [190].

Treatment of NOD mice with FhES resulted in significant decreases in the levels of auto-antigen specific IFN-γ, a switch in the isotype of auto-antibodies from a Th1 associated IgG2a to a Th2 induced IgG1, and the differentiation of helminth-M2 macrophages [190]. Importantly, these helminth-M2 macrophages promoted the development of Tregs *in vitro*, suggesting a mechanism by which NOD mice were protected from disease after FhES treatment. More recently, FhES has been shown to afford protection from MS, in the murine EAE model, via reduction of Th1/Th17 cell infiltration into the brain, and the induction of Th2/Treg cytokines by eosinophils and helminth-M2 macrophages [191]. The efficacy with which FhES treatment prevented autoimmunity in both T1D and MS models indicated that it represented a potent source of parasite-derived immune-modulators, which could be mined to isolate, identify and characterise novel therapeutic agents.

Table 1.4 Host immune response profiles induced by *Fasciola hepatica* and its excretory/secretory molecules (FhES)

Summary of study	Immune response outcomes	Ref
***F. hepatica* oral infection of cattle**	↑ M2 macrophage ↑ Th2/ Treg cytokines (IL-4, IL-10, TGF- β) ↑ Th2 antibody (IgG1) ↓ Th1 antibody (IgG2) ↓ Th1 cytokine (IFN-γ)	[181, 182] [185] [187-189] [187] [187, 192]
***F. hepatica* oral infection of mice**	↑ M2 Mphi ↑ Th2/ Treg cytokines (IL-4, IL-5, IL-10, TGF- β) ↑ Th2-associated antibody, IgG1 production ↓ Th1 cytokines (IL-2, IL-12, IFN-γ)	[183, 184] [28, 186] [186] [28, 186]
***F. hepatica* oral infection of mice models of MS (EAE)**	↓ in Th1 and Th17 type cells and cytokines (IL-17 and IFN-γ) ↑ in M2 macrophage and Treg cells and cytokines (IL-10, TGF- β)	[28]
FhES administration to cattle Mphi *in vitro*	↑ Th2/ Treg cytokines (IL-4, IL-10) ↑ M2 macrophage	[182]
FhES administration to mice via intraperitoneal injections	↑ M2 macrophage ↑ Th2/ Treg cytokines (IL-4, IL-5)	[183, 184] [183]
FhES administration to mice infected with or obtained vaccination of *B. pertussis* in mice	↑ Th2 cytokine (IL-4) ↓ Th1 cytokine (IFN-γ)	[193]
FhES administration to mice models of T1D (NOD)	↓ Th1 cytokine (IFN-γ) ↑ Th2 antibody (IgG1) ↑ M2 macrophage	[190]
FhES administration to mice models of MS (EAE)	↑ Th2/ Treg cytokines (IL-4, IL-5, IL-13, IL-33, TGF- β) ↓ in Th1 and Th17 type cells and cytokines (IL-17 and IFN-γ)	[191]

F. hepatica: *Fasciola hepatica*; M2 macrophages: Macrophages of T-helper 2 phenotype; Th2: T-helper 2; Treg: T-regulatory; Th1: T-helper 1; IL: Interleukin; Ig: Immunoglobulin; IFN-γ: Interferon Gamma; MS: Multiple Sclerosis; EAE: Experimental Autoimmune Encephalomyelitis; FhES: *Fasciola hepatica* Excretory/Secretory molecules; TGF- β: Transforming Growth Factor-β; *B. pertussis*: *Bordetella pertussis*. ↑ and ↓ denotes increase and decrease, respectively.

1.6 Identification of the individual immune-modulatory molecules of FhES

Size exclusion chromatography has been used to fractionate and characterise the protein content of FhES. Proteomics analyses of these fractions have revealed that FhES contains fewer proteins than the ES products of other parasites [194]. For example, examination of the secretome of the eggs from the closely related blood fluke, *Schistosoma mansoni* has identified 188 proteins [195]. In contrast, proteomic analysis of *F. hepatica* ES has identified only 160 proteins [155]. Indeed, when separated by one-dimensional electrophoresis, FhES consists of a relatively simple mixture of proteins (Fig 1.3). Predominant amongst these are the cysteine protease enzymes, with Cathepsin L1 (FhCL1) accounting for 67% of the total secreted Cathepsin L molecules by the *Fasciola* worm [196]. Within the remaining 32% of FhES, a number of different proteins have been characterised, such as fatty acid binding proteins, peroxiredoxin, serpins, and glutathione transferase. However, the most abundant appear to be a small (8kDa) protein, termed *F. hepatica* helminth defence molecule-1 (FhHDM-1) [155]. Interestingly, homologs of these abundant proteins among FhES (FhCL1 and FhHDM-1) have been identified in other helminth parasites, suggesting their conservation to perform vital roles for parasite survival.

To assess the therapeutic efficacy in comparison to FhES, recombinant forms of FhCL1 and FhHDM-1 (as the two most abundant molecules of FhES), were tested in animal models of autoimmunity. This study showed that neither FhPrx (Donnelly *et al.,* unpublished data) nor FhCL1 [197] prevented disease development in murine models of T1D or relapsing/remitting EAE. However, a short time course of treatment with FhHDM-1 prevented the development of T1D and reduced the clinical symptoms of EAE [197]. These data suggest that within the ES products of *F. hepatica*, FhHDM-1 may be the sole molecule with potential as an immune therapeutic.

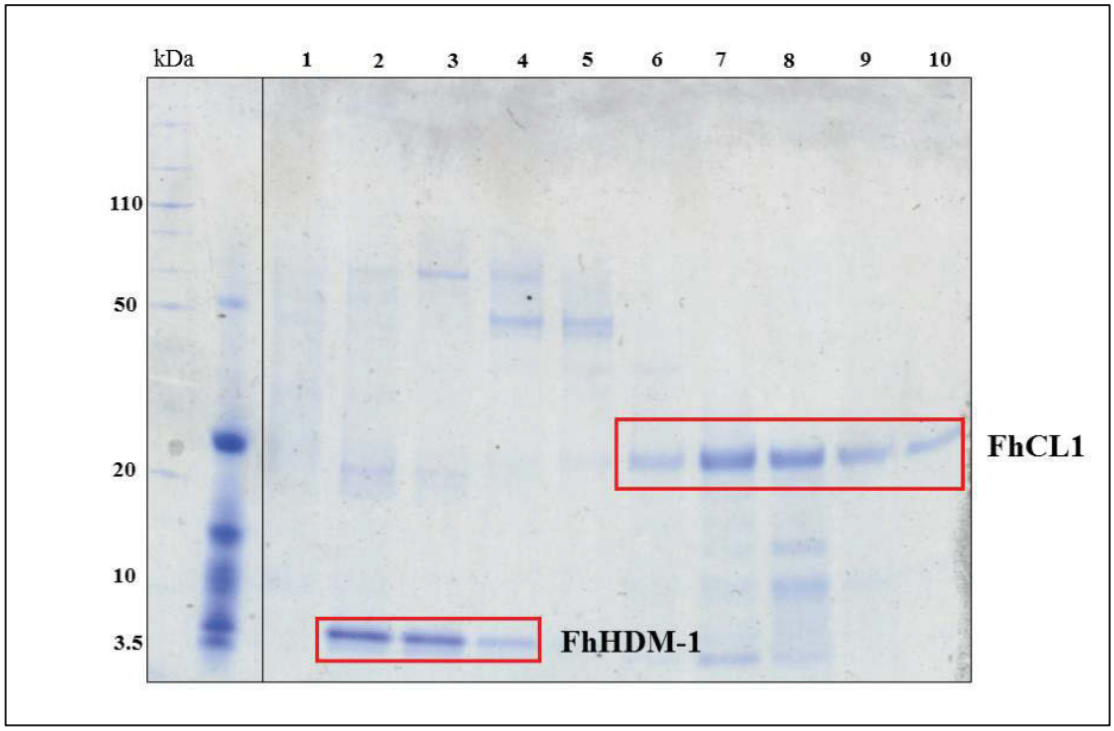

Figure 1.3 One-dimensional gel of *Fasciola hepatica* excretory/secretory (FhES) molecules. FhES was fractionated into ten fractions and run on a one-dimensional sodium dodecyl sulfate polyacrylamide electrophoresis (SDS-PAGE) gel. FhHDM-1 and FhCL1 (in red boxes) were the most abundant molecules found within FhES. The column on the left is the molecular weight ladder in kDa (Joyce To, 2015, unpublished).

1.7 FhHDM-1: A cathelicidin-like immune modulating peptide

FhHDM-1 is consistently expressed throughout all life-cycle stages of *F. hepatica* (NEJ flukes, 21-day immature liver stage flukes, and adults), and is regurgitated by the worm every 3h [198]. Therefore, the host is exposed to FhHDM-1 continually during the helminth's residence. The observation that antibodies against FhHDM-1 are present in the serum of sheep 4-8 week post-infection, supports the premise that FhHDM-1 is a key protein facilitating the survival of *F. hepatica*, throughout the migratory stage and long after the parasite has taken up residency in the bile ducts of the host [199]. Additionally, the relative abundance of FhHDM-1 within FhES also suggests that it performs a crucial function in ensuring parasite survival and longevity.

1.7.1 Structure of FhHDM-1

Reverse-phase high-performance liquid chromatography has revealed that FhHDM-1 is a small protein; 8kDa in size [199]. Further structural analysis identified a N-terminal signal peptide, adopting an α-helical secondary structure, and a hydrophobic C-terminal fragment of 34-residues (named FhHDM-1 p2) [199] (Fig. 1.4). The structural characteristics of FhHDM-1 resemble that of a class of mammalian antimicrobial/host defence peptides (HDPs), known as the cathelicidins. These peptides are an essential component of the mammalian innate immune response, thought to act primarily as bactericidal agents during infections due to their ability to disrupt bacterial membranes [200], although they can also affect certain fungi and viruses [201]. Testament to their anti-bacterial properties, the cathelicidins are widely distributed throughout the mammalian body, being found in the skin, alimentary canal, saliva, and sweat [202, 203].

Cathelicidins are now also recognised as molecules that are not simply anti-microbial agents, but function as important modulators of the innate immune system [202]. For example, PR-39 (a porcine HDP) facilitates tissue repair through the induction of syndecan proteoglycan synthesis [204] and angiogenesis [205]. This molecule is also directly anti-inflammatory, through its ability to inhibit the production of reactive oxygen species (ROS) by activated neutrophils [206]. Similarly, the human cathelicidin homolog, LL-37, can act as a chemoattractant for monocytes, neutrophils, T-cells, and

mast cells [207, 208]. Additionally, after cleavage of its precursor protein, CAP18, LL-37 can reduce the expression levels of pro-inflammatory cytokines, such as TNF, and pro-inflammatory genes, such as NFκB1 (p105/p50) and TNFα-induced protein 2 [209]. Considering the structural similarities between FhHDM-1 and the cathelicidins it was suggested that FhHDM-1 might exert similar biological functions.

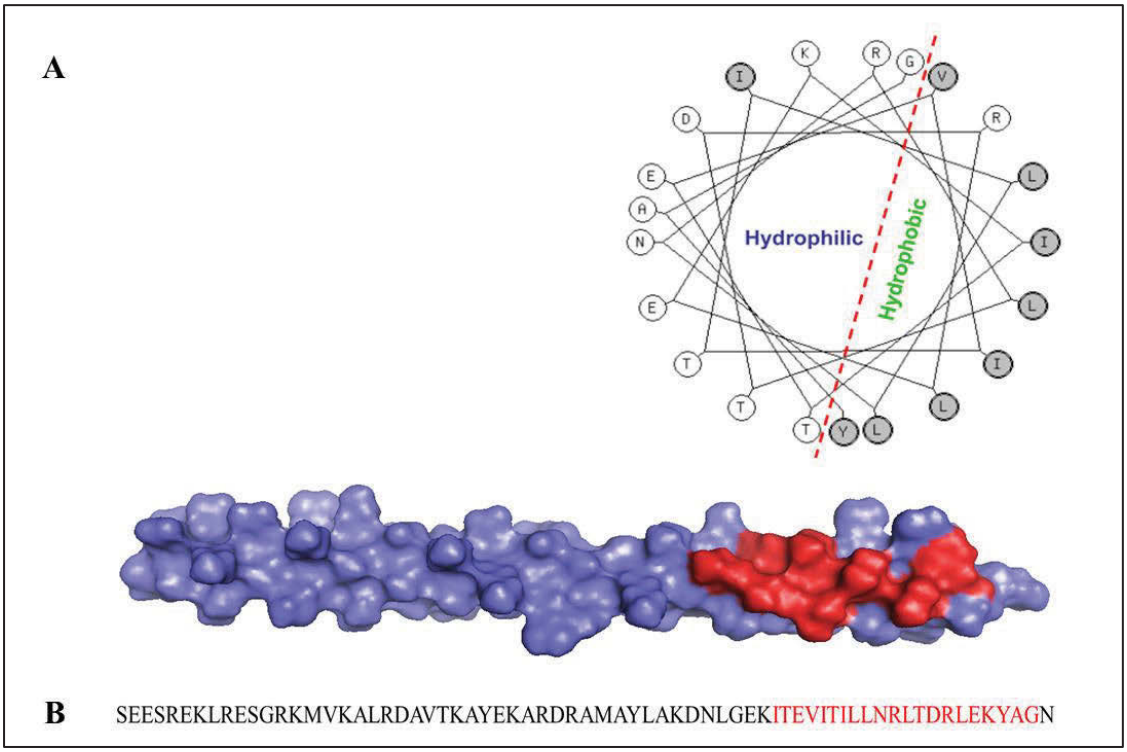

Figure 1.4 Structure of FhHDM-1. (A) A model of secondary structure of FhHDM-1 showing the α-helical secondary structure and a helical wheel diagram showing the amphipathic region towards the C-terminus. **(B)** The primary amino acid sequence of FhHDM-1. The amphipathic region for both the secondary structure (A) and primary sequence (B) is indicated in red. Adapted from [199].

1.7.2 FhHDM-1 is likely not anti-microbial, anti-parasiticidal or cytotoxic to mammalian cells

Cathelicidins are known to be anti-microbial, anti-parasiticidal, and cytotoxic to mammalian cells, especially due to the presence of a conserved amphipathic region. Despite possessing a similar amphipathic helix [199] (Fig. 1.4), FhHDM-1 p2 neither inhibited the growth of gram-negative (*Escherichia coli, Pseudomonas aeruginosa* and *Salmonella typhimurium*) and gram-positive (*Staphylococcus aureus* and *Staphylococcus epidermidis*) bacteria, nor reduced the viability of parasites, *Cryptosporidium parvum* and *C. hominis* (even at the highest concentration used [2.5μM]) [210]. Furthermore, FhHDM-1 p2 (even at a concentration of 50μM), neither induced cell death in murine macrophages nor caused lysis of human erythrocytes [210].

Similar to *F. hepatica*, genes encoded for cathelicidin-like peptides have also been identified in the genomes of all other human trematodes, including *S. mansoni*, *S. japonicum*, *Clonorchis sinensis*, *Paragonimus westermani,* and *Opisthorchis viverrini* [199]. The ability of the helminth cathelicidin-like peptides to suppress Th1 responses, whilst being non-cytotoxic and non-anti-microbial, suggests the conservation of an immune-modulatory function [210].

1.7.3 FhHDM-1 binds lipopolysaccharide

Host defence peptides, especially those that possess a hydrophobic helical structure, directly bind and neutralise bacterial endotoxin, lipopolysaccharide (LPS) [211, 212], which normally activates Th1 type M1 macrophages [213]. It follows that blocking the interaction between LPS and its cellular receptor would inhibit activation of the downstream Th1 pro-inflammatory response. Having established that FhHDM-1 (and FhHDM-1 p2) similarly adopts an amphipathic helix, Thivierge *et al.* directly compared FhHDM-1 to a panel of well-characterised HDPs (such as LL-37 [human], SMAP-29 [sheep], CRAMP [mice], and BMAP-28 [cattle]), with regards to its ability to directly bind and neutralise LPS [210]. As predicted from structural analyses, FhHDM-1 and FhHDM-1 p2 interacted with LPS [199], with similar efficacy to that of its mammalian counterparts [210]. This was confirmed in another study, where FhHDM-1, and the C-terminus equivalent to FhHDM-1 p2 (termed sFhMF6c), were able to bind to two serotypes of LPS [214]. The truncated versions of the C-terminus, as well as the remainder of the FhHDM-1 molecule that excluded the C-terminus (termed the N-

terminus), did not bind to either of the LPS serotypes, confirming that the whole segment of this particular region of the protein is necessary for its binding capability. Consistent with its ability to bind LPS, mammalian HDPs and FhHDM-1 p2 were able to suppress the levels of TNF secreted by LPS activated macrophages *in vitro* [199, 210]. The LPS-induced production of TNF and IL-1β was also inhibited by FhHDM-1 treatment *in vivo* [199], and this resulted in the protection of mice from LPS-induced sepsis [199]. It has been proposed that the parasites may secrete these peptides to prevent the initiation of pro-inflammatory responses elicited by bacteria, which would likely be released from the gastrointestinal tract as a by-product of the worm's migration [199].

1.7.4 FhHDM-1 modulates the biological activity of macrophages

Considering that the peritoneal cavity is populated primarily by macrophages, and that FhHDM-1 is secreted at this site during a typical infection with *F. hepatica*, it was perhaps not surprising that FhHDM-1 showed a high binding affinity for macrophages *in vivo* (in autoimmune NOD mice and immune competent BALB/C mice) [197]. It was also found that both the full-length FhHDM-1 peptide and the C-terminal portion, FhHDM-1 p2, bound directly to the membrane of both murine and human macrophages *in vitro* [215]. This interaction appeared to occur specifically with cholesterol motifs, via an electrostatic interaction, and was not associated with protein or receptor binding [215]. The amphipathic helix was critical for this interaction, as a similar peptide containing 6 amino acid substitutions, which reduced the hydrophobicity of the amphipathic helix, was unable to bind to the same motif [215]. This membrane association facilitated internalisation of FhHDM-1, and subsequent delivery of the peptide to endolysosomal compartments.

The functionality of the macrophage lysosome is dependent upon pH, with most enzymes within the organelle requiring an acidic pH for optimal catalytic activity [216]. The pH of the lysosome is tightly controlled by the actions of membrane vacuolar ATPases (vATPases), which regulate the flow of hydrogen ions into the vacuole [217]. *In vitro*, FhHDM-1 was shown to inhibit the vATPase activity of lysosomal vesicles [215], which led to the hypothesis that the peptide was modulating the pH, and therefore the activity of lysosomal proteases. Within macrophages, lysosomal proteases are vital for various immunological functions, such as antigen processing and presentation [218]

and induction of apoptosis [219]. Most importantly, functional lysosomal proteases are required for the effective processing of toll-like receptors (TLRs), and their subsequent pro-inflammatory signalling pathways [220]. With the known ability of FhHDM-1 to be internalised and localise to the lysosome [215], there may be intracellular signalling pathways that are targeted indirectly, through the modifications to lysosomal pH.

Consistent with this premise, FhHDM-1 was shown to inhibit the activation of lysosomal Cathepsin B, which is crucial for the activation of the NLRP3 inflammasome, after its release from disrupted phagolysosomes, to ultimately inhibit the production of biologically active IL-1β [221]. Given the growing evidence that the inflammasome plays an important role in the pathogenesis of autoimmune disease [222, 223], this further suggests that lysosomal modifications within macrophages induced by FhHDM-1 are central to its ability to prevent autoimmunity in multiple disease models.

1.8 Research questions and aims

The research to date has strongly indicated that FhHDM-1 is an anti-inflammatory peptide with potential as a therapeutic agent for autoimmune disease. However, further detailed information regarding its cellular binding abilities, mechanisms of action and potential off-target effects is required before FhHDM-1 can be progressed to pre-clinical and clinical trials. Additionally, for manufacturing the peptide for therapeutic applications, it would be advantageous if smaller derivatives of FhHDM-1 were equally efficacious.

Therefore, the aims of this research project were to:

i. Assess the anti-inflammatory activity of FhHDM-1
ii. Identify the minimal bioactive derivative of FhHDM-1
iii. Determine if FhHDM-1 interacted with neutrophils

1.8.1 Assessing the anti-inflammatory activity of FhHDM-1

As discussed previously (Section 1.7.3), FhHDM-1 reduced the levels of the pro-inflammatory cytokines, TNF and IL-1β, produced by macrophages in response to bacterial LPS [197, 199]. The experimental approach was designed to demonstrate that FhHDM-1 bound to LPS, thus preventing its binding to macrophage receptors, notably TLR-4, which is a known LPS receptor [224]. However, the evidence showing that FhHDM-1 is internalised by macrophages, and localises to the lysosome, suggests that the peptide may also impact upon intracellular signalling pathways to modulate the inflammatory response. Therefore, the activation of FhHDM-1 treated macrophages in response to LPS, after internalisation of the peptide, was investigated. Furthermore, to deduce if there were any intracellular pathways specifically targeted by FhHDM-1, the inhibition of macrophage activation in response to a range of TLR ligands was assessed (Chapters 3 & 4).

1.8.2 Determining the minimal bioactive derivative of FhHDM-1

FhHDM-1, being 8kDa in size, is considered a ‘large peptide’, and therefore, is a challenging molecule to chemically synthesise for an up-scaled production, which would be required for its use as a therapeutic peptide. Elucidation of the smallest

peptide derivative that displays comparable efficacy to that of the full length peptide would better facilitate large scale production and further allow for the accurate identification of the biological active regions of the peptide. Therefore, the cellular binding and internalisation, and the biological activity of a number of FhHDM-1 peptide derivatives were assessed (Chapter 5).

1.8.3 Determining the interaction of FhHDM-1 with neutrophils

It has been reported that FhHDM-1 interacts with, and is internalised by, murine and human macrophages [197, 215], as studies to date have only examined the binding of FhHDM-1 to macrophages in isolation. However, given the central role that neutrophils also play in the initiation and perpetuation of autoimmune disease, it was determined if FhHDM-1 interacted with, and exerted biological effects upon, neutrophils (Chapter 6).

Chapter 2: Materials and Methods

2.1 General Materials

2.1.1 General Chemicals and Reagents

Supplier	General chemicals and reagents
Baxter Healthcare (Illinois, USA)	Baxter (Bx) water for irrigation Bx saline for irrigation
Chem-supply (SA, Australia)	Glycine
Greiner Bio-one (Kremsmünster, Austria)	Conical Tubes (15ml and 50ml)
InvivoGen (CA, USA)	Polyinosinic:polycytidylic acid (High molecular weight; Poly (I:C))
Life Technologies (CA, USA)	Pre-heat inactivated Fetal Bovine Serum (HI FBS) Trypan Blue
Scientific Specialities Inc. (CA, USA)	Microtubes (1.5ml)
Sigma-Aldrich (St. Louis, MO, USA)	3,3',5,5' tetramethylbenzidine (TMB) Dimethylsulfoxide (DMSO) EtOH (100%) Lipopolysaccharide from *Escherichia coli* 011:B4 strain (5 x 10^4 EU/ml; LPS) Phosphate Buffered Saline (PBS) and PBS + 1% w/v Bovine Serum Albumin (BSA) sachets Tween 20 β-mercaptoethanol

2.1.2 General Buffers

All buffers were made up using milliQ water (MqH_2O).

1 x PBS: 0.1M PO_4^{3-}, 0.138M NaCl, 2.7mM KCl, pH 7.4

PBS azide (PBS/Az): PBS, 0.05% w/v NaN_3

PBS washing buffer (PBS/T): PBS + 0.05% v/v Tween 20

2.2 Preparation of Parasite Molecules

2.2.1 Fasciola hepatica *Helminth Defense Molecule (FhHDM-1), derivative peptides, cathelicidins and cathelicidin-like peptides*

The full length FhHDM-1 and its derivatives, cathelicidins (LL-37, CRAMP) and cathelicidin-like peptides (*Opisthorchis viverrini* helminth peptide, *Hydrophis cyanocinctus* sea snake peptide) used in all experiments were produced by chemical synthesis, to 95% purity and verified to have no endotoxin contamination. Synthetic peptides were produced by GL Biochem (Shanghai, China) or GenScript (NJ, USA). Lyophilised synthetic peptides were reconstituted in 100% DMSO, under aseptic conditions. For cellular assays, peptides in DMSO were diluted with appropriate cell media and/or saline to working concentrations of <1% DMSO. Other peptides were reconstituted in either Bx water or saline under aseptic conditions.

2.2.2 Amine labelling of FhHDM-1 and FhHDM-1.C2 peptide

FhHDM-1 was labelled with either Alexa Fluor 488 or Alexa Fluor 647 carboxylic acid, succinimidyl ester, according to the manufacturer's instructions. The FhHDM-1.C2 peptide was labelled with Alexa Fluor 488 dye. In brief, the peptides were diluted initially in 0.1M PBS to a concentration of 1mg/ml, and then incubated with 10 molar fold excess of either Alexa Fluor 488 or 647 dye, with rotation on a wheel (protected from light), at room temperature (RT), for 1-2h. After conjugation of the dye to the peptides, excess unconjugated dye was removed via dialysis using the Slide-A-Lyzer cassette with a 2,000 kDa molecular weight cut off (Thermo Fisher Scientific; Boston, MA, USA), in 3 changes of Bx saline. Following dialysis, peptides were assessed by 1D polyacrylamide gel electrophoresis, or via NanoDrop One/One (Thermo Fisher Scientific), to confirm the successful labelling of the peptides, and concentrations were then adjusted to 1mg/ml.

2.3 Cell culture

To prevent any bacterial contamination, all experiments involving tissue culture and procedures with human and murine derived products were performed aseptically within a Biosafety Cabinet Class-II (BSC-II), located within a PC2 certified laboratory, using sterile, disposable plasticware. The BSC-II cabinet was cleaned with 80% (v/v) EtOH and treated with UV light, before and after use.

2.3.1 General tissue culture reagents and materials

Polypropylene tissue culture plates (6, 12, 24 and 96 well) were supplied by BD Biosciences (San Diego, CA, USA). Roswell Park Memorial Institute (RPMI) 1640 media, 10,000U/ml Penicillin/Streptomycin (Pen/Strep) were supplied by Thermo Fisher Scientific. autoMACS® Rinsing Solution (RS), MACs BSA Stock Solution, Midi MACS™ separator and MACS® LS separation columns were supplied by Miltenyi Biotec (Bergisch Gladbach, Germany); 75cm^2 tissue culture flasks (T75) were supplied by Corning (NY, USA). Sterile 1 x PBS was made by dissolving 10 PBS tablets supplied by Astral Scientific (Uppsala, Sweden) into 1L of Bx water.

2.3.2 Animals

Female 6-8 week old BALB/C mice (ARC, Perth, Australia) were used for all murine experiments requiring primary cells. Mice were euthanased by CO_2 asphyxiation under the guidelines of the UTS Animal Care and Ethics Committee (Protocol number: 2015-000359). Bone marrow was collected from the femurs and tibias of mice through aspiration with a 26G needle and syringe using RT RPMI 1640 media. The cells were then aspirated through a 21G needle and syringe to produce a suspension of single cells. Peritoneal lavage was collected by injecting 5ml of ice cold sterile PBS into the peritoneum, which was then massaged, and cells were collected by withdrawing the injected media using a syringe. Spleens were harvested by sterile dissection and placed into ice-cold RPMI 1640 media.

2.3.3 Primary cells

2.3.3.1 Cell culture of murine bone marrow derived macrophages

Primary murine bone marrow derived macrophages (BMDMs) were isolated as previously described [225]. In brief, bone marrow from mice was placed into RPMI 1640 media through aspiration with a needle and syringe. Then, 2 x 10^7 cells were plated in a volume of 10ml in bacterial grade petri dishes (Techno Plas, SA, Australia), and cultured in BMDM media (RPMI 1640 media + 1% Pen/Strep + 10% v/v HI FBS + 715nM β-mercaptoethanol) with the addition of 50ng/ml recombinant murine macrophage colony stimulating factor (rM-CSF, eBioscience, CA, USA) at 37ºC/ 5% CO_2. After 3 days, an additional 10ml of BMDM media was added to the cells, which were cultured for a further 4 days. On day 7, non-adherent cells and supernatants were discarded, and the adherent cells were washed with saline, prior to being gently harvested using a tissue culture scraper. The phenotype and purity of differentiated cells was confirmed by flow cytometry (Section 2.5.3.1).

2.3.3.2 Cell culture of murine peritoneal macrophages

Primary murine peritoneal macrophages were isolated, via negative selection, from the peritoneal lavages of mice using the Macrophage Isolation Kit (Peritoneum) Mouse (Miltenyi Biotec), as per the manufacturer's protocol. In brief, peritoneal lavage was centrifuged (300xg; 10min) after collection and the cell pellet was resuspended in the appropriate volume of autoMACS® RS + 0.05% MACs BSA Stock Solution (MACs buffer) with the addition of the FcR Blocking Reagent and Macrophage (Peritoneum) Biotin-Antibody Cocktail. After incubation (10min; 4ºC), cells were washed with 1-2ml of MACs buffer and centrifuged (300xg; 10min). The cell pellet was then resuspended in MACs buffer with the addition of the Anti-Biotin Microbeads and incubated for 15min at 4ºC. After washing with 1-2ml of MACs buffer and centrifugation (300xg; 10min), the cell pellet was resuspended in MACs buffer for magnetic separation, using a Midi MACS™ separator and MACS® LS separation column. The flow through fraction was collected and centrifuged (300xg; 5min) to obtain a purified pellet of macrophages. The phenotype and purity of isolated murine peritoneal macrophages was confirmed by flow cytometry (Section 2.5.3.1).

2.3.3.3 Cell culture of murine T cells

Primary murine T cells were isolated, via negative selection, from the spleens of mice using the Pan T Cell Isolation Kit II Mouse (Miltenyi Biotec), as per the manufacturer's protocol. In brief, a spleen was separated into single cells by passage through a 70µm sieve with RPMI 1640 media. Cells were centrifuged (300xg; 10min), and the resultant pellet was resuspended in the appropriate volume of MACs buffer with the addition of the Biotin-Antibody Cocktail. After incubation (10min; 4°C), MACs buffer and Anti-Biotin Microbeads were added and cells were further incubated (15min; 4°C). After washing with 1-2ml of MACs buffer and centrifugation (300xg; 10min), the cell pellet was resuspended in MACs buffer for magnetic separation, using a Midi MACS™ separator and MACS® LS separation column. The flow through fraction was collected and centrifuged (300xg; 5min) to obtain a purified pellet of T cells. The phenotype and purity of isolated peritoneal T cells was confirmed by flow cytometry (Section 2.5.3.2).

2.3.3.4 Cell culture of murine neutrophils

Primary murine neutrophils were isolated, via negative selection, from bone marrow of mice using the murine Neutrophil Isolation Kit (Miltenyi Biotec), as per the manufacturer's protocol. In brief, bone marrow from mice was collected into RPMI 1640 media through aspiration with a needle and syringe. After centrifugation (300xg; 10min), the cell pellet was resuspended in the appropriate volume of MACs buffer with the addition of the Neutrophil Biotin-Antibody cocktail. After incubation (10min; 4°C), cells were washed with 10ml of MACs buffer and centrifuged (300xg; 10min). The cell pellet was then resuspended in MACs buffer for magnetic separation, using a Midi MACS™ separator and MACS® LS separation column. The flow through fraction was collected and centrifuged (300xg; 5min) to obtain a purified pellet of neutrophils. The phenotype and purity of isolated murine neutrophils was confirmed by flow cytometry (Section 2.5.3.3).

2.3.3.5 Cell culture of primary murine bone marrow derived dendritic cells

Primary murine bone marrow derived DCs were isolated as previously described [226]. In brief, bone marrow from mice was collected into RPMI 1640 media through aspiration with a needle and syringe. Then, 2 x 10^7 cells were plated in a volume of 10ml in bacterial grade petri dishes, and cultured in BMDM media with the addition of murine recombinant granulocyte macrophage colony stimulating factor (rGM-CSF,

Miltenyi Biotec) at 37ºC/ 5% CO_2. After 3 days, the culture media was replaced with a fresh 10ml of BMDM media per dish without the addition of rGM-CSF, and cells were cultured for a further 4 days. On day 7, non-adherent cells and supernatants were discarded, and the adherent cells were washed with saline, prior to being gently harvested using a tissue culture scraper. The phenotype and purity of differentiated cells was confirmed by flow cytometry (Section 2.5.3.4).

2.3.3.6 Cell culture of human peripheral blood leukocytes

Human peripheral blood leukocytes were collected from human buffy coats (Australian Red Cross). In brief, human buffy coats were diluted 1 in 3 with RPMI 1640 media and centrifuged (400xg; 5min). The clear top layer (serum) was carefully transferred with sterile pasteur pipettes into a new 15ml tube and centrifuged (400xg; 5min), with no brake. The top layer of plasma was carefully discarded using a sterile pasteur pipette, and the white cell layer (leukocyte population) above the red cell layer (erythrocytes) was carefully placed into a new 15ml tube. The collected white cell layer was incubated with red cell lysis buffer (Sigma-Aldrich) up to 15ml, for 3min at RT, and then centrifuged (400xg; 5min). This step was repeated until most of the contaminating erythrocytes were removed from the cell pellet. The leukocyte population was then resuspended in PBS to appropriate concentrations for staining as described in Section 2.5.4.3.

2.3.4 Cell-lines

2.3.4.1 RAW 264.7 murine macrophages

RAW 264.7 macrophages were purchased from the American Type Culture Collection (ATCC) and kept frozen in DMSO in liquid nitrogen (5 x 10^6 cells /ml). One week prior to experimental use, a single vial of stock was thawed, and cells were seeded into a T75 flask in R10 media (RPMI 1640 media + 10% v/v HI FBS), and maintained at 37ºC/ 5% CO_2. Cells were grown to 80% confluency. At this point (which occurred approximately every third day of culturing), adherent cells were washed twice with sterile Bx saline, and then harvested by incubation with TrypLE (5ml, 20min at 37ºC/ 5% CO_2; Thermo Fisher Scientific). An equivalent volume of R10 was added to stop the trypsin activity of the TrypLE, and then cells were collected using a cell scraper. Cells were centrifuged (300xg; 5min), and the resultant cell pellet was resuspended in R10 media. The cells were split 1 in 10 with R10 media and maintained with a total

volume of 20ml of R10 media per T75 flask. Cells were grown for at least 2-3 passages prior to experimental use, and only used between passages 3 and 18.

2.3.4.2 Baby Hamster Kidney cells with high or low Epidermal Growth Factor Receptor expression

Two clones of Baby Hamster Kidney (BHK) cells transfected to express differential levels of Epidermal Growth Factor Receptor (EGFR) were kindly donated by Prof. Valerius (Christian-Albrechts-University and University Hospital Schleswig-Holstein, Germany) and were kept frozen in DMSO in liquid nitrogen (5 x 10^6 cells/ml). One week prior to experimental use, a single vial of stock was thawed and seeded into a T75 flask in R10 and 5% Pen/Strep media (37ºC/ 5% CO_2). For BHK cells with high EGFR expression, the media was supplemented with 1mg/ml Geneticin (Life Technologies) to maintain the selective pressure required for EGFR expression. When 80% confluent, cells were harvested using TrypLE (5ml; Thermo Fisher Scientific) for 1min (37ºC/ 5% CO_2). Cells were then collected by centrifugation (300xg; 5min) and the resultant pellet was resuspended in R10 media alone (low EGFR expression) or R10 media with Geneticin (high EGFR expression). Cells were split twice a week, at a ratio between 1 in 5 and 1 in 10 with appropriate media, according to the cell confluency as observed by microscopy. The expression of EGFR on both cell lines was confirmed by flow cytometry (Section 2.5.3.5).

2.4 Functional assays

2.4.1 Cytokine assays

2.4.1.1 Treatment of murine primary bone-marrow derived macrophages, RAW 264.7 macrophages and murine neutrophils

FhHDM-1, and its derivative peptides, were resuspended initially in a small volume of saline, and then further resuspended in BMDM or R10 media (to various concentrations as required) for addition to BMDMs or RAW 264.7 macrophages, respectively (1 x 10^6 cells/ml in 96 well TC plates), and incubated for 1h (37ºC/ 5% CO_2). For experiments using murine neutrophils, FhHDM-1 was resuspended initially in a small volume of saline, and then further resuspended in BMDM media (to various concentrations as required), for addition to neutrophils (4 x 10^6 cells/ml in 96 well TC plates), and incubated for 30min (37ºC/ 5% CO_2). Negative control samples were treated with saline and the appropriate media.

2.4.1.2 Intraperitoneal injection of FhHDM-1

BALB/c mice received 100µl of FhHDM-1 in saline (0.1mg/ml), via intraperitoneal (i.p.) injection every second day, for a total of 6 injections. Twenty four hours after the last injection, mice were euthanased (as described in Section 2.3.2) and peritoneal macrophages were collected by lavage (Section 2.3.3.2). Peritoneal macrophages were plated on 96 well TC plates, at cell densities normalised to the sample that contained the lowest number of cells.

2.4.1.3 Stimulation of murine primary bone-marrow derived macrophages, RAW 264.7 macrophages, murine peritoneal macrophages, and murine neutrophils

Untreated or peptide treated BMDMs and RAW 264.7 macrophages were stimulated with LPS (10ng/ml) O/N (37ºC/ 5% CO_2), after which time supernatants were collected for the assay of TNF, and other cytokines and chemokines (as detected on the multiplex). For the detection of IFN-β, supernatants from LPS stimulated BMDMs were collected at 3h (37ºC/ 5% CO_2). Supernatants from untreated or peptide treated BMDMs and peritoneal macrophages stimulated with Poly (I:C) (20µg/ml) were collected after an O/N incubation (37ºC/ 5% CO_2). Supernatants from murine neutrophils, untreated or

treated with FhHDM-1, were collected after a 4h stimulation with LPS (100ng/ml; 37ºC/ 5% CO_2).

For experiments to determine the effect of FhHDM-1, and peptide derivatives, on 'washed' cells; peptides were incubated with cells, which were then washed with saline twice, prior to stimulation with the appropriate ligands.

2.4.1.4 Cytokine assay of stimulated murine primary bone-marrow derived macrophages, RAW 264.7 macrophages, murine peritoneal macrophages, and murine neutrophils

Supernatants from stimulated murine macrophages and neutrophils were assayed for TNF (BD Biosciences) or IFN-β (PBL Assay Science, NJ, USA) secretion using ELISA kits, as per the manufacturer's instructions. In brief, 96 well Nunc Maxisorp™ plates (Thermo Fisher Scientific) were coated with the kit capture antibody (unless plates were supplied pre-coated), provided by the manufacturer. Supernatants, diluted with blocking buffer (PBS + 10% v/v HI FBS) at 1:5 (for TNF assays) or at neat (for IFN-β assays), were incubated for 2h or 1h (for TNF and IFN-β determination, respectively) at RT. A standard curve was generated using the standard samples provided in the kits. After washing three times with PBS + 0.05% v/v Tween 20 (PBS/T), the wells were incubated with the detection antibody (1h, RT). After three washes with PBS/T, streptavidin-horse radish peroxidase antibody was added and the 96-well plate was incubated for 1h at RT. The TMB substrate was added to wells and colour development was stopped by the addition of 85% phosphoric acid (Sigma-Aldrich). The optical density (OD) was read at 425nm using the Infinite 200 Pro Tecan spectrophotometer (Tecan, Switzerland). Data was plotted as pg/ml or as percentages, where the amounts of cytokine produced by LPS or Poly (I:C)-only stimulated cells were adjusted to 100%. Dose curves were then produced by conducting non-linear regression analysis on GraphPad Prism software (GraphPad, CA, USA), and EC50s were calculated.

2.4.1.5 Multiplex assay of cytokines and chemokines from stimulated RAW 264.7 macrophages and murine neutrophils

For the assessment of the effect of FhHDM-1 and FhHDM-1.C2 on stimulated RAW 264.7 macrophages and murine neutrophils, cytokine and chemokine production (Table 2.1) was assessed using a Bio-Plex Pro Mouse Cytokine 23-Plex Immunoassay kit (Bio-

Rad Laboratories, CA, USA), according to the manufacturer's instructions. In brief, standards and beads were re-constituted in the supplied sample diluent. Cell supernatants were centrifuged (1,000xg; 15min; 4°C), to remove any cellular debris, diluted 1:4 with the provided blocking buffer, and added to the Bio-Plex plate. The plate was sealed, briefly shaken on an orbital plate shaker (130xg; 30sec), and incubated for 30min. The plate was then washed three times, with shaking (130xg; 30sec), prior to addition of detection antibodies, after which the plate was sealed and shaken (130xg; 30sec), and then incubated for 30min. The plate was again washed, prior to incubation with streptavidin conjugated to PE, with the plate sealed, and shaken (130xg; 30sec) for a 10min incubation, whilst protected from light. After the final wash, the samples were resuspended with the provided buffer and the plate was sealed and shaken at 130xg for 30sec, prior to taking readings on the Bio-Rad Bio-Plex 200 array reader for the detection of PE fluorescence. Data was converted to percentages, where the amount of cytokine produced by LPS-only stimulated cells was adjusted to 100%.

Table 2.1 Cytokines and chemokines detected by multiplex

Th1/Th17 cytokines	Th2/Treg cytokines	Chemokines
IL-1α	IL-4	Eotaxin
IL-1β	IL-5	KC
IL-2	IL-13	MCP-1
IL-3		MIP-1α
IL-6		MIP-1β
IL-9		RANTES
IL-12(p40)		
IL-12(p70)		
IL-17A		
G-CSF		
GM-CSF		
IFN-γ		
TNF		

2.4.1.6 Effect of FhHDM-1 and FhHDM-1.C2 on Th1 cytokine production by macrophages

BMDMs (5 x 10^5 cells/ml) in 96 well TC plates were treated with FhHDM-1 or FhHDM-1.C2 (15µM) for 1h (37ºC/ 5% CO_2). Cells were then washed with saline twice, prior to co-culture with T cells (1:1), and purified NA/LE Hamster anti-mouse CD3 antibody (Cat. no: 553057; BD Biosciences) at a concentration of 0.05µg/ml or 1µg/ml for 48h (37ºC/ 5% CO_2). For experiments assessing cell-cell contact between macrophages and T cells, the supernatant from BMDMs untreated or treated with peptides were collected, filtered through a 0.45µm sterile filter, and added to fresh BMDMs with T cells and anti-CD3 antibody. The supernatants were collected and IFN-γ was quantified using a mouse IFN-γ ELISA kit (BD Biosciences), as described in Section 2.4.1.4.

2.4.2 Cytotoxicity assays

2.4.2.1 Assessment of FhHDM-1 and peptide derivative cytotoxicity on RAW 264.7 macrophages

The release of lactate dehydrogenase (LDH) into the supernatant by cells treated with peptides was detected by a LDH non-cytotoxic assay (Promega, Wisconsin, USA). In brief, RAW 264.7 macrophages (1 x 10^6 cells/ml) were seeded onto a 96 well TC plate in R10 media and allowed to adhere O/N (37°C/ 5% CO_2). Media was replaced prior to incubation with FhHDM-1 and FhHDM.C2 (at various concentrations), diluted in an initial small volume of saline, and then resuspended in R10. The untreated cells received media alone, saline or DMSO, and all cells were incubated for 1h (37°C/5% CO_2). As a positive control for 100% cellular death, RAW 264.7 macrophages were lysed with a detergent provided in the LDH assay kit (37°C/5% CO_2). After incubation, 50µL of the cell supernatants were incubated with 50µL of substrate reagent for 10-30min at RT, protected from light. Then, 50µL of the provided stop solution was added to prevent any further colour development. Absorbance of samples were read within 1h at 490nm using the Infinite 200 Pro Tecan spectrophotometer. The percentage of cell death induced by peptides was calculated as compared to the cells treated with lysis buffer, which was adjusted 100% cell death.

2.4.3 Phagocytosis assays

2.4.3.1 Assessing the effect of FhHDM-1 on the ability of murine neutrophils to phagocytose E. coli *particles*

Murine neutrophils were assessed for the phagocytosis of *E. coli* particles (enzyme-labelled, fixation inactivated *E. coli*) in the presence of FhHDM-1 using the CytoSelect 96 well phagocytosis assay (*E.coli* substrate; Cell Biolabs, Inc., CA, USA), according to the manufacturer's instructions. In brief, murine neutrophils (1 x 10^6 cells/ml) in 96 well TC plates were incubated with FhHDM-1 (at various concentrations) or Cytochalasin D (2µM; Sigma-Aldrich) for 30min (37°C/ 5% CO_2), or pre-stimulated with LPS (100ng/ml) for 30min (37°C/ 5% CO_2), prior to peptide incubation. Then, the *E. coli* suspension was added to the cells and incubated for 3h (37°C/ 5% CO_2). The culture supernatant was then removed by centrifugation (300xg; 5min) and the cells were washed with ice cold 1 x PBS. The cells were then fixed with the provided fixing solution, washed twice, then blocked with the provided blocking solution for 30min at RT. After further washing, the cells were permeabilised by the provided permeabilisation solution and washed. The provided substrate solution was then added, and the cells were incubated for 10min at RT. Colour development was stopped by addition of a stopping solution, and the absorbance values were read at 450nm using the Infinite 200 Pro Tecan spectrophotometer. The percentage of *E. coli* uptake was calculated as compared to the cells incubated only with *E. coli* particles, which was adjusted to 100% phagocytosis.

2.5 Flow cytometry

All incubations of cells with fluorescently-labelled peptides or fluorescent antibodies were conducted on ice (4ºC) and protected from light, inside 1.5ml microtubes, unless stated otherwise.

2.5.1 General flow cytometry reagents and materials

Dead cell stains, Sytox Blue and TOPRO-3, were supplied by Thermo Fisher Scientific; Falcon 5ml polystyrene round-bottom tubes (FACs tubes) were supplied by Corning; and synthetic 70µm mesh was supplied by Sefar Pty Ltd (NSW, Australia). The general washing and running buffer (FSW) used for flow cytometry experiments was 1 x PBS + 1% w/v BSA + 2% v/v HI FBS + 0.1% sodium azide (FACs Stain Wash, FSW).

Table 2.2 Antibodies used in flow cytometry experiments

Antibody	Clone	Isotype	Supplier
Purified Rat Anti-MouseCD16/CD32 (Mouse BD Fc block)	2.4G2	-	BD Biosciences
Anti-human CD3 FITC	SK7 (or Leu-4)	Mouse IgG1, κ	BD Biosciences
Anti-human CD14 Pacific Blue	TüK4	Mouse IgG2a	Invitrogen
Anti-human CD16 FITC	3G8	Mouse IgG1, κ	BD Biosciences
Anti-human CD19 Pacific Blue	SJ25-C1	Mouse IgG1, κ	Invitrogen
Anti-human CD56 PE-Cy7	B159	Mouse IgG1, κ	BD Biosciences
Anti-human CD123 PE	9F5	Mouse IgG1, κ	BD Biosciences
Anti-human HLA-DR V450	L243	Mouse IgG2a, κ	BD Biosciences
Lineage Cocktail 1 (lin 1) (CD3, CD14, CD16, CD19, CD20, CD56) FITC	SJ25C1 (or SJ25-C1) NCAM16.2 (or NCAM 16) L27 SK7 (or Leu-4) MφP9 (or MφP-9) L27 3G8	Mouse IgG1, κ Mouse IgG2b, κ Mouse IgG1, κ Mouse IgG1, κ Mouse IgG2b, κ Mouse IgG1, κ Mouse IgG1, κ	BD Biosciences
IgG from human serum	-	-	Sigma-Aldrich
Anti-mouse CD3 PE	17A2	Rat IgG2b, κ	BD Biosciences
Anti-mouse CD11b APC	M1/70	Rat IgG2b, κ	BD Biosciences
Anti-mouse CD11b PE	M1/70	Rat IgG2b, κ	BD Biosciences
Anti-mouse CD11c APC-Cy7	HL3	Hamster IgG1, λ2	BD Biosciences
Anti-mouse CD62L PE-Cy7	MEL-14	Rat IgG2a, κ	BD Biosciences
Anti-mouse CD80 PE	16-10A1	Hamster IgG2, κ	BD Biosciences
Anti-mouse CD86 FITC	GL1	Rat IgG2a, κ	BD Biosciences
Anti-mouse EGFR Alexa Fluor 488	EP38Y	IgG	Abcam
Anti-mouse F4/80 PE	BM8	Rat IgG2a, κ	eBioscience

Cont'

Anti-mouse Ly6G FITC	1A8	Rat IgG2a, κ	BD Biosciences
Anti-mouse I-A/I-E (MHC II) Alexa Fluor 488	M5/114.15.2	Rat IgG2b, κ	BD Biosciences
Hamster IgG2, κ PE	B81-3	Hamster IgG2, κ	BD Biosciences
Rat IgG APC	A95-1	Rat IgG2b, κ	BD Biosciences
Rat IgG FITC	R35-95	Rat IgG2a, κ	BD Biosciences
Rat IgG PE-Cy7	R35-95	Rat IgG2a, κ	BD Biosciences

CD: cluster of differentiation; FITC: Fluorescein isothiocyanate; PE-Cy7: R-phycoerythrin Cyanine 7; PE: R-phycoerythrin; Lin-1: anti-human Lineage cocktail; APC: Allophycocyanin; APC-Cy7: Allophycocyanin Cyanine 7; HLA-DR: Human Leukocyte Antigen- antigen D Related; MHC II: Major Histocompatibility Complex Class II

2.5.2 Standard flow cytometry staining protocol

Isolated cells were placed into 1.5ml microtubes and initially incubated with mouse BD Fc block (BD Biosciences) for 5min at RT to prevent any non-specific binding of antibodies. The cells were then incubated with the appropriate antibody at 4ºC for 30min, protected from light. The cells were washed with 700µl of ice cold FSW to remove unbound antibodies and centrifuged via a pulse spin (<10,000xg; 6sec, repeated twice). The supernatant was removed and the wash with pulse spin was repeated. Cells were then resuspended in 500µl FSW and strained through synthetic mesh (for the dispersion of cells into a single cell suspension) into FACs tubes immediately prior to acquiring on either the BD LSR-II flow cytometer or BD LSR-Fortessa^{TM} X-20 flow cytometer. Sytox blue or TOPRO-3 dyes (0.5µl of 1 in 10 diluted dyes) were added per 500µl sample, just prior to acquisition, for the detection of any dead cells.

2.5.3 Assessment of purity of cell populations via flow cytometry

2.5.3.1 Assessing purity of primary murine macrophages

To confirm the derivation of primary murine BMDMs and the isolation of peritoneal macrophages, the cells were stained for CD11b and F4/80, respectively. As per the general protocol from Section 2.5.2, collected cells from Section 2.3.3 (BMDMs) and 2.3.4 (peritoneal macrophages) were blocked and stained with either anti-mouse CD11b PE and anti-mouse F4/80 PE antibodies (Table 2.2). Macrophages were washed to remove unbound antibodies, and data were acquired on the flow cytometer. Cell populations, >90% positive for CD11b and >95% positive for F4/80 were recorded (Fig. 2.1 and 2.2, respectively), verifying that near pure populations of murine BMDMs and peritoneal macrophages were obtained.

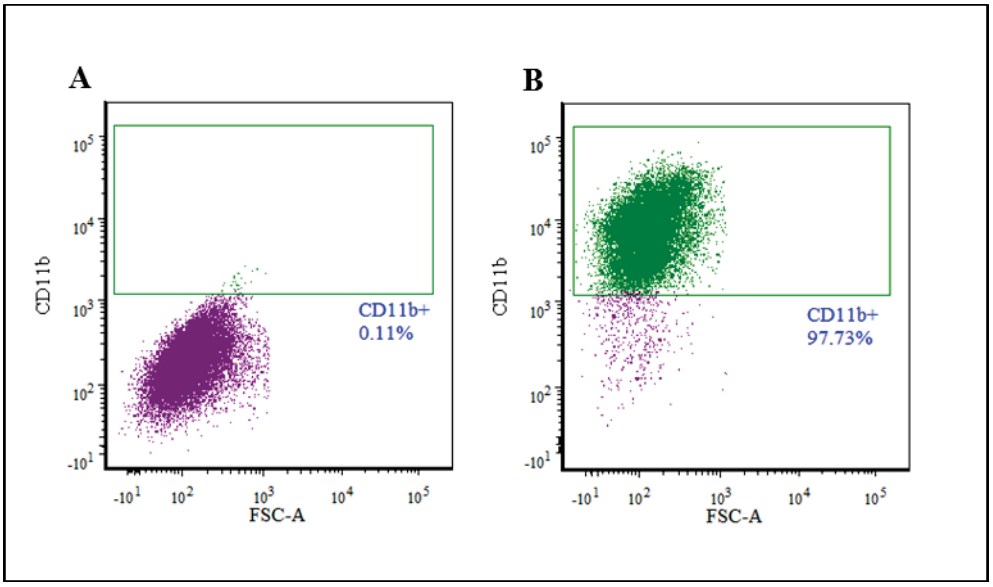

Figure 2.1 Assessment of the purity of primary murine bone marrow derived macrophages isolated by differentiation with M-CSF. Macrophages were derived from bone marrow using M-CSF. Cells were stained with an antibody against CD11b to determine the purity of macrophage populations. Plots show **(A)** unstained and **(B)** stained macrophage samples. The purity obtained was always in excess of 90%.

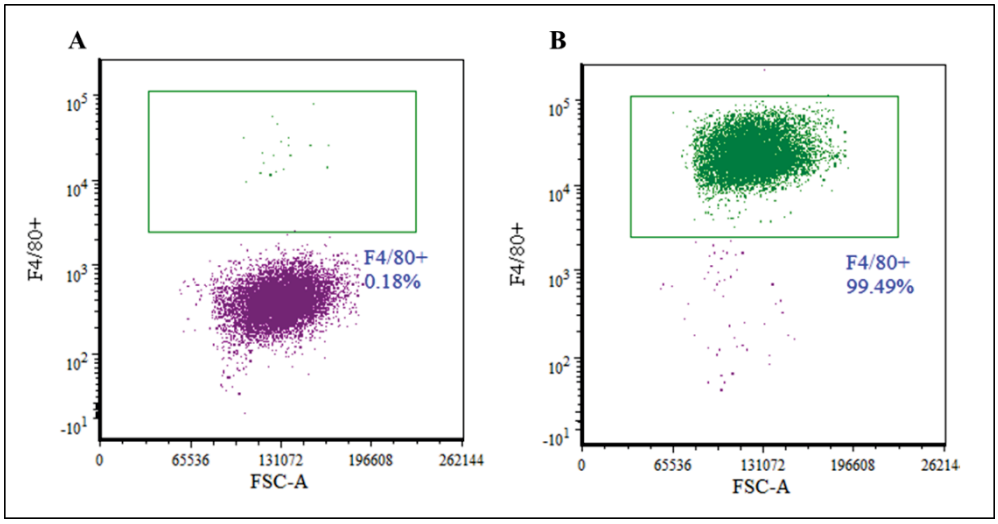

Figure 2.2 Assessment of the purity of primary murine peritoneal macrophages isolated by negative microbead selection. Macrophages were isolated from peritoneal lavages by negative microbead selection. Cells were stained with an antibody against F4/80 for assessment of macrophage purity. Plots show **(A)** unstained and **(B)** stained macrophage samples. The purity obtained was always in excess of 95%.

2.5.3.2 Assessing purity of primary murine T cells

To confirm the isolation of primary murine T cells, the cells were stained for CD3. As per the general protocol from Section 2.5.2, collected cells from Section 2.3.5 were blocked and stained with anti-mouse CD3 PE antibody (Table 2.2). Unbound antibodies were removed by washing and data were acquired on the flow cytometer. A cell population >95% positive for CD3 was recorded (Fig. 2.3), verifying that a near pure population of murine T cells was obtained.

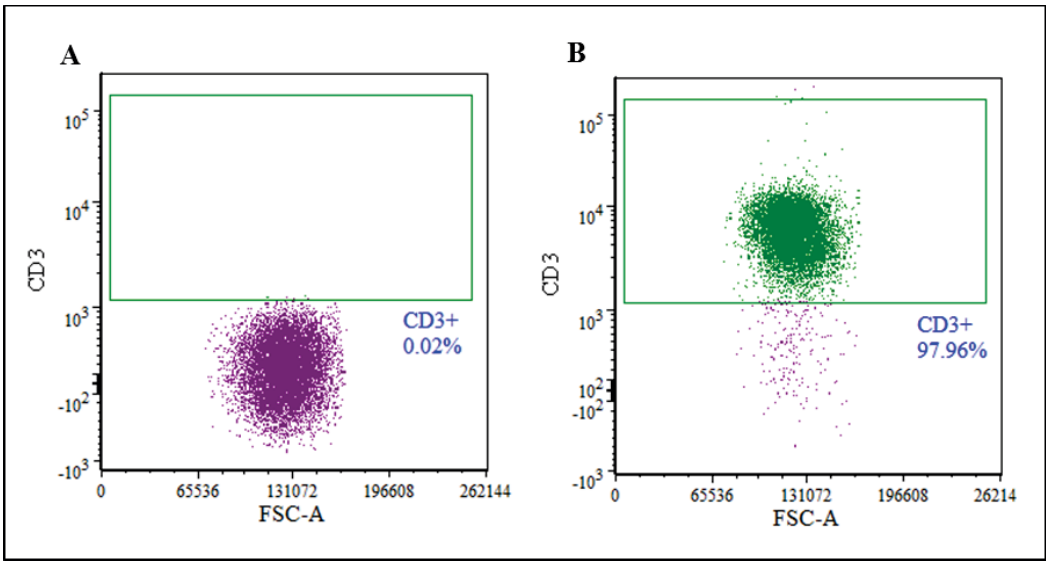

Figure 2.3 Assessment of the purity of primary murine T cells obtained by CD3 microbead isolation. T cells were isolated from spleen by CD3 microbead isolation. Cells were stained with an antibody against CD3 for assessment of T cell purity. These plots show **(A)** unstained and **(B)** stained T cells samples. The purity obtained was always in excess of 95%.

2.5.3.3 Assessing purity of primary murine neutrophils

To confirm the isolation of murine neutrophils, the cells were stained for CD11b and CD62L surface markers. As per the general protocol from Section 2.5.2, collected cells from Section 2.3.6 were blocked and stained with anti-mouse CD11b APC and anti-mouse Ly6G FITC antibodies (Table 2.2). Unbound antibodies were removed by washing and data were acquired on the flow cytometer. A cell population >90% positive for CD11b and Ly6G was recorded (Fig. 2.4) showing that a pure population of murine neutrophils was obtained.

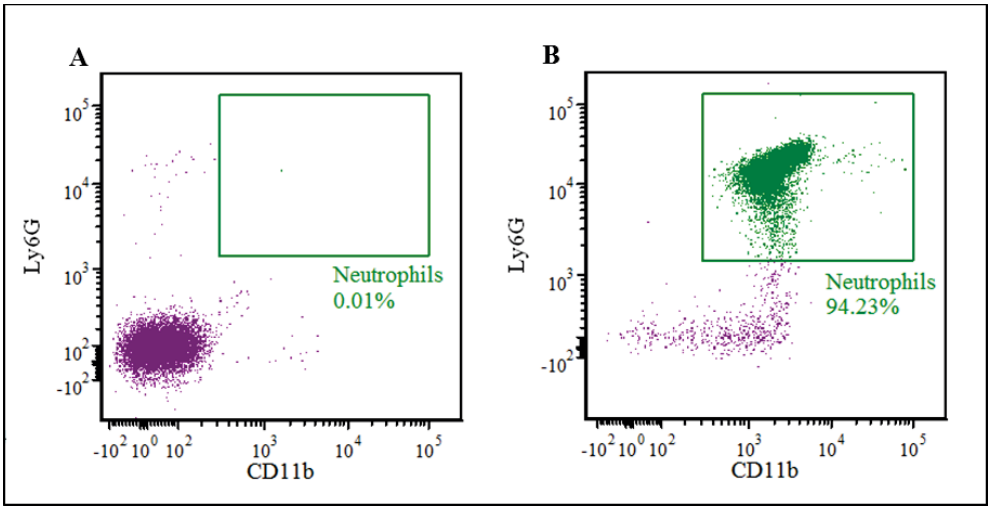

Figure 2.4 Assessment of the purity of primary murine neutrophils isolated by negative microbead selection. Neutrophils were isolated from bone marrow using negative microbead selection. Cells were stained with antibodies against CD11b and Ly6G for assessment of neutrophil purity. Plots show **(A)** unstained and **(B)** stained neutrophil samples. The purity obtained was always in excess of 90%.

2.5.3.4 Assessing purity of primary murine dendritic cells

To confirm the isolation of murine DCs, the cells were stained for CD11c. As per the general protocol from Section 2.5.2, collected cells (Section 2.3.3.5) were blocked and stained with anti-mouse CD11c APC-Cy™7 and Anti-mouse Ly6G FITC antibodies (Table 2.2). An antibody against the Ly6G surface marker (specific for neutrophils) was included to ensure that there were no neutrophils obtained from the differentiation process. Unbound antibodies were removed by washing, and data were acquired on the flow cytometer. Approximately 88% of cells were $CD11c^{+}/Ly6G^{-}$ (Fig. 2.5), verifying that a near pure population of murine DCs was obtained.

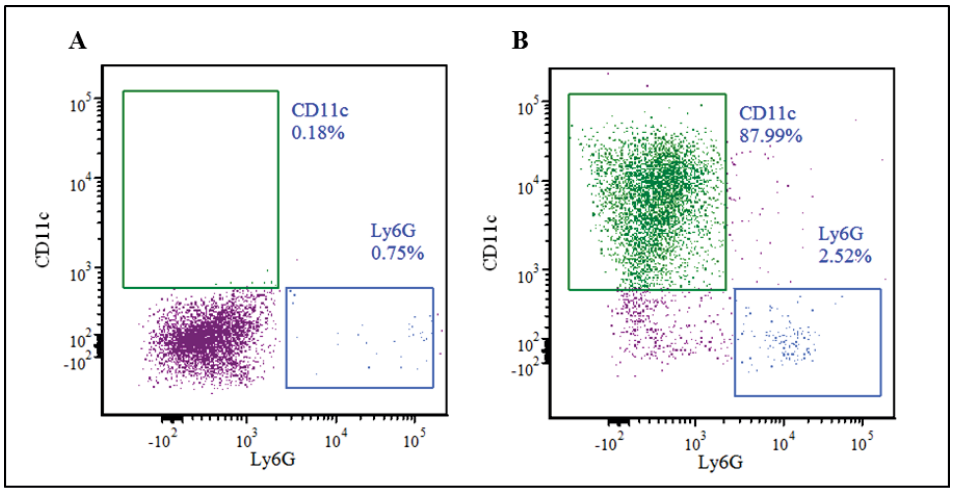

Figure 2.5 Assessment of the purity of primary murine dendritic cells isolated by differentiation with GM-CSF. Dendritic cells (DCs) were derived from bone marrow using GM-CSF. Cells were stained with antibodies against CD11c and Ly6G for assessment of DC purity. These plots show **(A)** unstained and **(B)** stained neutrophil samples. The purity obtained was always approximately 90%.

2.5.3.5 Assessing the surface expression of EGFR on BHK cells

To confirm the high or low expression of EGFR on BHK cells, collected cells (Section 2.3.8) were resuspended in PBS (1 x 10^6 cells/ml), and the FVS780 viability dye (BD Biosciences) was added (1µL per 1 x 10^6 cells of cells). Cells were vortexed immediately, and then incubated for 45min at RT protected from light. Cells were washed with FSW with pulse centrifugation (<10,000x; 6 sec, repeated twice; PC1). After aliquoting 2 x 10^6 cells per 1.5ml microtube, the cells were resuspended in 1ml of ice cold MeOH (80% v/v; Sigma-Aldrich) for 5min at -20°C. Cells were again collected by centrifugation (<10,000xg; 6 sec, repeated twice, then 500xg for 5min; PC2), and washed with 500µl of PBS with centrifugation (PC2) twice. Cell pellets were then resuspended in 1ml of PBS + 0.1%v/v Tween 20, and incubated for 20min at RT to enable cell permeabilisation. After centrifugation (PC2) and two washes with FSW and centrifugation (PC2), cells were resuspended in 50µL of staining buffer (PBS + 10%v/v normal goat serum + 0.3M glycine; SB) for 15min at RT. Cells were then incubated with either 50µl of anti-mouse EGFR Alexa Fluor 488 antibody (Abcam, Cambridge, UK) diluted 1:25 in SB, or anti-mouse MHCII Alexa Fluor 488 antibody (Table 2.2) diluted 1:25 in SB as an isotype control, and incubated, protected from light, for 30min at RT. Cells were then washed with 500µl of FSW, centrifuged (PC2) twice and resuspended in 350µL FSW and strained through mesh into FACs tubes immediately prior to data acquisition on the flow cytometer (Fig. 2.6).

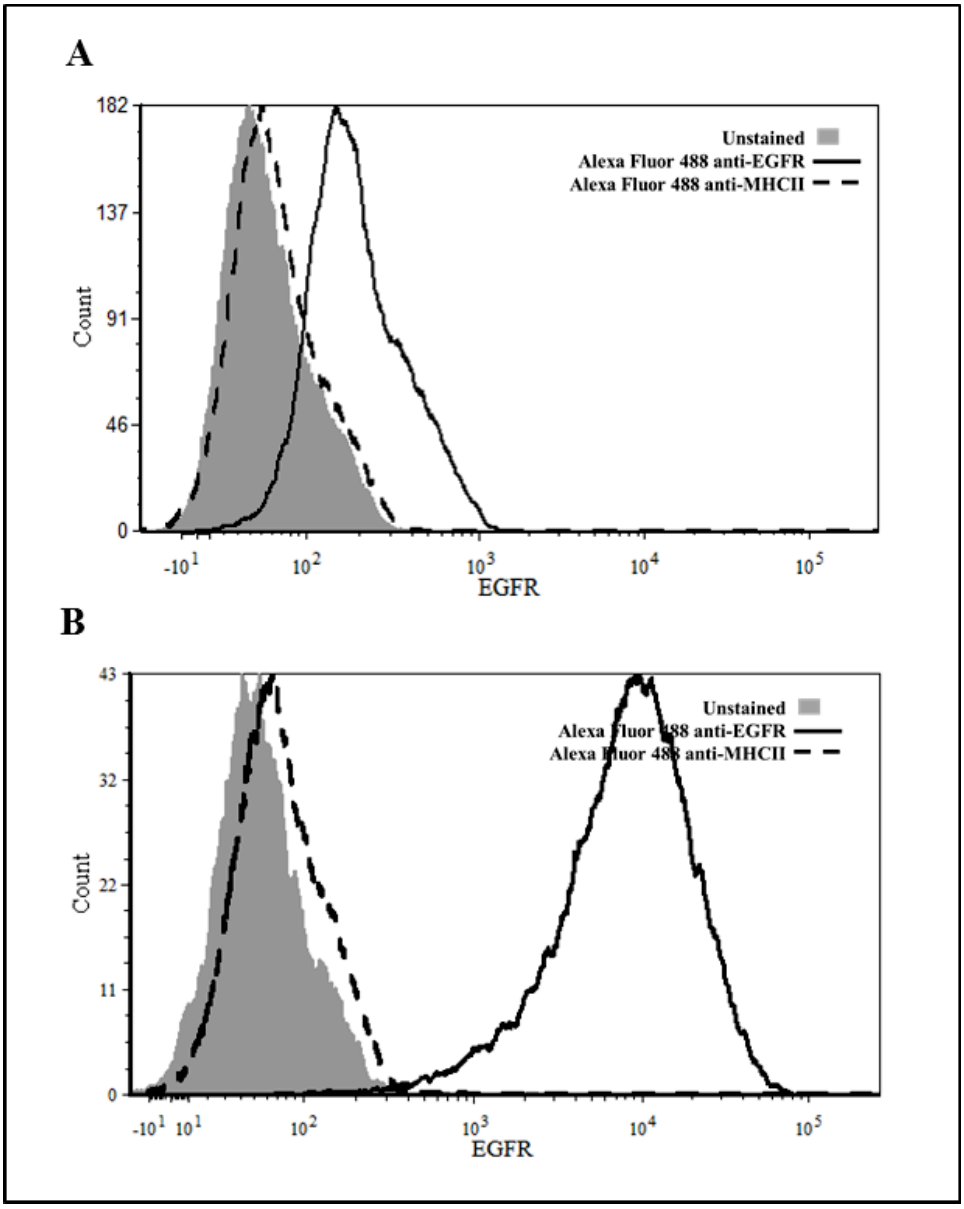

Figure 2.6 Assessment of the expression of EGFR on BHK cells expressing low or high EGFR levels. Baby Hamster Kidney (BHK) cells expressing low or high EGFR levels were stained for EGFR. Alexa Fluor 488 anti-EGFR (black line) and Alexa Fluor 488 anti-MHC II (isotype control, black dotted line) antibodies were used to determine EGFR expression on **(A)** EGFR low and **(B)** EGFR high expressing BHK cells. The grey histogram represents the unstained control.

2.5.4 Assessment of FhHDM-1 and peptide derivative binding with animal and human cell populations

2.5.4.1 Assessing the interaction of Alexa Fluor 488 labelled FhHDM-1 and FhHDM-1.C2 peptides with BMDMs, RAW 264.7 macrophages, BHK cells and murine neutrophils

BMDMs, RAW 264.7 macrophages, or BHK cells (1 x 10^6 cells/ml) in 1.5ml microtubes were incubated with 100µl of Alexa Fluor 488 labelled FhHDM-1 or FhHDM-1.C2 peptides in PBS (2.5µM) at 4ºC for 30min, protected from light. Murine neutrophils (1 x 10^6 cells/ml) in 1.5ml microtubes were incubated with Alexa Fluor 488 labelled FhHDM-1 (5µM) for 30min at 4ºC, protected from light. Cells were washed and data were acquired on the flow cytometer as per the general protocol (Section 2.5.2).

2.5.4.2 Assessing the interaction of biotin-labelled FhHDM-1.C1 and FhHDM-1.C2 peptides with RAW 264.7 macrophages

RAW 264.7 macrophages (1 x 10^6 cells/ml) plated in a 6 well TC plate were incubated with 1ml of biotin-labelled FhHDM-1.C1 or FhHDM-1.C2 peptides in saline (5µM) at 4ºC for 30min, protected from light. Cells were washed twice with saline and collected into 1.5ml microtubes. The cells were pelleted by centrifugation (300xg; 5min) and resuspended in 100µl of PBS with 1 in 200 diluted Alexa Fluor 488 labelled streptavidin (Life Technologies). The cells were incubated at 4ºC for 30min, protected from light, prior to washing and acquisition on the flow cytometer, as per the general protocol (Section 2.5.2).

2.5.4.3 Assessing the interaction of Alexa Fluor 647 labelled FhHDM-1 with human peripheral blood leukocytes

To assess the interaction of FhHDM-1 with human cells, Alexa Fluor 647 labelled FhHDM-1 was incubated with human peripheral blood leukocytes (Section 2.3.9). In brief, 4 x 10^6 cells in 1.5ml microtubes were incubated with either 20µg/ml of Alexa Fluor 647 labelled FhHDM-1 for 1h at 4ºC. Then, 50 µg/ml of IgG from human serum (20µl; Sigma-Aldrich) was added on top of each sample, and cells were incubated for 10min at 4ºC. Cells were then split into appropriate 1.5ml microtubes to be incubated with 80µl of master mixes containing the specific fluorochrome-conjugated antibodies for 30min at 4ºC. Four master mixes of antibodies were created to identify four different panels of cell populations, according to Table 2.3, adjusted to a total volume of 400µl

with FSW. Cells were then washed twice with FSW, and resuspended for data acquisition via flow cytometry, as per the general protocol (Section 2.5.2). The cell gating strategy for the identification of B cells, T cells, natural killer (NK) cells, monocytes, neutrophils, eosinophils, DCs, and basophils from human peripheral blood leukocytes is described in Section 2.5.4.4.

Table 2.3 Antibody master mixes for identification of individual human peripheral blood leukocyte populations

Panel	Cell population	Surface marker	Antibody colour	Volume of antibody (µl)	Volume of FSW (µl)	Total volume (all antibodies + FSW; µl)
1	B cells	CD19+	Pacific Blue	60	160	400
	T cells	CD3+	FITC	120		
	NK cells	CD56+	PE-Cy7	60		
2	Monocytes	CD14+	Pacific blue	30	370	400
3	Neutrophils	CD16+	FITC	120	280	400
	Eosinophils	CD16 –				
4	Other cell populations	Lin-1+	FITC	120	130	400
	DCs	HLA-DR+	V450	30		
	Basophils	CD123+	PE	120		

FSW: FACs Stain Wash; NK cells: Natural Killer cells; CD: cluster of differentiation; FITC: Fluorescein isothiocyanate; PE-Cy7: R-phycoerythrin Cyanine 7; Lin-1: anti-human Lineage cocktail; DCs: Dendritic cells; HLA-DR: Human Leukocyte Antigen- antigen D Related; PE: R-phycoerythrin; +/- denotes presence and absence of surface markers respectively.

2.5.4.4 Gating strategy for the identification of human peripheral blood leukocytes

The gating strategy for the identification of individual cell types within human peripheral blood leukocyte populations initially involved gating based on size (forward scatter) and granularity (side scatter), as detailed in Figure 2.7.

Subsequent identification (Fig. 2.8-2.11), utilised antibodies that bound to specific surface markers: anti-CD19 for B cells, anti-CD3 for T cells, anti-CD56 for NK cells, anti-CD14 for monocytes, and anti-CD16 for neutrophils [227, 228]. Eosinophils were distinguished by their lack of CD16 [229]. DCs and basophils do not have a distinguishable sole surface marker, however, an antibody cocktail of all the other surface markers (CD3, CD14, CD16, and CD56) was used to negatively gate for DCs and basophils, and these cells were further distinguished by HLA-DR and CD123 expression, where DCs were positive for both [228], and basophils were HLA-DR^- and $CD123^+$ [230].

For each assay, an unstained sample of peripheral blood leukocytes was included to ensure that any detection of surface marker expression was the result of a specific interaction with the antibody, rather than non-specific binding. Within each donor sample, the percentages of each cell population were recorded and compared to the percentages reported in the literature. The values obtained corroborated the previously reported reference percentage ranges, which further confirmed the successful identification of the specific cell populations.

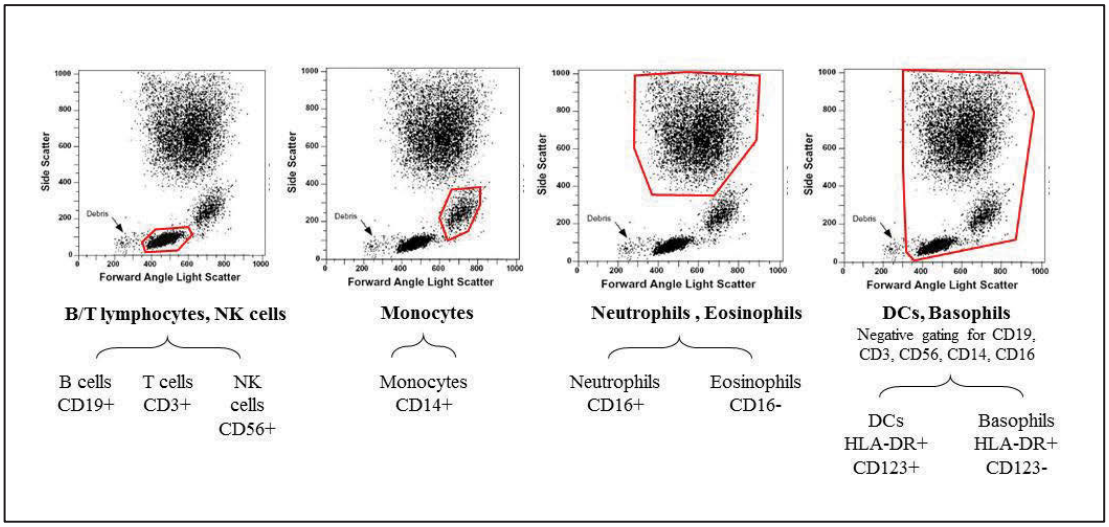

Figure 2.7 Human peripheral blood leukocyte populations were identified using differential surface markers by flow cytometry. Human peripheral blood leukocytes can initially be categorised into three groups of cell types depending upon their forward (size) and side (granularity) scatter profiles. B and T lymphocytes and natural killer (NK) cells are small in size and low in granularity. Monocytes are large in size and low in granularity. Neutrophils and eosinophils are high in granularity. Dendritic cells (DCs) and basophils are difficult to distinguish with forward and side scatter profiles alone. Leukocytes can be further distinguished by the presence/absence of surface markers. B cells are CD19 positive; T cells are CD3 positive; NK cells are CD56 positive; monocytes are CD14 positive; neutrophils are CD16 positive, and eosinophils are CD16 negative. DCs and basophils were negatively gated for all of these surface markers and distinguished by the fact that DCs are positive for both HLA-DR and CD123, whilst basophils are HLA-DR positive and CD123 negative. + and – denotes positive and negative, respectively. Adapted from [231].

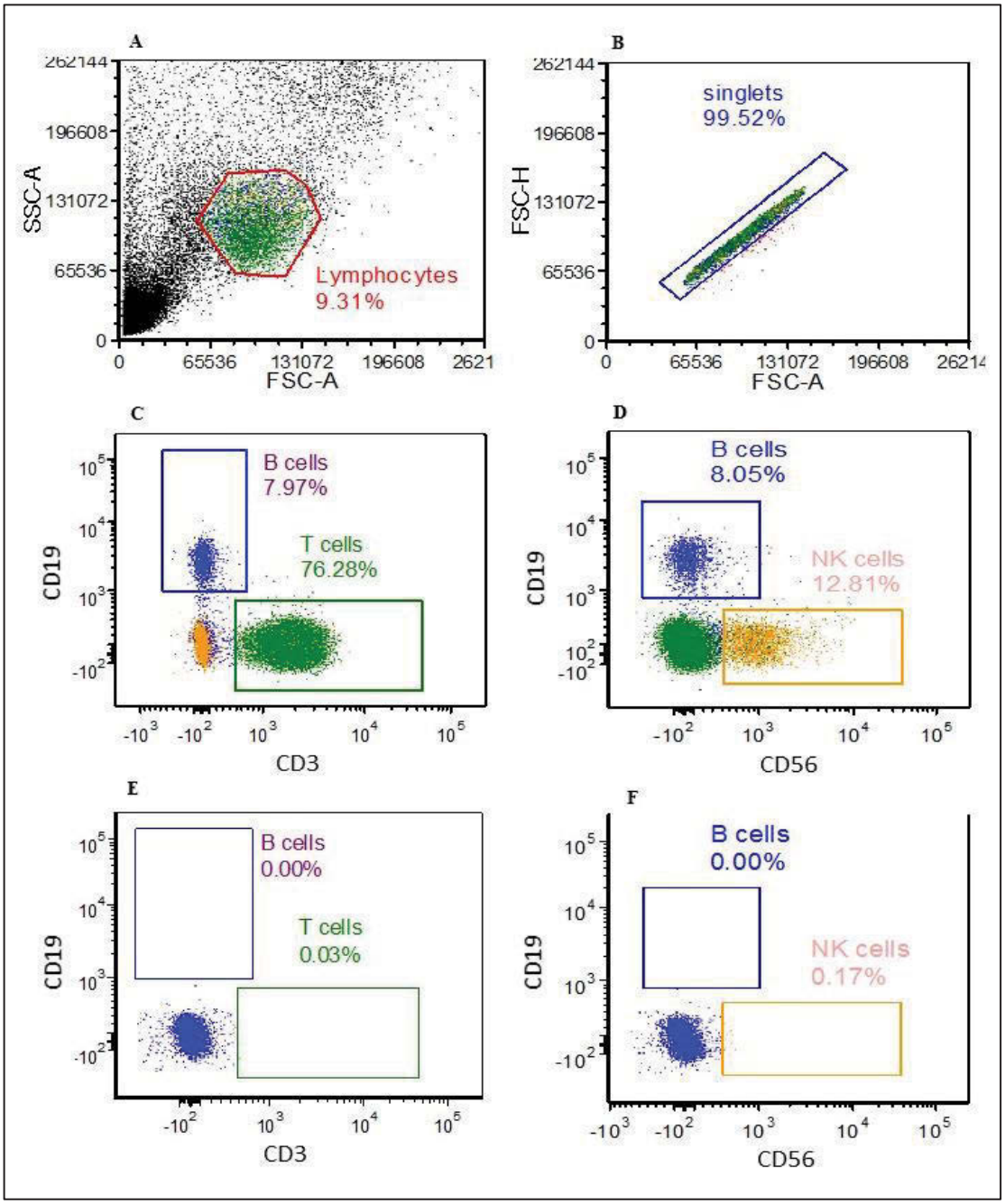

Figure 2.8 Human B- and T- lymphocytes and natural killer cells were identified by flow cytometry. (A) The lymphocyte population was initially determined by their forward (FSC-A) and side (SSC-A) scatter profiles. The percentage denotes the percentage of lymphocytes in the leukocyte population. **(B)** A single cell population of these lymphocytes was obtained by gating for FSC-A and forward scatter height (FSC-H) profile. **(C, D)** B- and T-lymphocytes and natural killer (NK) cells were further distinguished by presence of CD19, CD3 and CD56 surface markers, respectively. **(E,F)** Unstained controls. The percentages denote the percentage of B- and T-lymphocytes and NK cells within the single cell lymphocyte population. The x and y axes for (A) and (B) are cell counts; whilst for (C-F), the axes represent fluorescence intensities. This plot is representative of 4 independent experiments.

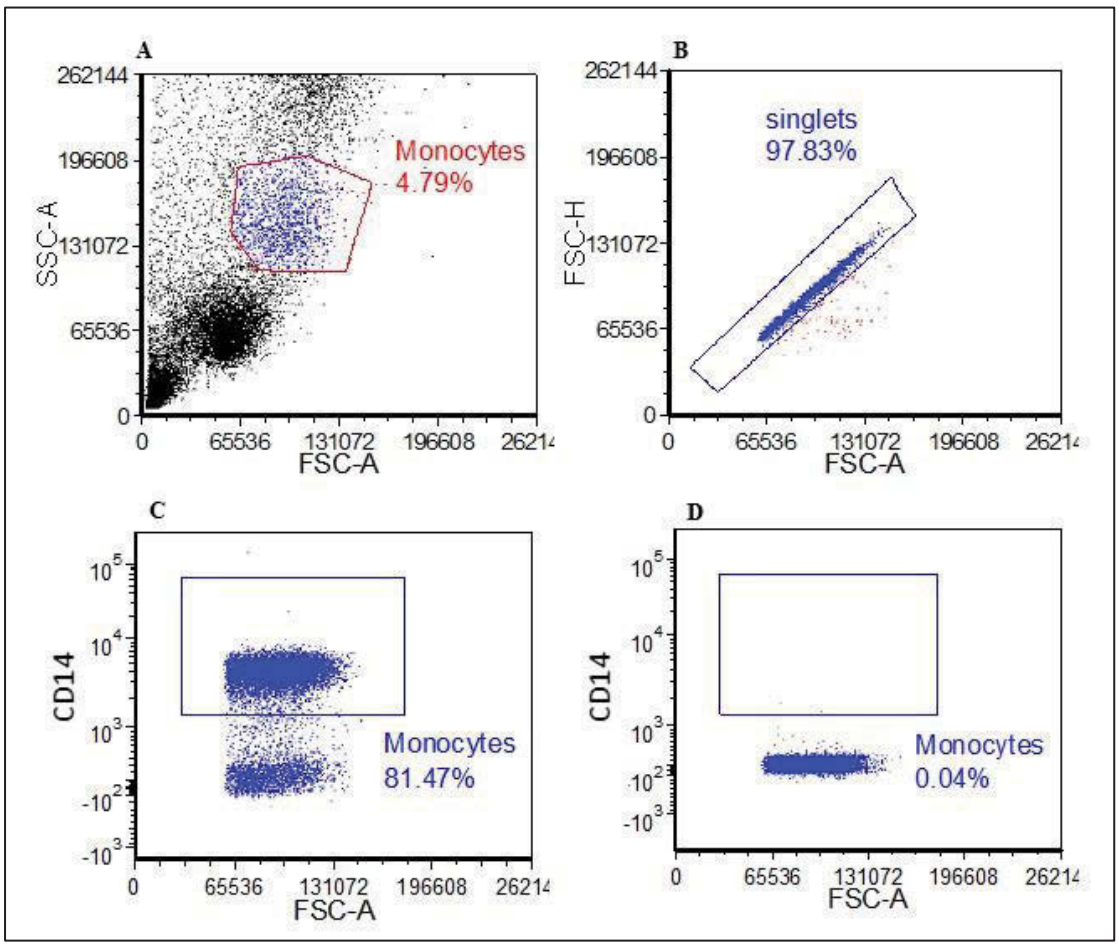

Figure 2.9 Human monocytes were identified by flow cytometry. (A) The monocyte population was initially determined by their forward (FSC-A) and side (SSC-A) scatter profiles. The percentage denotes the percentage of monocytes in the leukocyte population. **(B)** A single cell population of these monocytes was obtained by gating for FSC-A and forward scatter height (FSC-H) profile. **(C)** Monocytes were further confirmed by the presence of CD14. **(D)** Unstained control. The percentages denote the percentage of monocytes in the single cell population. The x and y axes for (A) and (B) are cell counts; whilst for (C) and (D), the axes represent fluorescence intensities. This plot is representative of 4 independent experiments.

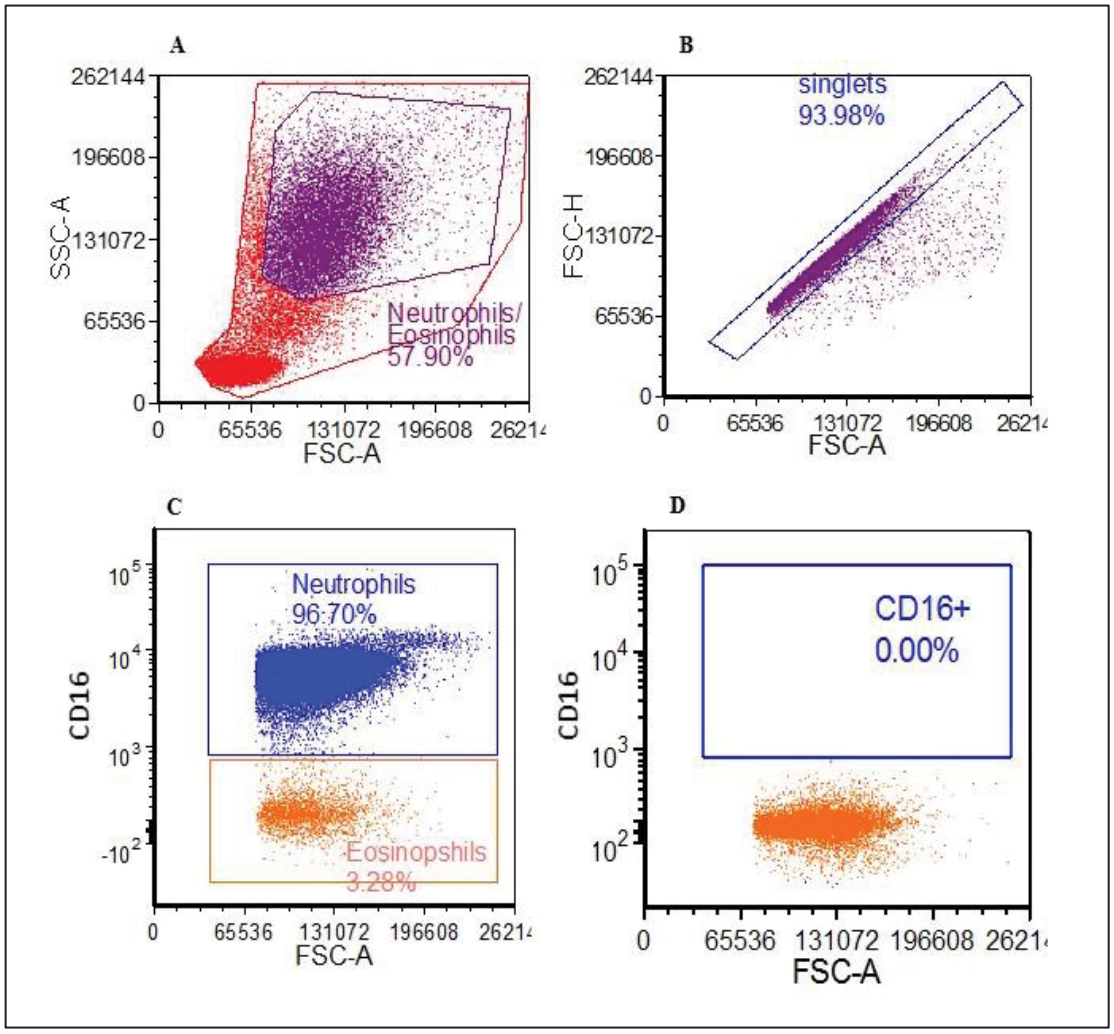

Figure 2.10 Human neutrophils and eosinophils were identified by flow cytometry. **(A)** The granulocyte population was initially identified on the basis of forward (FSC-A) and side (SSC-A) scatter profiles. The percentage denotes the percentage of granulocytes in the leukocyte population. **(B)** A single cell population of these granulocytes was obtained by gating for FSC-A and forward scatter height (FSC-H) profile. **(C)** Neutrophils and eosinophils were further confirmed by the presence or absence of CD16, respectively. **(D)** Unstained control. The percentages denote the percentage of neutrophils and eosinophils in the single cell population. The x and y axes for (A) and (B) are cell counts; whilst for (C) and (D), the axes represent fluorescence intensities. This plot is representative of 4 independent experiments.

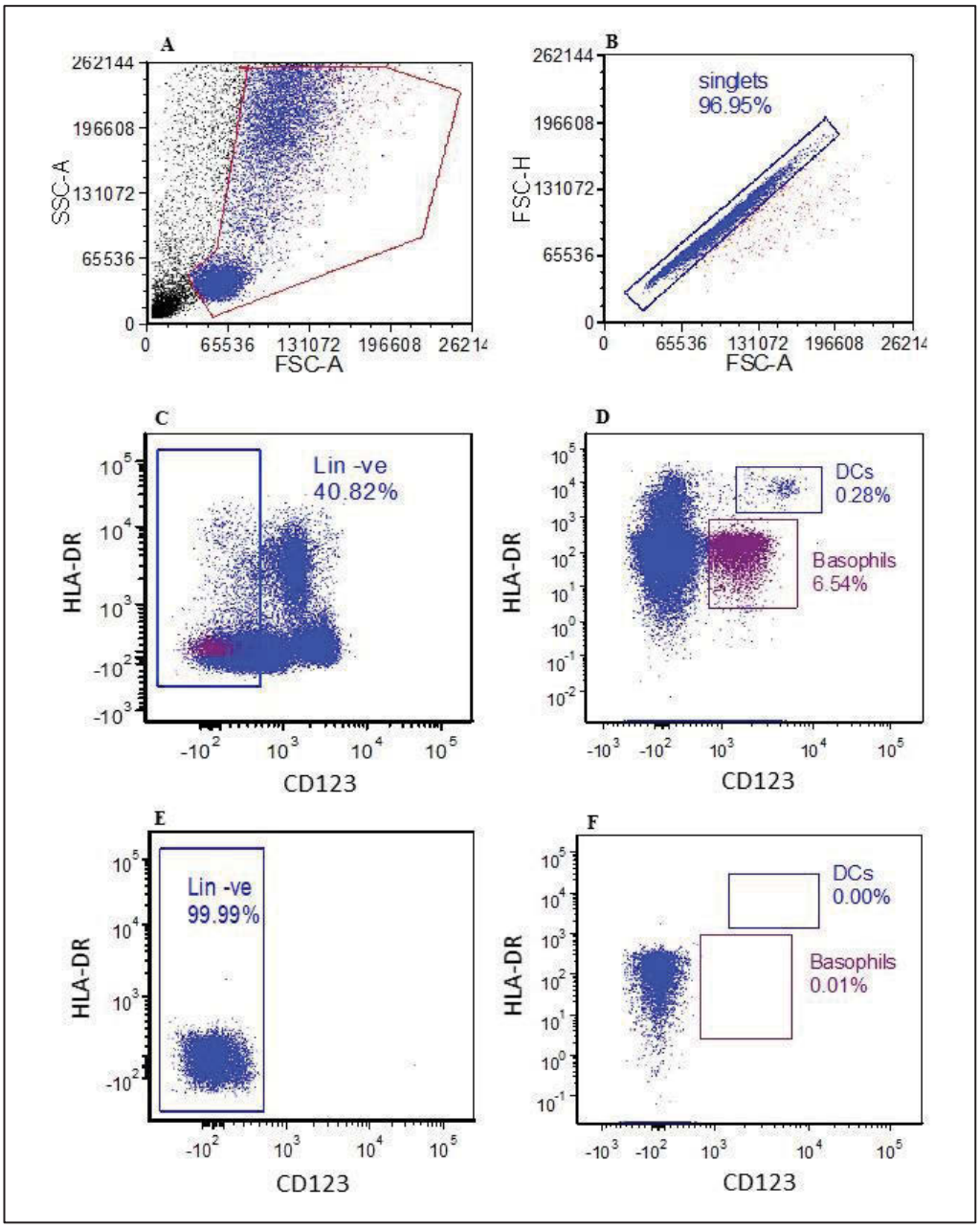

Figure 2.11 Human dendritic cells and basophils were identified by flow cytometry. **(A)** The main leukocyte population was gated based on forward (FSC-A) and side (SSC-A) scatter profiles. **(B)** A single cell population of these granulocytes was obtained by gating for FSC-A and forward scatter height (FSC-H) profile. **(C)** A lineage negative (Lin -ve) gating was used to exclude cells positive for CD3, CD14, CD16, CD19 and CD56. **(D)** Dendritic cells (DCs) and basophils were further confirmed by the presence of CD123, with DCs being further positive and basophils negative for HLA-DR, respectively. **(E,F)** Unstained control. The percentages denote the percentage of DCs and basophils in the Lin -ve gate. The x and y axes for (A) and (B) are cell counts; whilst for (C-F), the axes represent fluorescence intensities. This plot is representative of 4 independent experiments.

2.5.5 Assessment of cellular functions via flow cytometry

2.5.5.1 Assessing the effect of FhHDM-1 and peptide derivatives on murine macrophage viability

The uptake of TOPRO-3 dye, which labels cells with compromised membrane integrity, was used to determine cell viability. In brief, RAW 264.7 macrophages (1 x 10^6 cells/ml) were suspended in cold PBS. Then, 500µl samples were strained through mesh and placed in FACS tubes. After the addition of 1µL of 1 in 10 diluted TOPRO-3 dye, cells were analysed on the flow cytometer for 6000msec. Cells were then treated with peptides, FhHDM-1 or FhHDM.C2 (20µM), diluted in saline, and data were further acquired on the flow cytometer for a total of 28000msec. The uptake of TOPRO-3 was detected as an increase in red fluorescence, using the 660/40nm filter.

2.5.5.2 Assessing the effect of FhHDM-1 and FhHDM-1.C2 on murine macrophage lysosomal pH

The assessment of change in murine macrophage lysosomal pH by FhHDM-1 and FhHDM-1.C2 was detected using Lysosensor dye (Life Technologies). In brief, RAW 264.7 macrophages (1 x 10^6 cells/ml) in 12 well TC plates were incubated with FhHDM-1 or FhHDM-1.C2 (15µM) for 30min at (37ºC/ 5% CO_2), then washed twice with saline, prior to incubation with Lysosensor dye (5µM) for 5min (37ºC/ 5% CO_2). The cells were then washed with FSW, to remove any excess Lysosensor dye, resuspended in 500µl FSW, and then dispersed by passage through mesh into FACs tubes for flow cytometric analysis. An increase in lysosomal pH was detected as an increase in blue fluorescence, detected using the 450/50nm filter.

2.5.5.3 Assessing the effect of FhHDM-1 on murine neutrophil phagocytosis of Ovalbumin particles

The effect of FhHDM-1 on neutrophil phagocytosis of Ovalbumin particles was conducted using Alexa Fluor 488 labelled Ovalbumin (Life Technologies). In brief, murine neutrophils (1 x 10^6 cells/ml) in 1.5ml microtubes were incubated with FhHDM-1 (10µM) for 30min (37ºC/ 5% CO_2). Cells were then incubated with Alexa Fluor 488 labelled Ovalbumin (10µg/ml) for 1h (37ºC/ 5% CO_2), or further stimulated with LPS (1µg/ml) for 1h (37ºC/ 5% CO_2) prior to Ovalbumin incubation. Cells were then washed with FSW, passaged through a mesh into FACs tubes, and analysed by flow cytometry.

2.5.5.4 Assessing the effect of FhHDM-1 on the expression of murine neutrophil surface markers

To assess the effect of FhHDM-1 on the expression of murine neutrophil surface markers, the levels of CD11b and CD62L were determined. In brief, murine neutrophils (1 x 10^6 cells/ml) in 1.5ml microtubes were incubated with FhHDM-1 (10μM) for 30min (37ºC/ 5% CO_2), and then stimulated with phorbol myristate acetate (PMA, 100ng/ml; Sigma-Aldrich); or incubated with FhHDM-1 (5μM) for 30min (37ºC/ 5% CO_2), washed twice with saline prior to stimulation with LPS (1μg/ml) for 1h (37ºC/ 5% CO_2). As per the general protocol (Section 2.5.2), the cells were blocked and stained with anti-mouse CD11b APC and anti-mouse CD62L antibodies PE-Cy7 (Table 2.2). Rat IgG APC and rat IgG PE-Cy7 antibodies (Table 2.2) were used as isotype controls. Unbound antibodies were removed by washing and the cells were analysed on the flow cytometer.

2.5.5.5 Assessing the effect of FhHDM-1 treated murine neutrophils on murine dendritic cell activation

To assess the effect of FhHDM-1 on murine DC activation via murine neutrophils, the expression levels of CD80 and CD86 surface markers were detected. In brief, murine neutrophils (2 x 10^6 cells/ml) in 15ml conical tubes were incubated with FhHDM-1 (10μM) for 30min (37ºC/ 5% CO_2), prior to stimulation with LPS (1μg/ml) for 1h, or the combination of murine recombinant TNF (10ng/ml; Sigma Aldrich) for 20min and then LPS (37ºC/ 5% CO_2). Neutrophils were washed five times with saline (with centrifugation [300xg; 5min] to collect cells) prior to incubation with primary bone marrow derived DCs (1:1) for 16h in a 24 well TC plate (37ºC/ 5% CO_2). After the incubation, cells were then blocked and stained anti-mouse CD80 PE and anti-mouse CD86 FITC antibodies (Table 2.2), as per the general protocol (Section 2.5.2). Hamster IgG2, κ PE and rat IgG FITC antibodies (Table 2.2) were used as isotype controls. Unbound antibodies were removed by washing, and the cells were analysed on the flow cytometer.

2.5.6 Flow cytometry instrumentation and data analysis

For all flow cytometry experiments, either the BD LSR-II flow cytometer or BD LSR-Fortessa™ X-20 flow cytometer was used, with BD FACs DIVA software for acquisition of samples. Data analysis of flow cytometry experiments were conducted

using FCS Express 4 Research Edition (De Novo, CA, USA) or FlowJo (FlowJo LLC, Oregon, USA).

2.6 Microscopy

2.6.1 Standard microscopy staining protocol

Cells were seeded onto 10mm Fluorodish cell culture dishes (World Precision Instruments, Florida, USA) for all microscopy experiments. After incubation of cells with appropriate peptides in appropriate cell culture media, the supernatant was removed and cells were washed with PBS twice. Paraformaldehyde (4% v/v) was then used to fix samples at RT for 30min. After washing with PBS (for 1min three times) to remove excess paraformaldehyde, Microscopy Permeabilisation Solution (PBS + 0.1% v/v Triton-X100; Sigma-Aldrich, MPS) was added to permeabilise the cellular membranes for 1min. Cells were then washed with PBS three times prior to membrane or nuclear staining, or further processed with a quenching and blocking step for antibody-related experiments (Section 2.6.2.2). Staining with Alexa Fluor 647 Phalloidin (Life Technologies) diluted 1 in 60 with PBS was conducted for cellular membrane staining (20min at RT, protected from light), and/or 3% v/v 4',6-Diamidino-2-Phenylindole, Dihydrochloride (DAPI, Molecular Probes®, Life Technologies) in PBS for nuclear staining (15min at RT, protected from light). Two changes of glycerol (nPG, supplied by UTS Microscopy Imaging Facility) were then applied to the wells to prevent quenching of fluorescence. A 12mm glass coverslip was placed on top of the nPG to flatten the meniscus. Samples were imaged using the confocal microscope within 1 week after staining.

2.6.2 Assessment of FhHDM-1 and FhHDM-1.C2 peptide binding and internalisation by murine macrophages

2.6.2.1 Assessment of FhHDM-1.C2 binding to RAW 264.7 macrophages

RAW 264.7 macrophages were seeded (2 x 10^5 cells/ml) onto 10mm Fluorodish cell culture dishes and allowed to adhere for at least 2h (37ºC/ 5% CO_2). Cells were then incubated with R10 media only (for untreated) or with Alexa Fluor 488 labelled FhHDM-1.C2 (5µM) resuspended in R10 for 15min or 30min at 4ºC. The cells were then washed, fixed, permeabilised, as described in the standard microscopy staining protocol (Section 2.6.1). Alexa Fluor 647 Phalloidin was used for the staining of the cellular membrane, and DAPI was used for identification of the nucleus.

2.6.2.2 Assessment of FhHDM-1 and FhHDM-1.C2 peptide internalisation by RAW 264.7 macrophages

RAW 264.7 macrophages were seeded (2 x 10^5 cells/ml) onto 10mm Fluorodish cell culture dishes, and incubated for at least 2h (37ºC/ 5% CO_2). Cells were then incubated with R10 media only (for untreated), or with Alexa Fluor 488 labelled FhHDM-1 (2.5µM) for 45min, or Alexa Fluor 488 labelled FhHDM-1.C2 (5µM) for 15min, 30min and 45min, or with biotin-labelled FhHDM-1.C2 (5µM) for 15min (37ºC/ 5% CO_2). The cells were then washed, fixed, permeabilised, as described in the standard microscopy staining protocol (Section 2.6.1). For experiments with biotin-labelled peptides, further steps (as follows) were conducted. After further washing with PBS, excess paraformaldehyde was quenched using 100mM glycine. Cells were then washed and blocked with microscopy blocking solution (PBS + 2%v/v HI FBS + 0.1% v/v Tween 20; MBS) O/N at 4ºC. After washing, the cells were incubated with Alexa Fluor 488 labelled streptavidin (Life Technologies) diluted 1 in 20 with PBS + 2% (v/v) HI FBS for 1h at RT, protected from light. An Alexa Fluor 488 labelled streptavidin only sample was included to exclude any non-specific binding. After washing cells with PBS/T, Alexa Fluor 647 Phalloidin was used to stain the cellular membrane, or transmission detection (TD) was used to visualise the membrane. DAPI was used for nuclei staining.

2.6.3 Microscopy instrumentation and data analysis

For all microscopy experiments, the 60x objective on the Nikon A1 confocal microscope (Nikon, NY, USA) and NIS software (Nikon) was used for image acquisition of samples. Images were analysed by Imaris (Bitplane, UK) software. There were six to seven fields of view captured for each sample, and each whole visible cell was observed to quantify the numbers of green fluorescent dots (for the fluorescently-labelled or biotin-labelled peptide) to determine peptide binding and internalisation. Average percentages were calculated using numbers of whole visible cells with punctate green fluorescence close in proximity to the cellular membrane (binding) or within the cellular cytoplasm (internalisation) out of the total numbers of whole visible cells counted, ± SEMs.

2.7 Molecular biology

2.7.1 Gene expression levels in peptide-treated murine macrophages via microarray

2.7.1.1 Treatment of BMDMs and isolation of RNA

BMDMs (1 x 10^6 cells/ml) in 6 well TC plates were treated with BMDM media alone or with FhHDM-1 (15μM) for 1h (37ºC/ 5% CO_2). The cells were then left to incubate as untreated or with FhHDM-1 for 6 or 24h, or further stimulated with LPS (10ng/ml) for 6 or 24h (37ºC/ 5% CO_2). Supernatants were removed and cells were lysed with TRIzol™ reagent (Invitrogen) and RNA was isolated using the Qiagen RNeasy Plus Mini kit (Qiagen, Hilden, Germany). The aqueous phase of the Trizol preparation was obtained, according to the manufacturer's instructions, and applied to the gDNA-eliminating column of the RNeasy Plus Mini Kit, and then RNA was isolated, according to the manufacturer's instruction (Qiagen). RNA was submitted to the Ramaciotti Centre for Genomics (UNSW, Sydney, Australia) for gene expression microarray analyses using the Affymetrix Mouse Gene 2.1ST array.

2.7.1.2 Analysis of microarray data and network mapping

The data output from the microarray (Section 2.7.1.1), was analysed using Partek Genomics Suite (Partek Inc. USA). Data files were grouped according to treatment (untreated, FhHDM-1 only, LPS only, and LPS+FhHDM-1), and individual gene lists for the treatments at 6 and 24h were generated by one way ANOVA comparison of a combination of two groups, with a fold change cut off of >2, p-value with FDR<0.05 to identify the significantly altered genes between the two groups being analysed. Heat maps of the whole microarray data were created using Partek Genomics Suite (Partek Inc., MO, USA). A heat map of specific genes was created using Heml (Heatmap Illustrator, version 1.0, [232]). Pathway analysis was conducted using Ingenuity Pathway Analysis® (Qiagen), where comparison analysis was conducted between gene lists created for LPS versus untreated samples and LPS+FhHDM-1 versus LPS treated samples at both 6 and 24h time points. An activation Z-score was generated by the software to rank the most differentially regulated pathways.

2.7.2 Gene expression levels in peptide-treated murine macrophages via quantitative Real Time-PCR

2.7.2.1 Treatment of BMDMs and isolation of RNA

For experiments involving the gene expression levels of *SerpinB2*, *Havcr2* and *Lsp-1*, BMDMs (1 x 10^6 cells/ml) in 6 well TC plates were treated with BMDM media, or with FhHDM-1, FhHDM-1.C2, LL-37, CRAMP, *Opisthorchis viverrini* helminth peptide, or *Hydrophis cyanocinctus* sea snake peptide (15μM) for 24h (37^{o}C/ 5% CO_2). For experiments that observed the gene expression levels of *Il1β* and *iNOS*, BMDMs (1 x 10^6 cells/ml) in 6 well TC plates were treated with BMDM media, or with FhHDM-1, *Opisthorchis viverrini* helminth peptide (2.5μM) for 1h, washed twice with saline, prior to stimulation with LPS (10ng/ml) or Poly (I:C) (50ng/ml) for 6h (37^{o}C/ 5% CO_2).

Cellular RNA was isolated using the Isolate II RNA mini kit (Bioline, UK), following the manufacturer's protocol. In brief, after treatment of cells, cells were washed twice with saline. Lysis buffer (350μl with 3.5μl of β-mercaptoethanol) was added to each well, and the lysed cellular mixture was placed into a sterile 1.5ml microtube to vortex for 30sec. The sample was then placed into an Isolate I filter column and centrifuged (11,000xg; 1min). An equal volume of 70% v/v pure ethyl alcohol (EtOH, Sigma-Aldrich) was added, and tube contents were mixed well before loading into an Isolate II RNA mini column for centrifugation (11,000xg; 30sec). The sample was then washed with the membrane desalting buffer prior to DNAse I treatment. The samples were subjected to multiple washing steps with the kit RW1 and RW2 wash buffers, twice and once, respectively. The RNA was eluted into 40μl of Bx water and RNA quality and quantity was assessed via the NanoDrop One/One (Thermofisher Scientific). The absorbance at 260nm (A260) was measured to approximate RNA concentration. The absorbance at 280nm (A280) and 230nm (A230) were measured to assess the purity of the sample, where contaminating protein and phenol or guanidine thiocyanate can be detected at the respective absorbance. RNA was deemed of high quality if the ratio of A260/A280 was between the ranges of 1.8 and 2.2, and the A260/A230 ratio was >1.7 [233].

2.7.2.2 DNAse I treatment and cDNA synthesis

The concentrations of the RNA samples (from Section 2.7.2.1) were adjusted to the sample of the lowest RNA concentration by addition of Bx water. All reactions were conducted using 0.2ml thin walled PCR tubes (Axygen, California, USA). A further DNAse step was conducted using the DNAse I Amplification Grade (Sigma-Aldrich) for the removal of any contaminating gDNA, following the manufacturer's protocol. In brief, 1µl of 10x reaction buffer and 1µl of DNAse I was added to digest up to 1µg of Bx water diluted RNA. The samples were gently mixed by tapping the tube, and incubated for 15min at RT. Next, 1µl of stop solution was added to RNA (up to 1µg). Samples were heated for 10min at 70°C in a thermal cycler to denature the DNAse I. First strand cDNA was synthesised from purified RNA in a 20µl volume using the SuperScript® III First-Strand Synthesis for RT-PCR (Life Technologies), according to the manufacturer's protocol. Specifically, 1pg – 5µg of RNA (in Bx water) was incubated with 50ng/µl of random hexamers, 1µl of 10mM dNTP mix, to a total reaction volume of 10µl, in a thermal cycler at 65°C for 5min. The reaction was then placed on ice for 1min. The following reagents were then added, in order, to the reaction on ice: 2µl of 10x reverse transcriptase buffer, 4µl of 25mM $MgCl_2$, 2µl of 0.1M DTT, 1µl of RNaseOUT™ (recombinant RNase inhibitor, 40U/µl), and 1µl of SuperScript® III reverse transcriptase (200U/µl). A no reverse transcriptase control was included to ensure that non-specific amplification did not occur. The reaction was incubated in a thermal cycler at 25°C for 10min, and then 50°C for 50min, followed by a termination step at 85°C for 5min. Next, 1µl of the RNAse H was added to each sample to digest any remaining mRNA template off the cDNA. A master mix was used where possible to minimise variability in DNAse I treatment and cDNA synthesised between samples.

2.7.2.3 Quantitative real time quantitative RT-PCR

Primers amplifying regions of the target genes and the reference genes were purchased from Thermo Fisher Scientific. TaqMan primer probes are listed in Table 2.4. All reactions were conducted using 0.2ml thin walled PCR tubes (Axygen, California, USA). The RT-PCR reaction was conducted using the TaqMan™ Gene Expression Master Mix (AmpliTaq Gold® DNA Polymerase [Ultra Pure], Uracil-DNA glycosylase, dNTPs [with dUTP], ROX™ Passive Reference, and optimized buffer components; Applied Biosystems, Life Technologies), as per the manufacturer's protocol. In brief, in a total volume of 10µl, 2µl of cDNA (5ng, refer Section 2.7.2.2),

0.5µl of appropriate TaqMan primer probe (as listed in Table 2.4), 5µl of TaqMan™ Gene Expression Master Mix, and 2.5µl of Bx water was assayed in technical triplicates, in a MicroAmp® Optical 384-Well Reaction Plate with Barcode (Applied Biosystems, Life Technologies), which was sealed with a MicroAmp® Optical Adhesive Film (cat no: 4311971; Applied Biosystems, Life Technologies). A no cDNA control of Bx water was included. The PCR program was as follows: UNG activation (50˚C, 2 min), UNG inactivation (95˚C, 10 min), followed by 40 cycles of denaturation (95˚C, 15 sec) and annealing/extension (60˚C, 1 min). Analysis of amplification plots provided cycle threshold (C_t) values, and the quality of the plots provided confidence that the C_t values obtained were of the target product.

Table 2.4 Table of TaqMan primer probes

Gene		Assay ID	Dye
Actinb	β-actin	Mm00607939_s1	FAM-MGB
B2m	β-2- microglobulin	Mm00437762_m1	FAM-MGB
Gapdh	Glyceraldehyde- 3-phosphate dehydrogenase	Mm99999915_g1	FAM-MGB
Gusb	β-glucuronidase	Mm01197698_m1	FAM-MGB
Havcr2	Hepatitis A virus cellular receptor 2/ T-cell immunoglobulin and mucin-domain containing-3 (TIM-3)	Mm00454540_m1	FAM-MGB
Hmbs	Hydroxymethylbilane synthase	Mm01143545_m1	FAM-MGB
Hnrnpab	Heterogeneous Nuclear Ribonucleoprotein A/B	Mm01288699_m1	FAM-MGB
Hprt	Hypoxanthine-guanine phosphoribosyltransferase	Mm00446968_m1	FAM-MGB
Il1β	Interleukin 1 β	Mm00434228_m1	FAM-MGB
iNOS/Nos2	Nitric Oxide Synthase	Mm00440502_m1	FAM-MGB
Lsp-1	Lymphocyte-specific protein 1	Mm01268877_m1	FAM-MGB
Mau2	MAU2 Sister Chromatid Cohesion Factor	Mm00512415_m1	FAM-MGB
Ppia	Peptidylprolyl Isomerase A	Mm02342430_g1	FAM-MGB
Rpl13a	Ribosomal protein L13a	Mm01612987_g1	FAM-MGB
SerpinB2	Serpin Family B Member 2/ Plasminogen Activator Inhibitor 2 (PAI-2)	Mm00440905_m1	FAM-MGB
Stx5a	Syntaxin 5a	Mm00502335_m1	FAM-MGB

2.7.2.4 Quantification of relative gene expression levels

The most common method to quantify gene expression levels, and hence calculate the difference in relative gene expression levels between different treatment groups, is to use the $2^{-\Delta\Delta Ct}$ calculation method [234].

In brief, the following calculation steps were performed:

The difference in gene expression levels of the target gene and the reference gene were determined using a mean threshold cycle value (C_t) from three biological replicates of each gene expression measured.

The ΔC_t value (the difference in C_t value between the reference gene and the gene of interest) was then calculated using the formula:

$$\Delta C_t = C_{t\ \text{gene of interest}} - C_{t\ \text{reference gene}}$$

For the comparison of relative expression levels of the genes of interest between the untreated (vehicle control) samples and the treatment samples (either FhHDM-1 only or LPS only or combination of LPS+FhHDM-1), the $\Delta\Delta C_t$ (the difference in the change in C_t value between the untreated and the treated samples) was calculated using the formula (for each biological replicate of the treatment group):

$$\Delta\Delta C_t = \Delta C_t\text{(FhHDM-1, LPS, or LPS+FhHDM-1 treated sample)} - \Delta C_t\text{(untreated sample)}$$

Finally, the difference in relative gene expression levels between the untreated samples and each biological replicate of the treated samples was determined by the fold-change in expression, which was calculated using this formula:

$$\text{Fold-change in gene expression (between treatment groups)} = 2^{-\Delta\Delta Ct}$$

The choice of reference genes for each experimental assay is detailed in Section 2.7.4.

2.7.3 Molecular biology instrumentation and data analysis

For the DNAse I treatment and cDNA synthesis, the Eppendorf Mastercycler (Eppendorf, Hamburg, Germany) was used. The Quant Studio Flex 12K instrument (Applied Biosystems, Life Technologies) was used for real time quantification qRT-PCR experimentation.

2.7.4 Reference gene analysis

2.7.4.1 Identification of suitable reference genes from the microarray data and the literature

As described in Appendix A, two gene lists comparing LPS versus untreated samples, at both 6 and 24h timepoints, were generated by a one way ANOVA comparison of the two groups, from the microarray data analysis (Section 2.7.1.2) using Partek Genomics Suite software (Partek Inc.). A fold change cut off of -1.4<fold change<1.4 was then set, and a list of genes that were common to both lists was generated, in which three candidate reference genes (*Mau2, Stx5a* and *Hnrnpab*; Table 2.4) were then selected. Further reference genes (listed in Table 2.4) were identified from the literature, with the criteria being commonly used reference genes for normalisation of gene expression levels in LPS treated BMDMs.

2.7.4.2 Analysis of reference genes expression stability

In order to identify the most consistently expressed reference gene for specific experimental parameters, the C_t values obtained from qRT-PCR of samples were inputted into GeNorm, NormFinder and BestKeeper programs, according to the instructions supplied. This required that raw C_t values were transformed to different input formats for GeNorm and NormFinder analyses. For analysis using BestKeeper software, raw C_t values were inputted. The analysis provided by NormFinder assigns a stability ranking to candidate reference genes using an algorithm, which takes into account intra- and inter-variability (i.e. the variability in expression levels within and between the treatment groups, respectively) [235]. GeNorm determines the expression stability of a gene using a stepwise exclusion of the least stably expressed gene, generating an M value for each reference gene, and M values are then ranked [236]. The Bestkeeper software assigns a ranking to each candidate reference gene based on the SD between samples [237]. The ranking and identification of the most suitable

reference gene for each experimental condition was conducted as detailed in Section 2.7.4.3.

2.7.4.3 Analysis and identification of the most suitable reference gene

For experiments observing the effect of FhHDM-1, FhHDM-1.C2, other cathelicidins, and cathelicidin-like peptides on the gene expression levels of *SerpinB2*, *Havcr2* and *Lsp-1* in BMDMs at 24h, the C_t values of *Hnrnpab, Stx5a* (identified from Appendix A), *Actinb* and *Gapdh* (identified as commonly used within the literature) obtained from the qRT-PCR analyses were inputted into the ranking softwares, as previously described (Section 2.7.4.2). Of the three softwares, *Hnrnpab* was the highest-ranking reference gene using two of the three softwares and, therefore, was determined to be the most suitable reference gene (Table 2.5). This was consistently observed across 2 independent experiments.

For experiments observing the effect of FhHDM-1 and *Opisthorchis viverrini* helminth peptide on the gene expression levels of *Il1β* and *iNOS* in LPS or Poly (I:C) stimulated BMDMs at 6h, the C_t values of *Hnrnpab, Stx5a* (identified from Appendix A), *Gapdh* and *Hprt* (identified as commonly used within the literature) obtained from the qRT-PCR were inputted into the ranking softwares, as described in Section 2.7.4.2. All three softwares showed that *Stx5a* was the highest-ranking reference gene and hence identified as the most suitable reference gene for these experiments (Table 2.6). This was consistently observed across 3 independent experiments.

Table 2.5 *In silico* ranking of reference genes for experiments using BMDMs treated with FhHDM-1, FhHDM-1.C2, other cathelicidins and cathelicidin-like peptides

GeNorm	NormFinder	BestKeeper
Hnrnpab | Actinb	*Hnrnpab*	*Stx5a*
Gapdh	*Actinb*	*Actinb*
Stx5a	*Gapdh*	*Hnrnpab*
	Stx5a	*Gapdh*

The ranking of genes is displayed as the top being the most stable reference gene. | denotes that the genes were equally ranked as the most stable reference gene.

Table 2.6 *In silico* ranking of reference genes for experiments using LPS or Poly (I:C) stimulated BMDMs treated with FhHDM-1 and *Opisthorchis viverrini* helminth peptide

GeNorm	NormFinder	BestKeeper
Stx5a	*Stx5a*	*Stx5a | Hnrnpab*
Hnrnpab	*Hnrnpab*	*Gapdh*
Gapdh	*Gapdh*	*Hprt*
Hprt	*Hprt*	

The ranking of genes is displayed as the top being the most stable reference gene. | denotes that the genes were equally ranked as the most stable reference gene.

2.8 CPPpred analysis

For analysis of cell penetrating peptide (CPP) sequences within FhHDM-1, the predictive software CPPpred [238] was utilised. This online software allows the analysis of peptides between 5 and 30 amino acids in length, and ranks peptides from 0 to 1 according to predictive N-to-1 neural network algorithms of how likely a peptide is to be cell-penetrating. Scores closer to 1 indicate that CPPpred is more confident that the peptide will be cell-penetrating, while scores closer to 0 suggest that the peptide is highly unlikely to be cell-penetrating.

2.9 Statistical analysis

Data analysis was conducted using Microsoft Excel (Microsoft Windows) and GraphPad Prism (GraphPad, CA, USA) with statistical analysis conducted using the unpaired parametric student's t-test, unless stated otherwise. EC50s for cytokine inhibition by peptides were calculated using non-linear regression analysis, where a sigmoidal dose-response (variable slope) curve was generated. For the multiplex data, a two-way ANOVA comparison was conducted.

Chapter 3: Transcriptional profiling of macrophages treated with FhHDM-1

3.1 Introduction

Signals from both host and infecting pathogen result in the activation of gene expression programs that initiate macrophage-dependent immune responses. Biological outcomes associated with these changes in gene expression levels are varied. They include the induction or repression of genes that mediate inflammation, cell proliferation, migration, and cell survival [239]. Due to the potency of immune responses generated by even small changes in gene expression levels in macrophages, this process is tightly regulated and dysregulation is associated with excessive pro-inflammatory responses, as observed in conditions such as septic shock and inflammatory autoimmune diseases [240]. Accordingly, a therapeutic strategy which selectively modulates the transcriptional response of macrophages could potentially be used to prevent/suppress immune mediated disease.

Previous studies have shown that direct stimulation of macrophages with the human cathelicidin peptide, LL-37, regulated the expression levels of more than 900 genes [241]. Genes that were up-regulated included those encoding cytokine and chemokine receptors, cell surface antigens, cell adhesion and intercellular communication, whilst genes that were down-regulated included those encoding DNA repair proteins and inflammatory mediators [242]. Of significance for immune responsiveness, the anti-inflammatory cytokine, IL-10, was up-regulated, whilst the pro-inflammatory cytokine, IL-12, and the chemokine, macrophage-inflammatory protein (MIP)-1, were down-regulated by LL-37 treatment of macrophages [242]. Similarly, an insect-derived cationic alpha helical peptide (CEMA) has been shown to induce the expression of 35 genes in murine macrophages, including genes involved in intercellular communication and apoptosis [243]. These observations led to the proposal that cationic peptides may directly regulate macrophage function to selectively modulate responses to inflammatory signals. Consistent with this hypothesis, innate defence regulator (IDR)-1, a synthetic derivative of LL-37, regulated the expression levels of 566 genes in human monocytes [244]. Of these genes, several were transcription factors, and their activation resulted in reduced expression levels of pro-inflammatory cytokines, such as TNF, *in vivo* [244].

Structurally, FhHDM-1 is a cathelicidin-like peptide and, like LL-37, has been shown to inhibit the induction of pro-inflammatory macrophages in response to bacterial LPS [197, 199]. Therefore, the possibility that FhHDM-1 also directly altered macrophage gene expression levels to modulate inflammatory pathways was investigated.

3.2 Transcriptional profiling of FhHDM-1 treated murine macrophages

To determine changes in gene expression levels in macrophages following treatment with FhHDM-1, the global gene expression profile of BMDMs was measured using a 41,436 Affymetrix mouse gene array (Section 2.7.1). The fold changes in gene expression levels was analysed using Partek Genomics Suite (Partek Inc., USA).

The gene expression profiles, at 6 and 24h, in FhHDM-1 treated BMDMs and untreated BMDMs were remarkably similar (Fig. 3.1). Furthermore, gene lists generated by one-way ANOVA comparisons of untreated versus FhHDM-1 treated BMDMs at 6h showed that there were no significant differences in the expression levels of any genes in response to treatment with FhHDM-1 (with the cut-off at fold-change > 2, p-value with FDR < 0.05). However, at 24h, this analysis revealed a significant change in the expression levels of 6 genes (fold-change > 2, p-value with FDR < 0.05; Table 3.1). Of these 6 genes, only *SerpinB2* was upregulated, whereas the expression levels of the other 5 genes were reduced by 2 to 3.8 fold (Table 3.1). The finding that the expression levels of only 6 genes were modulated after 24h FhHDM-1 treatment is in stark contrast to the number of genes regulated by LL-37 and IDR-1 treatment, suggesting that, unlike these cathelicidin peptides, FhHDM-1 may be inducing a highly specific effect on macrophage function.

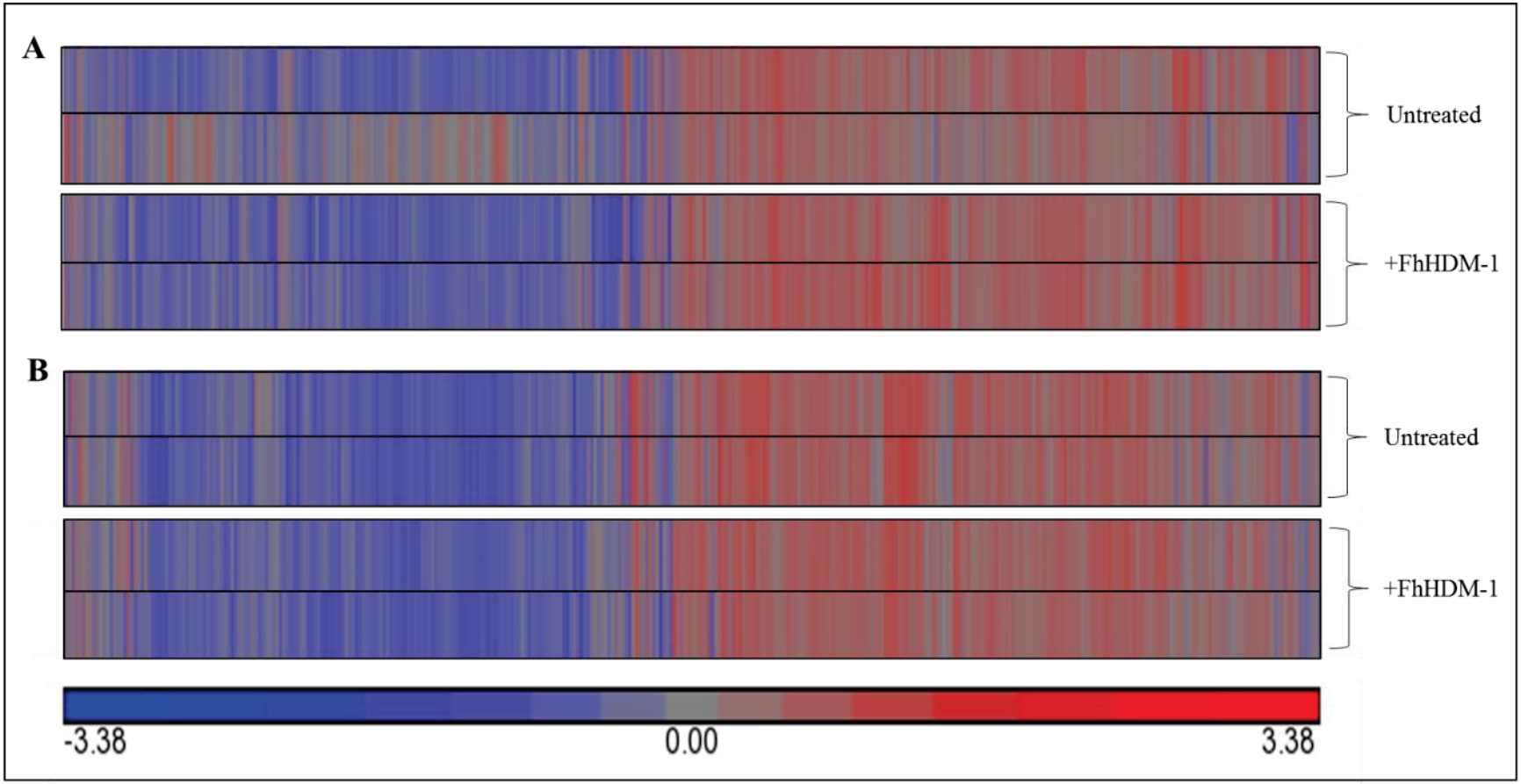

Figure 3.1 FhHDM-1 treatment does not induce any significant changes in gene expression profiles in murine BMDMs. BMDMs (1 x 10^6 cells/ml) were treated with FhHDM-1 (15µM; n = 2, replicates shown) for **(A)** 6h or **(B)** 24h at 37ºC. RNA was isolated for Agilent microarray analysis. A heat map was generated from gene expression analysis with Partek Genomics Suite. The colour-code key indicates log-fold increases (red) or decreases (blue) in gene expression levels.

Table 3.1 Genes significantly regulated by 24h FhHDM-1 treatment of murine BMDMs.

Gene Symbol	Protein	Foldchange (24h FhHDM-1 vs. 24h UT)	p-value (24h FhHDM-1 vs. 24h UT)
SerpinB2	Serine or cysteine peptidase inhibitor, Clade B, member 2	↑ (2.44)	$7.75E^{-08}$
Havcr2	Hep A virus cellular receptor 2	↓ (-2.1)	$1.15E^{-05}$
Lsp1	Lymphocyte specific protein 1	↓ (-2.2)	$2.07E^{-06}$
Hal	Histidine Ammonia Lyase	↓ (-2.3)	$1.82E^{-08}$
Cd72	CD72	↓ (-2.4)	$1.05E^{-05}$
Ogn	Osteoglycin	↓ (-3.8)	$2.20E^{-06}$

UT: Untreated; ↑ and ↓ denotes up- and down-regulation, respectively.

3.3 Analysis of *SerpinB2* expression levels and the inhibition of Th1 cytokine production in FhHDM-1 treated macrophages

As *SerpinB2* was the only gene to show increased expression levels in response to FhHDM-1 treatment of BMDMs, this was explored further. Firstly, the changes in expression levels were validated using qRT-PCR in two independent experimental replicates (Section 2.7.2). To calculate the fold change in expression levels of *SerpinB2*, a reference/normalisation gene, whose expression level was not regulated by the experimental conditions, was included.

Typically, in most published studies of macrophage inflammatory responses, the expression levels of *Actinb* and *Gapdh* are used for normalisation. However, an optimal reference gene should be determined for every set of experimental conditions [245]. Thus, a study (Tanaka *et al.* 2017; Appendix A) was undertaken to determine the expression levels of a total of 11 candidate reference genes in BMDMs, and the optimal reference gene was identified using NormFinder [235], GeNorm [236] and BestKeeper [237] softwares. This study was the first to identify and validate *Hnrnpab* and *Stx5a*, as optimal reference genes for the normalisation of gene expression data in experiments using BMDMs. The use of *Hnrnpab* as the most appropriate reference gene was determined by analysing the stability of gene expression across untreated and FhHDM-1 treated macrophages, from a panel of reference genes, as detailed in Section 2.7.4.3. Using this approach, the fold change in expression levels of *SerpinB2* was calculated, as compared to the expression levels of *Hnrnpab*. Macrophages treated with FhHDM-1 again showed a significant increase in the expression levels of *SerpinB2* (fold change of 12.7 ± 1.2; Fig. 3.2A), as compared to untreated cells, thus validating the microarray findings.

Analyses of the genomes of other helminth parasites have identified sequences for HDM-like peptides in all major human trematode parasites [199]. This suggests that a common mechanism of immune modulation is utilised by this family of parasites. To test this, BMDMs were treated with a synthetic HDM derived from the helminth, *Opisthorchis viverrini* (Ov-HDM), and the expression levels of *SerpinB2* were quantified by qRT-PCR (Section 2.7.2). Although the fold change was not as high, as

compared to macrophages treated with FhHDM-1, the Ov-HDM peptide also induced the up-regulation of *SerpinB2* (2.4 ± 0.1; Fig. 3.2B). Similarly, BMDMs treated with the mammalian cathelicidin peptide derived from human (LL-37) and mouse (CRAMP) also showed significantly increased expression levels of *SerpinB2* (3.2 ± 0.4 and 6.0 ± 0.3, respectively; Fig. 3.2B). In contrast, a peptide derived from the sea snake, *Hydrophis cyanocinctus*, which although cationic in nature is not classified as a cathelicidin, did not exert any significant effect on the expression levels of *SerpinB2* in macrophages (Fig. 3.2B).

A

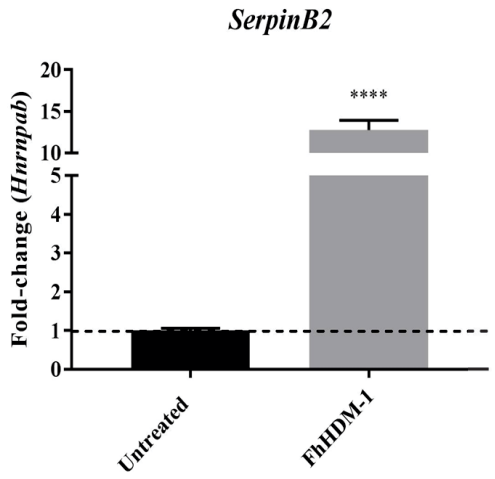

B

Sample	*SerpinB2* (Fold change ± SEM)
FhHDM-1	12.7 ± 1.2
LL-37	3.2 ± 0.4
CRAMP	6.0 ± 0.3
Opisthorchis viverrine helminth peptide	2.4 ± 0.1
Hydrophis cyanocinctus sea snake peptide	-1.3 ± 0.1

Figure 3.2 FhHDM-1 treated macrophages express *SerpinB2*, and this is conserved across other helminth, mammalian and sea snake cathelicidin-like peptides. BMDMs (1 x 10^6 cells/ml) were incubated with **(A)** FhHDM-1 and **(B)** other cathelicidin-like peptides (LL-37 [human], CRAMP [murine], *Opisthorchis viverrini* peptide [helminth], and *Hydrophis cyanocinctus* peptide [sea snake]; 15 μM) for 24h at 37°C. RNA was isolated, cDNA synthesised, and gene expression levels were analysed by qRT-PCR. Fold changes in expression levels of *SerpinB2* were calculated using the $\Delta\Delta C_t$ method, where a fold change of 1 (dotted line) indicates no change in expression level, as compared to untreated BMDMs. Genes were normalised to *Hnrnpab* expression levels. Data is the combination of two independent experiments (A) and three biological replicates (B) and expressed as means ± SEMs (**** $p \leq 0.0001$).

Expression of *SerpinB2* is induced throughout many inflammatory processes [246, 247], and is one of the most upregulated proteins in activated monocytes/macrophages [246]. Originally identified as an inhibitor of the urokinase-type plasminogen activator (uPA) [247], more recently, SerpinB2 has been associated with uPA-independent biological functions. Importantly, in the context of infections with helminth parasites, it has been shown that *SerpinB2* expression by macrophages regulates the development of Th1 adaptive immune responses [248].

Therefore, it was postulated that the increased expression levels of *SerpinB2* induced by FhHDM-1 treatment of macrophages would mediate a reduction in IFN-γ secretion by T cells. BMDMs (5 x 10^5 cells/ml) were treated with FhHDM-1 (15μM) for 24h (the time point in the array data set at which increased *SerpinB2* expression levels were observed) at 37ºC (Section 2.4.1.6). After washing the BMDMs to ensure that non-internalised FhHDM-1 was removed, murine T cells were added (T cells : BMDMs, 1:1) and the cells were co-cultured for 48h at 37ºC in the presence of αCD3 antibody (0.05μg/ml, 0.1μg/ml). The production of IFN-γ was then quantified by ELISA.

As expected, co-culturing BMDMs with T cells in the presence of αCD3 antibody promoted the production of IFN-γ (Fig. 3.3B,C). Consistent with the reported physiological role for SerpinB2, the addition of FhHDM-1 treated BMDMs to T cells significantly reduced their ability to produce IFN-γ in response to CD3 stimulation ($p < 0.0001$ for both 0.05μg/ml and 0.1μg/ml αCD3 antibody treatment, respectively; Fig. 3.3A,B).

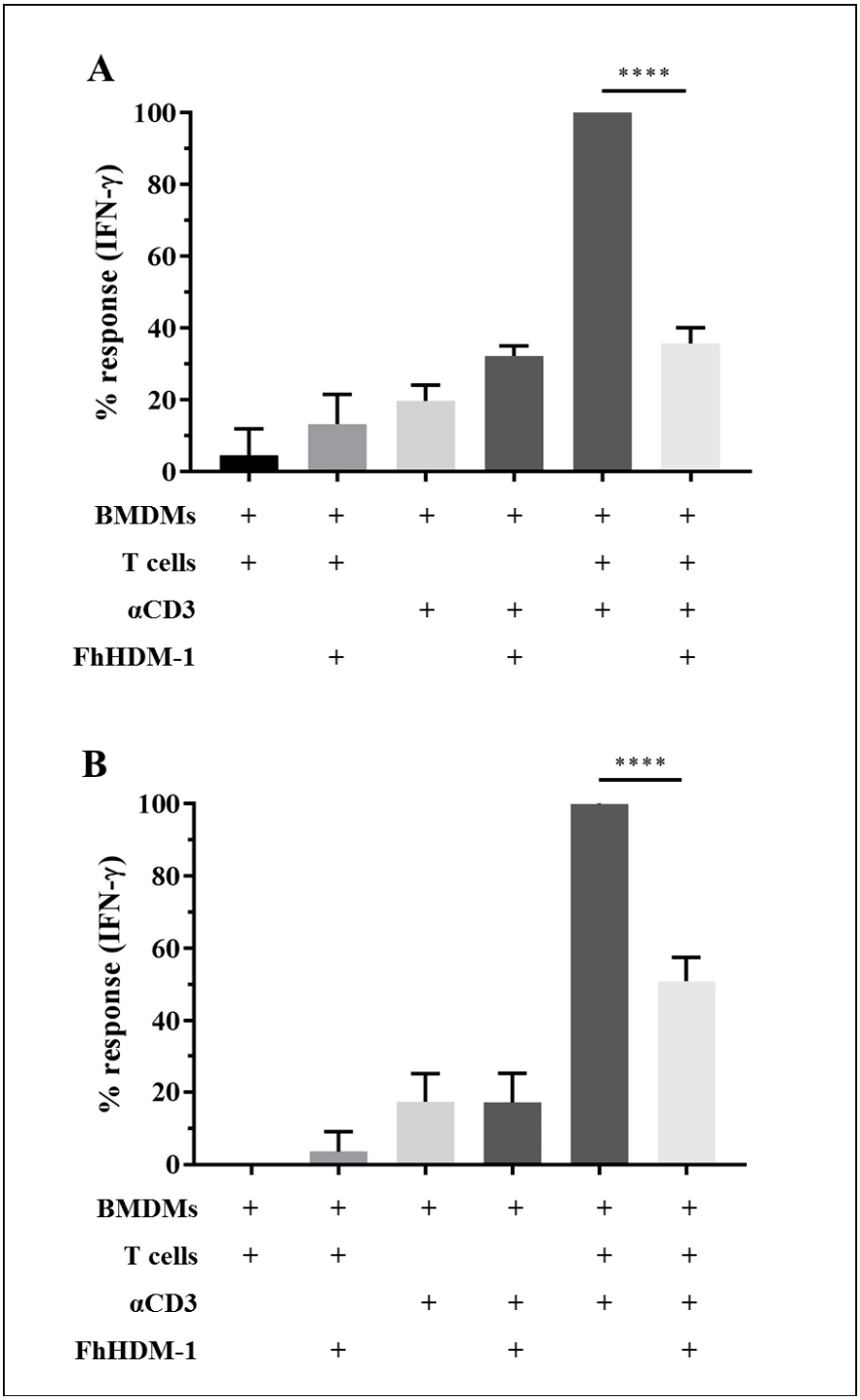

Figure 3.3 FhHDM-1 prevents IFN-γ secretion by T-cells via murine macrophages. BMDMs (5 x 10^5 cells/ml) were incubated with FhHDM-1 (15µM) for 24h at 37°C. Cells were washed twice with saline, and then co-cultured with T cells (1:1) in the presence of αCD3 antibody at **(A)** 0.05µg/ml or **(B)** 0.1µg/ml, for 48h at 37°C. Cell supernatants were assayed for IFN-γ secretion. Data was converted to percentages with untreated BMDMs + T cells + αCD3 antibody adjusted to 100%. Data is the combination of two independent experiments and expressed as means ± SEMs (**** $p \leq 0.0001$).

The mechanism(s) by which *SerpinB2* expression reduces Th1-promoting cytokine production in macrophages remains unknown, however it has been suggested that CD40 signalling activity may be affected [248]. CD40 is a primary co-stimulatory molecule present on antigen presenting cells, and its engagement with its ligand, CD154, on T cells is required for their activation [249]. Thus, to determine whether cell-cell contact was required for the reduction of IFN-γ production mediated by FhHDM-1 treated macrophages, the supernatants of untreated, or FhHDM-1 treated, BMDMs were collected, filtered (for removal of any remnant macrophage cells or cellular components) and added to fresh BMDMs and T cells, in the presence of αCD3 antibody (Section 2.4.1.6). As shown in Figure 3.4, T cells co-cultured with the supernatant of FhHDM-1 treated BMDMs were not inhibited in their secretion of IFN-γ. This suggests a requirement for cell-cell contact and also supports the microarray analysis, which showed that FhHDM-1 itself does not modulate the production of cytokines/chemokines by macrophages, which might impact upon T cell responses.

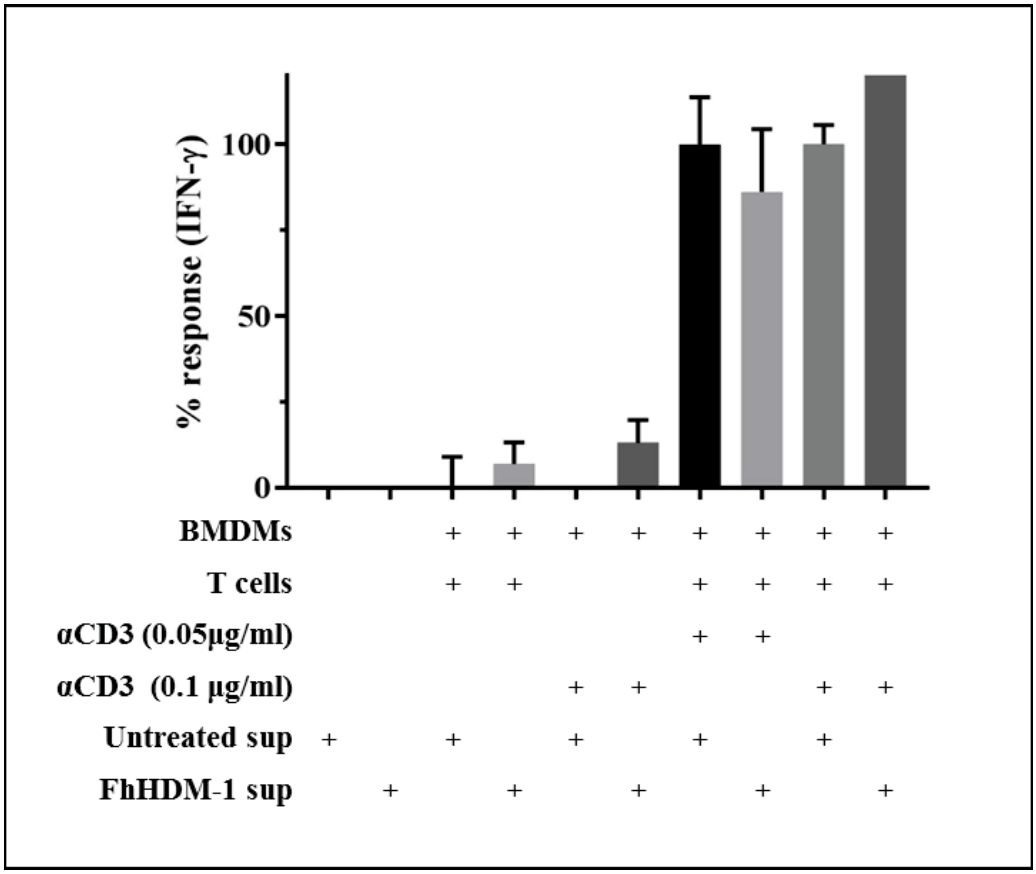

Figure 3.4 FhHDM-1 treated macrophages mediate the inhibition of Th1 cytokine production via cellular contact between macrophages and T cells. BMDMs (5 x 10^5 cells/ml) were incubated with FhHDM-1 (15 μM) for 24h at 37ºC. The supernatant (sup) was collected and co-cultured with fresh BMDMs, T cells and αCD3 antibody at two concentrations (0.05μg/ml, 0.1μg/ml) for 48h at 37ºC. Cell supernatants were assayed for IFN-γ secretion. Data was converted to percentages with untreated BMDMs + T cells + αCD3 antibody adjusted to 100%. Data is from six and four biological replicates (0.05μg/ml, 0.1μg/ml, respectively) and expressed as means ± SEMs.

3.4 Analysis of *Havcr2* and *Lsp-1* expression by helminth, mammalian and snake cathelicidin-like peptides

Of the 5 genes that showed reduced expression levels in macrophages following treatment with FhHDM-1 (Section 3.2; Table 3.1), there is very little published literature describing the function of *Hal*, *Cd72* or *Ogn*.

The gene, *Havcr2*, encodes the T cell immunoglobulin domain and mucin domain (TIM)-3 protein, which was initially identified as a membrane marker specific for Th1 lymphocytes. This surface marker functions as an immune checkpoint, negatively regulating Th1 cell activation [250]. Recent research has found that other cells, including monocytes and macrophages, can also express TIM-3 [251, 252]. While studies have demonstrated that it can regulate cytokine production [251, 253-255], cell activation [251], and the capture of apoptotic bodies [256, 257] within monocytes and macrophages, the function of TIM-3 in myeloid cells and the molecular mechanisms that this protein regulates are not yet fully understood [252]. Therefore, the consequence of the decreased expression levels induced by treatment with FhHDM-1 is not known. However, comparing the gene expression of macrophages treated with the Ov-HDM, LL-37 and CRAMP peptides indicates that a reduced expression levels of *Havcr2* (as detected via qRT-PCR) in macrophages is a common outcome for all cathelicidin-like peptides (Table 3.2).

Lsp-1 is an intracellular filamentous-actin binding protein that regulates leukocyte recruitment to inflamed sites. Mice deficient for this gene show enhanced healing of skin wounds [258] due to increased infiltration of leukocytes. While this effect is not specifically attributed to macrophages, the reduction of *Lsp-1* expression in FhHDM-1 treated mice might contribute to the promotion of wound healing observed during parasite infection. Once again, macrophages treated with Ov-HDM, LL-37 and CRAMP peptide also display a reduced expression levels of *Lsp-1* (Table 3.2).

However, as the sea snake peptide also reduced the expression levels of *Havcr2* and *Lsp-1* by comparable levels to those observed for the helminth and mammalian cathelicidin peptides (Table 3.2), more extensive analysis will be required to

demonstrate that the reduction in expression of these two genes is not simply a bystander effect, and not specifically related to FhHDM-1 treatment of macrophages.

Table 3.2 Regulation of *Havcr2* and *Lsp-1* expression by helminth, mammalian and snake cathelicidin-like peptides.

Sample	Genes (Fold change ± SEM)	
	Havcr2	***Lsp-1***
FhHDM-1	-1.5 ± 0.1	-1.9 ± 0.1
LL-37	-1.7 ± 0.1	-1.6 ± 0.1
CRAMP	-1.6 ± 0.02	-1.7 ± 0.1
Opisthorchis viverrine helminth peptide	-2.3 ± 0.01	-3.0 ± 0.1
Hydrophis cyanocinctus sea snake peptide	-1.5 ± 0.02	-2.8 ± 0.1

3.5 Discussion

Transcriptional profiling of macrophages treated with FhHDM-1 revealed that only a single gene, *SerpinB2,* was up-regulated. Furthermore, the increased expression levels of *SerpinB2* was associated with the inhibition of IFN-γ secretion from T cells (Fig. 3.3). Although the true biological function of SerpinB2 is not fully elucidated, its ability to mediate alterations to the inflammatory response has been demonstrated. In the context of autoimmunity, macrophages from the synovial fluid of patients with RA were shown to have a down-regulated expression of *SerpinB2* [259]. Further, polymorphisms in *SerpinB2* have been associated with the development of SLE (with increased Th1 responses) [260, 261]. These observations corroborate the role of SerpinB2 in the context of a parasite infection, as *SerpinB2* expression was shown to be critical in the elicitation of a functional Th2 response during infection with the helminths, *Heligmosomoides bakeri* [262] and *Schistosoma japonicum* [263]. This was observed to be dependent upon the presence of Th2 cytokines, IL-4 and IL-13, to induce *SerpinB2* expression in macrophages, and further promote the anti-inflammatory M2 phenotype [264]. Thus, the increased expression levels of *SerpinB2* in macrophages treated with FhHDM-1 is associated with decreased Th1 immune responses, and enhanced Th2 immune responses observed during infection of mouse models [186] and natural hosts [185] with *Fasciola hepatica*.

The discovery here that the treatment of macrophages with FhHDM-1 only regulated the expression of 6 genes (Section 3.2) was surprising, given that the human homolog, LL-37, and the synthetic derivative, IDR-1, reportedly modulated the expression levels of hundreds of genes [241, 244]. This striking difference may be due to the cell type studied, and the kinetics of gene expression profiling. The LL-37 study investigated its effects on RAW 264.7 macrophages (murine cell line) [242], whilst the IDR-1 study investigated its effects on human monocytes [244]. Both of these studies observed the effect of the respective peptides after 4h of incubation, while the genetic expression of macrophages treated with FhHDM-1 was assessed here at 6 and 24h. Although it is possible that FhHDM-1 has an immediate effect on macrophages, which could be quantified at an earlier time point, it is unlikely that within a 2h time frame, hundreds of genes would return to homeostatic levels of expression. However, it would be

worthwhile to assess the expression levels of genes at an earlier time point (≤ 4h) in a range of macrophage cell types, and to include macrophages treated with LL-37 in the same analysis. Despite these differences in experimental design, it is conceivable that FhHDM-1 has evolved to have a more specific effect on macrophage gene expression, as compared to the mammalian cathelicidins.

Of interest, the increase in *SerpinB2* gene expression levels was not restricted to treatment of macrophages with FhHDM-1, as another helminth homolog (Ov-HDM) and two mammalian cathelicidins (CRAMP and LL-37) also induced *SerpinB2* gene expression (Fig. 3.2B). This may be a novel mechanism conserved among the cathelicidins, and cathelicidin-like peptides, as part of their anti-inflammatory activity. The observation that a non-cathelicidin sea snake peptide did not upregulate *SerpinB2* expression levels (Fig. 3.2B), suggests possible differences in structure and charge distribution between this peptide and the cathelicidins, with the latter peptides possessing the specific characteristics required to induce *SerpinB2* expression. The regulation of *SerpinB2* expression is yet to be fully understood, however, studies have identified the regions and the proteins responsible for the regulation of the *SerpinB2* gene promoter [265]. This may provide insight as to how cathelicidins may affect the proteins and promoter regions necessary for *SerpinB2* up-regulation.

Macrophages treated with FhHDM-1 inhibited the expression of IFN-γ from T cells, which may have been mediated by the increased expression levels of *SerpinB2*. However, to confirm that *SerpinB2* is indeed functionally inhibiting the production of Th1 cytokines, further studies are required. The most direct approach would be to utilise macrophages derived from *SerpinB2*$^{-/-}$ mice. To date, little is known about the phenotype of these mice, except for their ability to produce more IgG2c and IFN-γ production by T cells, in response to Ovalbumin immunisation (in Complete Freud's Adjuvant, to elicit a Th1 response), suggesting that these mice show a bias for Th1 responses [248]. It would be anticipated that macrophages isolated from *SerpinB2*$^{-/-}$ mice and co-cultured with FhHDM-1 would be unable to inhibit T cell activation. Furthermore, infection of these mice with *F. hepatica* would allow for the determination of T cell activation *in vivo*. Based on the data presented in this chapter, *F. hepatica* infected *SerpinB2*$^{-/-}$ mice would be expected to display an increased Th1 response, in contrast to *F. hepatica* infected *SerpinB2*$^{+/+}$ mice.

Considering that the primary biological function attributed to FhHDM-1 has been the regulation of pro-inflammatory immune responses, it was of interest that one of the genes found to be reduced in expression (TIM-3 coded by *Havcr2*) has been associated with autoimmune disease. The expression of TIM-3 on T cells has been associated with the exacerbation of both EAE (murine MS) [266] and murine T1D [267]. While it is difficult to determine the biological effect of reduced macrophage expression of *Havcr2* in response to FhHDM-1, with its efficacy in suppressing development of EAE and T1D in mice [197], it warrants further investigation.

This chapter has focused on the use of transcriptional profiling to elucidate the mechanism of action by which FhHDM-1 modulates macrophage activity. While this is a valid starting point, and a commonly used strategy, to determine the biological impact of compounds, this approach does not consider other aspects of cellular function. This includes regulation of proteins (proteomics) and metabolic pathways (metabolomics) within cells, as these are also known to modulate inflammatory activity. For example, pro-inflammatory macrophages are associated with the induction of the glycolytic pathway, whilst the activation of anti-inflammatory M2 macrophages is associated with the metabolic use of oxidative phosphorylation to produce energy [268]. Therefore, these changes could be measured via mass spectrometry and live-cell metabolic assays. With increasing evidence that the metabolism is crucial for determining cellular function, the effect of FhHDM-1 on the proteome and metabolic pathways of macrophages will be a compelling area to pursue.

Chapter 4: Analysis of the anti-inflammatory effect of FhHDM-1 in murine macrophages

4.1 Introduction

Due to its ability to reduce pro-inflammatory cytokine production by macrophages in response to bacterial LPS, an anti-inflammatory mechanism of action for FhHDM-1 was postulated [197, 199]. This activity was hypothesised as important in mediating the fitness of the host, and thus supporting the parasite's survival. The damage caused to the intestinal epithelium as the juvenile parasites migrate from the intestine to the peritoneal cavity, results in the translocation of gut microbes to the systemic circulation. Mounting a pro-inflammatory response to these increased levels of circulating bacterial ligands (such as LPS) could result in the development of sepsis, which may be fatal to the host, and therefore the parasite. Developing strategies to minimise these host pro-inflammatory responses, ensures the parasite's long-term survival, while concomitantly reducing tissue damage for the host. Indeed, it has been reported that individuals infected with the related helminth parasite, *Schistosoma mansoni,* have circulating levels of endotoxin ten times higher than those reported for patients experiencing lethal septic shock [269]. The evidence that FhHDM-1 is secreted by the parasite as it migrates through the host tissue, and that it prevents the innate immune response to bacterial LPS, suggests that this peptide is a critical component of the mechanisms that have evolved to regulate the host inflammatory response during parasite infection.

The sequence and kinetics of activation of the intracellular signalling factors in macrophages, in response to LPS are well characterised [270, 271]. It is known that macrophages undergo a peak of inflammation at 6h after LPS stimulation and then a resolution phase, at 24h post-stimulation [272-274]. At the peak of inflammation, LPS upregulates the expression of genes involved in the intracellular signalling cascades, such as NF-κB signalling, and the production of pro-inflammatory cytokines and chemokines, including IFN and IL-6 [274-276]. The later resolution phase is associated with increased expression levels of genes encoding lysosomal proteins, to facilitate the preparation of the phagosome; and intracellular compartment proteins associated with secretion, such as components of the Golgi apparatus and endoplasmic reticulum [276]. Due to the detailed characterisation of events accompanying LPS stimulation of macrophages, this is a commonly used model to test efficacies, and to elucidate the mechanisms of action, of new anti-inflammatory compounds. Despite not observing

any significant alterations to gene expression levels in macrophages in response to FhHDM-1 (Chapter 3), the global gene expression levels in response to LPS after treatment of macrophages with FhHDM-1 was completed to determine whether the presence of FhHDM-1 altered pathways of inflammation. This would identify putative intracellular targets of FhHDM-1, and thus the mechanism(s) of action of the parasite peptide.

Significantly, the intracellular signalling pathways activated by LPS within macrophages are also shared by stimulation using many other pro-inflammatory ligands [272, 273]. Thus, by using LPS as an initial stimulatory ligand, broad any anti-inflammatory effects of FhHDM-1 could be examined, to provide a predictive mechanism of action for the peptide in the autoimmune context.

4.2 Transcriptional profiling of murine macrophages treated with FhHDM-1 in response to LPS stimulation

The suppression of LPS-mediated inflammatory responses by FhHDM-1 had previously been attributed to an interaction between the amphipathic c-terminal region of FhHDM-1 and LPS, which blocked the binding of LPS to its macrophage receptor (TLR-4). However, the evidence that FhHDM-1 was internalised by macrophages [215], suggested that the peptide could also impact upon intracellular pathways to inhibit the subsequent stimulation of macrophages by LPS. To confirm this hypothesis, it was important to initially observe the ability of FhHDM-1 to intracellularly prevent the activation of macrophages normally induced by LPS.

To measure this, BMDMs were treated with FhHDM-1 for 1h, then washed twice with saline to remove any excess extracellular FhHDM-1, prior to LPS stimulation, thus minimising direct interaction of FhHDM-1 with LPS (Section 2.4.1). As shown previously [199], the presence of FhHDM-1 (i.e. using a protocol in which macrophages were not washed) significantly inhibited the production of TNF, even at concentrations of FhHDM-1 as low as 2.5μM (Fig 4.1A). Although the addition of a washing step reduced the potency of inhibition, the pre-treatment of macrophages with FhHDM-1 also significantly reduced the production of TNF in response to LPS stimulation (Fig 4.1B). This suggests that internalised FhHDM-1 suppresses the pro-inflammatory response to LPS, independently of an interaction with the bacterial ligand, suggesting an ability of FhHDM-1 to modulate the intracellular signalling pathways induced by LPS.

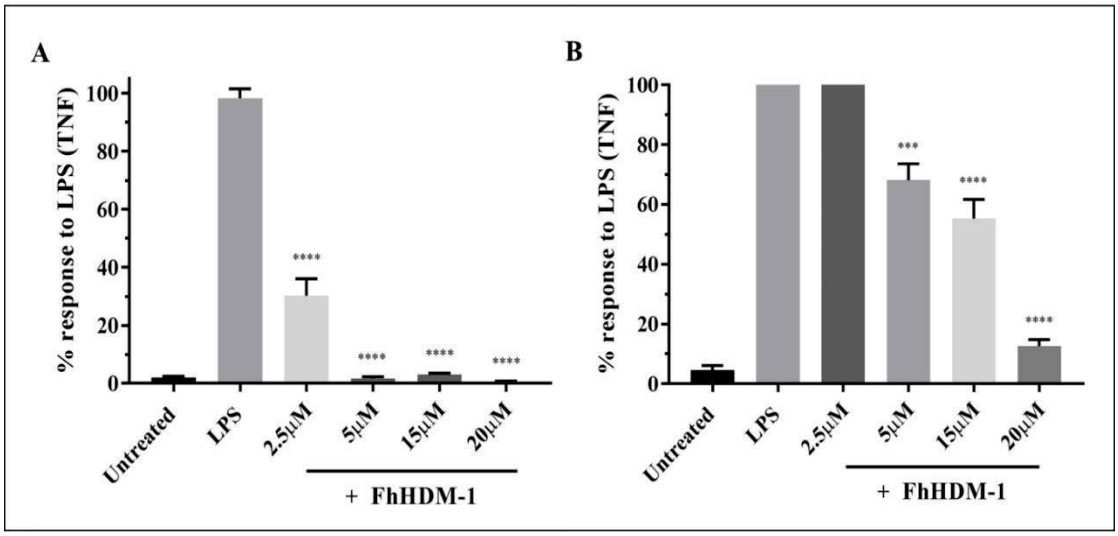

Figure 4.1 FhHDM-1 inhibits pro-inflammatory cytokine production by LPS stimulated murine macrophages. BMDMs (1 x 10^6 cells/ml) were treated with FhHDM-1 (at various concentrations) for 1h, and then **(A)** treated immediately, or **(B)** washed twice with saline prior to O/N stimulation with LPS (10ng/ml) at 37ºC. Cell supernatants were assayed for TNF secretion. Data was converted to percentage values with LPS-only stimulation samples adjusted to 100%. Data is the combination of fifteen (A) and five (B) independent experiments and expressed as means ± SEMs (statistical significance was determined by comparisons to the levels of TNF secreted by LPS-only treated samples; *** $p \leq 0.001$, **** $p \leq 0.0001$).

To identify the intracellular pathways targeted by FhHDM-1, the global gene expression profile of BMDMs stimulated with LPS-only (for a period of 6 or 24h) was compared to the genes expressed by BMDMs treated with FhHDM-1 and LPS using a 41,436 Affymetrix mouse gene array (Section 2.7.1). The fold changes in gene expression were analysed using Partek Genomics Suite (Partek Inc., USA).

As expected, at both time points of 6 and 24h (corresponding to the peak and resolution phases, respectively, of LPS inflammation in macrophages), LPS stimulated macrophages generated a distinct gene expression profile, as compared to that of untreated macrophages at the same time point (Fig. 4.2). Further analysis of gene lists, created using one-way ANOVA comparisons of LPS versus untreated samples (cut-off at fold-change>2, p-value with FDR<0.05), revealed that 3,255 and 28,747 genes (at 6 and 24h, respectively) were regulated in the presence of LPS. In support of its proposed anti-inflammatory activity, BMDMs treated with FhHDM-1 prior to LPS stimulation, generated a genetic profile that was more similar to the untreated samples, as compared to the LPS treated cells. Indeed, further analysis of gene lists showed that only 154 and 61 genes (at 6 and 24h, respectively) were differentially regulated between LPS and FhHDM-1 treated macrophages, as compared to untreated cells (Fig 4.2).

Analysis of gene lists generated from LPS and FhHDM-1 versus LPS-only treatment groups, showed that of the genes whose expression levels were modulated greater than 5 or 10 fold, most were down-regulated (65:251, 7:98 and 67:258, 12:123 for numbers of up- and down-regulated genes greater than 5 and 10 fold, at 6 and 24h, respectively; Fig. 4.3A). Closer inspection of these repressed genes showed that they were typical of a pro-inflammatory response [275]. For example, *Il6* (Fig. 4.3B), a gene that codes for the pro-inflammatory cytokine, IL-6, was up-regulated by LPS treatment at the peak of inflammation (fold change of 48, $p = 0.002$; Fig. 4.3B). In contrast, in the presence of FhHDM-1, this gene was the most significantly down-regulated gene at the 6h time point (fold change of -188, $p = 0.0004$; Fig. 4.3B). Consistent with the reduced expression levels of this gene, the production of IL-6 protein was also significantly inhibited when LPS-stimulated macrophages were pre-treated with FhHDM-1 (5 and 15μM; Fig. 4.3D).

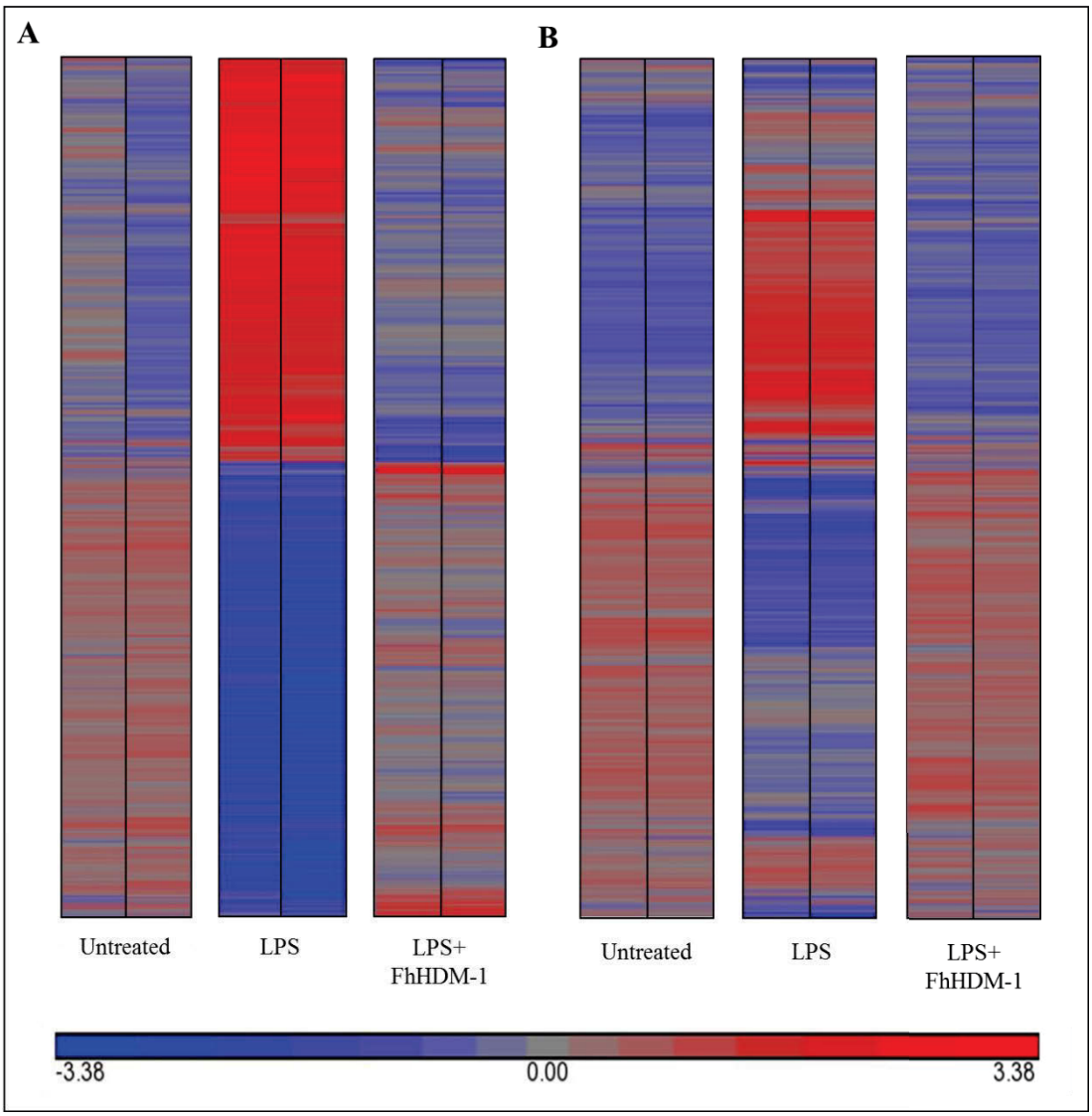

Figure 4.2 FhHDM-1 significantly alters the gene expression profile of LPS treated murine macrophages. BMDMs (1 x 10^6 cells/ml) were treated with FhHDM-1 (15µM; n = 2 replicates shown) for 1h, and then treated with LPS (10ng/ml) for **(A)** 6h or **(B)** 24h at 37ºC. RNA was isolated for Agilent microarray analysis. A heat map was generated from gene expression analysis with Partek Genomics Suite. The colour-code key indicates log-fold increases (red) or decreases (blue) in gene expression.

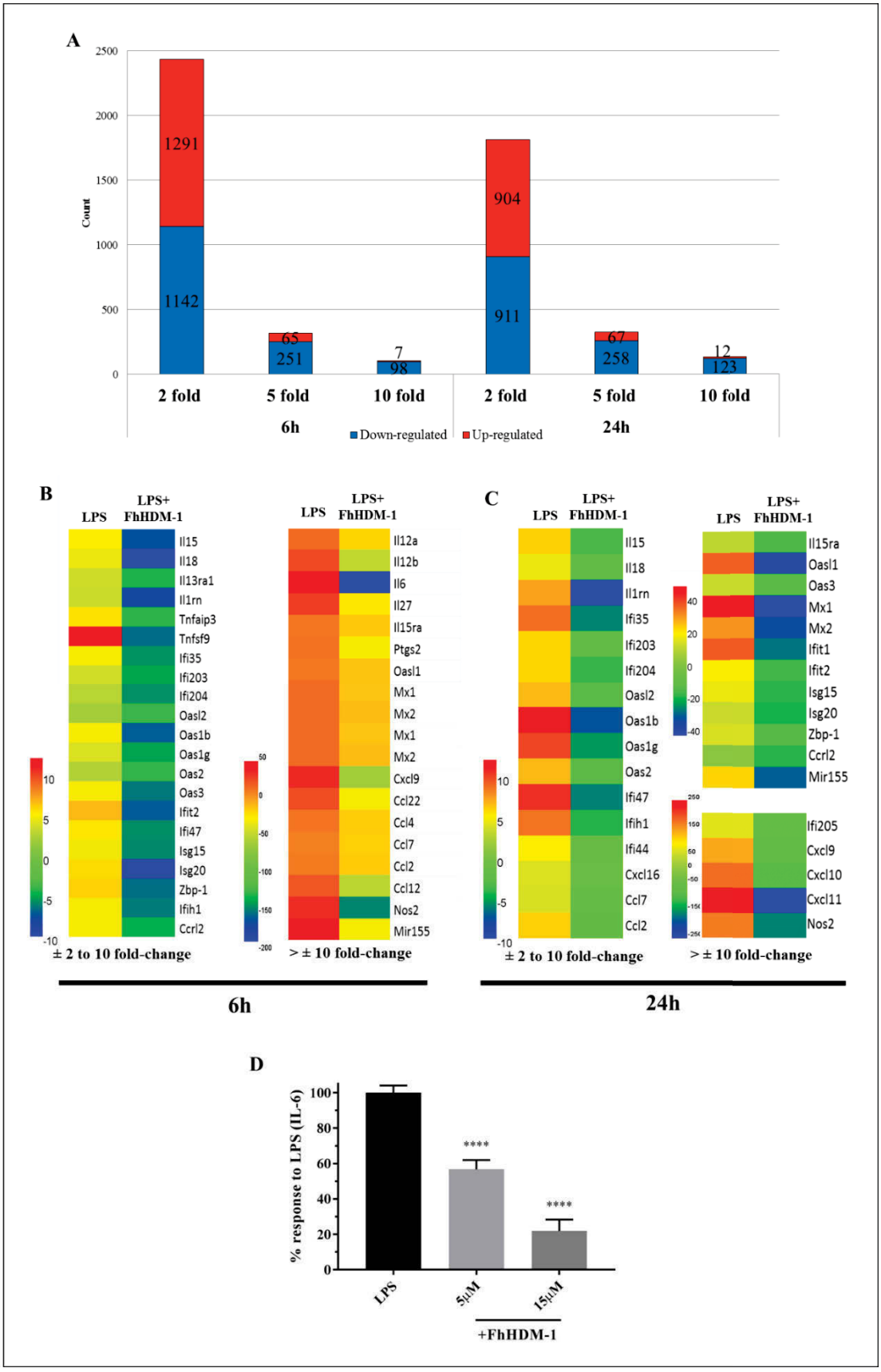
A
Count
2500
2000
1500
1000
500
0
1291
1142
65
251
7
98
904
911
67
258
12
123
2 fold
5 fold
10 fold
2 fold
5 fold
10 fold
6h
24h
Down-regulated
Up-regulated
B
LPS
LPS+ FhHDM-1
Il15
Il18
Il13ra1
Il1rn
Tnfaip3
Tnfsf9
Ifi35
Ifi203
Ifi204
Oasl2
Oas1b
Oas1g
Oas2
Oas3
Ifit2
Ifi47
Isg15
Isg20
Zbp-1
Ifih1
Ccrl2
± 2 to 10 fold-change
Il12a
Il12b
Il6
Il27
Il15ra
Ptgs2
Oasl1
Mx1
Mx2
Mx1
Mx2
Cxcl9
Ccl22
Ccl4
Ccl7
Ccl2
Ccl12
Nos2
Mir155
> ± 10 fold-change
6h
C
LPS
LPS+ FhHDM-1
Il15
Il18
Il1rn
Ifi35
Ifi203
Ifi204
Oasl2
Oas1b
Oas1g
Oas2
Ifi47
Ifih1
Ifi44
Cxcl16
Ccl7
Ccl2
± 2 to 10 fold-change
Il15ra
Oasl1
Oas3
Mx1
Mx2
Ifit1
Ifit2
Isg15
Isg20
Zbp-1
Ccrl2
Mir155
Ifi205
Cxcl9
Cxcl10
Cxcl11
Nos2
> ± 10 fold-change
24h
D
% response to LPS (IL-6)
100
80
60
40
20
0
****
****
LPS
5μM
15μM
+FhHDM-1

Figure 4.3 FhHDM-1 significantly down-regulates genes associated with inflammation, in LPS treated murine macrophages. Gene lists were created from one-way ANOVA comparisons of LPS and FhHDM-1 versus LPS-only treated BMDMs (cut-off at fold-change>2, p-value with FDR<0.05). **(A)** Numbers of genes that were up- and down-regulated by FhHDM-1 in the presence of LPS, in comparison to LPS-only samples, were categorised according to genes that were regulated more than 2, 5 or 10 fold at 6 and 24h. **(B,C)** Genes up-regulated by LPS-only samples were chosen for further analysis (from [275]), and compared with LPS and FhHDM-1 treated samples at (B) 6 and (C) 24h. Heat maps are categorised by genes that were regulated between 2 to 10 fold and greater than 10 fold. The '±' symbolises up- (+) and down- (-) regulation. **(D)** BMDMs (1 x 10^6 cells/ml) were treated with FhHDM-1, washed twice with saline prior to O/N stimulation with LPS (10ng/ml) at 37^{o}C. Cell supernatants were assayed for IL-6 via a multiplex. Data was converted to percentages with LPS-only stimulation adjusted to 100%. Data is the combination of two independent experiments, and expressed as means ± SEMs (statistical significance represents comparisons to the levels of TNF secreted by LPS-only samples; **** $p \leq 0.0001$).

4.3 Modulation of intracellular pathways in murine macrophages treated with FhHDM-1 in response to LPS stimulation

The array analysis clearly demonstrated that rather than targeting individual genes, FhHDM-1 treatment inhibited the expression of large numbers of genes in response to LPS stimulation, suggesting that whole pro-inflammatory pathways may be modulated. Therefore, the relationships between differentially expressed genes were analysed using Ingenuity Pathway Analysis® (IPA; Qiagen) to identify LPS-induced signalling pathways that were regulated by FhHDM-1 (Section 2.7.1). Within the top 30 significantly altered pathways at 6 (Fig. 4.4A) and 24h (Fig. 4.4B), the majority were inhibited. Unsurprisingly, those pathways were associated with the activation of the pro-inflammatory responses, including signalling by TREM1, pattern recognition receptor, IL-6, GM-CSF, interferon NF-κB, and toll-like receptor (Fig. 4.4A,B). Corroborating the evidence that treatment of macrophages with FhHDM-1 prevents the development of T1D in mice [132], the primary signalling pathways involved in inflammation and β-cell death were also predicted to be inhibited by the IPA analysis (pathway no. 19 and no. 26; Fig. 4.4A,B).

Of the top 30 pathways modulated at 6h, only seven pathways were predicted to be significantly activated in cells treated with both FhHDM-1 and LPS, as compared to cells stimulated with LPS only. Of these, the Liver X Receptor (LXR) activation pathway and the Peroxisome Proliferator Activated Receptor (PPAR) signalling pathway were the most highly activated (pathway no. 3 and no. 4, respectively; Fig. 4.4A). LXRs are nuclear receptors that are critical in cholesterol and fatty acid homeostasis [277, 278]. They are present on liver, intestine, kidney, spleen and adipose tissue, and work in partnership with the Retinoid X Receptor (RXR) as heterodimers when stimulated with natural ligands, such as oxysterols (monooxygenated derivative of cholesterol) [278]. LXRs have anti-inflammatory and immune regulatory roles [279], especially in macrophages, where they are able to trans-repress specific LPS stimulated pro-inflammatory genes [280, 281]. In the absence of LXR expression, mice are more susceptible to bacterial infection [282], and, furthermore, LXR agonists have been shown to reduce the incidence and inflammation in murine models of arthritis [283], MS [284], and other pro-inflammatory diseases [279, 285].

PPARs are also nuclear receptors vital for the regulation of lipid metabolism within cells. This leads to their critical role in the maintenance of alternatively activated macrophages, as up-regulation of fatty acid oxidation (by these PPARs) causes macrophages to develop an alternatively activated phenotype [286]. Furthermore, PPAR deficiency (in knockout mice) caused the loss of these anti-inflammatory macrophage populations, and promoted susceptibility to metabolic diseases, such as obesity-induced type 2 diabetes mellitus, non-alcoholic fatty liver disease [287], and insulin resistance [288].

There are two subtypes of LXRs: LXR-α and -β. Analysis of gene lists generated from the microarray analysis showed no difference in the fold change of *Nr1h3* and *Nrl1h2* (genes coding for LXR-α and -β, respectively) gene expression levels. For the PPARs, there are three subtypes: PPAR-α, -β/δ and -γ; which show distinct tissue distribution and ligand specificities [289]. Analysis of the gene lists showed no difference in the fold change of *PPAR-α* and *PPAR-β/δ* gene expression levels between the LPS-only versus LPS and FhHDM-1 treated samples. However, the expression of *PPAR-γ* was differentially regulated after LPS and FhHDM-1 treatment, as compared to LPS-only treatment. While the levels of *PPAR-γ* gene expression were down-regulated in response to LPS stimulation (fold changes of -5.33 and -8.4 for 6 and 24 h, respectively; Table 4.1), treatment of macrophages with FhHDM-1 prior to stimulation with LPS resulted in a significant increase in the expression levels of *PPAR-γ* (fold changes of 2.5 and 4.0 for 6 and 24h, respectively; Table 4.1). These combined observations of altered gene expression and predicted pathway activation, suggest that FhHDM-1 may be acting as a PPAR-γ agonist to mediate its anti-inflammatory effects.

Figure 4.4 FhHDM-1 represses pro-inflammatory signalling pathways. Generated gene lists of LPS versus untreated and LPS versus LPS and FhHDM-1 treatment were analysed with Ingenuity Pathway Analysis® to identify signalling pathways regulated by FhHDM-1 in the presence of LPS at **(A)** 6 and **(B)** 24h. The top 30 signalling pathways were ranked by the activation Z-score (with blue and orange indicating up- and down-regulation, respectively, of the signalling pathway by FhHDM-1).

Table 4.1 FhHDM-1 up-regulates *PPAR-γ* gene expression in response to LPS in murine macrophages.

Time point (h)	Samples comparison (Treatment 1 vs Treatment 2)	Fold change (Treatment 1 vs Treatment 2)	p-value (Treatment 1 vs Treatment 2)
6	LPS vs Untreated	↓ (-5.33)	$3.88E^{-09}$
24	LPS vs Untreated	↓ (-8.4)	$5.54E^{-10}$
6	LPS+FhHDM-1 vs LPS	↑ (2.5)	$4.02E^{-07}$
24	LPS+FhHDM-1 vs LPS	↑ (4.0)	$1.62E^{-08}$

LPS: Lipopolysaccharide; ↑ and ↓ denotes up- and down-regulation, respectively.

4.4 Assessment of the effect of FhHDM-1 as a PPAR-γ agonist

LXR and PPAR-γ agonists elicit overlapping, but distinct, repression patterns of specific pro-inflammatory genes in macrophages stimulated with various TLR ligands. Therefore, the differential expression of inflammatory genes is commonly utilised as a mechanism to elucidate a specific agonistic effect. For example, when macrophages are stimulated with LPS (TLR-4 ligand), *iNOS* gene expression levels are down-regulated by both LXR and PPAR-γ agonists, whilst only down-regulation of *iNOS* is observed with LXR agonists when macrophages are stimulated with Poly (I:C) (TLR-3 ligand) [280]. Furthermore, LXR agonists only reduce the gene expression levels of *IL1β* when macrophages are stimulated with LPS [and not Poly (I:C)]; whilst PPAR-γ agonists have no effect on the gene expression levels of *IL1β*, in response to LPS or Poly (I:C) stimulation of macrophages [280]. Thus, in order to confirm the predicted agonist effect of FhHDM-1 treatment, qRT-PCR was performed to quantify *IL1β* and *iNOS* gene expression levels in BMDMs treated with FhHDM-1, and subsequently stimulated with LPS or Poly (I:C) (Section 2.7.2). The genes were normalised to *Stx5a* expression levels, as it was identified to be the most stable reference gene expressed across the samples (Section 2.7.4). Consistent with the behaviour of a PPAR agonist, *IL1β* expression levels were unchanged in the presence of FhHDM-1, in response to both LPS and Poly (I:C) (Fig 4.5A). Furthermore, the expression levels of *iNOS* were significantly reduced by FhHDM-1 in response to LPS, but not in response to Poly (I:C) (Fig. 4.5B). This differential expression of genes in FhHDM-1 treated cells, is consistent with this peptide functioning as a PPAR-γ agonist.

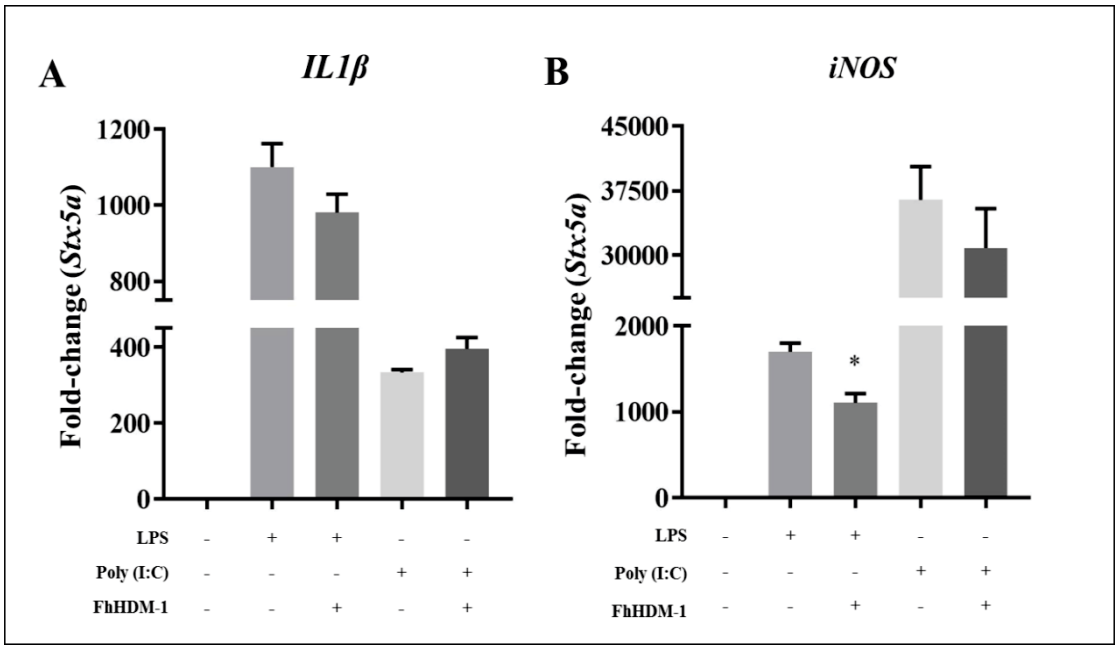

Figure 4.5 FhHDM-1 selectively down-regulates pro-inflammatory genes in response to TLR-4 and TLR-3 ligands. BMDMs (1 x 10^6 cells/ml) were treated with FhHDM-1 (2.5μM) for 1h, washed twice with saline, and then treated with LPS (10ng/ml) or Poly (I:C) (50ng/ml) for 6h at 37ºC. Messenger RNA was isolated, cDNA synthesised, and expression levels were analysed by quantitative real time RT-PCR. Fold changes in expression levels of **(A)** *IL1β* and **(B)** *iNOS* were calculated using the $\Delta\Delta C_t$ method. Genes were normalised to expression levels of *Stx5a*. Data is representative of four (A; LPS) and two [A; Poly (I:C)] and five (B; LPS) and three [B; Poly (I:C)] independent experiments, and is expressed as means ± SEMs (statistical significance was determined using a comparison to the gene expression levels after LPS or Poly (I:C) only treatment of macrophages; * $p \leq 0.05$).

The down-regulation of *Tnf* gene expression levels in macrophages has been observed with PPAR-γ agonists in response to both LPS and Poly (I:C) treatment of macrophages [290]. Consistent with the premise that it functions as a PPAR-γ agonist, FhHDM-1 has the ability to intracellularly modulate LPS stimulated macrophages to prevent the secretion of TNF (Section 4.2, Fig. 4.1B). In addition, FhHDM-1 reduced the production of TNF by macrophages in response to Poly (I:C) treatment, in a concentration dependent manner, in both non-washed and washed cells (Fig. 4.6A and B, respectively; Section 2.4.1). Furthermore, this inhibitory effect was also observed in peritoneal macrophages isolated from mice that had received intraperitoneal injections of FhHDM-1, and then stimulated *ex vivo* with Poly (I:C) (Fig. 4.6E; Section 2.4.1.2). These data indicate that FhHDM-1 exerts intracellular activity, and provides further evidence that the peptide is functioning as a PPAR-γ agonist.

Both LPS and Poly (I:C) signal through an adaptor protein, termed TRIF, for the production of pro-inflammatory interferons [291, 292]. The production of one of these interferons, IFN-β, in response to LPS and Poly (I:C) is negatively regulated by PPAR-γ agonists [293]. To determine whether FhHDM-1 also reduced the production of IFN-β by macrophages stimulated with both inflammatory ligands, an ELISA was performed. In support of the gene expression data, FhHDM-1 significantly inhibited the secretion of IFN-β by macrophages in response to both LPS (Fig. 4.6C) and Poly (I:C) (Fig. 4.6D), in a concentration dependent manner. The inhibitory effect was also observed in peritoneal macrophages isolated from FhHDM-1- treated mice and stimulated *ex vivo*, (Fig. 4.6F). These data again support the IPA prediction that FhHDM-1 functions as a PPAR-γ agonist.

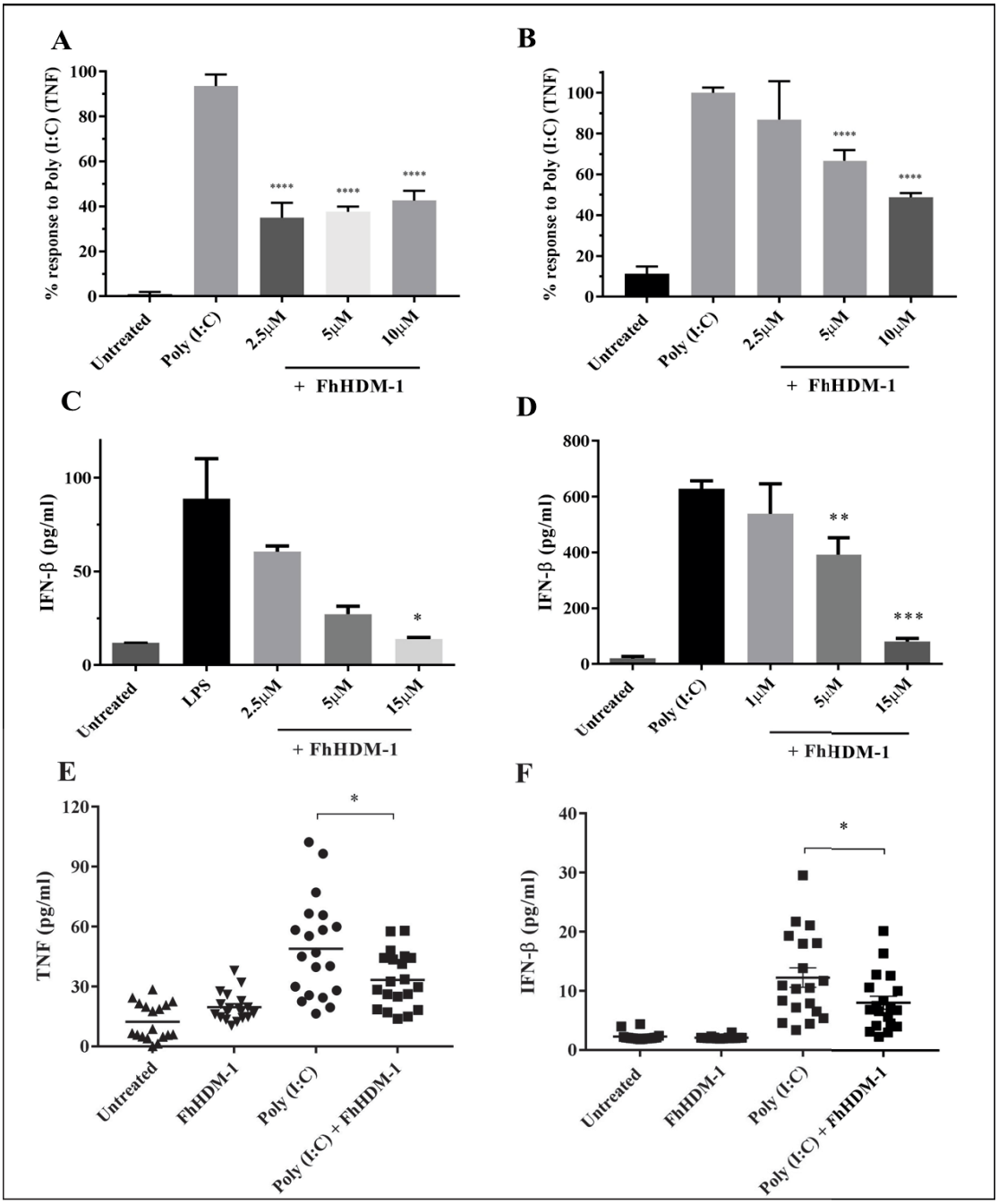

Figure 4.6 FhHDM-1 inhibits the production of pro-inflammatory cytokines, TNF and IFN-β, by LPS and Poly (I:C) stimulated murine macrophages. BMDMs (1 x 10^6 cells/ml) were treated with FhHDM-1 (at various concentrations) for 1h and then **(A,D)** treated immediately or **(B)** washed twice with saline prior to O/N stimulation with Poly I:C (20μg/ml) at 37ºC. **(C)** BMDMs (1 x 10^6 cells/ml) were treated with FhHDM-1 peptide (at various concentrations) for 1h and then stimulated with LPS (10ng/ml) for 3h at 37ºC. **(E,F)** BALB/c mice (n=20) were injected i.p. six times with 100μl of 0.1mg/ml of FhHDM-1 every second day prior to isolation of peritoneal macrophages. Cells were stimulated with Poly (I:C) (20μg/ml) and incubated for 18h at 37ºC. Cell supernatants were assayed for TNF and IFN-β. In A and B data was converted to percentage values with LPS-only stimulation samples adjusted to 100%. Data is the combination of four independent experiments (A,B) and three biological

Cont'

replicates (C,D). Data for E and F is collated from twenty mice. Error bars represent means ± SEMs (statistical significance was determined using comparisons to the levels of cytokines secreted by LPS- or Poly (I:C)-only samples; * $p \leq 0.05$, ** $p \leq 0.01$, *** $p \leq 0.001$, **** $p \leq 0.0001$).

Sequences for HDM-like peptides have been identified in the genome of all mammalian trematodes (Chapter 3, Section 3.3 and [199]). In addition, the analysis of changes in gene expression levels in macrophages treated with the synthetic HDM derived from the helminth parasite, *Opisthorchis viverrini* (Ov-HDM), showed that it regulated the gene expression of naïve macrophages in the same way as *Fasciola* FhHDM-1 (Chapter 3, Section 3.3, Table 3.2 and Section 3.4, Table 3.3), supporting a common mechanism of action for the parasite HDMs. Given the observation that FhHDM-1 was displaying PPAR-γ agonist activity, the repression of pro-inflammatory genes in macrophages treated with Ov-HDM was also assessed. Consistent with the result reported for FhHDM-1, the expression levels of *IL1β* in response to LPS stimulation was unaffected by the pre-treatment of macrophages with Ov-HDM (Fig. 4.7A), whilst *iNOS* expression was down-regulated (Fig. 4.7B). Although preliminary, this observation suggests that the family of parasite-derived HDM peptides exert similar biological activity in macrophages.

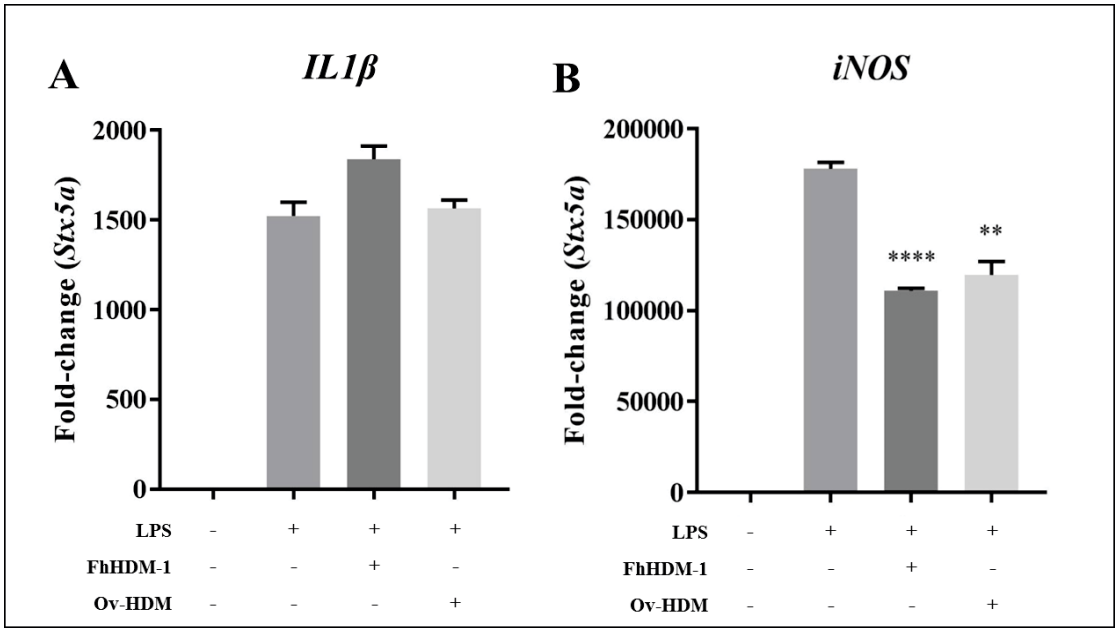

Figure 4.7 The helminth cathelicidin-like peptide from *Opisthorchis viverrini* also selectively down-regulates pro-inflammatory gene expression in macrophages in response to TLR-4 and TLR-3 ligands. BMDMs (1 x 10^6 cells/ml) were treated with FhHDM-1 or *Opisthorchis viverrini* peptide (Ov-HDM; 2.5μM) for 1 h, washed twice with saline, and then treated with LPS (10ng/ml) for 6h at 37ºC. Messenger RNA was isolated, cDNA synthesised, and the gene expression levels were analysed by qRT-PCR. Fold change in expression of **(A)** *Il1β* and **(B)** *iNOS* was calculated using the $\Delta\Delta C_t$ method. Genes were normalised to *Stx5a* expression levels. Data for FhHDM-1 is representative of four (A) and five (B) independent experiments. Data for Ov-HDM was from three biological replicates and is expressed as means ± SEMs (statistical significance was determined using a comparison to the gene expression of LPS only samples ** $p \leq 0.01$, **** $p \leq 0.0001$).

4.5 Discussion

This chapter further characterised the anti-inflammatory effects of FhHDM-1, and identified a selective down-regulation in the expression levels of pro-inflammatory genes when macrophages were exposed to the TLR-3 and TLR-4 ligands, Poly (I:C) and LPS, respectively (Section 4.4). This finding validated the global gene expression data, which predicted that FhHDM-1 treatment of macrophages promoted the activation of PPAR-γ signalling in response to TLR stimulation (Section 4.3).

While *in silico* analyses also predicted that the LXR/RXR pathway was induced, there was no evidence of enhanced expression levels of LXR genes in macrophages treated with both FhHDM-1 and LPS (Section 4.3). Further consideration of the alterations to expressed genes suggests that the prediction of LXR agonist activity may be due to common anti-inflammatory activities by LXRs and PPARs [280, 290]. Similar genes are repressed by both nuclear receptors, with *iNOS* being a common gene down-regulated by both LXR and PPAR-γ agonists [280] (and by FhHDM-1, as seen in Section 4.4, Fig. 4.5B). Furthermore, analyses of the genes from the LXR and PPAR pathways that were regulated by FhHDM-1 in LPS-stimulated macrophages showed that 11 genes were shared between both pathways. Due to this commonality, the pathway analysis likely predicted the activation of the LXR nuclear receptor. The subsequent and more comprehensive analysis of differential gene expression using different ligands, however, suggested that FhHDM-1 is unlikely to be using LXRs to mediate its inhibitory effect on macrophages. Thus, for the first time, the data produced here supports a hypothesis that FhHDM-1 is acting as a PPAR-γ agonist to mediate its anti-inflammatory effect.

Despite the evidence of differential gene expression induced by FhHDM-1, used here to support the predicted PPAR-γ agonist effect, there is contradiction in the literature as to which genes are selectively regulated by PPAR-γ agonists. The choice of genes used for the FhHDM-1 study was based on multiple studies by Ogawa *et al.,* which reported specific regulation of pro-inflammatory genes by PPAR-γ agonists in response to LPS and Poly (I:C) [280, 290]. This included the down-regulation of *Tnf* gene expression in macrophages in response to LPS and Poly (I:C); *iNOS* gene expression in

macrophages in response to LPS, but not Poly (I:C); and no effect on the gene expression of *IL1β*, in response to both LPS and Poly (I:C) [280, 290]. This is in agreement with studies using the PPAR-γ agonists, Pioglitazone (in human monocytes) [294] and 15-Deoxy-$\Delta^{12,14}$-prostaglandin J_2 (in murine macrophages) [295], which both reported inhibition of TNF production, in response to LPS. In contrast, it has been reported that the PPAR agonist, Troglitazone, does not suppress TNF production by macrophages in response to either LPS or Poly (I:C) [293]. Similarly, while the PPAR-γ agonists, GW7845 [290] and GW1929 [296, 297], suppress the production of IL-6 by LPS and Poly (I:C) stimulated murine macrophages, no inhibition of IL-6 protein secretion was observed in macrophages treated with Troglitazone [293]. Given these contrasting activities, to definitively prove an agonist effect for FhHDM-1, a direct measurement of PPAR activation should be completed.

To date, the mechanism of PPAR-γ trans-repression of genes is shown to involve a series of processes. Firstly, PPAR-γ agonists stimulate PPAR-γ to become SUMOylated (a process in which small ubiquitin-like modifier [SUMO] proteins attach to lysine residues in target proteins) [295]. Consequently, PPAR-γ blocks the release of nuclear receptor corepressor (NCoR) complexes [286], which are critical for actively silencing inflammatory genes within resting macrophages [286]. Thus, chromatin immunoprecipitation (ChIP) assays could be performed to determine whether FhHDM-1 prevents NCoR clearance and induces PPAR-γ recruitment to the promotor of *iNOS* (the gene observed to be inhibited by FhHDM-1).

The activation of PPAR-γ in macrophages has been linked to the alteration of metabolic activity within cells, specifically mediating a switch towards the use of oxidative phosphorylation rather than glycolysis. Importantly, the induction of glycolytic pathways is associated with the development of pro-inflammatory M1 macrophages [268], which are known to mediate a number of autoimmune diseases, such as T1D and MS [34]. Although there is no evidence directly reporting the attenuation of these diseases through modulation of macrophage metabolism, there is some evidence that agents, such as anti-glycolytics and antioxidants, regulate immune-metabolism and have therapeutic potential for the treatment of immune-mediated disease. For example, the anti-glycolitic, Rapamycin, an immunosuppressant drug widely used during organ transplantation [298], inhibits glucose metabolism and has shown efficacy in inhibiting

the development of murine MS [299]. Antioxidants scavenge and reduce the reactive oxygen species (ROS) that exacerbate autoimmunity [300]. Such examples of their therapeutic effect in autoimmunity include: epigallocatechin-3-gallate (found in green tea) ameliorated murine MS [301]; Resveratrol protected mice from developing rheumatoid arthritis [302]; and manganese prophyrins decreased aerobic glycolysis and prevented the development of T1D in mice [303-305]. With evidence highlighting the importance of metabolic activity in macrophage functions, and the involvement of PPAR-γ in this process, the likelihood that FhHDM-1 modulates metabolic activity to influence the inflammatory state of macrophages, and thus prevent immune mediated disease such as T1D and MS, warrants further investigation.

The use of PPARγ agonists has been widely acknowledged as an effective treatment strategy for inflammatory disorders, including type 2 diabetes mellitus [306] and dyslipidemia [307]. There is emerging evidence that PPAR-γ agonists have therapeutic potential in autoimmune/inflammatory disorders, such as psoriasis and psoriatic arthritis [308], inflammatory bowel diseases [309, 310], and RA [311, 312]. Experimentally, PPAR-γ agonists, have been shown to significant reduce the incidence of both T1D [313-317], and MS [318-322] in murine models. In clinical studies, patients with established T1D, who received the PPAR-γ agonist, Pioglitazone, showed moderate improvements in glycemic control [323-325]. In trials testing Pioglitazone in patients with relapsing remitting MS, there was no significant difference on the expanded disability status scale (used to quantify MS development) between the placebo and treatment groups after a year, however, magnetic resonance images showed reduced atrophy and lesions in those receiving Pioglitazone [326]. There have also been population-based studies that have associated PPAR-γ polymorphisms with delayed onset of MS in patients [327]. Although the precise mechanisms of action of such PPAR-γ agonists is not yet known, there is an overall dampening of the pro-inflammatory immune responses [289], which is an effect observed when FhHDM-1 has been used to protect mice from autoimmune disease.

Chapter 5: Determining the minimal bioactive derivative of FhHDM-1

5.1 Introduction

As previously described (Section 1.7), FhHDM-1 is a 68mer alpha helical peptide with an amphipathic C-terminus. Biochemical analysis showed that mammalian lysosomal cathepsin L, cleaved the full-length peptide to release a 21mer amphipathic C-terminal region (termed FhHDM-1.p2), which, in turn, inhibited lysosomal vATPase activity *in vitro* [215]. Disruption of the alpha helix structure, or the amphipathicity of FhHDM-1.p2, abolished biological activity [215]. Collectively, this data suggested that this 21mer amphipathic C-terminal region was the bioactive portion of FhHDM-1 [215]. However, when macrophages were treated with FhHDM-1.p2, an inhibitory effect on lysosomal function was not observed [221]. Furthermore, FhHDM-1.p2 did not protect NOD mice from developing T1D (Donnelly *et al.*, unpublished data). Therefore, whilst the biological activity of FhHDM-1 was clearly attributable to the presence of the alpha helix amphipathic C-terminus, the cellular and *in vivo* data suggest a requirement for all, or part, of the N-terminus for binding, uptake and delivery of the bioactive C-terminus to the lysosome of macrophages. Exposure of the full length FhHDM-1 to the Cathepsin L1 cysteine protease secreted by *F. hepatica*, also resulted in cleavage of the peptide and the release of the p2 peptide [199]. However, like the lysosomal Cathepsin L, this only occurs at an acidic pH, which may reflect a mechanism by which the helminth parasite controls the activation of the FhHDM-1 peptide.

Cell-penetrating peptides (CPPs) are a group of small peptides, which promote the transport of molecular cargo across the plasma membrane, thereby providing cellular and subcellular specificity [328, 329]. Structurally, CPPs can be linear, cyclic, cationic (rich in R and K residues), anionic, hydrophobic, hydrophilic, amphipathic, non-amphipathic, random-coiled, α-helical, or β-sheet in formation [330]. However, more than half of the known CPPs contain amphipathic α-helices [331]. Notably, the N-terminal region of FhHDM-1 contains a high proportion (33.4%) of R and K residues, and its predominant secondary structure adopts an alpha helical formation. This observation, combined with the cellular analysis, suggests that a CPP exists within the sequence of FhHDM-1, and that this structure is required for the internalisation of FhHDM-1.

To investigate the existence of a CCP region, the sequence of FhHDM-1 was assessed by the predictive software, CPPpred [238] (Fig. 5.1A), which ranks peptides from 0 to 1, according to predictive algorithms that determine the probability that a peptide is cell-penetrating (Section 2.8). Scores closer to 1 indicate that CPPpred is more confident that the peptide will be cell-penetrating, while scores closer to 0 suggest that the peptide is highly unlikely to be cell-penetrating. To locate any potential CPP domains within FhHDM-1, the sequence was analysed in three sections: the N-terminus, the middle section, and the amphipathic C-terminus. In agreement with the cellular assays, the C-terminus was awarded a score of 0.255. Similarly, the 14 amino acid sequence from N-terminus (FhHDM-1.N) was also given a low score (0.319). However, analysis of the middle peptide section (FhHDM-1.M) generated a score of 0.682, indicating the likely presence of a CPP sequence in FhHDM-1. Further analysis of different amino acid sequences within this region revealed that a sequence of 5 amino acids, 'KARDR', located to the N-terminus side of the amphipathic region, generated the highest score (0.799). Based on this analysis, a series of peptide derivatives of FhHDM-1 were synthesised (kindly provided by Prof. John Dalton, Queen's University, Belfast, Ireland) for assessment of cellular uptake and biological activity (Fig. 5.1B). Throughout this chapter FhHDM-1.p2 has been termed FhHDM-1.C1.

A

Peptide description	Sequence	Score (0-1)
FhHDM-1.N	SEESREKLRESGRK	0.319
FhHDM-1.M	SGRKMVKALRDAVTKAYEKARDRAMAYLA	0.682
Amphipathic helix region	ITEVITILLNRLTDRLEKYAG	0.255
Carrier-protein	KARDR	0.799
Carrier-protein + 4AA towards N-terminus (FhHDM-1.C3)	KAYEKARDR	0.523
Carrier-protein + 2AA towards N-terminus (FhHDM-1.C4)	YEKARDR	0.429
Truncated FhHDM-1.C1	AMAYLAKDNLGEKITEVITILLNRLTDRLE	0.258

B

```
FhHDM-1     SEESREKLRESGRKMVKALRDAVTKAYEKARDRAMAYLAKDNLGEKITEVITILLNRLTDRLEKYAGN

FhHDM-1.M             SGRKMVKALRDAVTKAYEKARDRAMAYLA

FhHDM-1.N   SEESREKLRESGRK

FhHDM-1.C1                                      AMAYLAKDNLGEKITEVITILLNRLTDRLEKYAGN

FhHDM-1.C2.                                   KARDRAMAYLAKDNLGEKITEVITILLNRLTDRLEKYAGN

FhHDM-1.C3                                 KAYEKARDRAMAYLAKDNLGEKITEVITILLNRLTDRLEKYAGN

FhHDM-1.C4                                   YEKARDRAMAYLAKDNLGEKITEVITILLNRLTDRLEKYAGN

FhHDM-1.C5                                    KARDRAMAYLAKDNLGEKITEVITILLNRLTDRLEK
```

Figure 5.1 A sequence of 5 amino acids located to the N-terminus side of the amphipathic region of FhHDM has cell-penetrating capability *in silico*. (A) An *in silico* analysis was conducted using CPPpred, where different sections of the full length FhHDM-1 were scored for cell-penetrating capability. A score above 0.5 suggests that the peptide is cell-penetrating. Scores closer to 1 indicate a higher confidence that the peptide will be cell-penetrating, and scores closer to 0 suggest that the peptide is very unlikely to be cell-penetrating. **(B)** Sequences were derived from the full-length FhHDM-1 using CPPpred analysis. FhHDM-1.M is the middle section, which excludes both the amphipathic helix and the end terminus. FhHDM-1.N is the N-terminus of the peptide, and FhHDM-1.C1 (also known as FhHDM-1.p2) is the C-terminus section. Variations of the FhHDM-1.C1 peptides were designed based on the CPPpred analysis, where an additional 5 amino acids (carrier protein-like sequence) towards the N-terminus were included (indicated in red). FhHDM-1.C3 and FhHDM-1.C4 include an additional 4 and 2 amino acids, respectively (indicated in green), whilst FhHDM-1.C5 is a truncated form of FhHDM-1.C2 from the C-terminus.

5.2 Assessment of the ability of FhHDM-1, and its peptide derivatives, to inhibit TNF cytokine secretion by LPS stimulated macrophages

To initially screen the bioactivity of the FhHDM-1 peptide derivatives, their ability to inhibit the production of TNF by macrophages stimulated with LPS was assessed. RAW 264.7 macrophages were treated with FhHDM-1, or the various peptide derivatives (15µM), for 1h, prior to O/N stimulation with LPS (10ng/ml) (Section 2.4.1). As expected, treatment of macrophages with LPS induced the production of TNF (6332 ± 177 pg/ml), which was significantly reduced when cells were pre-treated with the full length FhHDM-1 (3832 ± 336 pg/ml; p= 0.0060; Fig. 5.2A). While the amphipathic FhHDM-1.p2 peptide (here termed FhHDM-1.C1) displayed an inhibitory effect, in agreement with previous cellular assays, this effect was significantly less pronounced than that observed for the full-length peptide (p= 0.0258). Also consistent with previous observations, peptides missing some (FhHDM-1.C5) or all (peptides N and M) of the amphipathic helix showed no inhibitory effect on TNF production. However, the addition of the N-terminal 'KARDR' sequence to the amphipathic C-terminus (i.e. FhHDM-1.C2; Fig. 5.2A) inhibited TNF production to the same extent as the full length FhHDM-1. Extension of this N-terminal sequence (FhHDM-1.C3 and C4) did not enhance the biological activity any further. These data suggest that the amino acid sequence KARDR may represent an essential cell penetrating sequence, which directs the peptide to the lysosome.

As FhHDM-1.C2 was the shortest sequence that inhibited TNF production, and therefore the minimal bioactive derivative, this peptide was selected for further analysis. Comparison of log-doses of FhHDM-1 and FhHDM-1.C2 (Fig. 5.2B; Section 2.4.1) showed no difference in the activity of these peptides. As shown in Figure 5.2B, the curves for both peptides were identical (p = 0.0990), revealing no difference in the EC50s (0.8215 and 0.9846 for FhHDM-1 and FhHDM-1.C2, respectively). This suggested that FhHDM-1.C2 exerted similar inhibitory activity, as compared to the full-length peptide.

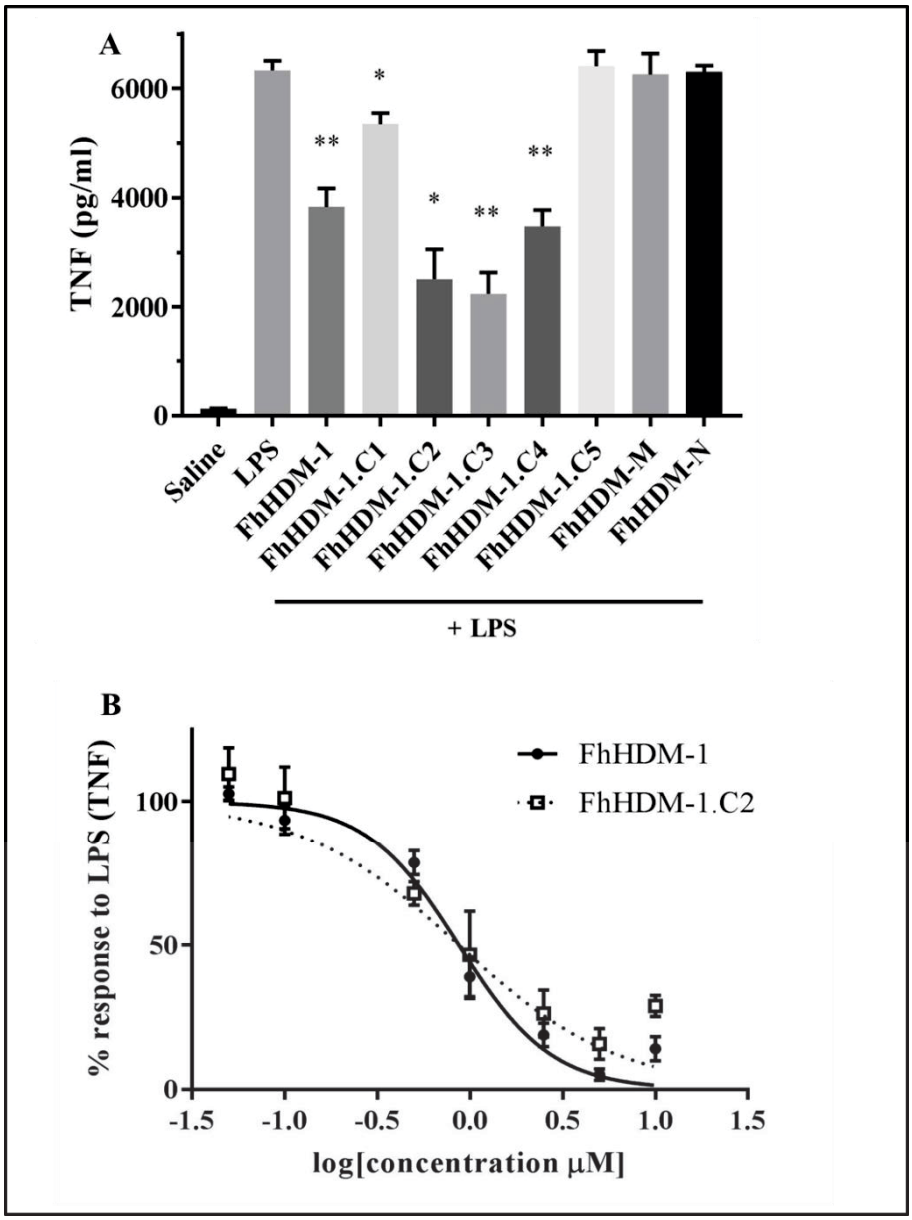

Figure 5.2 The complete amphipathic helix and the N-terminal amino acids of FhHDM-1 are required for the suppression of TNF production by LPS stimulated RAW 264.7 macrophages. (A) RAW 264.7 macrophages (1 x 10^6 cells/ml) were treated with FhHDM-1, or the peptide derivatives (15μM), for 1h prior to O/N stimulation with LPS (10ng/ml). Cell supernatants were assayed for TNF. Data is representative of two independent experiments and expressed as a means of triplicates ± SEMs (statistical significance represents a comparison to the levels of TNF secreted by LPS-only samples; * $p \leq 0.05$, ** $p \leq 0.01$). **(B)** RAW 264.7 macrophages (1 x 10^6 cells/ml) were treated with FhHDM-1 and FhHDM-1.C2 at various concentrations for 1h prior to O/N stimulation with LPS (10ng/ml). Dose response curves were generated by adjusting LPS-only stimulation to 100%, and then calculating the amount of TNF produced by LPS stimulated macrophages in the presence of FhHDM-1 and FhHDM-1.C2 as percentages. Data is the combination of three independent experiments and expressed as means ± SEMs.

It has been previously shown that FhHDM-1 binds LPS, an ability that is mediated by the presence of the amphipathic region [199, 214]. Therefore, any inhibitory effect on the ability of macrophages to produce pro-inflammatory cytokines may be attributable to the ability of FhHDM-1 peptide derivatives to bind LPS, and hence prevent pro-inflammatory stimulation of macrophages. To demonstrate that FhHDM-1.C2 was not simply 'mopping up' LPS, thereby preventing its ability to stimulate macrophages, cells were incubated with the peptides for 1h, and then washed to remove excess peptide, prior to the addition of LPS (Section 2.4.1). Under these experimental conditions, FhHDM-1 and FhHDM-1.C2 retained their ability to significantly inhibit TNF production in response to LPS stimulation, in both RAW 264.7 macrophages and BMDMs (Fig. 5.3). In comparison, FhHDM-1.C1 had no inhibitory effect on TNF production (Fig. 5.3B), which supports the premise that the C-terminal region alone is not effectively internalised by macrophages. Collectively, these data suggest that the ability of the peptides to prevent LPS stimulation of macrophages is not attributable to LPS binding. Rather these data indicate that the 'KARDR' sequence mediates the uptake and lysosomal localisation of FhHDM-1 and FhHDM-1.C2, resulting in the inhibition of intracellular signalling pathways.

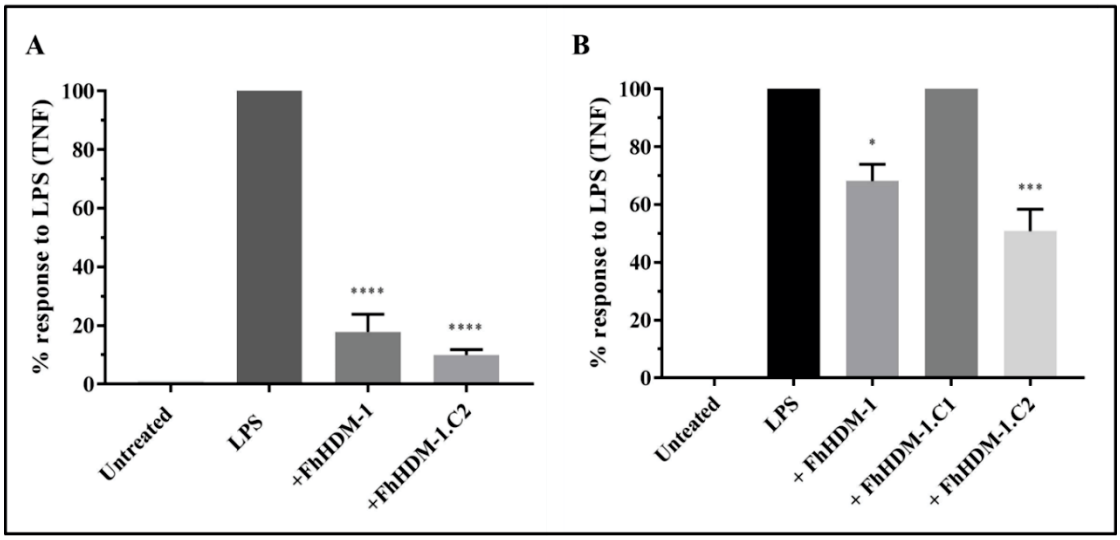

Figure 5.3 FhHDM-1 and FhHDM-1.C2 directly modulate macrophage function to prevent TNF production. (A) RAW 264.7 macrophages and **(B)** BMDMs (1 x 10^6 cells/ml) were treated with FhHDM-1 and FhHDM-1.C2 (15μM) for 1h, and then washed with saline twice, prior to O/N stimulation with LPS (10ng/ml). Cell supernatants were assayed for TNF secretion. Data was converted to percentage values with LPS-only stimulation samples adjusted to 100%. Data is the combination of three and two, (A) and (B), respectively, independent experiments and expressed as means ± SEMs (** $p \leq 0.01$, *** $p \leq 0.001$, **** $p \leq 0.0001$).

5.3 Determination of FhHDM-1 and FhHDM-1.C2 cytotoxicity

Mammalian cathelicidin peptides function as effective antimicrobial agents by inserting into bacterial membranes to induce cell death. However, this ability also makes cathelicidin peptides cytotoxic to mammalian cells [210]. It has previously been shown that, despite having similar structural features to the mammalian cathelicidins, FhHDM-1.C1 neither displayed bactericidal activity nor cytotoxicity to mammalian cells [210]. However, to ensure that the addition of the 'KARDR' sequence did not introduce a cytotoxic effect, the uptake of TOPRO-3 by peptide-treated cells was measured [210]. When a cell is undergoing death, the plasma membrane is compromised allowing uptake of the fluorescently labelled TOPRO-3. Thus, RAW 264.7 macrophages incubated with TOPRO-3 were analysed by flow cytometry for 6000msec (Fig. 5.4A; Section 2.5.5.1). Peptides were then added to the cells (20μM; as indicated by the red arrow on Fig. 5.4A), and the continued uptake of TOPRO-3 was recorded for a total of 28000msec. As expected, the addition of saline (negative control) to cells did not alter the uptake of TOPRO-3, whilst treatment with CRAMP (murine cathelidicin) immediately and significantly increased the fluorescent signal, indicating instant cellular death. In comparison, and as previously described, FhHDM-1.C1 induced only a marginal increase in TOPRO-3 fluorescence. Similarly, the full length FhHDM-1 and FhHDM-1.C2 induced minimal cell death, with only a slight increase in fluorescence being observed, as compared to treatment of macrophages with CRAMP.

To confirm these results, the release of lactate dehydrogenase (LDH; a soluble cytosolic enzyme released upon loss of membrane integrity) was also measured (Section 2.4.2.1). RAW 264.7 macrophages were incubated with varying concentrations of FhHDM-1 or FhHDM-1.C2 for 1h at 37^{o}C. The amount of LDH released by macrophages was calculated as a percentage, where complete cell lysis induced by a detergent (positive control) was adjusted to 100%. Saline and DMSO (vehicle controls), were used as negative controls to determine baseline levels of LDH released by resting cells (Fig. 5.4B; blue horizontal line). Neither the full length FhHDM-1 nor the FhHDM-1.C2 peptide (even at a concentration of 20μM) resulted in a significant release of LDH above baseline levels (in the presence of saline or DMSO). These data corroborated the data using TOPRO3 to assess cell death. Therefore, FhHDM-1 and FhHDM-1.C2 were

not cytotoxic to macrophages, and, therefore, their ability to inhibit TNF production by macrophages could not be attributed to the induction of cell death.

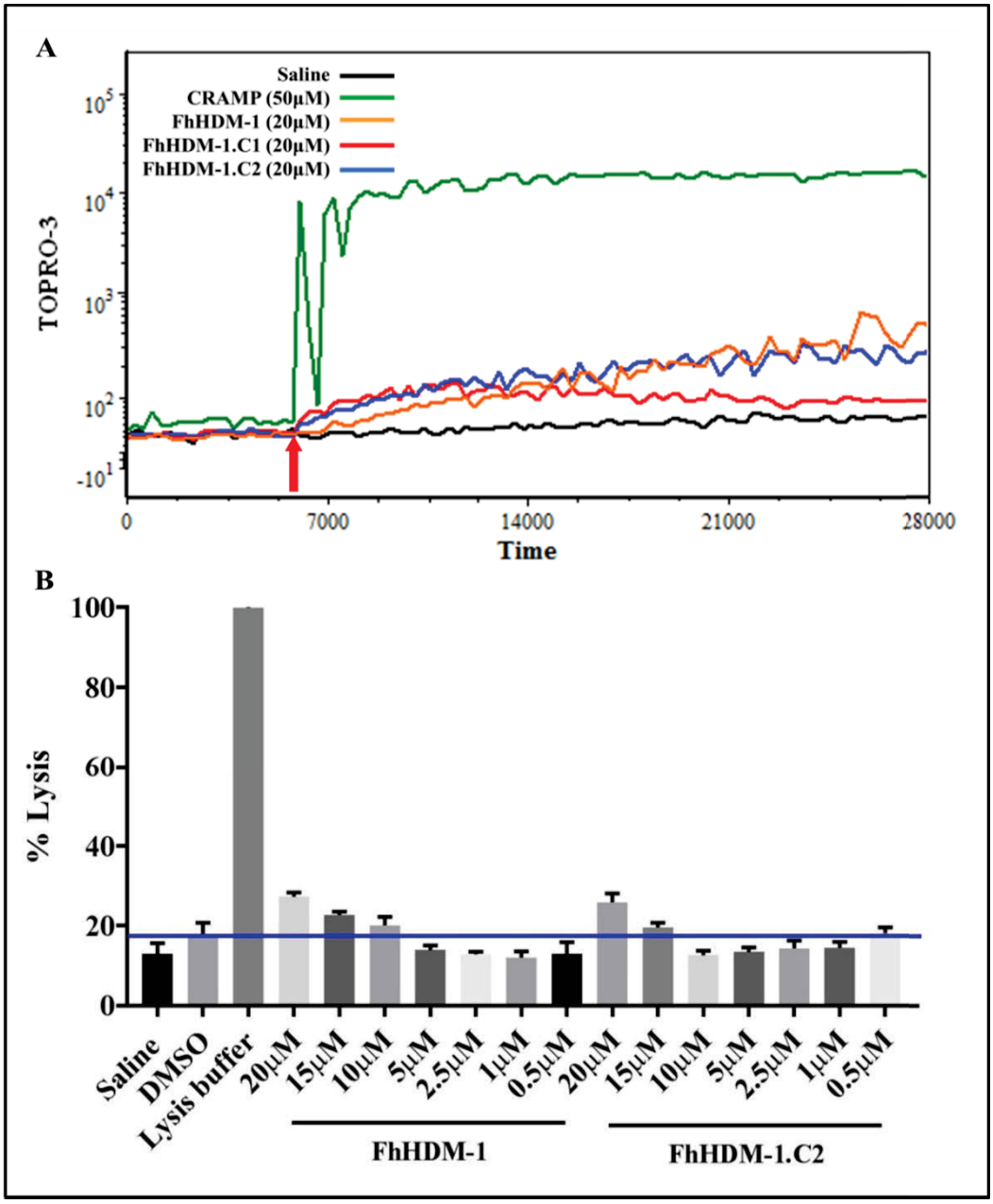

Figure 5.4 FhHDM-1 and FhHDM-1.C2 are not cytotoxic to macrophages. (A) RAW 264.7 macrophages (1 x 10^6 cells/ml) were analysed by flow cytometry for the uptake of the vital fluorescent dye, TOPRO-3. Fluorescence was recorded for the first 6000msec, and then peptides (FhHDM-1, FhHDM.C1, FhHDM.C2 [20µM], or CRAMP [50µM]) were added, as indicated by the red arrow. The uptake of TOPRO-3, was measured for a further 28000msec. Data shown is representative of four independent experiments. **(B)** RAW 264.7 macrophages (1 x 10^6 cells/ml) were incubated with varying concentrations of FhHDM-1 and FhHDM-1.C2 for 1h. The release of LDH by cells was measured and expressed as the percentage of cells treated with lysis buffer (normalised to 100%). The blue horizontal line indicates baseline levels of LDH released by DMSO treated cells. Data shown are representative of three independent experiments and presented as means ± SEMs.

5.4 Assessment of the ability of FhHDM-1 and FhHDM-1.C2 to bind murine macrophages

The mechanisms by which CPPs promote the uptake of associated molecules are influenced by the physico-chemical properties of the penetrating peptide, the associated molecular cargo, and the type of cell/tissue. Two general models of uptake have been proposed: (i) energy-independent translocation across the plasma membrane to the cytosolic compartment [332, 333], and (ii) endocytosis [334, 335]. It has already been established that the uptake of FhHDM-1 by macrophages occurs via energy dependent endocytosis [215]. To determine whether the addition of the 'KARDR' sequence to the amphipathic C-terminus of FhHDM-1 is sufficient to mediate uptake and targeting to the endolysosome, the binding and localisation of fluorescently labelled FhHDM-1.C2 was investigated. As previously described (Section 2.2.2), FhHDM-1.C2 was fluorescently labelled with Alexa Fluor 488 (direct detection) or synthesised with a biotin tag (indirect detection using an Alexa Fluor 488-labelled streptavidin).

To determine the ability of the peptide to bind to macrophages, and to assess the contribution of any passive uptake, RAW 264.7 macrophages were incubated with biotin-labelled FhHDM-1.C2 (5μM) at 4^{o}C for 30min (Section 2.5.4.2). As a comparative control, the binding of a biotin-labelled FhHDM-1.C1 to macrophages was also assessed. The incubation was conducted at 4^{o}C to decrease the metabolism of macrophages, which allows discrimination of peptide/macrophage interaction from active uptake of the peptides. The addition of FhHDM-1.C1 resulted in a small, yet significant, increase in the fluorescence of macrophages, as compared to controls ($p=0.0167$; Fig. 5.5B), suggesting an interaction. However, the addition of FhHDM-1.C2 resulted in a much greater increase in fluorescence levels ($p = 0.0028$; Fig. 5.5B). This significant difference in the peptides binding capabilities is further reflected by the large differences in MFIs (390 ± 30 and 2048 ± 101, for FhHDM-1.C1 and FhHDM-1.C2, respectively; $p = 0.0020$; Fig. 5.5B). This data confirms the predictive CPP analysis that the addition of the 'KARDR' sequence enhances the ability of the peptides to interact with macrophages.

To further confirm that FhHDM-1.C2 was binding to macrophages, and to compare its binding ability to the full length peptide, RAW 264.7 macrophages and BMDMs were incubated with Alexa Fluor 488 labelled FhHDM-1 and FhHDM-1.C2 (2.5μM) at 4ºC for 30min (Section 2.5.4.1). As expected, the peptides interacted with both cell types, as indicated by the increased fluorescence of the cells, as compared to controls (Fig. 5.5C,E). From these data sets, the MFIs of FhHDM-1 samples in both cell types were significantly greater, as compared to FhHDM-1.C2 samples (Fig. 5.5D,F). While this observation suggests that the shorter C2 peptide may bind with less efficiency, this data must be interpreted with caution. To fluorescently label these peptides, the Alexa Fluor tag is attached to the primary amines of amino acids [336]. With FhHDM-1.C2 being a much shorter sequence, there is likely less dye attached, as compared to the full-length peptide, which in the flow cytometric analysis may present as reduced fluorescence, and hence be interpreted as reduced binding, even though the amount of Alexa-Fluor dye may not necessarily equate to the number of peptides that have bound to the cells. In comparison, the biotin-labelled peptides (Figure 5.5A) were synthesized to have only a single biotin moiety per molecule, thereby allowing quantitative comparisons of binding. Therefore, a quantitative comparison of binding cannot be made between these two peptides using this experimental approach. However, as there was a significant increase in fluorescence intensity as compared to the unstained samples, it can be concluded that both FhHDM-1 and FhHDM-1.C2 bind to macrophages.

It has been recently reported, that the murine cathelicidin, CRAMP, has the ability to prevent T1D in murine models. The ability of CRAMP to prevent autoimmunity was attributed to its interaction with the epidermal growth factor receptor (EGFR), which was expressed on intra-islet macrophages [337]. Through its interaction with EGFR, CRAMP was able to induce regulatory macrophages, which subsequently activated disease protective Tregs [337]. Due to their classification as cathelicidin-like peptides, FhHDM-1 and FhHDM-1.C2 were thus assessed for their ability to interact with EGFR. Here, baby hamster kidney (BHK) cells that had been transfected to express either low or high levels of EGFR (provided by Professor Thomas Valerius from Christian-Albrechts-University and University Hospital Schleswig-Holstein, Germany) were incubated with Alexa Fluor 488-labelled FhHDM-1 or FhHDM-1.C2 (2.5μM) at 4ºC for 30min (Section 2.5.4.1). The BHK cells were also confirmed for their high- or low-expression of EGFR via flow cytometry (Section 2.5.3.5). There was no difference in

the quantity of Alexa Fluor 488 fluorescence detected using either EGFR high- or low-expressing cells. These data suggest that there was no increase in the levels of FhHDM-1 binding with increased levels of EGFR expression (Fig. 5.5G). Similarly, there was no difference in fluorescence levels between the EGFR high or low expressing cells after co-culture with FhHDM-1.C2 (Fig. 5.5H). Therefore, it can be concluded that neither FhHDM-1 nor FhHDM-1.C2 interact with EGFR. Interestingly, cells incubated with FhHDM-1 displayed a higher level of fluorescence than those treated with the FhHDM-1.C2 derivative. This may indicate a differential preference between the peptides for yet to be identified receptors, or a level of non-specific binding mediated by the full-length peptide.

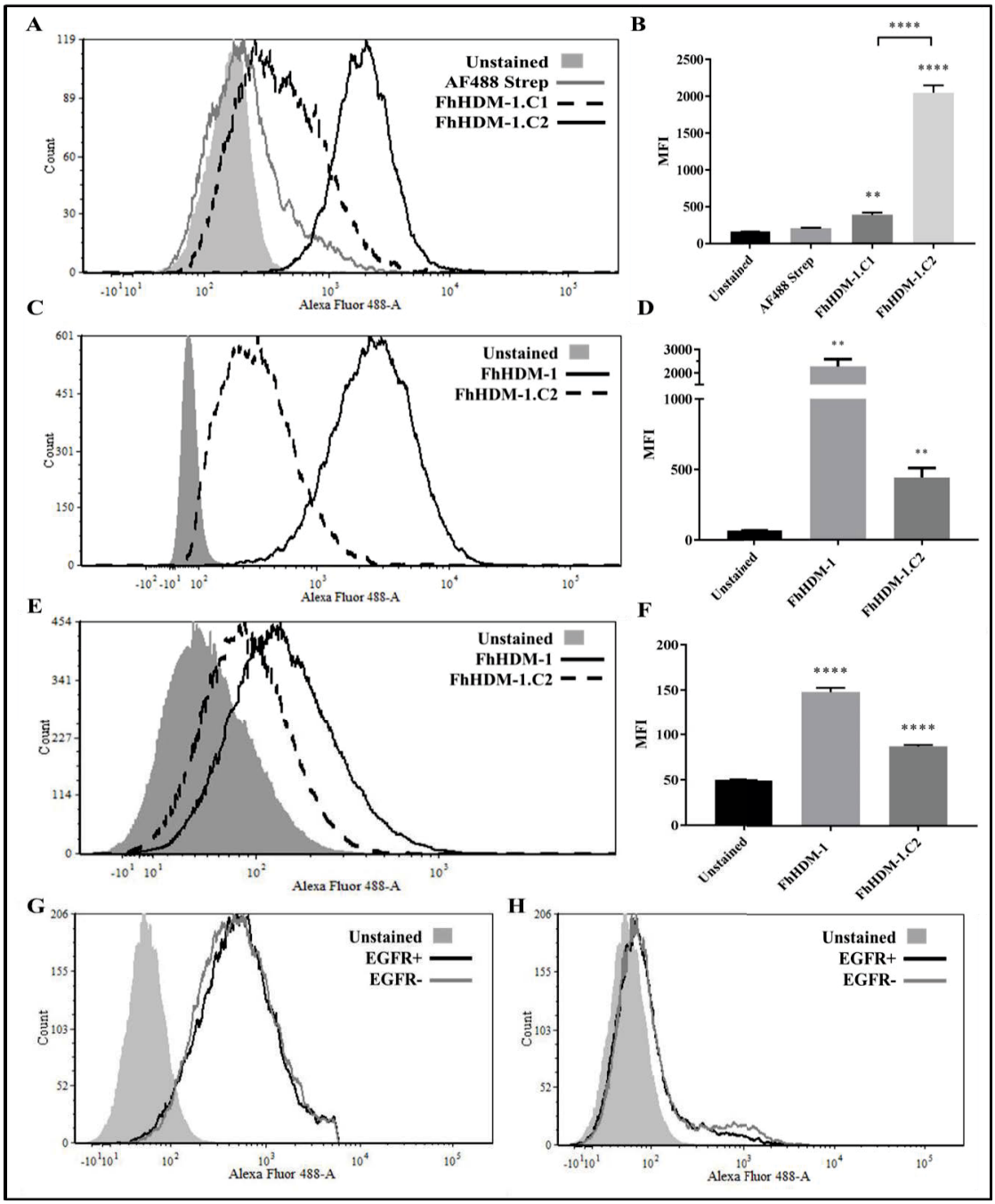

Figure 5.5 FhHDM-1.C2 binds to murine macrophages to a similar extent as full length FhHDM-1. (A) RAW 264.7 macrophages (1 x 10^6 cells/ml) were incubated with biotin-labelled FhHDM-1.C1 and FhHDM-1.C2 peptides (5µM) at 4ºC for 30min. To quantify peptide binding, an Alexa Fluor 488 labelled streptavidin was used. **(C)** RAW 264.7 macrophages and **(E)** BMDMs (1 x 10^6 cells/ml) were incubated with Alexa Fluor 488-labelled FhHDM-1 or FhHDM-1.C2 peptides (2.5µM) at 4ºC for 30 min. **(B)**, **(D)** and **(F)** are the mean fluorescence intensities (MFIs) from experiments **(A)**, **(C)** and **(E)**, respectively. Baby hamster kidney cells with high (+) or low (-) expression of EGFR (1 x 10^6 cells/ml) were incubated with Alexa Fluor 488-labelled **(G)** FhHDM-1 or **(H)** FhHDM-1.C2 peptides (2.5µM) at 4ºC for 30 min. Data is representative of three (A,B), two (C,D), one (E,F), and two (G,H) independent experiments. Data in (B), (D) and (F) expressed as means ± SEMs (* $p \leq 0.05$, ** $p \leq 0.01$).

Although the binding studies were conducted at 4^{o}C (to prevent uptake of peptides), flow cytometric analyses cannot distinguish between intra- and extra-cellular fluorescence. Therefore, confocal microscopy was utilised to further investigate the binding and internalisation of peptides. Due to high auto-fluorescence in the green channel (which is utilised for the detection of peptide) BMDMs could not be used for these experiments. Instead, RAW 264.7 macrophages were incubated with Alexa Fluor 488 labelled FhHDM-1.C2 (5μM) at 4^{o}C for 15min (Fig. 5.6B,E) and 30min (Fig. 5.6C,F; Section 2.6.2.1). The cellular membrane was visualised using Alexa Fluor 647 Phalloidin (red), and the nucleus was stained with DAPI (blue). Compared to the unstained control (Fig. 5.6A,D), there was intense green, punctate, fluorescence distributed along the membrane (stained red), indicative of FhHDM-1.C2 binding to the cellular membrane, at both 15min (Fig. 5.6B,E) and 30min (Fig. 5.6C,F). This was further confirmed by the overlay of images of the peptide and membrane staining, which produced a yellow colour suggesting co-localisation (Fig. 5.6C). Quantitative analyses suggested that, on average, 85 ± 6% and 95 ± 3% of macrophages had some level of peptide binding at 15min and 30min, respectively. Of these macrophages that exhibited peptide binding, approximately 13 ± 4% and 14 ± 2% of cells for 15min and 30min incubation times with peptide, respectively, were observed to have intra-cellular FhHDM-1.C2. This suggests that there was some degree of passive uptake, however, it can be concluded that the majority of the peptide was on the surface of the macrophage membrane, indicating binding of the peptide. Overall, these microscopic analyses corroborate the flow cytometry data that FhHDM-1.C2 binds to murine macrophages.

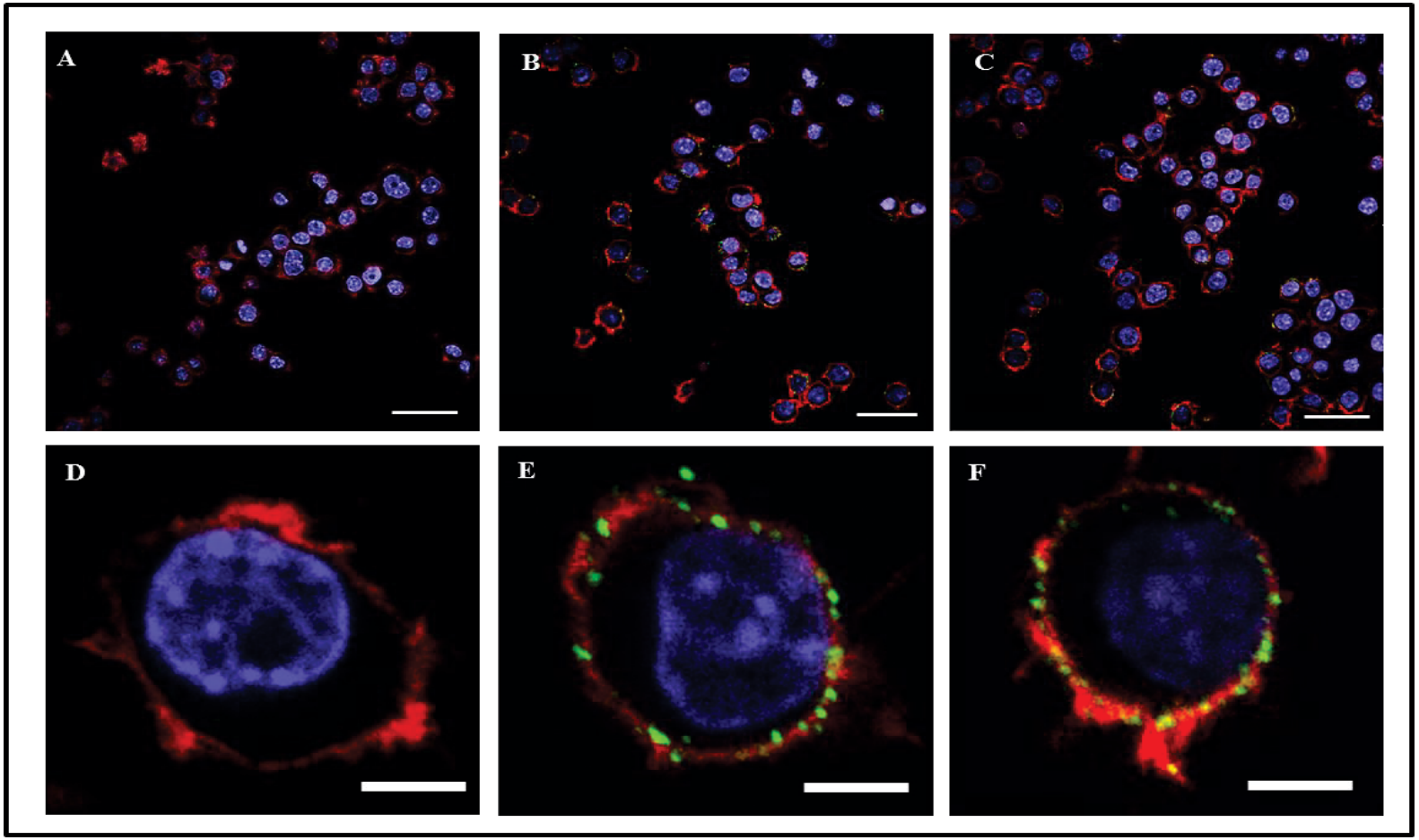

Figure 5.6 FhHDM-1.C2 binds to murine macrophages. RAW 264.7 macrophages were incubated with Alexa Fluor 488 labelled FhHDM-1.C2 (5µM; green) at 4ºC for 15min (B,E) and 30min (C,F), or were untreated (A,D). Confocal microscopy was conducted, where seven fields of view were captured for each sample. The cells were stained for the membrane (red; Alexa Fluor 647 Phalloidin) and the nucleus (blue; DAPI). Images are representative of seven fields of view, from two independent experiments. Scale bar: 30µm (A-C) and 5µm (D-F).

5.5 Assessment of the internalisation of FhHDM-1 and FhHDM-1.C2 by murine macrophages

To determine whether, after interacting with the macrophage membrane, FhHDM-1.C2 was actively internalised, RAW 264.7 macrophages were incubated at 37ºC with Alexa Fluor 488 labelled FhHDM-1.C2 (5μM) over a time course of 15, 30 and 45min (Section 2.6.2.2). For comparison, Alexa Fluor 488-labelled FhHDM-1 was incubated with cells for 45 min. Images were taken via confocal microscopy, in which the transmission detection (TD) was used to determine the outline of the cellular membrane, whilst DAPI was used to visualise nuclei. In agreement with previously published data, FhHDM-1 (green; Fig. 5.7B), was observed intracellularly at 45 min. Supporting the possibility that the residues 'KARDR' served to transport the peptide intracellularly, FhHDM-1.C2 was visualised intracellularly at all time points (Fig. 5.7C-E). However, the numbers of cells positive for green peptide fluorescence was significantly lower at 45 mins, as compared to the earlier time points (Fig. 5.7E). Quantitative analysis showed that 75 ± 5% of cells were positive for FhHDM-1.C2 internalisation at 15min, whilst there was only 25 ± 6% positivity at 45min.

The internalisation of FhHDM-1.C2 at 15min was confirmed using the biotin labelled FhHDM-1.C2. As shown in Figure 5.8A and 5.8B, green, punctate fluorescence was observed within the cytoplasmic region of the cells, as compared to untreated controls (Fig. 5.8B), verifying internalisation of FhHDM-1.C2 by macrophages (Fig. 5.8D). Quantitative analysis determined that 99.6 ±0.4% of cells had internalised FhHDM-1.C2.

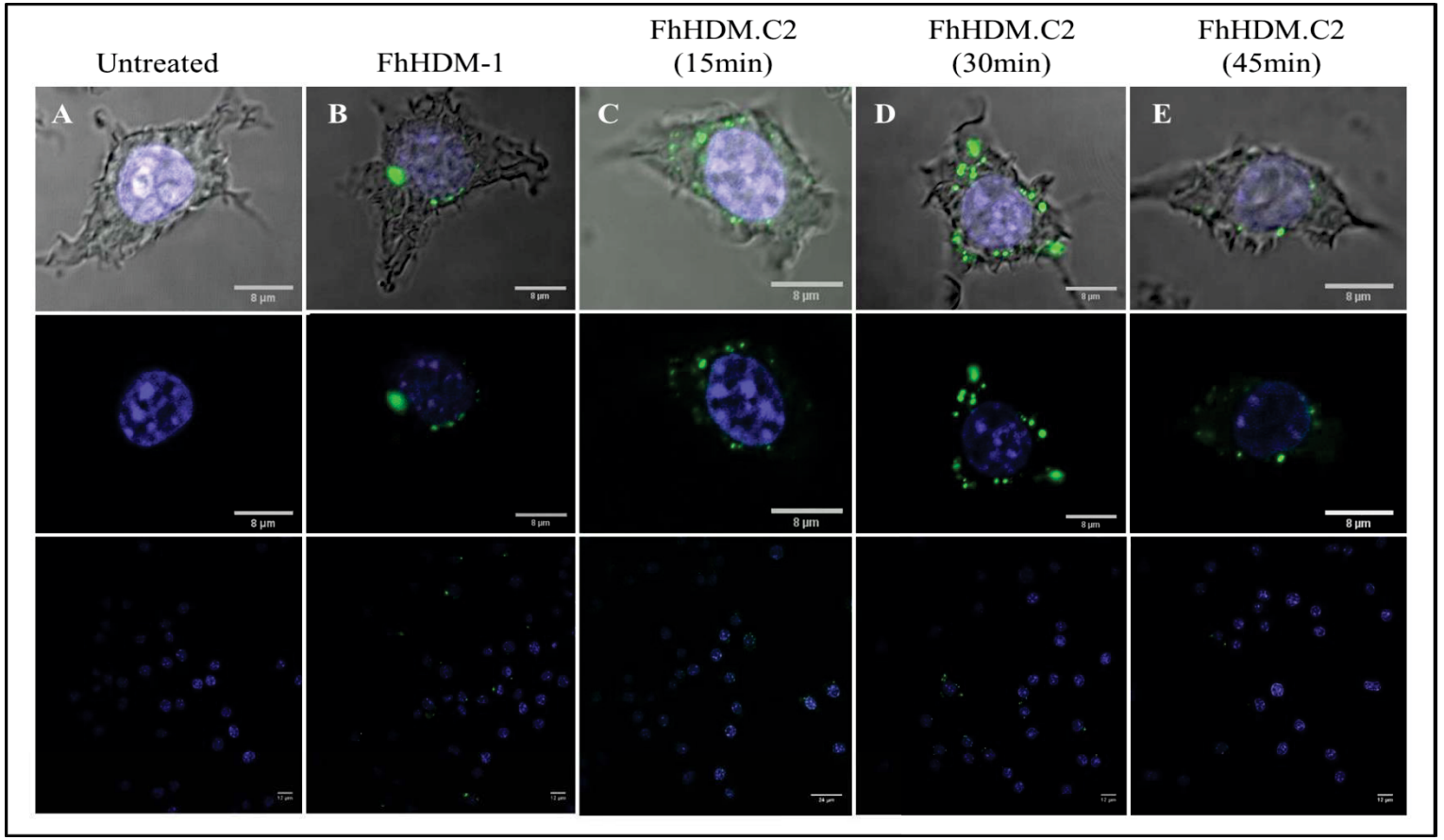

Figure 5.7 FhHDM-1.C2 is internalised by murine macrophages, to a similar extent as the full length FhHDM-1. RAW 264.7 macrophages were incubated with Alexa Fluor 488 labelled peptides (green) at 37°C. **(A)** untreated RAW 264.7 macrophages; **(B)** FhHDM-1 (2.5µM) for 45min; or FhHDM-1.C2 (5µM) for **(C)** 15min, **(D)** 30min and **(E)** 45min. Confocal microscopy was conducted, where seven fields of view were captured for each sample, with images being representative of three independent experiments. The bottom panel shows a representative field of view; middle panel shows a representative cell; and top panel shows a single cell with transmission view for visualisation of the cell membrane. Cells were also stained for the nucleus (blue; DAPI). Scale bars in the top and middle panel are 8µm and scale bars in the bottom panel are 12µm.

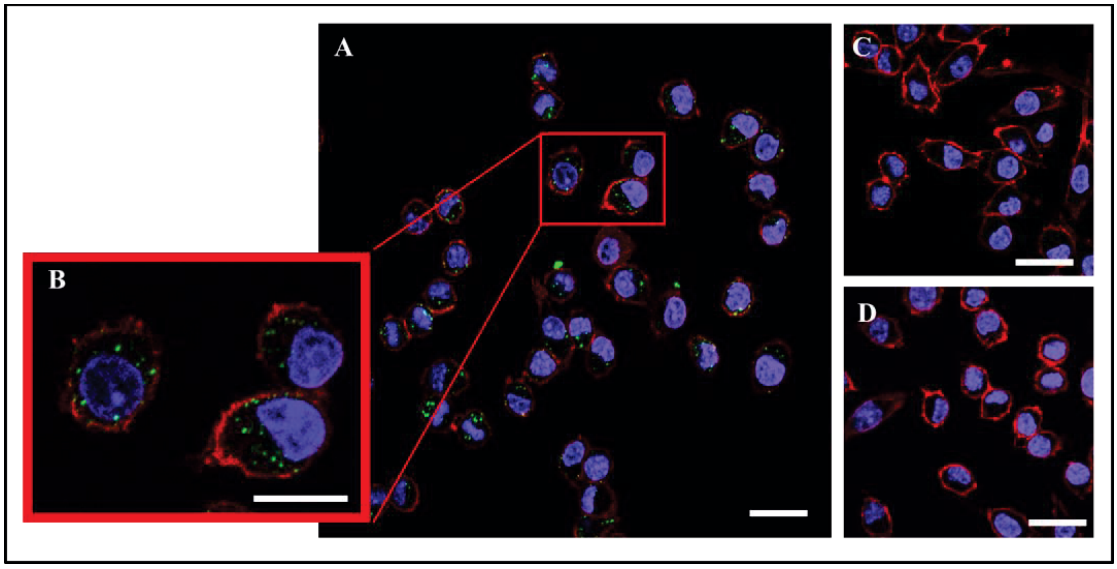

Figure 5.8 FhHDM-1.C2 is internalised by murine macrophages. RAW 264.7 macrophages were incubated with **(A)** biotin-labelled FhHDM-1.C2 (5µM; green) for 15min at 37ºC. Alexa Fluor 488-strepdavidin was further used for detection of peptide. **(B)** Higher magnification of cells from **(A)**; **(C)** Untreated RAW 264.7 macrophages; **(D)** secondary antibody only control. Confocal microscopy was conducted, where six fields of view were captured. The cells were stained for the membrane (red; Phalloidin Alexa Fluor 647) and the nucleus (blue; DAPI). Scale bar:12µm.

5.6 Assessment of lysosomal changes in macrophages induced by FhHDM-1 and FhHDM-1.C2

Once internalised, FhHDM-1 is known to localise to the lysosome. As *in vitro* biochemical analysis revealed that the peptide inhibited lysosomal vATPase [215], it was postulated that intracellularly FhHDM-1 prevented the acidification of lysosomes to mediate its effect. To determine definitively whether FhHDM-1 raised lysosomal pH, and whether FhHDM-1.C2 mimicked this effect, a fluorescent dye, Lysosensor, was utilised. This dye is a ratiometric probe used to indicate the pH of lysosomes; where it produces blue fluorescence in more neutral and alkaline environments, but fluoresces yellow, in more acidic environments. RAW 264.7 macrophages were incubated with either FhHDM-1 or FhHDM-1.C2 (15μM; 30min at 37^{o}C), washed twice with saline (to remove any excess peptide), incubated with Lysosensor, and then analysed by flow cytometry (Section 2.5.5.2). The dead cell stain, TOPRO-3 (y-axis of all plots in Fig. 5.9) was added to the cells, just prior to data acquisition on the flow cytometer, to exclude dead cells. The plots in Figure 5.9 exclude the cells that were TOPRO-3 positive. As shown in Figure 5.9A and 5.9D, a gate was created around the unstained population. Cells that were not treated with FhHDM-1 peptides, but stained with Lysosensor, represented approximately 17% of cells within this gate (Fig. 5.9B and 5.9E). The decrease in the population within this gate indicates an increase in blue fluorescence. Therefore, these samples show the baseline fluorescence from the Lysosensor dye itself. In the presence of either FhHDM-1 (Fig. 5.9C) or FhHDM-1.C2 (Fig. 5.9D), there was a further decrease in the percentage of cells (approximately 3% and 5% for FhHDM-1 and FhHDM-1.C2, respectively) within this gate, suggesting an increase in blue fluorescence, and therefore an increase in lysosomal pH to produce an alkaline environment. These data suggest that FhHDM-1.C2 modulates the biological activity of macrophages in the same way as the full length FhHDM-1, namely by preventing lysosomal acidification.

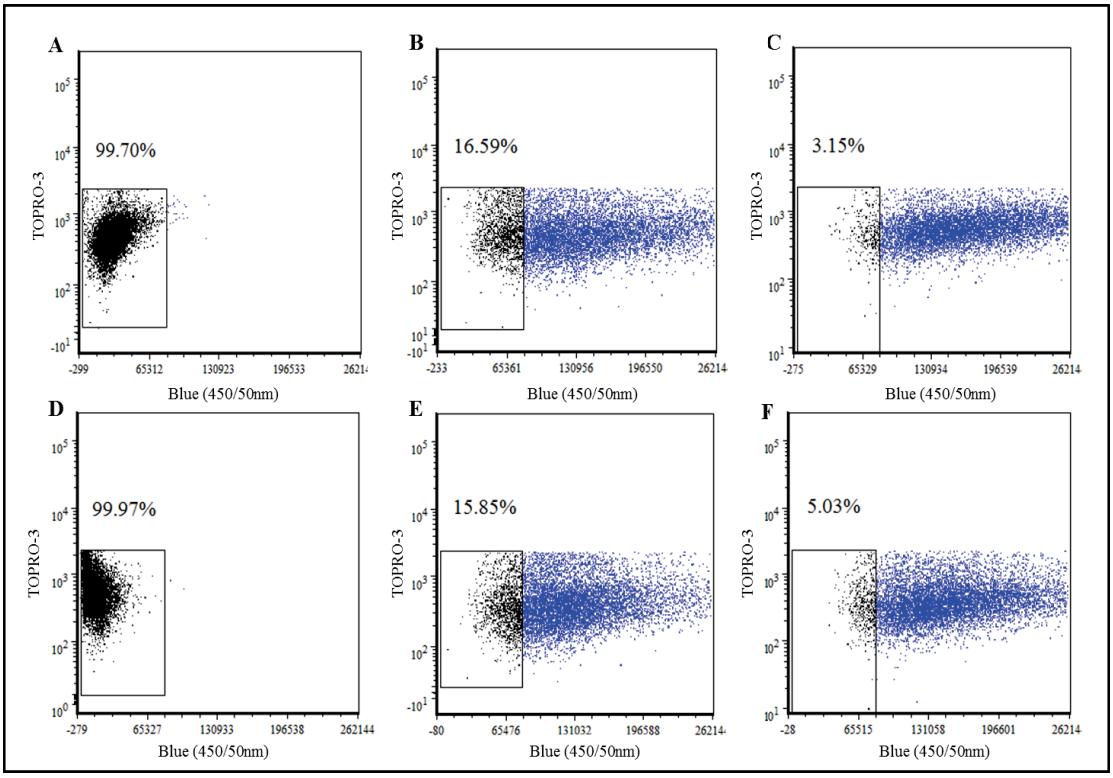

Figure 5.9 FhHDM-1.C2 increases macrophage lysosomal pH similar to that of the full length, FhHDM-1. RAW 264.7 macrophages (1 x 10^6 cells/ml) were incubated with **(C)** FhHDM-1 or **(F)** FhHDM-1.C2 (15µM) for 30min at 37ºC. Lysosensor (5µM) was then added to each sample **(B,C,E,F)** for 5min and macrophages were assessed for the emission of blue fluorescence (detected at 450/50nm). An increase in blue fluorescence indicates an increase in lysosomal pH. A gate was created, based on the unstained population **(A,D)**. The x-axis denotes the blue fluorescence (450/50nm), and the y-axis denotes the uptake of TOPRO-3. Data is representative of eight (A,D), thirteen (B,E), five (C), and eight (F) replicates.

5.7 Assessment of the modulation of macrophage function by FhHDM-1 and FhHDM-1.C2

Having established that FhHDM-1.C2 was replicating the effects of the full-length peptide with respect to inhibiting lysosomal acidification (Section 5.6), it was next determined whether the biological activities of the peptides were the same.

Firstly, the abilities of the peptides to modulate cytokine production by macrophages were compared. This analysis extended preliminary studies using FhHDM-1, which only focused on TNF and IFN-β secretion (Chapter 4, Section 4.2 and 4.4), to include a range of pro-inflammatory (Th1/Th17) cytokines, anti-inflammatory/regulatory (Th2/Treg) cytokines, and chemokines using a multiplex (Section 2.4.1.5). As previously done, macrophages were treated with the peptide for 1h, and then washed prior to stimulation with LPS. For all LPS-only stimulated samples, more than 10 pg/ml of cytokine/chemokine was detected, and, therefore these concentrations were considered biologically relevant, as this is a cut-off used for analyses of healthy human samples [338] and in the context of disease diagnosis [339]. For ease of comparison, the amount of cytokines/chemokines produced are presented as a percentage, with the LPS-only stimulated sample adjusted to 100% (Fig 5.10). Consistent with the TNF inhibition observed previously (Section 5.2, Figure 5.3) FhHDM-1 significantly inhibited the production of TNF, to less than 10% of the LPS-only samples (Fig. 5.10). FhHDM-1 also inhibited other pro-inflammatory cytokines and chemokines, including IL-6, G-CSF, MIP-1β and RANTES. Interestingly, Th2 /Treg cytokines were also inhibited by FhHDM-1 in response to LPS stimulation (Fig. 5.10).

It would be of interest to confirm the inhibition of anti-inflammatory cytokines by FhHDM-1 using an M2-driving stimulus such as IL-4. In corroboration of the binding and lysosomal studies, FhHDM-1.C2 inhibited production of all the cytokines/chemokines to the same extent as FhHDM-1. All the columns were statistically significant ($0.0001 \leq p \leq 0.01$), as compared to their respective LPS-only stimulated samples. From this data set, it can be concluded that both FhHDM-1 and FhHDM-1.C2 are capable of reducing (although, to varying degrees) the ability of

murine macrophages to produce predominantly cytokines/chemokines that are associated with a Th1/Th17 immune profile.

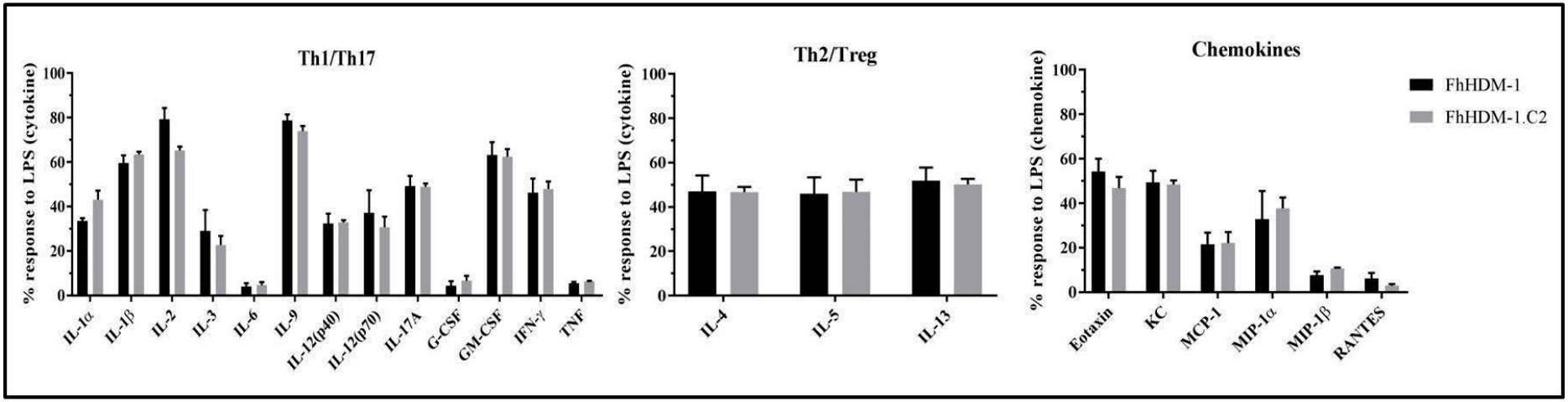

Figure 5.10 FhHDM-1.C2 is as effective as full-length FhHDM-1 in inducing the inhibition of cytokine/chemokine production in murine macrophages. RAW 264.7 macrophages (1 x 10^6 cells/ml) were treated with FhHDM-1 or FhHDM-1.C2 (15μM) for 1h. Cells were then washed twice with saline, prior to O/N stimulation with LPS (10ng/ml). Cell supernatants were assayed for pro-inflammatory (Th1/Th17), anti-inflammatory/regulatory (Th2/Treg), and chemokine via a multiplex. Data was converted to percentages with LPS-only stimulation adjusted to 100% for each cytokine/chemokine. Data is the combination of two independent experiments and expressed as means ± SEMs. For the clarity of visualisation, the LPS-only sample is not shown. All the columns were statistically significant (as compared to their respective LPS-only stimulated samples); varying from $p \leq 0.01$ and $p \leq 0.0001$ in significance.

As previously demonstrated (Chapter 3, Section 3.4), treatment of macrophages with FhHDM-1 reduced the expression levels of *Havcr2* and *Lsp1*, which are associated with the generation of pro-inflammatory immune responses. In contrast, FhHDM-1 significantly enhanced the expression levels of *SerpinB2*, which mediates the ability of macrophages to prevent the proliferation of Th1 cells *in vitro.*

Similarly, macrophages treated with FhHDM-1.C2 showed decreased expression levels of both *Havcr2* and *Lsp-1* (-1.4±0.1 and -2.0±0.3 fold decreases for *Havcr2* and *Lsp-1*, respectively; Fig. 5.11B,C), with almost the same fold change as observed for FhHDM-1 treatment of macrophages (-1.5±0.1 and -1.9±0.1 fold decreases for *Havcr2* and *Lsp-1*, respectively; Fig. 5.11B,C). In addition, treatment of BMDMs with FhHDM-1.C2 significantly increased the expression levels of *SerpinB2* (2.4±0.3 fold increase; Fig. 5.11A), although the fold change was not as large as that seen when the full-length peptide was incubated with macrophages (12.7±1.2 fold increase; Fig. 5.11A). Despite this difference in expression levels of *SerpinB2*, T cells co-cultured with FhHDM-1.C2 treated BMDMs displayed a significantly reduced ability to secrete IFN-γ, as compared to T cells co-cultured with untreated BMDMs (Fig. 5.12; Section 2.4.1.6). This supports the hypothesis that FhHDM-1.C2 contains the amino acid sequence responsible for the bioactivity, which regulates expression levels of *Havcr2, Lsp-1* and *SerpinB2*, to modulate the immune response.

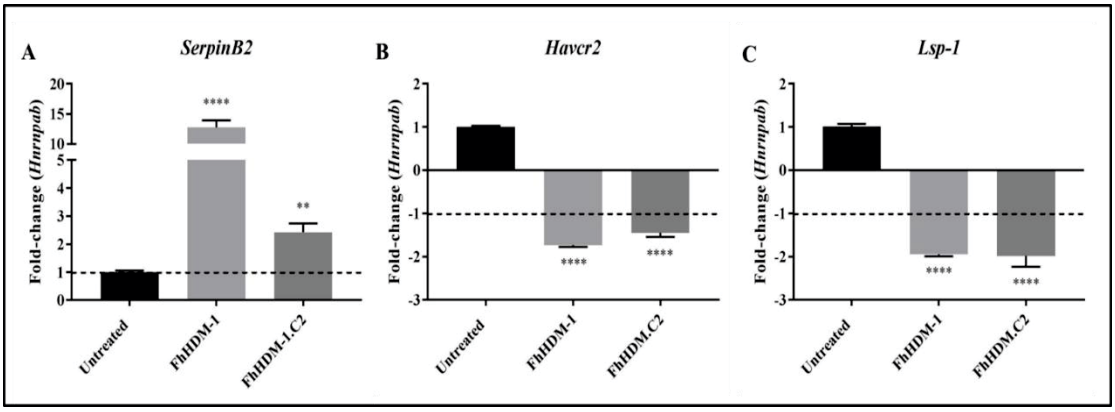

Figure 5.11 FhHDM-1.C2 modulates the expression levels of *Havcr2, Lsp-1* and *SerpinB2* in BMDMs in a similar manner to that of the full length FhHDM-1. BMDMs (1 x 10^6 cells/ml) were incubated with FhHDM-1 or FhHDM-1.C2 (15 µM) for 24h at 37ºC. Messenger RNA was isolated, cDNA was synthesised, and gene expression levels were analysed by quantitative real time RT-PCR. Fold changes in expression of **(A)** *SerpinB2*, **(B)** *Havcr2* and **(C)** *Lsp-1* was calculated using the $\Delta\Delta C_t$ method, where 1 or -1 (dotted lines) indicates no change, as compared to the untreated samples. Gene expression was normalised to *Hnrnpab*. Data is the combination of two independent experiments and expressed as means ± SEMs. Significance is calculated against the untreated samples (** $p \leq 0.01$, *** $p \leq 0.001$, **** $p \leq 0.0001$).

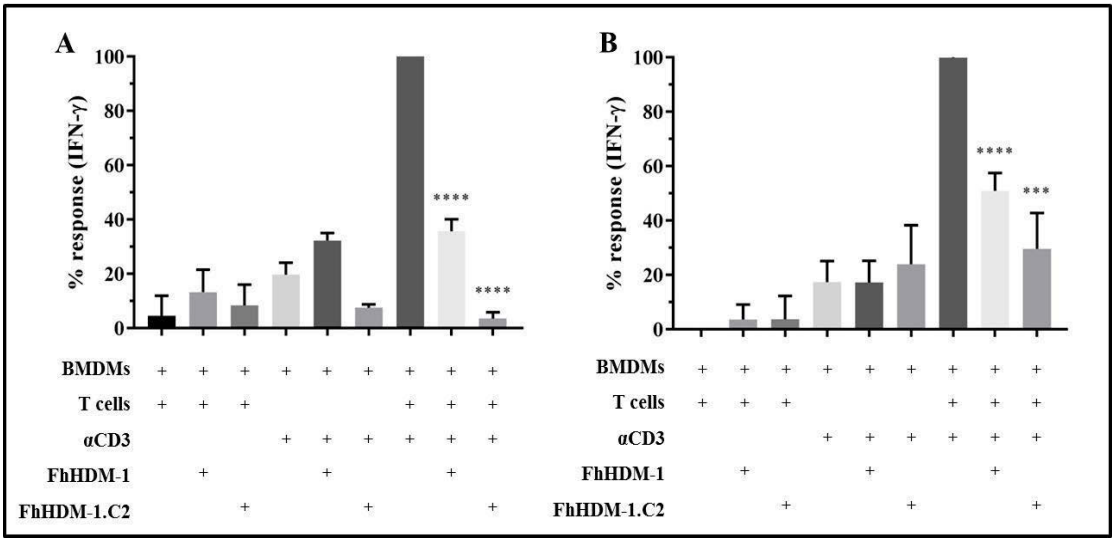

Figure 5.12 The ability of FhHDM-1.C2 to inhibit Th1 immune responses is comparable to that of the full length FhHDM-1. BMDMs (5 x 10^5 cells/ml) were incubated with FhHDM-1 or FhHDM-1.C2 (15 µM) for 24h at 37ºC. Cells were washed twice with saline, and then co-cultured with T cells (1:1) in the presence of α-CD3 antibody at **(A)** 0.05µg/ml or **(B)** 0.1µg/ml for 48h at 37ºC. Cell supernatants were assayed for IFN-γ. Data was converted to percentages with untreated BMDMs + T cells + α-CD3 antibody adjusted to 100%. Data is the combination of two (A) and two (B) independent experiments and expressed as means ± SEMs (*** $p \leq 0.001$, **** $p \leq 0.0001$).

5.8 Discussion

The data presented here confirmed the hypothesis that the bioactivity of FhHDM-1 resides in the C-terminal region of the peptide, and identified a sequence of amino acids that has predicted structural analogy with CPPs. Furthermore, the analysis suggests that this sequence mediates binding to macrophages, and likely targets the bioactive C-terminus to the lysosome.

The addition of the 'KARDR' sequence enhanced the interaction of the parasite peptide with macrophages, suggesting the presence of a binding domain. However, the target receptor is yet to be identified. Although characterised as a binding partner for the murine cathelicidin, CRAMP, EGFR was neither utilised by the full length nor C2 parasite peptide for entry into cells. However, this analysis did reveal an interesting difference between the behaviour of the two FhHDM-1 variants, with FhHDM-1.C2 showing no significant interaction with BHK cells, while the full-length peptide, FhHDM-1, bound to the cell membrane. This suggests that there may be undiscovered binding domains within the N-terminus of the full-length peptide, which may interact differently with specific cell types. Alternatively, this difference may be attributed to the previously identified affinity of FhHDM-1 for cholesterol [215]. The full-length peptide contains a cholesterol-binding motif (L/V-[X]1-5-Y-[X]1-5-R/K, spanning residues VTKAYEKAR) that is highly conserved across all known cholesterol-binding proteins. However, due to its truncation, this sequence is not present in the FhHDM-1.C2 peptide. This could be confirmed *in vitro* by quantifying the binding capability of FhHDM-1.C2 and FhHDM-1.C4 (which contains KAYEKAR) to cholesterol lipids using phospholipid ELISAs, as previously described [215].

Although FhHDM-1.C2 was clearly internalised by macrophages, the possibility that, similar to the full length FhHDM-1, the peptide localised to the lysosome was concluded based on the alteration of lysosomal pH. A more definitive demonstration of endolysosomal localisation is warranted. This could be achieved using confocal microscopy to visualise the co-localisation of peptides with fluorescently tagged antibodies binding to specific proteins expressed by lysosomes, (LAMP1 and LAMP2), early endosomes (Rab5 and EEA1), or late endosomes (Rab7).

Despite the lack of microscopic evidence, the decrease in fluorescent signal from FhHDM-1.C2 after internalisation by macrophages (Section 5.5; Fig. 5.7) supports the possibility that FhHDM-1.C2 is being trafficked to the endolysosome, where it is being degraded. Alternatively, it could be that FhHDM-1.C2 is localised within the cytoplasm after uptake where it is susceptible to degradation by the proteasome. This is a significantly different outcome, as compared to the internalised full-length peptide, which can still be visualised up to, and after, 45min incubation with macrophages. Previous studies have shown that FhHDM-1 localises to the endolysosome, and that it is relatively resistant to cleavage by protease enzymes. The only proteolytic event that occurs is the separation of the C-terminal amphipathic region from the N-terminus [215]. If the FhHDM-1.C2 is indeed trafficking to the endolysosome, and as it is missing 28 amino acids, it may be more susceptible to degradation by lysosomal proteases. This could be investigated *in vitro* using recombinant murine and human protease enzymes. However, despite this apparent reduction in stability, the efficacy of FhHDM-1.C2 is not impaired. The peptide displays the same EC50 as the full-length peptide, inhibiting the production of cytokines and chemokines with the same potency. This suggests that the peptides mediate their effect rapidly and that this is then maintained in the cell for a prolonged period.

Interestingly, as these analyses were being finalised, an article was published which supports both the experimental approach and the outcomes. In this study [214], the complete N- terminus of FhHDM-1 was analysed using CPPred, and, consistent with the current analysis, was awarded a score of 0.777 [214]. The authors therefore suggested that the entire N-terminus represented the cell-binding domain, while the bioactivity potency was located within the C-terminus. While the findings in this chapter are in agreement with this published work, by analysing smaller sections of the N-terminus, a 5 amino acid sequence, ‘KARDR’, with a closer proximity to a CPP has been identified (Section 5.1; Fig. 5.1A). However, further investigations are required to confirm that the ‘KARDR’ sequence represents a lysosomal targeting CPP. One simple demonstration would be to attach a variety of fluorescently tagged small peptides to the ‘KARDR’ sequence, and to then follow intracellular uptake by macrophages using confocal microscopy. Additionally, the cellular distribution of the FhHDM-1 C-terminus synthesized to a known CPP sequence, such as HIV-TAT [340], could be compared to the FhHDM-1.C2. The expectation would be that the HIV-TAT peptide

would direct the FhHDM-1 C-terminus peptide to the cytoplasm and have no effect on lysosomal function.

While this information is important to understanding how FhHDM-1 modulates immune cell function, the identification of a potential lysosomal targeting CPP has much broader implications. For example, CPPs are currently being investigated in the treatment of lysosomal storage diseases, which are caused by a deficiency in, or low abundance of, lysosomal enzymes, leading to accumulation of material in lysosomes and dysfunctional lysosomal systems [341]. These CPPs are used in enzyme replacement therapies, in which missing lysosomal enzymes are delivered and are able to restore lysosomal function [328, 342]. Another therapeutic avenue of CPPs is the delivery of vaccine antigens for the treatment of cancer and infectious diseases [343]. One of the most encouraging applications has been in DC vaccine based treatments, where enhanced delivery of antigens was observed, the antigen processed within the endolysosomes, and consequently presented by MHC class II molecules for induction of T cell activation [342]. This warrants a novel therapeutic avenue for FhHDM-1 and its derivative peptides, more specifically for the prospective lysosomal targeting CPP, which has been discovered in this study.

Chapter 6: Interaction of FhHDM-1 with neutrophils

6.1 Introduction

To date, elucidation of the immune modulatory effect(s) of FhHDM-1 has focused on its interactions with macrophages. This is because macrophages were identified as the primary cellular target for FhHDM-1 in mice. The interaction between FhHDM-1 and murine peritoneal macrophages was determined by flow cytometry, 20 mins after the intraperitoneal injection of fluorescently labelled FhHDM-1. Of the three most predominant immune cell populations within the peritoneal cavity (macrophages, B cells and T cells), FhHDM-1 preferentially bound to macrophages *in vivo*, in both autoimmune-prone NOD mice and immune competent BALB/c mice [197]. However, if FhHDM-1 is to be ultimately used as a human therapeutic, it would likely be delivered by other routes, such as intravenously or subcutaneously, and thus would have exposure to a broader range of immune cells, as compared to those residing in the peritoneal cavity.

Neutrophils play pivotal roles in the initiation of autoimmunity. In murine models of T1D, there is intricate communication between neutrophils and B cells, which results in the activation of pancreatic plasmacytoid DCs. Through their ability to prime autoreactive T cells for clonal expansion and trafficking to the islets, these DC populations are pivotal to the initiation of autoimmunity [41, 344]. In fact, the infiltration of neutrophils into pancreatic islets (as early as 2 weeks of age) [345] precedes that of macrophages (at approximately 4 weeks of age) [346], and their elimination/inhibition exerts positive effects on disease prevention. In MS, neutrophils mediate the maturation of DCs and macrophages, and in concert these cell types mediate the inflammation of the central nervous system (CNS) [42]. Therefore, early recruitment of neutrophils is critical for the development of the pro-inflammatory environment in T1D and MS. Further, the co-occurrence of T1D and MS has been reported in several human studies [347], suggesting shared mechanisms of disease development, in which neutrophils play a major role.

With the known significance of neutrophils in the pathogenesis of autoimmune diseases, especially T1D and MS, it was of interest to determine whether FhHDM-1 could also interact with neutrophils and modify their biological activity, as shown for

macrophages. It is yet to be determined if FhHDM-1 will be similarly efficacious in preventing/treating other autoimmune diseases, however, this study in investigating interaction of the peptide with neutrophils may broaden the therapeutic efficacy of FhHDM-1.

6.2 Determining the interaction of FhHDM-1 with human neutrophils

The initial studies to determine the cellular target of FhHDM-1 may have been biased due to the relative abundance of certain cell populations within the peritoneal cavity of mice [132]. In addition, validation of the peptide's cellular target among human cell populations is an important determinant of the potential for clinical translation of the peptide. Therefore, human peripheral blood leukocytes were used to screen the interaction of FhHDM-1 with major immune cell populations, in which neutrophils are known to predominate [348]. To achieve this, FhHDM-1 was labelled with an Alexa Fluor 647 fluorescent tag, and then incubated with human peripheral blood leukocytes obtained from fresh human buffy coats (Section 2.5.4.3). After 1h at 4^{o}C, cells were washed, and incubated with human IgG to prevent any non-specific binding of antibodies. Cells were then labelled with specific fluorochrome conjugated surface marker antibodies for the identification of individual cell populations by flow cytometry (the gating strategy is detailed in Section 2.5.4.4).

Binding of FhHDM-1 was assessed as a positive signal for Alexa Fluor 647 fluorescence within the respective cell gates. The same voltage settings were used to assess binding in all cell populations, which allowed for direct comparisons in the levels of interaction of FhHDM-1 between different cell types. Slight increases in fluorescence levels, above those detected for unstained control samples, were observed for all cell types. However, the largest increases in fluorescence levels, and hence binding, occurred within the neutrophil and monocyte populations, where the increase in FhHDM-1 positive cells was significantly greater than the unstained control. Calculation of the geometric mean of the area under the histogram confirmed these results, clearly showing that the FhHDM-1 interaction with neutrophils and monocytes (MFI of 1697 and 1034 for neutrophils and monocytes, respectively) was much greater than it's binding to any other cell type (Fig. 6.1B). The binding of FhHDM-1 to monocytes was not surprising, given the reported interactions of FhHDM-1 with both murine and human macrophages ([215] and Chapter 5). The binding of FhHDM-1 to human neutrophils was a novel finding, and this preliminary finding was confirmed using neutrophils from multiple donors.

Although, there was some variability in the actual value of geometric means, a similar pattern of binding was found in samples from two additional human donors (Figures 6.2A,B). In all cases, the level of FhHDM-1 interaction to monocytes and neutrophils was clearly greater than its binding to any other cell type. However, in the cells from a fourth donor, several cell types appeared as positive for FhHDM-1 fluorescence (Figure 6.2C). Additionally, the overall geometric means of fluorescence for cells from this fourth donor were lower than all previous analyses, reflecting an atypical binding profile for FhHDM-1. Despite this, both neutrophils and monocytes were consistently more positive, than any other cell type, for FhHDM-1 binding.

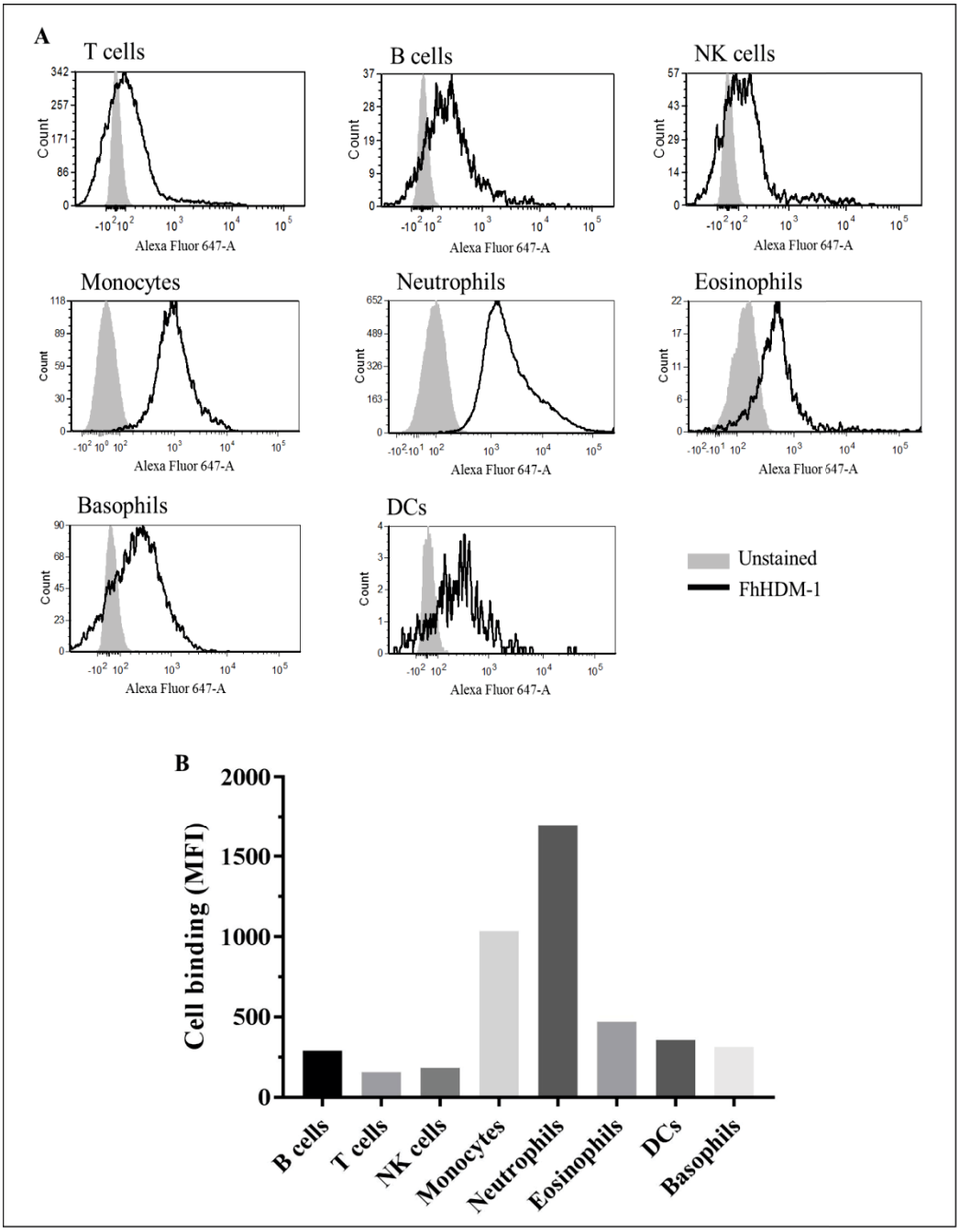

Figure 6.1 FhHDM-1 binds to human neutrophils and monocytes. (A) Alexa-Fluor 647 labelled FhHDM-1 (2.5µM) binding to human B and T lymphocytes, natural killer (NK) cells, monocytes, neutrophils, eosinophils, basophils, and dendritic cells (DCs). For each histogram, the grey filled histogram represents the unstained sample and the black line represents FhHDM-1 binding. The x-axis is the intensity of fluorescence for Alexa-Fluor 647 (indicating the binding of FhHDM-1), and the y-axis is the cell count. **(B)** The mean fluorescence intensities (MFI; y-axis) of Alexa-Fluor 647 labelled FhHDM-1 were calculated for each cell population (x-axis). Data is representative of four donors.

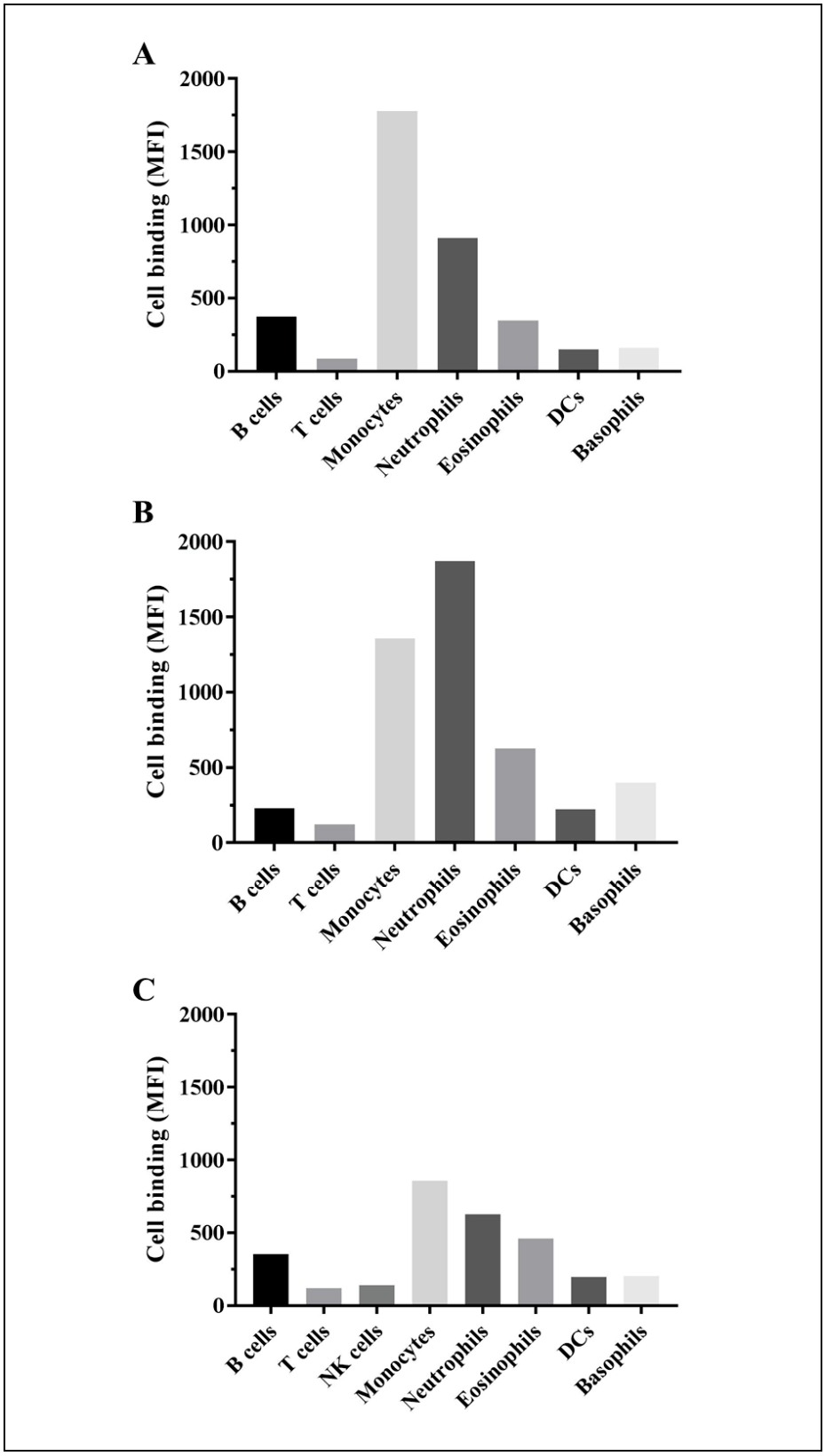

Figure 6.2 FhHDM-1 binds to human neutrophils and monocytes. The mean fluorescence intensities (MFI; y-axis) of Alexa-Fluor 647 labelled FhHDM-1 were calculated for each human peripheral blood leukocyte population (x-axis). **(A-C)** are the data from three donors.

6.3 Assessment of the modulation the biological function of murine neutrophils by FhHDM-1

Neutrophils comprise 60% of the total human leukocyte population, and, as such, are the most abundant leukocyte in blood [348]. Neutrophils perform critical roles in resolving bacterial and fungal infections [349] through multiple mechanisms, including phagocytosis and intracellular degradation of microbial products [350], and secretion of pro-inflammatory chemokines and cytokines (notably TNF and IL-8) [351-353]. These cells typically exist in a resting state, mainly within the bone marrow, and once primed/partially activated by cytokines and chemokines (such as TNF, IFN-γ, IL-6 and C-X-C-motif chemokine ligand [CXCL] -1, CXCL-2 and CXCL-12 [354, 355]), they are released into the blood stream, to migrate to the site of inflammation, where they become fully activated by pathogenic products [39]. Neutrophil migration, activation and death are tightly controlled processes to prevent excessive inflammation [38], given that mediators secreted by neutrophils exert potent pro-inflammatory effects, and to ensure subsequent resolution of the inflammatory response. There are many phenotypic changes that occur when neutrophils are partially/fully activated. These include changes in the expression levels of adhesion molecules. For example, neutrophil activation is associated with decreased expression levels of the adhesion molecule, CD62L (also known as L-selectin), which facilitates a higher degree of rolling along the endothelium of the blood vessels. Subsequently, levels of CD11b are increased, which provides migration arrest allowing neutrophils to transmigrate through the endothelial lining towards the pro-inflammatory site [39].

Given the binding of FhHDM-1 to neutrophils, it was next determined if the interaction of FhHDM-1 exerted any effect on the activation status, or biological activity, of neutrophils. The three primary readouts measured were (1) phagocytosis; (2) surface marker activation, and (3) cytokine/chemokine production.

These analyses were performed using murine neutrophils, which, like their murine counterparts, bound FhHDM-1. There is inherently great variability in the activation status and threshold of human neutrophils, due to genetic and environmental factors, and with the use of mice, these confounding factors are abrogated. In addition,

demonstration of modulatory activity on murine cells is important for the interpretation of outcomes in rodent models of disease. Murine neutrophils were isolated from the bone marrow of mice by negative magnetic bead selection (Section 2.3.3.4), with a purity of ~95% obtained for all experiments (Section 2.5.3.3). Initially, the ability of FhHDM-1 to interact with murine neutrophils was demonstrated, to confirm that the interaction with neutrophils was not specific to human cells. As expected, incubation of murine neutrophils with Alexa Fluor 488 labelled FhHDM-1 resulted in a significant increase in fluorescence, as compared to unstained cells ($p = 0.0305$; Fig. 6.3B). This validated that FhHDM-1 similarly bound to murine neutrophils, and validated their use in further experiments to elucidate the immune modulatory effects of FhHDM-1.

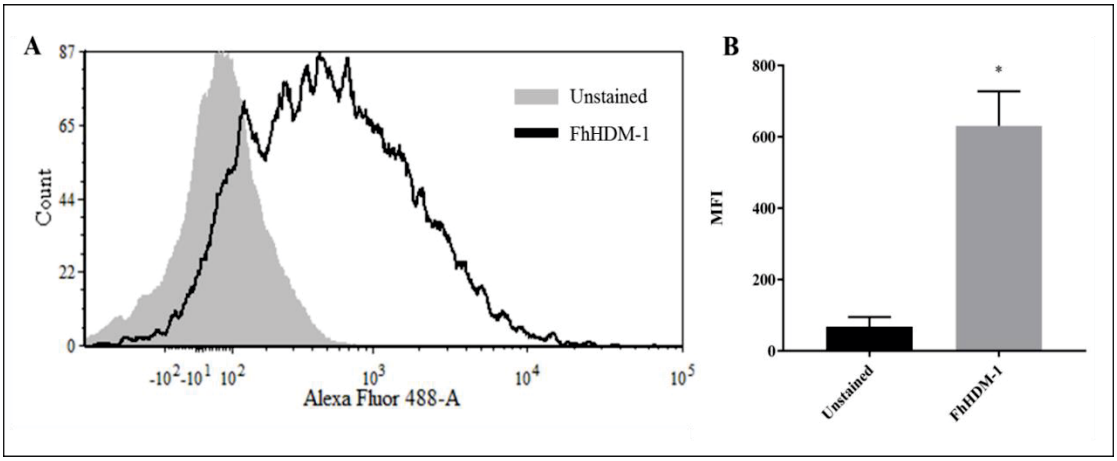

Figure 6.3 FhHDM-1 binds to murine neutrophils. Murine neutrophils (1 x 10^6 cells/ml) were incubated with Alexa Fluor 488 labelled FhHDM-1 (5µM) for 30min at 4°C. **(A)** The grey filled histogram represents the unstained and the black line represents Alexa Fluor 488 labelled FhHDM-1. **(B)** The mean fluorescence intensity (MFI) of **(A)** and other biological replicates. Data is representative of two independent experiments and expressed as means ± SEMs (* $p \leq 0.05$).

6.3.1 Ability of FhHDM-1 to modulate phagocytosis of resting and activated murine neutrophils

Similar to macrophages and DCs, neutrophils possess phagocytic activity [356]. Phagocytosis is a crucial early process in the resolution of microbial infections, and as part of the innate immune system, neutrophils are very efficient in the uptake and clearance of pathogenic products. In fact, their ability to do this exceeds that of macrophages [350]. In the context of autoimmunity, efficient phagocytic clearance of apoptotic cells is crucial in preventing the potential release of immunogenic material from the dying cells as it undergoes secondary necrosis. Accordingly, reduced phagocytic capacity has been associated with autoimmune disorders in both murine models and human studies [357]. Therefore, it was of interest to determine if FhHDM-1 modulated the ability of neutrophils to phagocytose.

Initially, murine neutrophils were treated with FhHDM-1 (10μM; a concentration of peptide shown to be biologically effective in previous assays [Chapters 3-5]) for 30min at 37^{o}C, and then incubated with Alexa Fluor 488 labelled Ovalbumin (10μg/ml; Ova 488) for 1h at 37^{o}C (Section 2.5.5.3). Uptake of Ovalbumin via phagocytosis was measured as an increase in cellular fluorescence by flow cytometry. The presence of FhHDM-1 inhibited the uptake of Ova 488 in resting neutrophils, as compared to untreated neutrophils ($p = 0.0003$; Fig. 6.4A). To investigate whether FhHDM-1 also inhibited the phagocytic activity of activated neutrophils, cells were stimulated with LPS, a biological stimulus commonly used to activate neutrophils [358, 359]. Although statistical significance was not reached, LPS-activated neutrophils did display increased phagocytic uptake (Fig. 6.7A). Consistent with its impact on resting cells, the pre-treatment of LPS activated neutrophils with FhHDM-1 also inhibited the uptake of Ova 488 ($p = 0.0015$; Fig. 6.4A). This suggests that FhHDM-1 has the ability to decrease the phagocytic activity of both resting and LPS-activated neutrophils.

To examine this effect using a biologically relevant particle, neutrophils were co-incubated with *Escherichia coli* particles. A commercially available ELISA was used (Cell Biolabs, Inc.) to quantify the amount of internalised enzyme-labelled labelled *E. coli* particles by addition of the enzyme substrate, and measurement of the subsequent colour development by optical density (Section 2.4.3.1). Murine neutrophils were incubated with FhHDM-1 (at various concentrations) for 30min prior to the addition of

E. coli particles. After 3h at 37^{o}C, cells were washed to remove non-phagocytosed material. After permeabilisation, enzyme substrate was added and the optical density (OD) of each sample was measured at 450nm. Similar to the result seen with Ovalbumin, treatment of both resting and LPS activated neutrophils with FhHDM-1 inhibited the uptake of *E. coli* particles in a dose dependent manner (Fig. 6.4B,C).

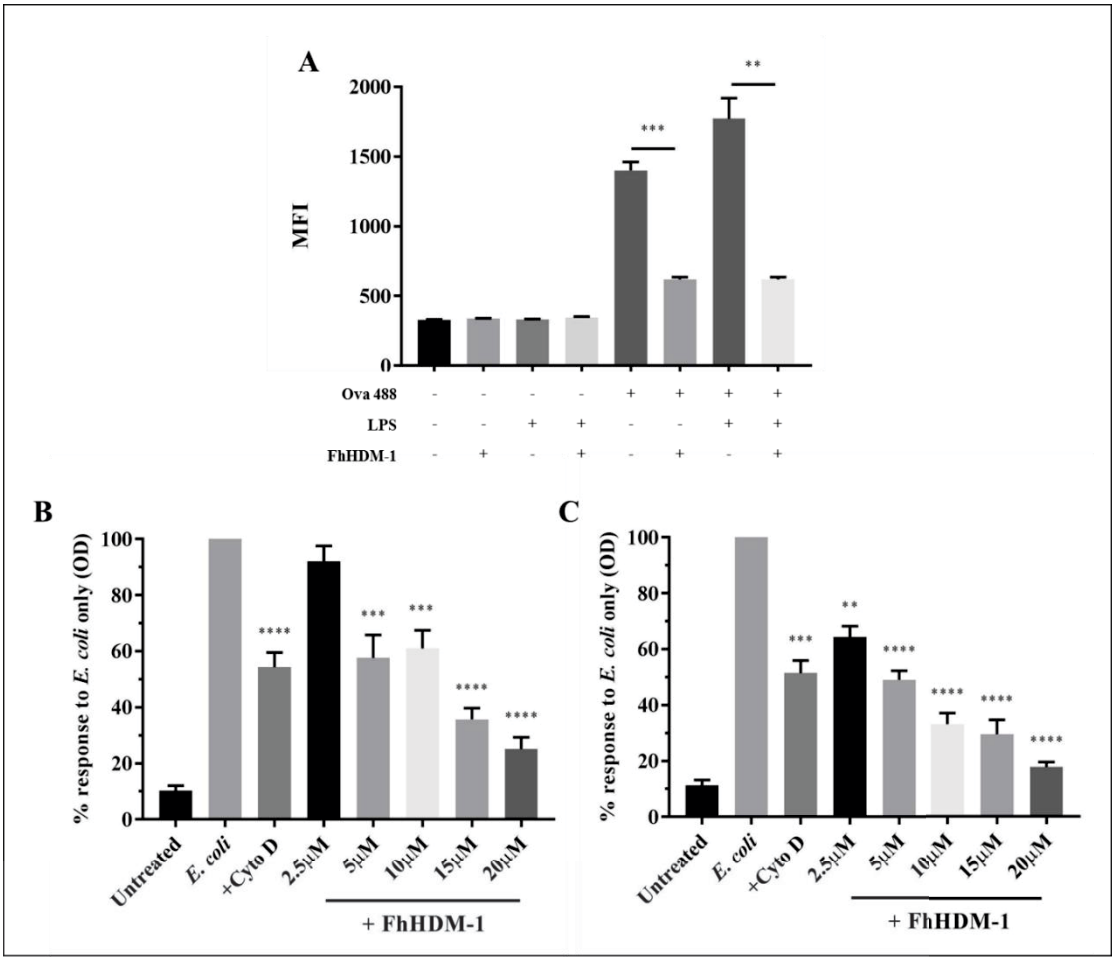

Figure 6.4 FhHDM-1 inhibits the phagocytosis of Ovalbumin and *E. coli* particles by resting and LPS activated murine neutrophils. **(A)** Murine neutrophils (1 x 10^6 cells/ml) were incubated with FhHDM-1 (10μM) for 30min at 37ºC and incubated with Alexa Fluor 488 Ovalbumin (10μg/ml; Ova 488) for 1h at 37ºC, or further stimulated with LPS (1μg/ml) for 1h at 37ºC prior to Ova 488 addition. **(B,C)** Murine neutrophils (1 x 10^6 cells/ml) were incubated with (B) FhHDM-1 (at various concentrations), or Cytochalasin D (2μM; positive control) for 30min at 37ºC, or (C) pre-stimulated with LPS (100ng/ml) for 30min at 37ºC, prior to peptide incubation. Enzyme-labelled *E.coli* particles were added and incubated for 3h at 37ºC. Amount of phagocytosed *E.coli* particles was measured as absorbance (OD read at 450nm). Data was converted to percentage values with *E. coli* only samples adjusted to 100%. Data is the representative of two independent experiments (A) or the combination of three (B) and two (C) independent experiments and expressed as means ± SEMs (statistical significance represents a comparison to the MFIs detected by Ova 488 + resting or LPS- activated neutrophils [A]; and OD levels detected by *E.coli* only samples [B,C]; ** $p \leq 0.01$, *** $p \leq 0.001$, **** $p \leq 0.0001$).

6.3.2 Assessment of the effect of FhHDM-1 on surface marker expression on resting and activated murine neutrophils

During the migration of neutrophils, CD62L is shed as a mechanism to increase the ability of neutrophils to roll along the endothelium of the blood vessels. In contrast, the expression of CD11b is enhanced, to aid in adhesion to the endothelium [39]. These changes in expression levels are characteristic of neutrophil activation and are measureable by flow cytometry [229]. Thus, to determine whether exposure to FhHDM-1 affected the maturation of neutrophils, the levels of expression of CD11b and CD62L were measured.

Murine neutrophils were activated by the addition of phorbol myristate acetate (PMA; 100ng/ml), a known synthetic stimulus for neutrophil surface marker activation [229, 360, 361], for 15min at 37^{o}C (Section 2.5.5.4). As expected, the expression of CD11b significantly increased and the levels of CD62L significantly decreased, as compared to resting, non-activated neutrophils ($p = 0.0199$ and $p < 0.0001$ for CD11b and CD62L, respectively; Fig. 6.5A). The addition of FhHDM-1 (10μM) had no effect on the expression levels of either marker in PMA activated neutrophils ($p = 0.2717$ and $p = 0.7630$ for CD11b and CD62L, respectively; Fig. 6.5A). In addition, FhHDM-1 did not modulate the levels of CD11b and CD62L in resting neutrophils ($p = 0.7617$ and $p = 0.1997$ for CD11b and CD62L, respectively; Fig. 6.5A).

To further assess the effect of FhHDM-1 binding, the expression of CD62L and CD11b was also measured on neutrophils activated with bacterial LPS. Not only is this a more biologically relevant stimulus of neutrophil activation, but FhHDM-1 has also been shown to have an inhibitory effect on LPS activation pathways (Chapter 4). While the increase in fluorescence was not as pronounced as compared to PMA stimulation, the expression of CD11b was enhanced and the expression of CD62L reduced in response to LPS ($p = 0.0028$ and $p = 0.0004$ for CD11b and CD62L, respectively; Fig 6.5B). To determine the effect of FhHDM-1 on these expression levels and to negate any interaction between FhHDM-1 and LPS [199, 214], neutrophils were treated with FhHDM-1 (5μM) for 30min at 37^{o}C, and then washed to remove any excess extracellular FhHDM-1, prior to stimulation with LPS (1μg/ml) for 1h at 37^{o}C. Again,

FhHDM-1 had no effect on the level of expression of either CD11b or CD62L ($p = 0.7132$ and $p = 0.1907$ for CD11b and CD62L, respectively; Fig. 6.5B).

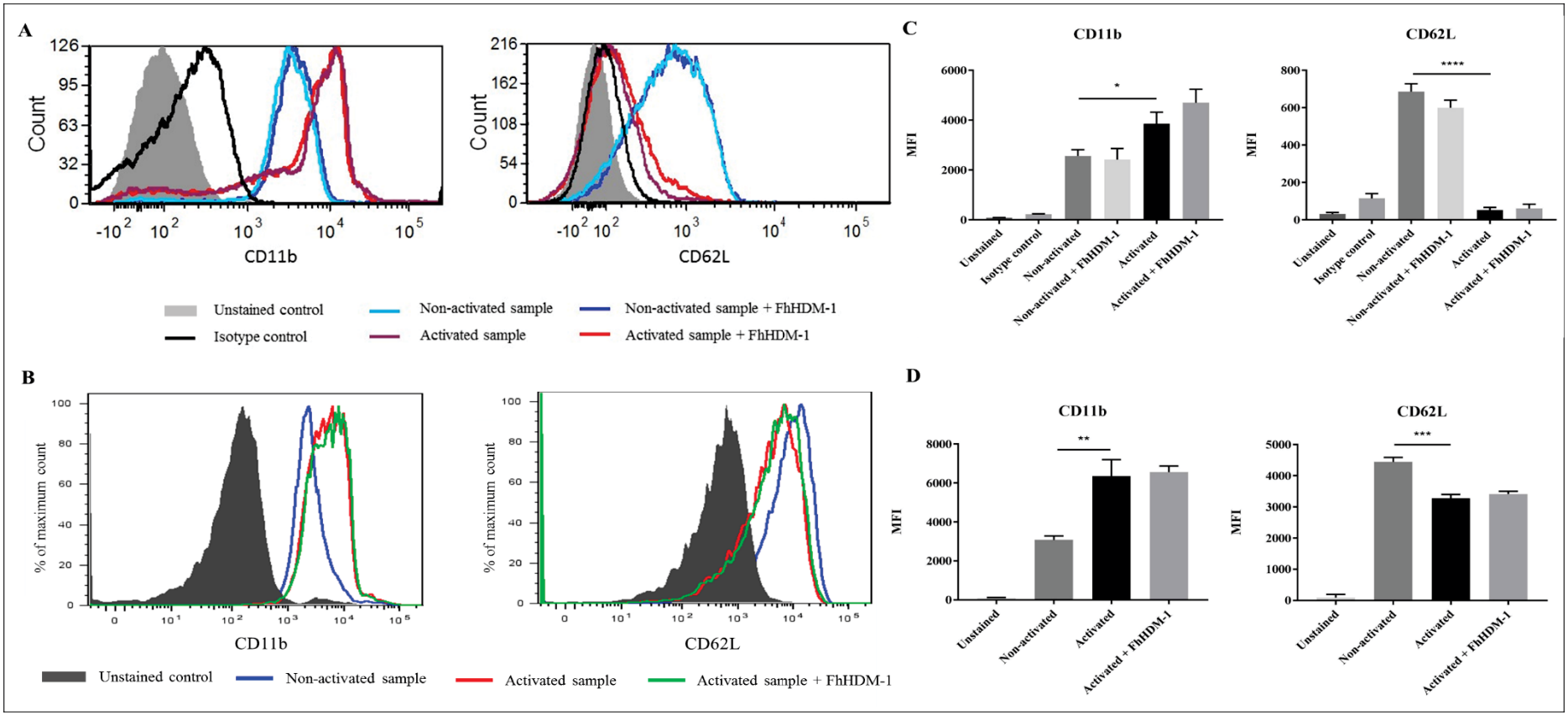

Figure 6.5 FhHDM-1 does not affect the expression levels of the neutrophil surface markers, CD11b and CD62L. Murine neutrophils (1 x 10^6 cells/ml) were incubated with **(A)** FhHDM-1 (10µM), for 30min at 37ºC and further stimulated with phorbol myristate acetate (PMA; 100ng/ml), or **(B)** incubated with FhHDM-1 (5µM) for 30min at 37ºC, washed twice with saline prior to stimulation with LPS (1µg/ml) for 1h at 37ºC. Expression levels of the activation markers, CD11b and CD62L, were determined by flow cytometry. The x-axis is the fluorescence intensity and the y-axis is the cell count, where for (B), cell count is represented as % of maximum cell count. **(C,D)** MFI of (A) and (B) and other biological replicates. Data is representative of three (A,B) independent experiments and expressed as means ± SEMs (* $p \leq 0.05$, ** $p \leq 0.01$, *** $p \leq 0.001$, **** $p \leq 0.0001$).

6.3.3 Effect of FhHDM-1 on pro-inflammatory cytokine and chemokine production by LPS stimulated murine neutrophils

Similar to macrophages, neutrophils contribute to the inflammatory response via the secretion of pro-inflammatory cytokines [351-353]. Therefore, the effect of FhHDM-1 on the production of TNF by neutrophils in response to LPS was investigated.

Murine neutrophils were incubated with FhHDM-1 (at various concentrations) for 30min at 37ºC, and then stimulated with LPS (100ng/ml) for 4h at 37ºC (Section 2.4.1.1). As reported for macrophages, FhHDM-1 inhibited the production of TNF by neutrophils with the near complete abrogation of TNF production, even at a concentration as low as 0.5μM (Fig. 6.6A). Similar to the peptide's immune modulatory effects on macrophages, washing neutrophils after treatment with FhHDM-1 reduced the peptide's potency in reducing TNF secretion, as compared to the non-washed neutrophils (EC50s of 0.1553 and 0.7718 for non-washed and washed cells, respectively). However, there was still a significant concentration dependent decrease in TNF production (Fig. 6.6B). This suggests that FhHDM-1 may be functioning via a similar mechanism to that occurring in macrophages (i.e. internalisation and modulation of intracellular signalling pathways).

To confirm that the decrease in TNF production was not simply due to reduced cell viability in FhHDM-1 treated cells, a dead cell stain (Sytox Blue, Life Technologies) was utilised to measure cell viability. Similar to the TOPRO-3 dye, when a cell is undergoing death, the plasma membrane is compromised, allowing uptake of the fluorescently labelled Sytox Blue dye. The gating strategy excluded any Sytox Blue positive cells, to identify the live cell population, which showed that close to 100% of neutrophils were viable (Fig. 6.6 C,D). Across ten independent experiments, treatment of cells with FhHDM-1 at 15μM (higher than the highest concentration tested for TNF production), consistently showed no cytotoxicity, with cell viability remaining unchanged, as compared to untreated neutrophils ($p = 0.5955$; Fig. 6.6E). Therefore, FhHDM-1 was not cytotoxic to murine neutrophils, and, accordingly, any inhibition in TNF production was attributable to the modulation of murine neutrophil function by FhHDM-1.

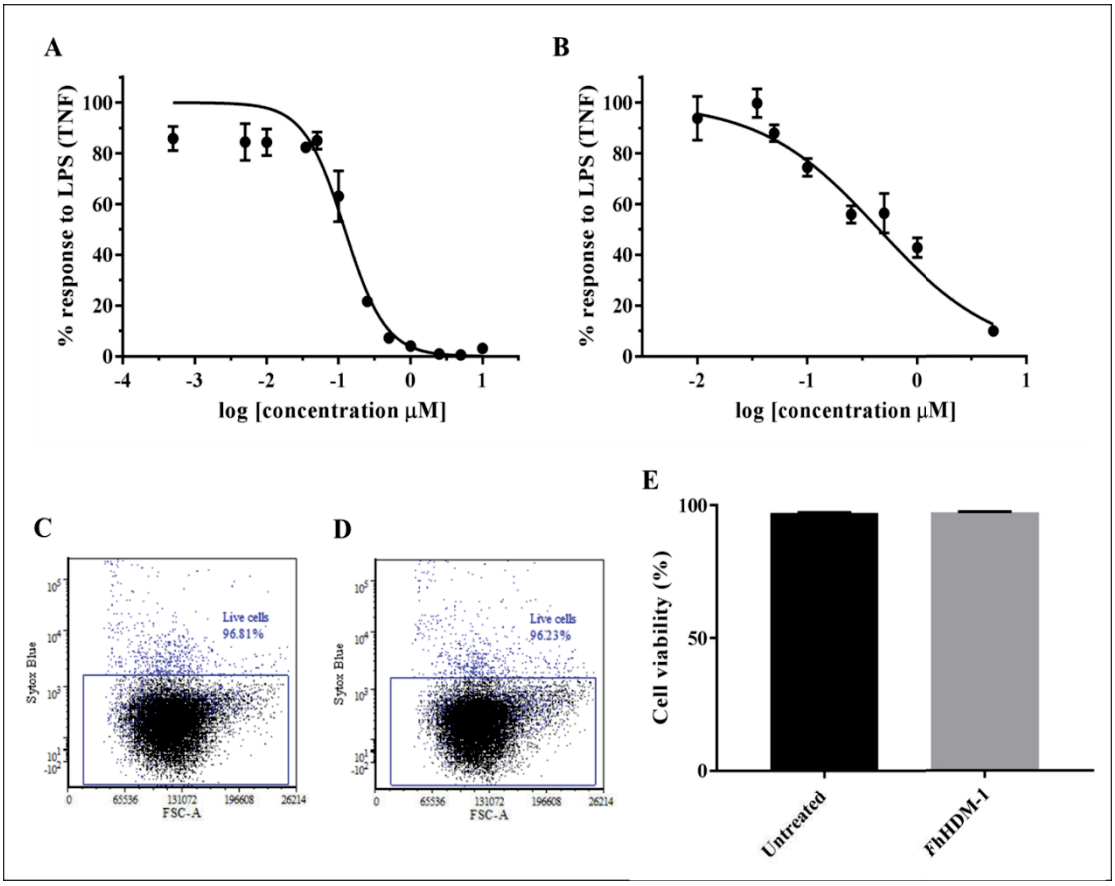

Figure 6.6 FhHDM-1 inhibits the production of TNF by LPS stimulated murine neutrophils. Murine neutrophils (4 x 10^6 cells/ml) were incubated with FhHDM-1 (at various concentrations) for 30min at 37°C and **(A)** immediately stimulated or **(B)** washed twice with saline, prior to stimulation with LPS (100ng/ml) for 4h at 37°C. Cell supernatants were assayed for TNF secretion. Dose response curves were generated by normalising LPS-only stimulation to 100%, and then calculating the amount of TNF produced by LPS stimulated neutrophils in the presence of FhHDM-1. **(C,D)** are representative plots for data **(E)**, where murine neutrophils (1 x 10^6/ml) were treated with FhHDM-1 (15µM) for 30min at 37°C. Sytox Blue was used as a viability stain, and, therefore, the Sytox Blue negative cells were gated for viable cells, with dot plots shown for untreated (C) and FhHDM-1 (D) cells. Data is the combination of five (A) three (B) and ten (E) independent experiments and expressed as means ± SEMs.

Having shown that FhHDM-1 inhibited TNF cytokine production by LPS activated neutrophils, it was determined whether this modulatory effect extended to a broad range of cytokines and chemokines, as had been observed for FhHDM-1 treated macrophages (Chapter 5, Section 5.7). A multiplex was again utilised to determine this. Here, some cytokines/chemokines were produced at levels below the 'biologically relevant' cut-off of 10pg/ml (as detailed in Chapter 5, Section 5.7). Therefore, only the cytokines/chemokines that were above this cut-off concentration were further analysed, and converted as a percentage with the LPS-only stimulated sample adjusted to 100%, for ease of comparisons (Fig. 6.7). Similar to the immune modulatory effect of FhHDM-1 on macrophages, the majority of Th1/Th17 cytokines and chemokines produced by neutrophils in response to LPS were significantly down-regulated by pre-treatment of cells with FhHDM-1, although the extent of inhibition was variable. Specifically, production of Eotaxin was completely inhibited, whilst levels of IL-1β, IL-6, GM-CSF, KC, MCP-1, MIP-1α, and MIP-1β were reduced to 50% (or below) by FhHDM-1 treatment of LPS stimulated neutrophils, as compared to the respective LPS-only samples (Fig. 6.7). Although the inhibition of TNF was not statistically significant, there was still a reduction of TNF production, down to ~60%, as compared to the LPS-only sample (Fig. 6.7). This could be attributed to the small sample size (n =2) of this assay; however, it was established that FhHDM-1 inhibited the production of TNF by LPS stimulated murine neutrophils in Figure 6.6.

In comparison to the inhibitory effect observed in macrophages (Chapter 5, Section 5.7, Fig. 5.10), IL-1β, IL-6, GM-CSF, TNF, Eotaxin, KC, MCP-1, MIP-1α, and MIP-1β were commonly decreased in secretion by both macrophages and neutrophils treated with FhHDM-1, in response to LPS stimulation. This may allude to some mechanistic similarities of signalling pathways for the modulation of pro-inflammatory cytokine/chemokine production within macrophages and neutrophils induced by FhHDM-1.

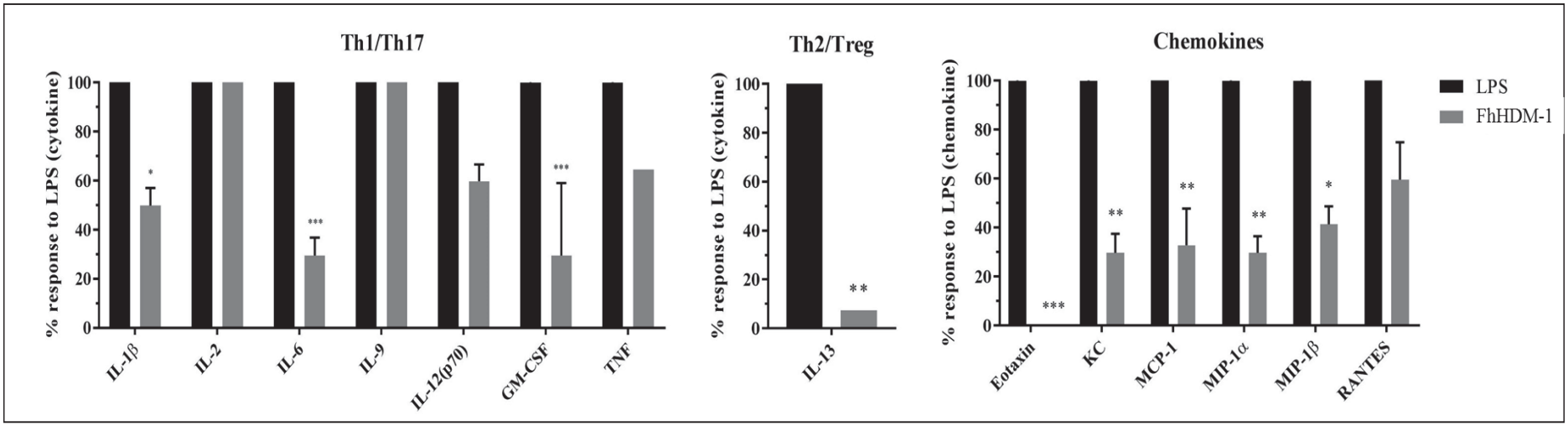

Figure 6.7 FhHDM-1 down-regulates the secretion of pro-inflammatory cytokines and chemokines by LPS stimulated murine neutrophils. Murine neutrophils (4 x 10^6 cells/ml) were incubated with FhHDM-1 (5μM) for 30min at 37ºC. Cells were then washed twice with saline, prior to stimulation with LPS (100ng/ml) for 4h at 37ºC. Cell supernatants were assayed for pro-inflammatory (Th1/Th17), anti-inflammatory/regulatory (Th2/Treg) cytokines and chemokines via a multiplex. Data was converted to percentages, with LPS-only stimulation normalised to 100% for each cytokine/chemokine. Data is the combination of two biological replicates and expressed as means ± SEMs (statistically significance was determined using a two-way ANOVA, as compared to their respective LPS-only stimulated samples; * $p \leq 0.05$, ** $p \leq 0.01$, *** $p \leq 0.001$, **** $p \leq 0.0001$).

6.4 Assessment of the ability of FhHDM-1 treated neutrophils to activate murine dendritic cells

Neutrophils play a significant role in the initiation of autoimmune diseases, such as T1D and MS. In particular, neutrophils secrete pro-inflammatory cytokines, and other unknown soluble proteins, which subsequently activate local DCs within the pancreas or CNS, to initiate T1D [41] and MS [42], respectively. Having demonstrated that FhHDM-1 treatment of neutrophils reduced the secretion of pro-inflammatory cytokines, it was of interest to determine whether this in turn modulated the activation of DCs.

Murine neutrophils were treated with FhHDM-1 (10μM) for 30min at 37ºC, and then stimulated with either LPS (1μg/ml) for 1h at 37ºC, or a combination of TNF (10ng/ml) and LPS [362] (Section 2.5.5.5). Neutrophils were then washed five times (to ensure that no LPS or TNF was present for the stimulation of DCs) prior to incubation with primary bone marrow derived DCs (1:1 neutrophils:DCs) for 16h at 37ºC. The expression of surface markers, CD80 and CD86, on DCs were measured via flow cytometry as indicators of DC activation. As expected, there was a slight, but statistically significant, increase in the surface expression levels of CD80 and CD86 on DCs co-incubated with neutrophils that had been activated with LPS ($p = 0.0018$ and $p = 0.0010$ for CD80 and CD86, respectively; Fig. 6.8A,C), and the combination of LPS/TNF ($p = 0.0146$ and $p = 0.0065$ for CD80 and CD86, respectively; Fig. 6.8B,D). Excitingly, neutrophils that had been pre-treated with FhHDM-1 had a reduced ability to activate DCs, as illustrated by a significant decrease in the expression levels of CD80 and CD86 on DCs co-cultured with either LPS ($p = 0.0357$ and $p = 0.0018$ for CD80 and CD86, respectively; Fig. 6.8A,C), or LPS/TNF activated neutrophils ($p = 0.0236$ and $p = 0.0008$ for CD80 and CD86, respectively; Fig. 6.8B,D). This supports the hypothesis that by modulating the production of pro-inflammatory cytokines by neutrophils, FhHDM-1 indirectly inhibits the activation of DCs.

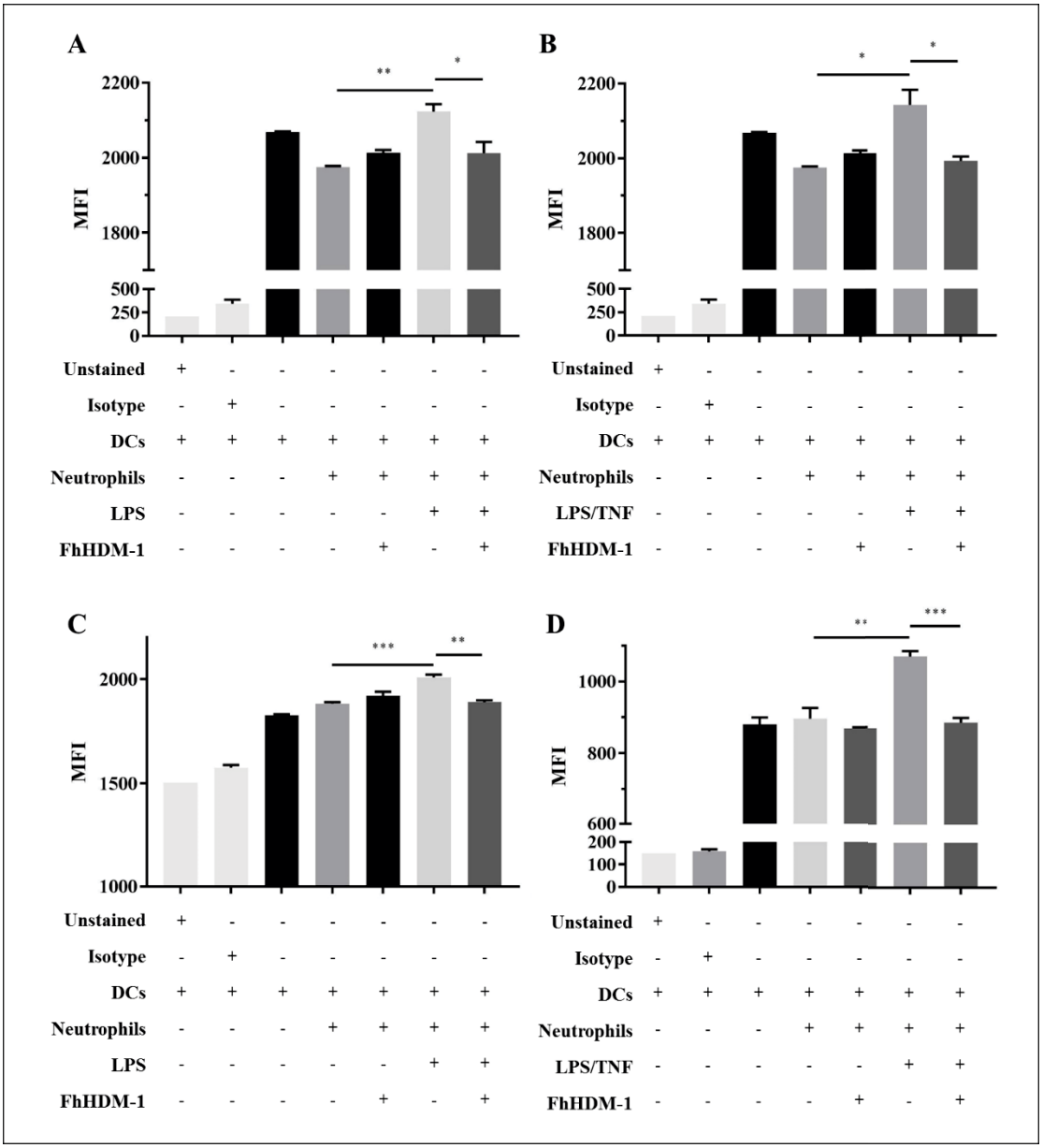

Figure 6.8 FhHDM-1 prevents dendritic cell activation by activated murine neutrophils. Murine neutrophils (2 x 10^6 cells/ml) were incubated with FhHDM-1 (10μM) for 30min at 37ºC. Then, neutrophils were either stimulated with **(A,C)** LPS (1μg/ml) for 1h or **(B,D)** the combination of TNF (10ng/ml) for 20min, then LPS at 37ºC. Neutrophils were then washed five times prior to incubation with primary bone marrow derived dendritic cells (DCs; 1:1) for 16h at 37ºC. The expression levels of (A,B) CD80 and (C,D) CD86 on DCs were measured via flow cytometry. Unstained and isotype controls were included. Data is representative of two independent experiments and expressed as means ± SEMs (* $p \leq 0.05$, ** $p \leq 0.01$, *** $p \leq 0.001$).

6.5 Discussion

The ability of FhHDM-1 to interact with neutrophils was a novel and exciting discovery, as neutrophils are emerging as crucial immune cells that cooperate with macrophages for the initiation of autoimmune disorders. Similar to the effect on macrophages, FhHDM-1 induced no change in surface marker expression levels (Section 6.3.2, Fig. 6.5), and reduced the production of pro-inflammatory cytokines/chemokines (Section 6.3.3, Fig. 6.6 and 6.7) by activated murine neutrophils. This may indicate a similar mechanism of action by FhHDM-1 in modulating intracellular signalling pathways within these two innate immune cell types.

The ability of FhHDM-1 to prevent the phagocytic uptake of Ovalbumin and *E. coli* particles (Section 6.3.1, Fig. 6.4) was an unexpected outcome, as phagocytosis (of dextran) by macrophages was reportedly not affected by FhHDM-1 treatment [221]. This disparity in results may be due to the type of particles used for the assessment of phagocytic ability. The biological impact of preventing phagocytic activity for both cell types should be further investigated, specifically assessing the uptake of apoptotic cells. Aberrations in phagocytosis of apoptotic cells is associated with autoimmunity [357]. Phagocytosis is a multi-step process, involving the initial recognition of microbes or apoptotic cells by specialised receptors, the internalisation of the target into cargos for digestion, and the subsequent secretion of immune modulatory products, such as cytokines and chemokines [363]. Although mechanisms linking phagocytosis and autoimmunity are yet to be defined, defects or modulations in any of these processes would putatively determine immune outcome. It is yet to be determined whether FhHDM-1 exerts any effects on these processes in neutrophils and macrophages.

The binding of FhHDM-1 to multiple types of immune cells may be detrimental for the development of the peptide as a therapeutic, as it may cause unwanted side effects. This is, however, unlikely to be the case, as it was demonstrated that FhHDM-1 does not affect changes in surface marker expression levels in neutrophils and FhHDM-1 is not cytotoxic (Section 6.3.3, Fig. 6.6C-E). More importantly, without inducing changes to surface marker expression levels, FhHDM-1 was still able to prevent pro-inflammatory cytokine/chemokine secretion by neutrophils. This suggests that, similar to its effect on

macrophages, FhHDM-1 is selectively inhibiting the activation of neutrophil pro-inflammatory activity. Therefore, FhHDM-1 offers great potential as a therapeutic for autoimmune disorders, as neutrophils (along with macrophages) play a crucial role in the initiation of autoimmunity. Recently, it has been reported that therapies targeting neutrophils attenuate autoimmune diseases, including T1D, MS and IBD. For example, blocking of the neutrophil receptors, CXCR1/2 (receptors for chemokine, IL-8), decreased the influx of neutrophils into the pancreas [41, 345]), and prevented the onset of T1D [364]. This strategy also delayed the clinical symptoms [365] and abrogated the breakdown of the blood-brain barrier, thereby reducing infiltration of leukocytes into the CNS of a murine model of MS [366]. Similarly, the severity of murine IBD was decreased by the modulation of neutrophil activity by CXCR1/2 [367, 368]. Although, the effect of FhHDM-1 on the expression levels of CXCR1/2 on neutrophils is unknown, it may explain the lack of neutrophil infiltration into the brain parenchyma in EAE mice that were treated with FhHDM-1 (Donnelly *et al.,* unpublished data).

The inhibition of DC activation via neutrophils was an important finding as it highlighted an indirect biological outcome of the anti-inflammatory actions of FhHDM-1. However, the mechanism of this inhibitory effect on DCs needs to be further defined to determine if it is mediated via a reduction in the secreted soluble products of neutrophils or changes that impact the neutrophils/DCs cellular interactions. This could be assessed using Transwell assays (separating direct DCs and neutrophil interaction), or by incubating the DCs with the supernatant of FhHDM-1 treated neutrophils. Additionally, antibodies against the secreted pro-inflammatory cytokines/chemokines could be used in an attempt to reverse the inhibitory effect (as conducted in [42]). In addition, it would be informative to determine whether neutrophils isolated from EAE mice treated with FhHDM-1 were also inhibited in their ability to activate DCs, as this would add to our understanding of the peptide's mechanism of action in models of autoimmunity.

Chapter 7: General Discussion

The helminth excreted/secreted peptide, FhHDM-1, has been identified as the immune-modulatory molecule within FhES with therapeutic efficacy demonstrated in two murine models of autoimmune disease: T1D and MS. To date, no other single immune-modulatory helminth peptide has been able to prevent disease in multiple models of autoimmunity.

Despite differences in the pathogenesis of T1D and MS, the diseases share characteristics with respect to the initiation and perpetuation phases of autoimmunity. The co-occurrence of MS and T1D has been reported by several studies, suggesting that they have common aetiological components [347]. Most notably, are the involvement of pro-inflammatory M1 macrophages and neutrophils, as key innate immune cells involved in establishing the pro-inflammatory environment within the target tissues, which facilitates the initiation of autoimmunity [348, 369], and amplification of the Th1/Th17 responses that drive the development of disease [29]. Therefore, the observations that FhHDM-1 prevented the initiation and perpetuation of autoimmunity in both MS and T1D, led to the hypothesis that FhHDM-1 operated via anti-inflammatory mechanisms.

The data presented here confirmed this hypothesis, demonstrating that FhHDM-1 specifically inhibited the activation of pro-inflammatory macrophages and neutrophils (Chapters 3, 4 and 6). Furthermore, these cells were shown to subsequently prevent the amplification of pro-inflammatory immune responses, as evidenced by the fact that FhHDM-1 treated macrophages suppressed the secretion of the IFN-γ by T cells, and FhHDM-1 treated neutrophils suppressed the activation of pro-inflammatory DCs. Collectively, these data indicated that FhHDM-1 is likely mediating its protective effects through the inhibition of the pro-inflammatory innate immune signals, which are required for the establishment and maintenance autoimmune disease.

Prior to the current study, the mechanism(s) of action of FhHDM-1 was yet to be characterised. Studies to date had elucidated some activities of the peptide, including the ability to bind and neutralise LPS, which significantly reduced M1 macrophage production of pro-inflammatory cytokines, TNF, IL-6, and IL-1β [197, 199, 210]. *In vitro* assays also showed inhibition of lysosomal vATPase activity by FhHDM-1 [215], and disrupted NLRP3 inflammasome formation, through inactivation of lysosomal

Cathepsin B [221]. All such evidence pointed towards the lysosome as a crucial point of action for FhHDM-1. It was suggested that FhHDM-1 may alter the acidic lysosomal environment, which is critical for the functioning of lysosomal proteases, which are required for appropriate processing of TLRs and intracellular pro-inflammatory signalling pathways [220]. Therefore, this study aimed to determine the intracellular signalling pathways targeted by FhHDM-1 to modulate pro-inflammatory responses.

Through analysing the transcriptional profile of macrophages treated with FhHDM-1 in the context of a pro-inflammatory immune signal, it became evident that the peptide was potentially functioning as a PPAR-γ agonist (Chapter 4), a previously unidentified mechanism of action for FhHDM-1, and an activity never before described for a parasite derived protein.

PPARγ is a key regulator of lipid metabolism within the macrophage [286], and recent reports have suggested the existence of bi-directional crosstalk between lysosomal biogenesis and lipid metabolism [370]. This leads to the question of whether the localization of FhHDM-1 to the lysosome, and subsequent inhibition of acidification, results in the activation of PPARγ (as hypothesised in Fig. 7.1). This would be of great interest, as it has been previously reported that IL-4 treated macrophages (as occurring during chronic helminth infection) actually require active, acidic, lysosomes to degrade lipids to fatty acids, which, in turn, activate PPARγ to induce a switch to a M2 phenotype [370]. This apparent contradiction in the relationship between lysosomal activity, and induction of PPARγ, may simply be due to the action of different signals (IL-4 versus FhHDM-1), and may indicate varied biological functions for PPARγ, which are dependent upon the local immune environment. Certainly, during the first 24h of infection with *Fasciola hepatica*, FhHDM-1 is one of the most abundantly secreted proteins by the parasite (Dalton, personal communication), and directly interacts with the cells of the host's innate immune response. At the same time, there is no evidence of IL-4 production, and the macrophages are not switched to an M2 phenotype; however the expression levels of the genes encoding pro-inflammatory cytokines (TNF, IL-12 and IL-6) are suppressed by 2-8 fold (Donnelly, personal communication). Thus, the inhibition of lysosomal activity, subsequent activation of PPARγ, and inhibition of M1 macrophages may actually be a phenomenon observed during the early stages of infection with *F. hepatica* and mediated by secretion of

FhHDM-1. In contrast, IL-4 induced lysosomal lipolysis, subsequent activation of PPARγ, and induction of M2 macrophages may be a requirement for the chronic stages of infection, when wound repair mechanisms are more critical.

On the other hand, the activation of PPAR-γ in macrophages treated with FhHDM-1 may be a mechanism occurring independently of lysosomal acidification, but which subsequently inhibits lysosomal biogenesis. Indeed, macrophages deficient for PPAR-γ exhibit enhanced lysosomal maturation when infected with *Mycobacterium tuberculosis* [371], and mouse prostate epithelial cells deficient in PPAR-γ show increased formation of lysosomes [372, 373]. This suggests that PPAR-γ induction can decrease lysosomal activity, which further supports the evidence that FhHDM-1 disrupts lysosomal activity. Interestingly, expression of the surface marker, CD36, is induced by PPAR-γ agonists [374-376], and has been shown to inhibit vATPase activity [377]. Potentially, FhHDM-1 may be thus preventing lysosomal acidification via direct inhibition of vATPase (as previously hypothesised), and/or indirectly via the induction of CD36 (Fig 7.1).

The finding that the inhibition of IFN-γ production by T cells, was dependent upon cell-to-cell contact with FhHDM-1 treated macrophages (Chapter 3), certainly supports the possibility that cell surface proteins were altered. Furthermore, CD36 has been associated with the suppression of DC-mediated T cell proliferation, and production of Th1 cytokines, in response to malarial parasites [378, 379]. Therefore, FhHDM-1 may indeed modulate surface CD36 expression levels on macrophages to suppress Th1 responses.

This study also showed that FhHDM-1 treatment of macrophages induced expression of another candidate that mediates the suppression of pro-inflammatory T cells: *SerpinB2* (Chapter 3). It is therefore of interest that PPAR-γ has been shown to induce the expression of SerpinE1 (also known as Plasminogen activator inhibitor-1) in human endothelial cells [380]. Although, it is not the same protein as SerpinB2, as a transcription factor, it is possible that PPAR-γ also regulates the expression of SerpinB2 in macrophages (as hypothesised in Fig. 7.1).

The influence of cellular metabolism on the activity of macrophages has become a prominent area of research, in which, it has been reported that the use of the glycolytic pathway for energy production, is associated with a switch to the M1 pro-inflammatory phenotype of macrophage [268]. Importantly, PPAR-γ is a critical regulator of oxidative phosphorylation, a metabolic pathway which promotes the development and activity of non-inflammatory immune cells, and produces the energy required by the cell in the absence of the glycolytic pathway [286]. This may therefore implicate an indirect consequence of PPAR-γ activation by FhHDM-1, which involves the immunometabolism of macrophages. Here, FhHDM-1 may induce downstream oxidative phosphorylation of macrophages, thereby driving macrophages away from the pro-inflammatory M1 phenotype (Fig. 7.1).

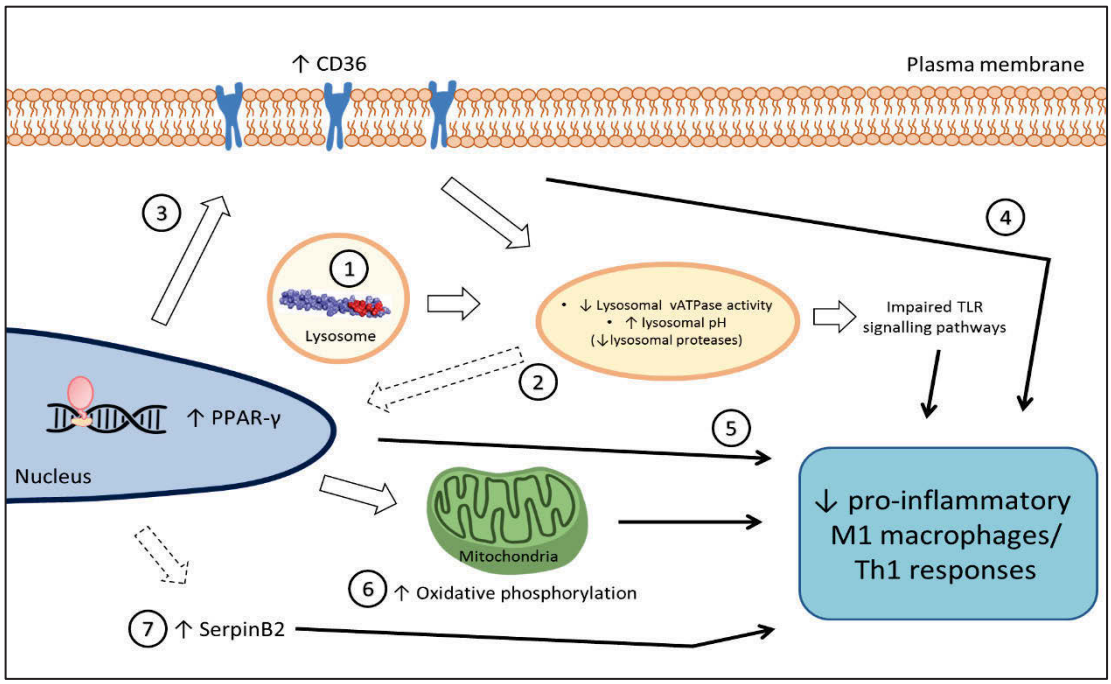

Figure 7.1 FhHDM-1 treatment of macrophages results in the inhibition of pro-inflammatory immune responses. FhHDM-1 localises to the lysosomes (1) resulting in an increase in lysosomal pH (Chapter 5), potentially through the inhibition of vATPase activity, leading to inhibition of lysosomal proteases and impaired TLR signalling pathways (Chapter 4). However, treatment of macrophages with FhHDM-1 also activated the PPAR-γ transcription factor (Chapter 4). Given the intracellular localisation of FhHDM-1, it is possible that alterations to lysosomal pH signal the activation of PPAR-γ (2). The consequence of this activation are putatively multifactorial. (3) Increased expression levels of CD36, which, in turn, recruits fatty acids to inhibit lysosomal vATPase activity and increase lysosomal pH. (4) CD36 on the surface of macrophages inhibits the development of Th1 cells. (5) PPAR-γ directly down-regulates the expression levels of pro-inflammatory cytokines, including TNF, IFN-β and *iNOS* (Chapter 4). (6) PPAR-γ activation drives a metabolic switch towards oxidative phosphorylation, thereby preventing the utilisation of glycolytic pathways to induce M1 macrophages. (7) PPAR-γ increases the expression of SerpinB2, which mediates the suppression of Th1 cells (Chapter 3). Collectively, these mechanisms (directly, or indirectly) down-regulate pro-inflammatory M1 macrophages, and consequently Th1 responses. Dotted arrows indicate hypothesised links. ↑ and ↓ denote increase and decrease, respectively.

In addition to its potential as an anti-inflammatory agent, IPA analysis suggested two additional therapeutic effects for FhHDM-1. Firstly, this investigation supported the previous demonstration that FhHDM-1 would prevent the development of T1D. However, the data suggested a new mechanism of action, namely the inhibition of cell death pathways induced by pro-inflammatory cytokines. Thus, treatment with FhHDM-1 was predicted to prevent pancreatic β cell apoptosis (Chapter 4, Section 4.3). Remarkably, treatment of a murine model of T1D with the PPAR-γ agonist, Pioglitazone, has been shown to increase pancreatic β cell mass, resulting in lowered insulitis and protection from T1D [317]. Confirmation of this activity for FhHDM-1 will implicate a novel mechanism of action for the peptide, to directly target pancreatic β cell survival, in addition to its anti-inflammatory effects to prevent the development of T1D.

Secondly, the IPA analysis indicated that FhHDM-1 down-regulated HMGB1 signalling and IL-17 mediated allergic inflammation (Chapter 4, Section 4.3, Fig. 4.4A, Pathway no. 5 and no. 12, respectively). HMGB1 is a pro-inflammatory mediator in asthma [381] and IL-17 is a pro-inflammatory cytokine that allows neutrophil-dominated inflammation for the development of allergic asthma [382]. To assess the accuracy of this prediction, FhHDM-1 was delivered intravenously to mice after sensitization with an allergen, 1h prior to challenge. Corroborating the IPA output, allergen induced inflammation was observed in mice treated with FhHDM-1, with a significant decrease in the infiltration of neutrophils and eosinophils to the lung (Tanaka *et al.,* manuscript under review). A few studies have also implicated PPAR-γ agonists as treatment for asthma, however, there is contradictory data. While murine studies have shown the therapeutic potential of PPAR-γ agonists [383, 384], clinical studies have only reported moderate benefits [385, 386]. Despite such discrepancies, it will be of interest to further investigate the potential of FhHDM-1 as a therapy for allergic asthma.

The development of FhHDM-1 as a therapeutic requires a further understanding of the binding and active domains of the peptide. This will be important for the identification of the peptide's cellular receptor, and also to inform the development of optimised peptide derivatives. This study made significant advances and identified the minimal

peptide required to mimic the bioactivity of the full length, FhHDM-1 (FhHDM-1.C2; Chapter 5). Further investigations into the activity of this shorter peptide will allow the determination of the vital amino acid sequences that mediate biological functionality, and support the advancement of FhHDM-1 as a highly promising therapeutic for immune-mediated diseases.

Bibliography

1. Cox, F.E., 2002, 'History of human parasitology', *Clinical Microbiology Reviews*, 15: 595-612.
2. Reinhard, K.J., Hevly, R.H., & Anderson, G.A., 1987, 'Helminth remains from prehistoric Indian coprolites on the Colorado Plateau', *The Journal of Parasitology*, 73: 630-639.
3. Laird, D.J., De Tomaso, A.W., Cooper, M.D., & Weissman, I.L., 2000, '50 million years of chordate evolution: seeking the origins of adaptive immunity', *Proceedings of the National Academy of Sciences of the United States of America*, 97: 6924-6926.
4. Jackson, J.A., Friberg, I.M., Little, S., & Bradley, J.E., 2009, 'Review series on helminths, immune modulation and the hygiene hypothesis: immunity against helminths and immunological phenomena in modern human populations: coevolutionary legacies?', *Immunology*, 126: 18-27.
5. Allen, J.E. & Maizels, R.M., 2011, 'Diversity and dialogue in immunity to helminths', *Nature Reviews. Immunology*, 11: 375-388.
6. McSorley, H.J., Hewitson, J.P., & Maizels, R.M., 2013, 'Immunomodulation by helminth parasites: Defining mechanisms and mediators', *International Journal for Parasitology*, 43: 301-310.
7. Hotez, P.J., Brindley, P.J., Bethony, J.M., King, C.H., Pearce, E.J., & Jacobson, J., 2008, 'Helminth infections: the great neglected tropical diseases', *The Journal of Clinical Investigation*, 118: 1311-1321.
8. Díaz, A. & Allen, J.E., 2007, 'Mapping immune response profiles: The emerging scenario from helminth immunology', *European Journal of Immunology*, 37: 3319-3326.
9. Panzer, M., Sitte, S., Wirth, S., Drexler, I., Sparwasser, T., & Voehringer, D., 2011, 'Rapid *in vivo* conversion of effector T cells into Th2 cells during helminth infection', *The Journal of Immunology*, 188: 615-623.
10. Anthony, R.M., Rutitzky, L.I., Urban, J.F.J., Stadecker, M.J., & Gause, W.C., 2007, 'Protective immune mechanisms in helminth infection', *Nature Reviews. Immunology*, 7: 975-987.
11. Maizels, R.M. & McSorley, H.J., 2016, 'Regulation of the host immune system by helminth parasites', *Journal of Allergy and Clinical Immunology*, 138: 666-675.
12. Herbert, D.R., Orekov, T., Roloson, A., Ilies, M., Perkins, C., O'Brien, W., Cederbaum, S., Christianson, D.W., Zimmermann, N., Rothenberg, M.E., & Finkelman, F.D., 2010, 'Arginase I suppresses IL-12/IL-23p40-driven intestinal inflammation during acute schistosomiasis', *The Journal of Immunology*, 184: 6438-6446.
13. Terrazas, C., de Dios Ruiz-Rosado, J., Amici, S.A., Jablonski, K.A., Martinez-Saucedo, D., Webb, L.M., Cortado, H., Robledo-Avila, F., Oghumu, S., Satoskar, A.R., Rodriguez-Sosa, M., Terrazas, L.I., Guerau-de-Arellano, M., & Partida-Sánchez, S., 2017, 'Helminth-induced Ly6Chi monocyte-derived alternatively activated macrophages suppress experimental autoimmune encephalomyelitis', *Scientific Reports*, 7: 40814.
14. Novak, M.L. & Koh, T.J., 2013, 'Macrophage phenotypes during tissue repair', *Journal of Leukocyte Biology* 93: 875-881.
15. Mosser, D.M. & Edwards, J.P., 2008, 'Exploring the full spectrum of macrophage activation', *Nature Reviews. Immunology*, 8: 958-969.
16. Loke, P., Nair, M.G., Parkinson, J., Guiliano, D., Blaxter, M., & Allen, J.E., 2002, 'IL-4 dependent alternatively-activated macrophages have a distinctive *in vivo* gene expression phenotype', *BMC Immunology*, 3: 7.
17. Nair, M.G., Gallagher, I.J., Taylor, M.D., Loke, P., Coulson, P.S., Wilson, R.A., Maizels, R.M., & Allen, J.E., 2005, 'Chitinase and Fizz family members are a generalized feature of nematode infection with selective upregulation of Ym1 and Fizz1 by antigen-presenting cells', *Infection and Immunity*, 73: 385-394.
18. Terrazas, L.I., Montero, D., Terrazas, C.A., Reyes, J.L., & Rodriguez-Sosa, M., 2005, 'Role of the programmed Death-1 pathway in the suppressive activity of alternatively

activated macrophages in experimental cysticercosis', *International Journal for Parasitology*, 35: 1349-1358.
19. MacDonald, A.S., Maizels, R.M., Lawrence, R.A., Dransfield, I., & Allen, J.E., 1998, 'Requirement for *In Vivo* Production of IL-4, But Not IL-10, in the Induction of Proliferative Suppression by Filarial Parasites', *The Journal of Immunology*, 160: 4124-4132.
20. Rőszer, T., 2015, 'Understanding the Mysterious M2 Macrophage through Activation Markers and Effector Mechanisms', *Mediators of Inflammation*, 2015: 16.
21. Thomas, A.C. & Mattila, J.T., 2014, "'Of Mice and Men": Arginine Metabolism in Macrophages', *Frontiers in Immunology*, 5: 479.
22. Yang, Z., Grinchuk, V., Urban, J.F.J., Bohl, J., Sun, R., Notari, L., Yan, S., Ramalingam, T., Keegan, A.D., Wynn, T.A., Shea-Donohue, T., & Zhao, A., 2013, 'Macrohpages as IL-25/IL33-responsive cells play an important role in the induction of Type 2 immunity', *PLoS One*, 8: e59441.
23. Grencis, R.K., Humphreys, N.E., & Bancroft, A.J., 2014, 'Immunity to gastrointestinal nematodes: mechanisms and myths', *Immunological Reviews*, 260: 183-205.
24. Gause, W.C., Wynn, T.A., & Allen, J.E., 2013, 'Type 2 immunity and wound healing: evolutionary refinement of adaptive immunity by helminths', *Nature Reviews. Immunology*, 13: 607-614.
25. Esser-von Bieren, J., Volpe, B., Sutherland, D.B., Burgi, J., Verbeek, J.S., Marsland, B.J., Urban, J.F., Jr., & Harris, N.L., 2015, 'Immune antibodies and helminth products drive CXCR2-dependent macrophage-myofibroblast crosstalk to promote intestinal repair', *PLoS Pathogens*, 11: e1004778.
26. Herbert, D.R., Holscher, C., Mohrs, M., Arendse, B., Schwegmann, A., Radwanska, M., Leeto, M., Kirsch, R., Happ, P., Mossmann, H., Claussen, B., Forster, I., & Brombacher, F., 2004, 'Alternative macrophage activation is essential for survival during schistosomiasis and downmodulates T helper 1 responses and immunopathology ', *Immunity*, 20: 623-635.
27. Mangan, N.E., Fallon, R.E., Smith, P., van Rooijen, N., McKenzie, A.N., & Fallonn, P.G., 2004, 'Helminth infection protects mice from anaphylaxis *via* IL-10 producing B cells', *The Journal of Immunology*, 173: 6346-6356.
28. Walsh, K.P., Brady, M.T., Finlay, C.M., Boon, L., & Mills, K.H., 2009, 'Infection with a helminth parasite attenuates autoimmunity through TGF-β-mediated suppression of Th17 and Th1 responses', *The Journal of Immunology*, 183: 1577-1586.
29. Anaya, J.M., 2010, 'The autoimmune tautology', *Arthritis Research and Therapy*, 12: 147.
30. Lissner, D., Schumann, M., Batra, A., Kredel, L.I., Kuhl, A.A., Erben, U., May, C., Schulzke, J.D., & Siegmund, B., 2015, 'Monocyte and M1 Macrophage-induced Barrier Defect Contributes to Chronic Intestinal Inflammation in IBD', *Inflammatory Bowel Diseases*, 21: 1297-1305.
31. Bedoya, S.K., Lam, B., Lau, K., & Larkin, J., 2013, 'Th17 Cells in Immunity and Autoimmunity', *Clinical and Developmental Immunology*, 2013: 16.
32. Damsker, J.M., Hansen, A.M., & Caspi, R.R., 2010, 'Th1 and Th17 cells: adversaries and collaborators', *Annals of the New York Academy of Sciences*, 1183: 211-221.
33. Mulherin, D., Fitzgerald, O., & Bresnihan, B., 1996, 'Synovial tissue macrophage populations and articular damage in rheumatoid arthritis', *Arthritis and Rheumatology*, 39: 115-124.
34. Steinfelder, S., O'Regan, N.L., & Hartmann, S., 2016, 'Diplomatic Assistance: Can Helminth-Modulated Macrophages Act as Treatment for Inflammatory Disease?', *PLOS Pathogens*, 12: e1005480.
35. Jung, S., Huitinga, I., Schmidt, B., Zielasek, J., Dijkstra, C.D., Toyka, K.V., & Hartung, H.-P., 1993, 'Selective elimination of macrophages by dichlormethylene diphosphonate-containing liposomes suppresses experimental autoimmune neuritis', *Journal of the Neurological Sciences*, 119: 195-202.

36. Huitinga, I., van Rooijen, N., de Groot, C.J., Uitdehaag, B.M., & Dijkstra, C.D., 1990, 'Suppression of experimental allergic encephalomyelitis in Lewis rats after elimination of macrophages', *The Journal of Experimental Medicine*, 172: 1025-1033.
37. Lee, K., Amano, K., & Yoon, J., 1988, 'Evidence for Initial Involvement of Macrophage in Development of Insulitis in NOD Mice', *Diabetes*, 37: 989-991.
38. Kaplan, M.J., 2013, 'Role of neutrophils in systemic autoimmune diseases', *Arthritis Research and Therapy*, 15: 219.
39. Wright, H.L., Moots, R.J., Bucknall, R.C., & Edwards, S.W., 2010, 'Neutrophil function in inflammation and inflammatory diseases', *Rheumatology (Oxford)*, 49: 1618-1631.
40. Rumble, J.M., Huber, A.K., Krishnamoorthy, G., Srinivasan, A., Giles, D.A., Zhang, X., Wang, L., & Segal, B.M., 2015, 'Neutrophil-related factors as biomarkers in EAE and MS', *The Journal of Experimental Medicine*, 212: 23-35.
41. Diana, J., Simoni, Y., Furio, L., Beaudoin, L., Agerberth, B., Barrat, F., & Lehuen, A., 2013, 'Crosstalk between neutrophils, B-1a cells and plasmacytoid dendritic cells initiates autoimmune diabetes', *Nature Medicine*, 19: 65-73.
42. Steinbach, K., Piedavent, M., Bauer, S., Neumann, J.T., & Friese, M.A., 2013, 'Neutrophils amplify autoimmune central nervous system infiltrates by maturing local APCs', *The Journal of Immunology*, 191: 4531-9.
43. Bosch, X., 2011, 'Systemic Lupus Erythematosus and the Neutrophil', *New England Journal of Medicine*, 365: 758-760.
44. Warde, N., 2011, 'Autoimmunity: The role of neutrophils in SLE: untangling the NET', *Nature Reviews. Rheumatology*, 7: 252.
45. Lande, R., Ganguly, D., Facchinetti, V., Frasca, L., Conrad, C., Gregorio, J., Meller, S., Chamilos, G., Sebasigari, R., Riccieri, V., Bassett, R., Amuro, H., Fukuhara, S., Ito, T., Liu, Y.J., & Gilliet, M., 2011, 'Neutrophils activate plasmacytoid dendritic cells by releasing self-DNA-peptide complexes in systemic lupus erythematosus', *Science Translational Medicine*, 3: 73ra19.
46. Cascão, R., Rosário, H.S., Souto-Carneiro, M.M., & Fonseca, J.E., 2010, 'Neutrophils in rheumatoid arthritis: More than simple final effectors', *Autoimmunity Reviews*, 9: 531-535.
47. Dominical, V.M., Bertolo, M.B., Almeida, C.B., Garrido, V.T., Miguel, L.I., Costa, F.F., & Conran, N., 2011, 'Neutrophils of rheumatoid arthritis patients on anti-TNF-alpha therapy and in disease remission present reduced adhesive functions in association with decreased circulating neutrophil-attractant chemokine levels', *Scandinavian Journal of Immunology*, 73: 309-318.
48. Wright, H.L., Moots, R.J., & Edwards, S.W., 2014, 'The multifactorial role of neutrophils in rheumatoid arthritis', *Nature Reviews. Rheumatology*, 10: 593-601.
49. Wipke, B.T. & Allen, P.M., 2001, 'Essential role of neutrophils in the initiation and progression of a murine model of rheumatoid arthritis', *Journal of Immunology*, 167: 1601-1608.
50. Diana, J., Gahzarian, L., Simoni, Y., & Lehuen, A., 2011, 'Innate immunity in type 1 diabetes', *Discovery Medicine*, 11: 513-20.
51. Billiau, A., Heremans, H., Vandekerckhove, F., Dijkmans, R., Sobis, H., Meulepas, E., & Carton, H., 1988, 'Enhancement of experimental allergic encephalomyelitis in mice by antibodies against IFN-gamma', *The Journal of Immunology*, 140: 1506-1510.
52. Ferber, I.A., Brocke, S., Taylor-Edwards, C., Ridgway, W., Dinisco, C., Steinman, L., Dalton, D., & Fathman, C.G., 1996, 'Mice with a disrupted IFN-gamma gene are susceptible to the induction of experimental autoimmune encephalomyelitis (EAE)', *The Journal of Immunology*, 156: 5-7.
53. Matthys, P., Vermeire, K., Mitera, T., Heremans, H., Huang, S., & Billiau, A., 1998, 'Anti-IL-12 antibody prevents the development and progression of collagen-induced arthritis in IFN-gamma receptor-deficient mice', *European Journal of Immunology*, 28: 2143-2151.

54. Yang, X.D., Tisch, R., Singer, S.M., Cao, Z.A., Liblau, R.S., Schreiber, R.D., & McDevitt, H.O., 1994, 'Effect of tumor necrosis factor alpha on insulin-dependent diabetes mellitus in NOD mice. I. The early development of autoimmunity and the diabetogenic process', *Journal of Experimental Medicine*, 180: 995-1004.
55. Veldhoen, M., Hocking, R.J., Flavell, R.A., & Stockinger, B., 2006, 'Signals mediated by transforming growth factor-beta initiate autoimmune encephalomyelitis, but chronic inflammation is needed to sustain disease', *Nature Immunology*, 7: 1151-1156.
56. Mangan, P.R., Harrington, L.E., O'Quinn, D.B., Helms, W.S., Bullard, D.C., Elson, C.O., Hatton, R.D., Wahl, S.M., Schoeb, T.R., & Weaver, C.T., 2006, 'Transforming growth factor-beta induces development of the T(H)17 lineage', *Nature*, 441: 231-234.
57. Bettelli, E., Carrier, Y., Gao, W., Korn, T., Strom, T.B., Oukka, M., Weiner, H.L., & Kuchroo, V.K., 2006, 'Reciprocal developmental pathways for the generation of pathogenic effector TH17 and regulatory T cells', *Nature*, 441: 235-238.
58. Zhu, S. & Qian, Y., 2012, 'IL-17/IL-17 receptor system in autoimmune disease: mechanisms and therapeutic potential', *Clinical science (London, England : 1979)*, 122: 487-511.
59. Zaccone, P., Fehervari, Z., Phillips, J.M., Dunne, D.W., & Cooke, A., 2006, 'Parasitic worms and inflammatory diseases', *Parasite Immunology*, 28: 515-523.
60. Aoyama, H., Hirata, T., Sakugawa, H., Watanabe, T., Miyagi, S., Maeshiro, T., Chinen, T., Kawane, M., Zaha, O., Nakayoshi, T., Kinjo, F., & Fujita, J., 2007, 'An inverse relationship between autoimmune liver diseases and *Strongyloides stercoralis* infection', *The American Journal of Tropical Medicine and Hygiene*, 76: 972-976.
61. Alcalde-Cabero, E., Almazan-Isla, J., Garcia-Merino, A., de Sa, J., & de Pedro-Cuesta, J., 2013, 'Incidence of multiple sclerosis among European Economic Area populations, 1985-2009: the framework for monitoring', *BMC Neurology*, 13: 58.
62. Eszter Muller, K., Laszlo Lakatos, P., Papp, M., & Veres, G., 2014, 'Incidence and paris classification of pediatric inflammatory bowel disease', *Gastroenterology Research and Practice*, 2014: 904307.
63. Wilson, M.S., Taylor, M.D., O'Gorman, M.T., Balic, A., Barr, T.A., Filbey, K., Anderton, S.M., & Maizels, R.M., 2010, 'Helminth-induced CD19+CD23hi B cells modulate experimental allergic and autoimmune inflammation', *European Journal of Immunology*, 40: 1682-1696.
64. Barnett, M.H., Williams, D.B., Day, S., Macaskill, P., & McLeod, J.G., 2003, 'Progressive increase in incidence and prevalence of multiple sclerosis in Newcastle, Australia: a 35-year study', *Journal of the Neurological Sciences*, 213: 1-6.
65. Fleming, J.O. & Cook, T.D., 2006, 'Multiple sclerosis and the hygiene hypothesis', *Neurology*, 67: 2085-2086.
66. Fleming, J.O. & Weinstock, J.V., 2015, 'Clinical trials of helminth therapy in autoimmune diseases: rationale and findings', *Parasite Immunology*, 37: 277-292.
67. Correale, J. & Farez, M., 2007, 'Association between parasite infection and immune responses in multiple sclerosis', *Annals of Neurology*, 61: 97-108.
68. Correale, J. & Farez, M.F., 2011, 'The impact of parasite infections on the course of multiple sclerosis', *Journal of Neuroimmunology*, 233: 6-11.
69. Fumagalli, M., Pozzoli, U., Cagliani, R., Comi, G.P., Riva, S., Clerici, M., Bresolin, N., & Sironi, M., 2009, 'Parasites represent a major selective force for interleukin genes and shape the genetic predisposition to autoimmune conditions', *The Journal of Experimental Medicine*, 206: 1395-1408.
70. Maizels, R.M., 2009, 'Parasite immunomodulation and polymorphisms of the immune system', *Journal of Biology*, 8: 62.
71. Elliott, D.E. & Weinstock, J.V., 2009, 'Helminthic therapy: using worms to treat immune-mediated disease', *Advances in Experimental Medicine and Biology*, 666: 157-166.
72. Rook, G.A., 2010, '99th Dahlem conference on infection, inflammation and chronic inflammatory disorders: darwinian medicine and the 'hygiene' or 'old friends' hypothesis', *Clinical and Experimental Immunology*, 160: 70-79.

73. Strachan, D.P., 1989, 'Hay fever, hygiene and household size', *BMJ*, 299: 1259-1260.
74. Rook, G.A.W., 2009, 'Review series on helminths, immune modulation and the hygiene hypothesis: The broader implications of the hygiene hypothesis', *Immunology*, 126: 3-11.
75. Brady, M.T., O'Neill, S.M., Dalton, J.P., & Mills, K.H., 1999, '*Fasciola hepatica* suppresses a protective Th1 response against *Bordetella pertussis*', *Infection and Immunity*, 67: 5372-5378.
76. McSorley, H.J. & Maizels, R.M., 2012, 'Helminth infections and host immune regulation', *Clinical Microbiology Reviews*, 25: 585-608.
77. van Riet, E., Hartgers, F.C., & Yazdanbakhsh, M., 2007, 'Chronic helminth infections induce immunomodulation: Consequences and mechanisms', *Immunobiology*, 212: 475-490.
78. Wiria, A.E., Djuardi, Y., Supali, T., Sartono, E., & Yazdanbakhsh, M., 2012, 'Helminth infection in populations undergoing epidemiological transition: a friend or foe?', *Seminars in Immunopathology*, 34: 889-901.
79. Maizels, R.M., Balic, A., Gomez-Escobar, N., Nair, M., Taylor, M.D., & Allen, J.E., 2004, 'Helminth parasites--masters of regulation', *Immunological Reviews*, 201: 89-116.
80. Espinoza-Jiménez, A., Rivera-Montoya, I., Cárdenas-Arreola, R., Morán, L., & Terrazas, L.I., 2010, 'Taenia crassiceps Infection Attenuates Multiple Low-Dose Streptozotocin-Induced Diabetes', *Journal of Biomedicine and Biotechnology*, 2010: 11.
81. Bodammer, P., Waitz, G., Loebermann, M., Holtfreter, M.C., Maletzki, C., Krueger, M.R., Nizze, H., Emmrich, J., & Reisinger, E.C., 2011, '*Schistosoma mansoni* infection but not egg antigen promotes recovery from colitis in outbred NMRI mice', *Digestive Diseases and Sciences*, 56: 70-78.
82. Osada, Y., Shimizu, S., Kumagai, T., Yamada, S., & Kanazawa, T., 2009, '*Schistosoma mansoni* infection reduces severity of collagen-induced arthritis via down-regulation of pro-inflammatory mediators', *International Journal for Parasitology*, 39: 457-464.
83. Song, X., Shen, J., Wen, H., Zhong, Z., Luo, Q., Chu, D., Qi, Y., Xu, Y., & Wei, W., 2011, 'Impact of Schistosoma japonicum infection on collagen-induced arthritis in DBA/1 mice: a murine model of human rheumatoid arthritis', *PLoS One*, 6: e23453.
84. Elliott, D.E., Li, J., Blum, A., Metwali, A., Qadir, K., Urban, J.F., Jr., & Weinstock, J.V., 2003, 'Exposure to schistosome eggs protects mice from TNBS-induced colitis', *American Journal of Physiology- Gastrointestinal and Liver Physiology*, 284: G385-G391.
85. Gruden-Movsesijan, A., Ilic, N., Mostarica-Stojkovic, M., Stosic-Grujicic, S., Milic, M., & Sofronic-Milosavljevic, L., 2010, 'Mechanisms of modulation of experimental autoimmune encephalomyelitis by chronic Trichinella spiralis infection in Dark Agouti rats', *Parasite Immunology*, 32: 450-459.
86. Broadhurst, M.J., Ardeshir, A., Kanwar, B., Mirpuri, J., Gundra, U.M., Leung, J.M., Wiens, K.E., Vujkovic-Cvijin, I., Kim, C.C., Yarovinsky, F., Lerche, N.W., McCune, J.M., & Loke, P., 2012, 'Therapeutic helminth infection of macaques with idiopathic chronic diarrhea alters the inflammatory signature and mucosal microbiota of the colon', *PLoS Pathogens*, 8: e1003000.
87. Liu, Q., Sundar, K., Mishra, P.K., Mousavi, G., Liu, Z., Gaydo, A., Alem, F., Lagunoff, D., Bleich, D., & Gause, W.C., 2009, 'Helminth infection can reduce insulitis and type 1 diabetes through CD25- and IL-10-independent mechanisms', *Infection and Immunity*, 77: 5347-5358.
88. Hunter, M.M., Wang, A., Parhar, K.S., Johnston, M.J., Van Rooijen, N., Beck, P.L., & McKay, D.M., 2010, '*In vitro*-derived alternatively activated macrophages reduce colonic inflammation in mice', *Gastroenterology*, 138: 1395-1405.
89. Weisser, S.B., Kozicky, L.K., Brugger, H.K., Ngoh, E.N., Cheung, B., Jen, R., Menzies, S.C., Samarakoon, A., Murray, P.J., Lim, C.J., Johnson, P., Boucher, J.L., van Rooijen, N., & Sly, L.M., 2014, 'Arginase activity in alternatively activated

macrophages protects PI3Kp110delta deficient mice from dextran sodium sulfate induced intestinal inflammation', *European Journal of Immunology*, 44: 3353-3367.
90. Leung, G., Wang, A., Fernando, M., Phan, V.C., & McKay, D.M., 2013, 'Bone marrow-derived alternatively activated macrophages reduce colitis without promoting fibrosis: participation of IL-10', *American Journal of Physiology. Gastrointestinal and Liver Physiology*, 304: G781-792.
91. Smith, P., Mangan, N.E., Walsh, C.M., Fallon, R.E., McKenzie, A.N., van Rooijen, N., & Fallon, P.G., 2007, 'Infection with a helminth parasite prevents experimental colitis via a macrophage-mediated mechanism', *Journal of Immunology*, 178: 4557-4566.
92. Hunter, M.M., Wang, A., Hirota, C.L., & McKay, D.M., 2005, 'Neutralizing anti-IL-10 antibody blocks the protective effect of tapeworm infection in a murine model of chemically induced colitis', *Journal of Immunology*, 174: 7368-7375.
93. Elliott, D.E., Setiawan, T., Metwali, A., Blum, A., Urban, J.F., Jr., & Weinstock, J.V., 2004, 'Heligmosomoides polygyrus inhibits established colitis in IL-10-deficient mice', *European Journal of Immunology*, 34: 2690-2698.
94. Elliott, D.E., Metwali, A., Leung, J., Setiawan, T., Blum, A.M., Ince, M.N., Bazzone, L.E., Stadecker, M.J., Urban, J.F., Jr., & Weinstock, J.V., 2008, 'Colonization with Heligmosomoides polygyrus suppresses mucosal IL-17 production', *Journal of Immunology*, 181: 2414-2419.
95. Hang, L., Setiawan, T., Blum, A.M., Urban, J., Stoyanoff, K., Arihiro, S., Reinecker, H., & Weinstock, J.V., 2010, '*Heligmosomoides polygyrus* infection can inhibit colitis through direct interaction with innate immunity', *Journal of immunology (Baltimore, Md. : 1950)*, 185: 3184-3189.
96. Osada, Y., Yamada, S., Nabeshima, A., Yamagishi, Y., Ishiwata, K., Nakae, S., Sudo, K., & Kanazawa, T., 2013, '*Heligmosomoides polygyrus* infection reduces severity of type 1 diabetes induced by multiple low-dose streptozotocin in mice via STAT6- and IL-10-independent mechanisms', *Experimental Parasitology*, 135: 388-396.
97. Wilson, M.S., Ramalingam, T.R., Rivollier, A., Shenderov, K., Mentink-Kane, M.M., Madala, S.K., Cheever, A.W., Artis, D., Kelsall, B.L., & Wynn, T.A., 2011, 'Colitis and intestinal inflammation in IL10-/- mice results from IL-13Ralpha2-mediated attenuation of IL-13 activity', *Gastroenterology*, 140: 254-264.
98. Hunter, M.M., Wang, A., Hirota, C.L., & McKay, D.M., 2007, 'Helminth infection enhances disease in a murine TH2 model of colitis', *Gastroenterology*, 132: 1320-1330.
99. Wang, A., Fernando, M., Leung, G., Phan, V., Smyth, D., & McKay, D.M., 2010, 'Exacerbation of Oxazolone Colitis by Infection with the Helminth *Hymenolepis diminuta* : Involvement of IL-5 and Eosinophils', *The American Journal of Pathology*, 177: 2850-2859.
100. Beer, R.J., 1976, 'The relationship between *Trichuris trichiura* (Linnaeus 1758) of man and *Trichuris suis* (Schrank 1788) of the pig', *Research in Veterinary Science*, 20: 47-54.
101. Summers, R.W., Elliott, D.E., Urban, J.F.J., Thompson, R., & Weinstock, J.V., 2005, 'Trichuris suis therapy in Crohn's disease', *Gut*, 54: 87-90.
102. Changhua, L., Xiaorong, Z., Dongchuan, Q., Shuhua, X., Hotez, P.J., Defu, Z., Hulian, Z., Mingden, L., Hainan, R., Bing, Z., Haichou, X., Hawdon, J., & Zheng, F., 1999, 'Epidemiology of human hookworm infections among adult villagers in Hejiang and Santai Counties, Sichuan Province, China', *Acta Tropica*, 73: 243-249.
103. Diemert, D.J., Bethony, J.M., & Hotez, P.J., 2008, 'Hookworm vaccines', *Clinical Infectious Diseases*, 46: 282-288.
104. Jouvin, M.H. & Kinet, J.P., 2012, '*Trichuris suis* ova: testing a helminth-based therapy as an extension of the hygiene hypothesis', *The Journal of Allergy and Clinical Immunology*, 130: 3-10
105. Croese, J., O'Neil, J., Masson, J., Cooke, S., Melrose, W., Pritchard, D., & Speare, R., 2006, 'A proof of concept study establishing Necator americanus in Crohn's patients and reservoir donors', *Gut*, 55: 136-137.

106. Helmby, H., 2015, 'Human helminth therapy to treat inflammatory disorders - where do we stand?', *BMC Immunology*, 16: 12.
107. Lopes, F., Matisz, C., Reyes, J.L., Jijon, H., Al-Darmaki, A., Kaplan, G.G., & McKay, D.M., 2016, 'Helminth Regulation of Immunity: A Three-pronged Approach to Treat Colitis', *Inflammatory Bowel Diseases*, 22: 2499-2512.
108. Medicine, N.Y.U.S.o. *Mucosal Immunity of Ulcerative Colitis Patients Undergoing Therapy With Trichuris Suis Ova (MUCUS)*. 2016; Available from: https://clinicaltrials.gov/ct2/show/results/NCT01433471.
109. Correale, J., 2014, 'Helminth/Parasite treatment of multiple sclerosis', *Current Treatment Options in Neurology*, 16: 296.
110. Nottingham, U.o. *Worms for Immune Regulation of Multiple Sclerosis (WIRMS)*. 2016; Available from: https://clinicaltrials.gov/ct2/show/NCT01470521.
111. Evans, H. & Mitre, E., 2015, 'Worms as therapeutic agents for allergy and asthma: understanding why benefits in animal studies have not translated into clinical success', *The Journal of Allergy and Clinical Immunology*, 135: 343-353.
112. Attout, T., Martin, C., Babayan, S.A., Kozek, W.J., Bazzocchi, C., Oudet, F., Gallagher, I.J., Specht, S., & Bain, O., 2008, 'Pleural cellular reaction to the filarial infection Litomosoides sigmodontis is determined by the moulting process, the worm alteration, and the host strain', *Parasitology International*, 57: 201-211.
113. Filbey, K.J., Grainger, J.R., Smith, K.A., Boon, L., van Rooijen, N., Harcus, Y., Jenkins, S., Hewitson, J.P., & Maizels, R.M., 2014, 'Innate and adaptive type 2 immune cell responses in genetically controlled resistance to intestinal helminth infection', *Immunology and Cell Biology*, 92: 436-448.
114. Sewell, D., Qing, Z., Reinke, E., Elliot, D., Weinstock, J., Sandor, M., & Fabry, Z., 2003, 'Immunomodulation of experimental autoimmune encephalomyelitis by helminth ova immunization', *International Immunology*, 15: 59-69.
115. La Flamme, A.C., Ruddenklau, K., & Backstrom, B.T., 2003, 'Schistosomiasis decreases central nervous system inflammation and alters the progression of experimental autoimmune encephalomyelitis', *Infection and Immunity*, 71: 4996-5004.
116. Reyes, J.L., Espinoza-Jimenez, A.F., Gonzalez, M.I., Verdin, L., & Terrazas, L.I., 2011, 'Taenia crassiceps infection abrogates experimental autoimmune encephalomyelitis', *Cellular Immunology*, 267: 77-87.
117. Wu, Z., Nagano, I., Asano, K., & Takahashi, Y., 2010, 'Infection of non-encapsulated species of Trichinella ameliorates experimental autoimmune encephalomyelitis involving suppression of Th17 and Th1 response', *Parasitology Research*, 107: 1173-1188.
118. Saunders, K.A., Raine, T., Cooke, A., & Lawrence, C.E., 2007, 'Inhibition of autoimmune type 1 diabetes by gastrointestinal helminth infection', *Infection and Immunity*, 75: 397-407.
119. Mishra, P.K., Patel, N., Wu, W., Bleich, D., & Gause, W.C., 2013, 'Prevention of type 1 diabetes through infection with an intestinal nematode parasite requires IL-10 in the absence of a Th2-type response', *Mucosal Immunology*, 6: 297-308.
120. Hubner, M.P., Shi, Y., Torrero, M.N., Mueller, E., Larson, D., Soloviova, K., Gondorf, F., Hoerauf, A., Killoran, K.E., Stocker, J.T., Davies, S.J., Tarbell, K.V., & Mitre, E., 2012, 'Helminth protection against autoimmune diabetes in nonobese diabetic mice is independent of a type 2 immune shift and requires TGF-beta', *The Journal of Immunology*, 188: 559-568.
121. Cooke, A., Tonks, P., Jones, F.M., O'Shea, H., Hutchings, P., Fulford, A.J., & Dunne, D.W., 1999, 'Infection with Schistosoma mansoni prevents insulin dependent diabetes mellitus in non-obese diabetic mice', *Parasite Immunology*, 21: 169-176.
122. El-Wakil, H.S., Aboushousha, T.S., El Haddad, O., Gamil, N.B., Mansour, T., & El-Said, H., 2002, 'Effect of schistosoma mansoni egg deposition on multiple low doses streptozotocin induced insulin dependent diabetes', *Journal of the Egyption Society of Parasitology*, 32: 987-1002.

123. Setiawan, T., Metwali, A., Blum, A.M., Ince, M.N., Urban, J.F., Jr., Elliott, D.E., & Weinstock, J.V., 2007, 'Heligmosomoides polygyrus promotes regulatory T-cell cytokine production in the murine normal distal intestine', *Infection and Immunity*, 75: 4655-4663.
124. Sutton, T.L., Zhao, A., Madden, K.B., Elfrey, J.E., Tuft, B.A., Sullivan, C.A., Urban, J.F., Jr., & Shea-Donohue, T., 2008, 'Anti-Inflammatory mechanisms of enteric Heligmosomoides polygyrus infection against trinitrobenzene sulfonic acid-induced colitis in a murine model', *Infection and Immunity*, 76: 4772-4782.
125. Xia, C.M., Zhao, Y., Jiang, L., Jiang, J., & Zhang, S.C., 2011, 'Schistosoma japonicum ova maintains epithelial barrier function during experimental colitis', *World Journal of Gastroenterology*, 17: 4810-4816.
126. Zhao, Y., Zhang, S., Jiang, L., Jiang, J., & Liu, H., 2009, 'Preventive effects of Schistosoma japonicum ova on trinitrobenzenesulfonic acid-induced colitis and bacterial translocation in mice', *Journal of Gastroenterology and Hepatology*, 24: 1775-1780.
127. Moreels, T.G., Nieuwendijk, R.J., De Man, J.G., De Winter, B.Y., Herman, A.G., Van Marck, E.A., & Pelckmans, P.A., 2004, 'Concurrent infection with Schistosoma mansoni attenuates inflammation induced changes in colonic morphology, cytokine levels, and smooth muscle contractility of trinitrobenzene sulphonic acid induced colitis in rats', *Gut*, 53: 99-107.
128. Melon, A., Wang, A., Phan, V., & McKay, D.M., 2010, 'Infection with Hymenolepis diminuta is more effective than daily corticosteroids in blocking chemically induced colitis in mice', *Journal of Biomedicine and Biotechnology*, 2010: 384523.
129. Khan, W.I., Blennerhasset, P.A., Varghese, A.K., Chowdhury, S.K., Omsted, P., Deng, Y., & Collins, S.M., 2002, 'Intestinal nematode infection ameliorates experimental colitis in mice', *Infection and Immunity*, 70: 5931-5937.
130. Persaud, R., Wang, A., Reardon, C., & McKay, D.M., 2007, 'Characterization of the immuno-regulatory response to the tapeworm Hymenolepis diminuta in the non-permissive mouse host', *International Journal for Parasitology*, 37: 393-403.
131. Donskow-ŁYsoniewska, K., Majewski, P., Brodaczewska, K., JÓŹWicka, K., & Doligalska, M., 2012, 'Heligmosmoides polygyrus fourth stages induce protection against DSS-induced colitis and change opioid expression in the intestine', *Parasite Immunology*, 34: 536-546.
132. Ledesma-Soto, Y., Callejas, B.E., Terrazas, C.A., Reyes, J.L., Espinoza-Jimenez, A., Gonzalez, M.I., Leon-Cabrera, S., Morales, R., Olguin, J.E., Saavedra, R., Oghumu, S., Satoskar, A.R., & Terrazas, L.I., 2015, 'Extraintestinal Helminth Infection Limits Pathology and Proinflammatory Cytokine Expression during DSS-Induced Ulcerative Colitis: A Role for Alternatively Activated Macrophages and Prostaglandins', *BioMed Research International*, 2015: 563425.
133. Adisakwattana, P., Nuamtanong, S., Kusolsuk, T., Chairoj, M., Yenchitsomanas, P.T., & Chaisri, U., 2013, 'Non-encapsulated *Trichinella* spp., *T. papuae*, diminishes severity of DSS-induced colitis in mice', *Asian Pacific Journal of Allergy and Immunology*, 31: 106-114.
134. Cho, M.K., Park, M.K., Kang, S.A., Choi, S.H., Ahn, S.C., & Yu, H.S., 2012, 'Trichinella spiralis infection suppressed gut inflammation with CD4(+)CD25(+)Foxp3(+) T cell recruitment', *The Korean Journal of Parasitology*, 50: 385-390.
135. He, Y., Li, J., Zhuang, W., Yin, L., Chen, C., Li, J., Chi, F., Bai, Y., & Chen, X.P., 2010, 'The inhibitory effect against collagen-induced arthritis by Schistosoma japonicum infection is infection stage-dependent', *BMC Immunology*, 11: 28.
136. Summers, R.W., Elliott, D.E., Qadir, K., Urban, J.F., Jr., Thompson, R., & Weinstock, J.V., 2003, 'Trichuris suis seems to be safe and possibly effective in the treatment of inflammatory bowel disease', *The American Journal of Gastroenterology*, 98: 2034-2041.

137. Sandborn, W.J., Elliott, D.E., Weinstock, J., Summers, R.W., Landry-Wheeler, A., Silver, N., Harnett, M.D., & Hanauer, S.B., 2013, 'Randomised clinical trial: the safety and tolerability of Trichuris suis ova in patients with Crohn's disease', *Alimentary Pharmacology and Therapeutics*, 38: 255-263.
138. Scholmerich, J., Fellermann, K., Seibold, F.W., Rogler, G., Langhorst, J., Howaldt, S., Novacek, G., Petersen, A.M., Bachmann, O., Matthes, H., Hesselbarth, N., Teich, N., Wehkamp, J., Klaus, J., Ott, C., Dilger, K., Greinwald, R., & Mueller, R., 2016, 'A Randomised, Double-blind, Placebo-controlled Trial of Trichuris suis ova in Active Crohn's disease', *Journal of Crohn's and Colitis*, 11: 390-399.
139. Summers, R.W., Elliott, D.E., Urban, J.F.J., Thompson, R.A., & Weinstock, J.V., 2005, 'Trichuris suis therapy for active ulcerative colitis: a randomized controlled trial', *Gastroenterology*, 128: 825-832.
140. Fleming, J.O., Isaak, A., Lee, J.E., Luzzio, C.C., Carrithers, M.D., Cook, T.D., Field, A.S., Boland, J., & Fabry, Z., 2011, 'Probiotic helminth administration in relapsing-remitting multiple sclerosis: a phase 1 study', *Multiple Sclerosis*, 17: 743-754.
141. Fleming, J., Hartman, L., Maksimovic, J., Nace, S., Luzzio, C., Koehn, M., Ritter, A., Risa, T., Lawler, B., Maser, A., Mundt, P., Rolak, L., Cook, T., Field, A., & Fabry, Z., 2014, 'Clinical Trial of Helminth-induced Immunomodulatory Therapy (HINT 2) in Relapsing-Remitting Multiple Sclerosis (P3.149)', *Neurology*, 82.
142. Benzel, F., Erdur, H., Kohler, S., Frentsch, M., Thiel, A., Harms, L., Wandinger, K.-P., & Rosche, B., 2012, 'Immune monitoring of Trichuris suis egg therapy in multiple sclerosis patients', *Journal of Helminthology*, 86: 339-347.
143. Voldsgaard, A., Bager, P., Garde, E., Akeson, P., Leffers, A.M., Madsen, C.G., Kapel, C., Roepstorff, A., Thamsborg, S.M., Melbye, M., Siebner, H., Sondergaard, H.B., Sellebjerg, F., & Sorensen, P.S., 2015, 'Trichuris suis ova therapy in relapsing multiple sclerosis is safe but without signals of beneficial effect', *Mult Scler*, 21: 1723-9.
144. Rosche, B., Wernecke, K.D., Ohlraun, S., Dorr, J.M., & Paul, F., 2013, 'Trichuris suis ova in relapsing-remitting multiple sclerosis and clinically isolated syndrome (TRIOMS): study protocol for a randomized controlled trial', *Trials*, 14: 112.
145. Berit Rosche, C.U., Berlin, Germany. *Trichuris Suis Ova (TSO)in Recurrent Remittent Multiple Sclerosis and Clinically Isolated Syndrome (TRIOMS)*. 2016; Available from: https://clinicaltrials.gov/ct2/show/NCT01413243.
146. Khan, A.R. & Fallon, P.G., 2013, 'Helminth therapies: Translating the unknown unknowns into known knowns', *International Journal for Parasitology*, 43: 293-299.
147. Ruyssers, N.E., De Winter, B.Y., De Man, J.G., Loukas, A., Herman, A.G., Pelckmans, P.A., & Moreels, T.G., 2008, 'Worms and the treatment of inflammatory bowel disease: are molecules the answer?', *Clinical and Developmental Immunology*, 2008: 567314.
148. Briggs, N., Weatherhead, J., Sastry, K.J., & Hotez, P.J., 2016, 'The Hygiene Hypothesis and Its Inconvenient Truths about Helminth Infections', 10: e0004944.
149. Smits, H.H., Hammad, H., van Nimwegen, M., Soullie, T., Willart, M.A., Lievers, E., Kadouch, J., Kool, M., Kos-van Oosterhoud, J., Deelder, A.M., Lambrecht, B.N., & Yazdanbakhsh, M., 2007, 'Protective effect of Schistosoma mansoni infection on allergic airway inflammation depends on the intensity and chronicity of infection', *The Journal of Allergy and Clinical Immunology*, 120: 932-940.
150. Farah, I.O., Langoi, D., Nyaundi, J., & Hau, J., 2007, 'Schistosome-induced pathology is exacerbated and Th2 polarization is enhanced during pregnancy', *In Vivo*, 21: 599-602.
151. Mejia, R. & Nutman, T.B., 2012, 'Screening, prevention, and treatment for hyperinfection syndrome and disseminated infections caused by Strongyloides stercoralis', *Current Opinion in Infectious Diseases*, 25: 458-463.
152. McKay, D.M., 2008, 'The therapeutic helminth?', *Trends in Parasitology*, 25: 109-114.
153. Johnston, M.J., MacDonald, J.A., & McKay, D.M., 2009, 'Parasitic helminths: a pharmacopeia of anti-inflammatory molecules', *Parasitology*, 136: 125-147.

154. Wammes, L.J., Mpairwe, H., Elliott, A.M., & Yazdanbakhsh, M., 2014, 'Helminth therapy or elimination: epidemiological, immunological, and clinical considerations', *The Lancet. Infectious Diseases*, 14: 1150-1162.
155. Robinson, M.W., Menon, R., Donnelly, S.M., Dalton, J.P., & Ranganathan, S., 2009, 'An integrated transcriptomics and proteomics analysis of the secretome of the helminth pathogen *Fasciola hepatica*: proteins associated with invasion and infection of the mammalian host', *Molecular and Cellular Proteomics*, 8: 1891-1907.
156. Berasaín, P., Goñi, F., McGonigle, S., Dowd, A., Dalton, J.P., Frangione, B., & Carmona, C., 1997, 'Proteinases secreted by Fasciola hepatica degrade extracellular matrix and basement membrane components', *The Journal of Parasitology*, 83: 1-5.
157. Hewitson, J.P., Grainger, J.R., & Maizels, R.M., 2009, 'Helminth immunoregulation: The role of parasite secreted proteins in modulating host immunity', *Molecular and Biochemical Parasitology*, 167: 1-11.
158. Harnett, W. & Harnett, M.M., 2010, 'Helminth-derived immunomodulators: can understanding the worm produce the pill?', *Nature Reviews. Immunology.*, 10: 278-284.
159. Ditgen, D., Anandarajah, E.M., Meissner, K.A., Brattig, N., Wrenger, C., & Liebau, E., 2014, 'Harnessing the Helminth Secretome for Therapeutic Immunomodulators', *BioMed Research International*, 2014: 964350.
160. Schnoeller, C., Rausch, S., Pillai, S., Avagyan, A., Wittig, B.M., Loddenkemper, C., Hamann, A., Hamelmann, E., Lucius, R., & Hartmann, S., 2008, 'A helminth immunomodulator reduces allergic and inflammatory responses by induction of IL-10-producing macrophages', *Journal of Immunology*, 180: 4265-4272.
161. Goodridge, H.S., Wilson, E.H., Harnett, W., Campbell, C.C., Harnett, M.M., & Liew, F.Y., 2001, 'Modulation of Macrophage Cytokine Production by ES-62, a Secreted Product of the Filarial Nematode Acanthocheilonema viteae', *The Journal of Immunology*, 167: 940-945.
162. Goodridge, H.S., Marshall, F.A., Wilson, E.H., Houston, K.M., Liew, F.Y., Harnett, M.M., & Harnett, W., 2004, 'In vivo exposure of murine dendritic cell and macrophage bone marrow progenitors to the phosphorylcholine-containing filarial nematode glycoprotein ES-62 polarizes their differentiation to an anti-inflammatory phenotype', *Immunology*, 113: 491-498.
163. McInnes, I.B., Leung, B.P., Harnett, M., Gracie, J.A., Liew, F.Y., & Harnett, W., 2003, 'A Novel Therapeutic Approach Targeting Articular Inflammation Using the Filarial Nematode-Derived Phosphorylcholine-Containing Glycoprotein ES-62', *The Journal of Immunology*, 171: 2127-2133.
164. Harnett, M.M., Kean, D.E., Boitelle, A., McGuiness, S., Thalhamer, T., Steiger, C.N., Egan, C., Al-Riyami, L., Alcocer, M.J., Houston, K.M., Gracie, J.A., McInnes, I.B., & Harnett, W., 2008, 'The phosphorycholine moiety of the filarial nematode immunomodulator ES-62 is responsible for its anti-inflammatory action in arthritis', *Annals of the Rheumatic Diseases*, 67: 518-523.
165. Pineda, M.A., McGrath, M.A., Smith, P.C., Al-Riyami, L., Rzepecka, J., Gracie, J.A., Harnett, W., & Harnett, M.M., 2012, 'The parasitic helminth product ES-62 suppresses pathogenesis in collagen-induced arthritis by targeting the interleukin-17–producing cellular network at multiple sites', *Arthritis & Rheumatism*, 64: 3168-3178.
166. Rodgers, D.T., Pineda, M.A., McGrath, M.A., Al-Riyami, L., Harnett, W., & Harnett, M.M., 2014, 'Protection against collagen-induced arthritis in mice afforded by the parasitic worm product, ES-62, is associated with restoration of the levels of interleukin-10-producing B cells and reduced plasma cell infiltration of the joints', *Immunology*, 141: 457-66.
167. Imai, S., Tezuka, H., & Fujita, K., 2001, 'A factor of inducing IgE from a filarial parasite prevents insulin-dependent diabetes mellitus in nonobese diabetic mice', *Biochemical Biophysical Research Communications*, 286: 1051-1058.
168. Ruyssers, N.E., De Winter, B.Y., De Man, J.G., Loukas, A., Pearson, M.S., Weinstock, J.V., Van den Bossche, R.M., Martinet, W., Pelckmans, P.A., & Moreels, T.G., 2009,

'Therapeutic potential of helminth soluble proteins in TNBS-induced colitis in mice', *Inflammatory bowel diseases*, 15: 491-500.
169. Ferreira, I., Smyth, D., Gaze, S., Aziz, A., Giacomin, P., Ruyssers, N., Artis, D., Laha, T., Navarro, S., Loukas, A., & McSorley, H.J., 2013, 'Hookworm excretory/secretory products induce interleukin-4 (IL-4)+ IL-10+ CD4+ T cell responses and suppress pathology in a mouse model of colitis', *Infection and Immunity*, 81: 2104-2111.
170. Cançado, G.G., Fiuza, J.A., de Paiva, N.C., Lemos Lde, C., Ricci, N.D., Gazzinelli-Guimarães, P.H., Martins, V.G., Bartholomeu, D.C., Negrão-Corrêa, D.A., Carneiro, C.M., & Fujiwara, R.T., 2011, 'Hookworm products ameliorate dextran sodium sulfate-induced colitis in BALB/c mice', *Inflammatory bowel diseases*, 17: 2275-2286.
171. Yang, X., Yang, Y., Wang, Y., Zhan, B., Gu, Y., Cheng, Y., & Zhu, X., 2014, 'Excretory/secretory products from Trichinella spiralis adult worms ameliorate DSS-induced colitis in mice', *PLoS One*, 9: e96454.
172. Endharti, A.T., Baskoro, A.D., & Norahmawati, E., 2017, 'Therapeutic effect of soluble worm protein acting as immune regulatory on colitis', *Asian Pacific Journal of Tropical Biomedicine*, 7: 70-77.
173. Johnston, M.J., Wang, A., Catarino, M.E., Ball, L., Phan, V.C., MacDonald, J.A., & McKay, D.M., 2010, 'Extracts of the rat tapeworm, Hymenolepis diminuta, suppress macrophage activation in vitro and alleviate chemically induced colitis in mice', *Infection and Immunity*, 78: 1364-1375.
174. Andrews, S.J., *The life-cycle of Fasciola hepatica*, in *Fasciolosis*, J.P. Dalton, Editor. 1999, CAB International: Oxford. p. 1-29.
175. Garcia, H.H., Moro, P.L., & Schantz, P.M., 2007, 'Zoonotic helminth infections of humans: echinococcosis, cysticercosis and fascioliasis', *Current Opinion in Infectious Diseases*, 20: 489-494.
176. Rondelaud, D., Vignoles, P., Abrous, M., & Dreyfuss, G., 2001, 'The definitive and intermediate hosts of *Fasciola hepatica* in the natural watercress beds in central France', *Parasitology Research*, 87: 475-478.
177. Vaughan, J.L., Charles, J.A., & Boray, J.C., 1997, 'Fasciola hepatica infection in farmed emus (Dromaius novaehollandiae)', *Australian Veterinary Journal*, 75: 811-813.
178. Mas-Coma, S., Valero, M.A., & Bargues, M.D., 2009, 'Chapter 2. Fasciola, lymnaeids and human fascioliasis, with a global overview on disease transmission, epidemiology, evolutionary genetics, molecular epidemiology and control', *Advances in Parasitology*, 69: 41-146.
179. Mas-Coma, S., Bargues, M.D., & Valero, M.A., 2005, 'Fascioliasis and other plant-borne trematode zoonoses', *International Journal for Parasitology*, 35: 1255-1278.
180. Cwiklinski, K., Dalton, J.P., Dufresne, P.J., La Course, J., Williams, D.J., Hodgkinson, J., & Paterson, S., 2015, 'The *Fasciola hepatica* genome: gene duplication and polymorphism reveals adaptation to the host environment and the capacity for rapid evolution', *Genome Biology*, 16: 71.
181. Flynn, R.J., Irwin, J.A., Olivier, M., Sekiya, M., Dalton, J.P., & Mulcahy, G., 2007, 'Alternative activation of ruminant macrophages by *Fasciola hepatica', Veterinary Immunology and Immunopathology*, 120: 31-40.
182. Flynn, R.J. & Mulcahy, G., 2008, 'Possible role for toll-like receptors in interaction of *Fasciola hepatica* excretory/secretory products with bovine macrophages', *Infection and Immunity*, 76: 678-684.
183. Donnelly, S., O'Neill, S.M., Sekiya, M., Mulcahy, G., & Dalton, J.P., 2005, 'Thioredoxin peroxidase secreted by Fasciola hepatica induces the alternative activation of macrophages', *Infection and Immunity*, 73: 166-173.
184. Donnelly, S., Stack, C.M., O'Neill, S.M., Sayed, A.A., Williams, D.L., & Dalton, J.P., 2008, 'Helminth 2-Cys peroxiredoxin drives Th2 responses through a mechanism involving alternatively activated macrophages', *The Journal of the Federation of American Societies for Experimental Biology*, 22: 4022-4032.

185. Flynn, R.J. & Mulcahy, G., 2008, 'The roles of IL-10 and TGF-beta in controlling IL-4 and IFN-gamma production during experimental *Fasciola hepatica* infection', *International Journal for Parasitology*, 38: 1673-1680.
186. O'Neill, S.M., Brady, M.T., Callanan, J.J., Mulcahy, G., Joyce, P., Mills, K.H., & Dalton, J.P., 2000, 'Fasciola hepatica infection downregulates Th1 responses in mice', *Parasite Immunology*, 22: 147-155.
187. Clery, D., Torgerson, P., & Mulcahy, G., 1996, 'Immune responses of chronically infected adult cattle to Fasciola hepatica', *Veterinary Parasitology*, 65: 71-82.
188. Mulcahy, G., O'Connor, F., McGonigle, S., Dowd, A., Clery, D.G., Andrews, S.J., & Dalton, J.P., 1998, 'Correlation of specific antibody titre and avidity with protection in cattle immunized against Fasciola hepatica', *Vaccine*, 16: 932-939.
189. Hoyle, D.V., Dalton, J.P., Chase-Topping, M., & Taylor, D.W., 2003, 'Pre-exposure of cattle to drug-abbreviated Fasciola hepatica infections: the effect upon subsequent challenge infection and the early immune response', *Veterinary Parasitology*, 111: 65-82.
190. Lund, M.E., O'Brien, B.A., Hutchinson, A.T., Robinson, M.W., Simpson, A.M., Dalton, J.P., & Donnelly, S., 2014, 'Secreted proteins from the helminth Fasciola hepatica inhibit the initiation of autoreactive T cell responses and prevent diabetes in the NOD mouse', *PLoS One*, 9: e86289.
191. Finlay, C.M., Stefanska, A.M., Walsh, K.P., Kelly, P.J., Boon, L., Lavelle, E.C., Walsh, P.T., & Mills, K.H., 2016, 'Helminth Products Protect against Autoimmunity via Innate Type 2 Cytokines IL-5 and IL-33, Which Promote Eosinophilia', *The Journal of Immunology*, 196: 703-714.
192. Brown, W.C., Davis, W.C., Dobbelaere, D.A., & Rice-Ficht, A.C., 1994, 'CD4+ T-cell clones obtained from cattle chronically infected with Fasciola hepatica and specific for adult worm antigen express both unrestricted and Th2 cytokine profiles', *Infection and Immunity*, 62: 818-827.
193. O'Neill, S.M., Mills, K.H.G., & Dalton, J.P., 2001, '*Fasciola hepatica* cathepsin L cysteine proteinase suppresses *Bordetella pertussis*-specific interferon-gamma production *in vivo', Parasite Immunology*, 23: 541-547.
194. Boukli, N.M., Delgado, B., Ricaurte, M., & Espino, A.M., 2011, 'Fasciola hepatica and Schistosoma mansoni: identification of common proteins by comparative proteomic analysis', *The Journal of Parasitology*, 97: 852-861.
195. Cass, C.L., Johnson, J.R., Califf, L.L., Xu, T., Hernandez, H.J., Stadecker, M.J., Yates, J.R., 3rd, & Williams, D.L., 2007, 'Proteomic analysis of Schistosoma mansoni egg secretions', *Molecular and Biochemical Parasitology*, 155: 84-93.
196. Robinson, M.W., Tort, J.F., Lowther, J., Donnelly, S.M., Wong, E., Xu, W., Stack, C.M., Padula, M., Herbert, B., & Dalton, J.P., 2008, 'Proteomics and phylogenetic analysis of the cathepsin L protease family of the helminth pathogen Fasciola hepatica: expansion of a repertoire of virulence-associated factors.', *Molecular and Cellular Proteomics*, 7: 1111-1123.
197. Lund, M.E., Greer, J., Dixit, A., Alvarado, R., McCauley-Winter, P., To, J., Tanaka, A., Hutchinson, A.T., Robinson, M.W., Simpson, A.M., O'Brien, B.A., Dalton, J.P., & Donnelly, S., 2016, 'A parasite-derived 68-mer peptide ameliorates autoimmune disease in murine models of Type 1 diabetes and multiple sclerosis', *Scientific Reports*, 6: 37789.
198. Dalton, J.P., Robinson, M.W., Mulcahy, G., O'Neill, S.M., & Donnelly, S., 2013, 'Immunomodulatory molecules of Fasciola hepatica: Candidates for both vaccine and immunotherapeutic development', *Veterinary Parasitology*, 195: 272-285.
199. Robinson, M.W., Donnelly, S., Hutchinson, A.T., To, J., Taylor, N.L., Norton, R.S., Perugini, M.A., & Dalton, J.P., 2011, 'A family of helminth molecules that modulate innate cell responses via molecular mimicry of host antimicrobial peptides', *PLoS Pathogens*, 7: e1002042.

200. Zanetti, M., Gennaro, R., Skerlavaj, B., Tomasinsig, L., & Circo, R., 2002, 'Cathelicidin peptides as candidates for a novel class of antimicrobials', *Current Pharmaceutical Design*, 8: 779-793.
201. Nizet, V. & Gallo, R.L., 2003, 'Cathelicidins and innate defense against invasive bacterial infection', *Scandinavian Journal of Infectious Diseases*, 35: 670-676.
202. Gallo, R.L., Murakami, M., Ohtake, T., & Zaiou, M., 2002, 'Biology and clinical relevance of naturally occurring antimicrobial peptides', *Journal of Allergy and Clinical Immunology*, 110: 823-831.
203. Murakami, M., Ohtake, T., Dorschner, R.A., & Gallo, R.L., 2002, 'Cathelicidin antimicrobial peptides are expressed in salivary glands and saliva', *Journal of Dental Research*, 81: 845-850.
204. Gallo, R.L., Ono, M., Povsic, T., Page, C., Eriksson, E., Klagsbrun, M., & Bernfield, M., 1994, 'Syndecans, cell surface heparan sulfate proteoglycans, are induced by a proline-rich antimicrobial peptide from wounds', *Proceedings of the National Academy of Sciences of the United States of America*, 91: 11035-11039.
205. Li, J., Post, M., Volk, R., Gao, Y., Li, M., Metais, C., Sato, K., Tsai, J., Aird, W., Rosenberg, R.D., Hampton, T.G., Sellke, F., Carmeliet, P., & Simons, M., 2000, 'PR39, a peptide regulator of angiogenesis', *Nature Medicine*, 6: 49-55.
206. Shi, J., Ross, C.R., Leto, T.L., & Blecha, F., 1996, 'PR-39, a proline-rich antibacterial peptide that inhibits phagocyte NADPH oxidase activity by binding to Src homology 3 domains of p47 phox', *Proceedings of the National Academy of Sciences of the United States of America*, 93: 6014-6018.
207. De, Y., Chen, Q., Schmidt, A.P., Anderson, G.M., Wang, J.M., Wooters, J., Oppenheim, J.J., & Chertov, O., 2000, 'LL-37, the neutrophil granule- and epithelial cell-derived cathelicidin, utilizes formyl peptide receptor-like 1 (FPRL1) as a receptor to chemoattract human peripheral blood neutrophils, monocytes, and T cells', *The Journal of Experimental Medicine*, 192: 1069-1074.
208. Niyonsaba, F., Iwabuchi, K., Someya, A., Hirata, M., Matsuda, H., Ogawa, H., & Nagaoka, I., 2002, 'A cathelicidin family of human antibacterial peptide LL-37 induces mast cell chemotaxis', *Immunology*, 106: 20-26.
209. Mookherjee, N., Brown, K.L., Bowdish, D.M., Doria, S., Falsafi, R., Hokamp, K., Roche, F.M., Mu, R., Doho, G.H., Pistolic, J., Powers, J.P., Bryan, J., Brinkman, F.S., & Hancock, R.E., 2006, 'Modulation of the TLR-mediated inflammatory response by the endogenous human host defense peptide LL-37', *The Journal of Immunology*, 176: 2455-2464.
210. Thivierge, K., Cotton, S., Schaefer, D.A., Riggs, M.W., To, J., Lund, M.E., Robinson, M.W., Dalton, J.P., & Donnelly, S.M., 2013, 'Cathelicidin-like Helminth Defence Molecules (HDMs): Absence of Cytotoxic, Anti-microbial and Anti-protozoan Activities Imply a Specific Adaptation to Immune Modulation', *PLOS Neglected Tropical Diseases*, 7: e2307.
211. Rosenfeld, Y. & Shai, Y., 2006, 'Lipopolysaccharide (Endotoxin)-host defense antibacterial peptides interactions: role in bacterial resistance and prevention of sepsis', *Biochimica et Biophysica Acta*, 1758: 1513-1522.
212. Hirsch, T., Metzig, M., Niederbichler, A., Steinau, H.U., Eriksson, E., & Steinstraesser, L., 2008, 'Role of host defense peptides of the innate immune response in sepsis', *Shock*, 30: 117-126.
213. Zheng, X., Hong, Y., Feng, G., Zhang, G., Rogers, H., Lewis, M.A.O., Williams, D.W., Xia, Z., Song, B., & Wei, X., 2013, 'Lipopolysaccharide-Induced M2 to M1 Macrophage Transformation for IL-12p70 production Is blocked by mediated up-regulation of EBI3 expression', *PLoS ONE*, 8: e63967.
214. Martínez-Sernández, V., Mezo, M., González-Warleta, M., Perteguer, M.J., Gárate, T., Romarís, F., & Ubeira, F.M., 2017, 'Delineating Distinct Heme-Scavenging and Binding Functions of Domains in MF6p/HDM Proteins from Parasitic Flatworms', *Journal of Biological Chemistry*.

215. Robinson, M.W., Alvarado, R., To, J., Hutchinson, A.T., Dowdell, S.N., Lund, M., Turnbull, L., Whitchurch, C.B., O'Brien, B.A., Dalton, J.P., & Donnelly, S., 2012, 'A helminth cathelicidin-like protein suppresses antigen processing and presentation in macrophages via inhibition of lysosomal vATPase', *FASEB Journal*, 26: 4614-4627.
216. Turk, V., Stoka, V., Vasiljeva, O., Renko, M., Sun, T., Turk, B., & Turk, D., 2012, 'Cysteine cathepsins: From structure, function and regulation to new frontiers', *Biochimica et Biophysica Acta (BBA) - Proteins and Proteomics*, 1824: 68-88.
217. Holliday, L.S., 2014, 'Vacuolar H+-ATPase: An Essential Multitasking Enzyme in Physiology and Pathophysiology', *New Journal of Science*, 2014: 21.
218. van Kasteren, S.I. & Overkleeft, H.S., 2014, 'Endo-lysosomal proteases in antigen presentation', *Current Opinion in Chemical Biology*, 23: 8-15.
219. Stoka, V., Turk, B., & Turk, V., 2005, 'Lysosomal cysteine proteases: structural features and their role in apoptosis', *IUBMB Life*, 57: 347-53.
220. Kawai, T. & Akira, S., 2011, 'Toll-like Receptors and Their Crosstalk with Other Innate Receptors in Infection and Immunity', *Immunity*, 34: 637-650.
221. Alvarado, R., To, J., Lund, M.E., Pinar, A., Mansell, A., Robinson, M.W., O'Brien, B.A., Dalton, J.P., & Donnelly, S., 2017, 'The immune modulatory peptide FhHDM-1 secreted by the helminth Fasciola hepatica prevents NLRP3 inflammasome activation by inhibiting endolysosomal acidification in macrophages', *The FASEB Journal*, 31: 85-95.
222. Strowig, T., Henao-Mejia, J., Elinav, E., & Flavell, R., 2012, 'Inflammasomes in health and disease', *Nature*, 481: 278-86.
223. Yang, C.A. & Chiang, B.L., 2015, 'Inflammasomes and human autoimmunity: A comprehensive review', *Journal of Autoimmunity*, 61: 1-8.
224. Blasius, A.L. & Beutler, B., 2010, 'Intracellular Toll-like Receptors', *Immunity*, 32: 305-315.
225. Zhang, X., Goncalves, R., & Mosser, D.M., 2008, 'The isolation and characterization of murine macrophages', *Current Protocols in Immunology*, Chapter 14: Unit 14 1.
226. Lutz, M.B., Kukutsch, N., Ogilvie, A.L., Rossner, S., Koch, F., Romani, N., & Schuler, G., 1999, 'An advanced culture method for generating large quantities of highly pure dendritic cells from mouse bone marrow', *Journal of Immunological Methods*, 223: 77-92.
227. Autissier, P., Soulas, C., Burdo, T.H., & Williams, K.C., 2010, 'Evaluation of a 12-color flow cytometry panel to study lymphocyte, monocyte, and dendritic cell subsets in humans', *Cytometry. Part A: The Journal of the International Society for Analytical Cytology*, 77: 410-419.
228. Maecker, H.T., McCoy, J.P., & Nussenblatt, R., 2012, 'Standardizing immunophenotyping for the Human Immunology Project', *Nature Reviews. Immunobiology*, 12: 191-200.
229. Dorward, D.A., Lucas, C.D., Alessandri, A.L., Marwick, J.A., Rossi, F., Dransfield, I., Haslett, C., Dhaliwal, K., & Rossi, A.G., 2013, 'Technical advance: autofluorescence-based sorting: rapid and nonperturbing isolation of ultrapure neutrophils to determine cytokine production', *Journal of Leukocyte Biology*, 94: 193-202.
230. Han, X., Jorgensen, J.L., Brahmandam, A., Schlette, E., Huh, Y.O., Shi, Y., Awagu, S., & Chen, W., 2008, 'Immunophenotypic study of basophils by multiparameter flow cytometry', *Archives of Pathology and Laboratory Medicine*, 132: 813-819.
231. Riley, R.S. & Idowu, M., *Principles and Applications of Flow Cytometry*. 2009: Department of Pathology, Medical College of Virginia/VCU Health Systems, Virginia Commonwealth University. p. 1-14.
232. Deng, W., Wang, Y., Liu, Z., Cheng, H., & Xue, Y., 2014, 'HemI: a toolkit for illustrating heatmaps', *PLoS One*, 9: e111988.
233. Wieczorek, D., Delaurier, L., & Schagat, T. *Methods of RNA Quality Assessment*. 2012 [cited 2017 17/10]; Available from: http://www.promega.com.au/resources/pubhub/methods-of-rna-quality-assessment/.

234. Livak, K.J. & Schmittgen, T.D., 2001, 'Analysis of Relative Gene Expression Data Using Real-Time Quantitative PCR and the 2−ΔΔCT Method′, *Methods*, 25: 402-408.
235. Andersen, C.L., Jensen, J.L., & Orntoft, T.F., 2004, 'Normalization of real-time quantitative reverse transcription-PCR data: a model-based variance estimation approach to identify genes suited for normalization, applied to bladder and colon cancer data sets′, *Cancer Research*, 64: 5245-5250.
236. Vandesompele, J., De Preter, K., Pattyn, F., Poppe, B., Van Roy, N., De Paepe, A., & Speleman, F., 2002, 'Accurate normalization of real-time quantitative RT-PCR data by geometric averaging of multiple internal control genes′, *Genome Biology*, 3: Research0034.
237. Pfaffl, M.W., Tichopad, A., Prgomet, C., & Neuvians, T.P., 2004, 'Determination of stable housekeeping genes, differentially regulated target genes and sample integrity: BestKeeper--Excel-based tool using pair-wise correlations′, *Biotechnology Letters*, 26: 509-515.
238. Holton, T.A., Pollastri, G., Shields, D.C., & Mooney, C., 2013, 'CPPpred: prediction of cell penetrating peptides′, *Bioinformatics*, 29: 3094-6.
239. Wynn, T.A. & Vannella, K.M., 2016, 'Macrophages in Tissue Repair, Regeneration, and Fibrosis′, *Immunity*, 44: 450-462.
240. Fujiwara, N. & Kobayashi, K., 2005, 'Macrophages in inflammation′, *Current Drug Targets Inflammation and Allergy*, 4: 281-286.
241. Hancock, R.E., Haney, E.F., & Gill, E.E., 2016, 'The immunology of host defence peptides: beyond antimicrobial activity′, *Nature Reviews Immunology*, 16: 321-334.
242. Scott, M.G., Davidson, D.J., Gold, M.R., Bowdish, D., & Hancock, R.E.W., 2002, 'The Human Antimicrobial Peptide LL-37 Is a Multifunctional Modulator of Innate Immune Responses′, *The Journal of Immunology*, 169: 3883-3891.
243. Scott, M.G., Rosenberger, C.M., Gold, M.R., Finlay, B.B., & Hancock, R.E., 2000, 'An alpha-helical cationic antimicrobial peptide selectively modulates macrophage responses to lipopolysaccharide and directly alters macrophage gene expression′, *The Journal of Immunology*, 165: 3358-3365.
244. Scott, M.G., Dullaghan, E., Mookherjee, N., Glavas, N., Waldbrook, M., Thompson, A., Wang, A., Lee, K., Doria, S., Hamill, P., Yu, J.J., Li, Y., Donini, O., Guarna, M.M., Finlay, B.B., North, J.R., & Hancock, R.E., 2007, 'An anti-infective peptide that selectively modulates the innate immune response′, *Nature Biotechnology*, 25: 465-472.
245. Bustin, S.A., Benes, V., Garson, J.A., Hellemans, J., Huggett, J., Kubista, M., Mueller, R., Nolan, T., Pfaffl, M.W., Shipley, G.L., Vandesompele, J., & Wittwer, C.T., 2009, 'The MIQE guidelines: minimum information for publication of quantitative real-time PCR experiments′, *Clinical Chemistry*, 55: 611-622.
246. Darnell, G.A., Schroder, W.A., Gardner, J., Harrich, D., Yu, H., Medcalf, R.L., Warrilow, D., Antalis, T.M., Sonza, S., & Suhrbier, A., 2006, 'SerpinB2 Is an Inducible Host Factor Involved in Enhancing HIV-1 Transcription and Replication′, *Journal of Biological Chemistry*, 281: 31348-31358.
247. Medcalf, R.L. & Stasinopoulos, S.J., 2005, 'The undecided serpin. The ins and outs of plasminogen activator inhibitor type 2′, *The FEBS Journal*, 272: 4858-4867.
248. Schroder, W.A., Le, T.T., Major, L., Street, S., Gardner, J., Lambley, E., Markey, K., MacDonald, K.P., Fish, R.J., Thomas, R., & Suhrbier, A., 2010, 'A physiological function of inflammation-associated SerpinB2 is regulation of adaptive immunity′, *The Journal of Immunology*, 184: 2663-2670.
249. Grewal, I.S. & Flavell, R.A., 1996, 'The role of CD40 ligand in costimulation and T-cell activation′, *Immunological Reviews*, 153: 85-106.
250. Topalian, S.L., Drake, C.G., & Pardoll, D.M., 2015, 'Immune checkpoint blockade: a common denominator approach to cancer therapy′, *Cancer cell*, 27: 450-461.
251. Han, G., Chen, G., Shen, B., & Li, Y., 2013, 'Tim-3: An Activation Marker and Activation Limiter of Innate Immune Cells′, *Frontiers in Immunology*, 4: 449.

252. Ocaña-Guzman, R., Torre-Bouscoulet, L., & Sada-Ovalle, I., 2016, 'TIM-3 Regulates Distinct Functions in Macrophages', *Frontiers in Immunology*, 7.
253. Yang, X., Jiang, X., Chen, G., Xiao, Y., Geng, S., Kang, C., Zhou, T., Li, Y., Guo, X., Xiao, H., Hou, C., Wang, R., Lin, Z., Li, X., Feng, J., Ma, Y., Shen, B., Li, Y., & Han, G., 2013, 'T Cell Ig Mucin-3 Promotes Homeostasis of Sepsis by Negatively Regulating the TLR Response', *The Journal of Immunology*, 190: 2068-2079.
254. Zhang, Y., Ma, C.J., Wang, J.M., Ji, X.J., Wu, X.Y., Moorman, J.P., & Yao, Z.Q., 2012, 'Tim-3 regulates pro- and anti-inflammatory cytokine expression in human CD14+ monocytes', *Journal of Leukocyte Biology*, 91: 189-196.
255. Ma, C.J., Li, G.Y., Cheng, Y.Q., Wang, J.M., Ying, R.S., Shi, L., Wu, X.Y., Niki, T., Hirashima, M., Li, C.F., Moorman, J.P., & Yao, Z.Q., 2013, 'Cis Association of Galectin-9 with Tim-3 Differentially Regulates IL-12/IL-23 Expressions in Monocytes via TLR Signaling', *PLOS ONE*, 8: e72488.
256. Nakayama, M., Akiba, H., Takeda, K., Kojima, Y., Hashiguchi, M., Azuma, M., Yagita, H., & Okumura, K., 2009, 'Tim-3 mediates phagocytosis of apoptotic cells and cross-presentation', *Blood*, 113: 3821-3830.
257. DeKruyff, R.H., Bu, X., Ballesteros, A., Santiago, C., Chim, Y.E., Lee, H., Karisola, P., Pichavant, M., Kaplan, G.G., Umetsu, D.T., Freeman, G.J., & Casasnovas, J.M., 2010, 'T Cell/Transmembrane, Ig, and Mucin-3 Allelic Variants Differentially Recognize Phosphatidylserine and Mediate Phagocytosis of Apoptotic Cells', *The Journal of Immunology*, 184: 1918-1930.
258. Wang, J., Jiao, H., Stewart, T.L., Lyons, M.V., Shankowsky, H.A., Scott, P.G., & Tredget, E.E., 2007, 'Accelerated wound healing in leukocyte-specific, protein 1-deficient mouse is associated with increased infiltration of leukocytes and fibrocytes', *Journal of Leukocyte Biology*, 82: 1554-1563.
259. Soler Palacios, B., Estrada-Capetillo, L., Izquierdo, E., Criado, G., Nieto, C., Municio, C., Gonzalez-Alvaro, I., Sanchez-Mateos, P., Pablos, J.L., Corbi, A.L., & Puig-Kroger, A., 2015, 'Macrophages from the synovium of active rheumatoid arthritis exhibit an activin A-dependent pro-inflammatory profile', *The Journal of Pathology*, 235: 515-526.
260. Palafox-Sánchez, C.A., Vázquez-Del Mercado, M., Orozco-Barocio, G., García-De la Torre, I., Torres-Carrillo, N., Torres-Carrillo, N.M., Illades-Aguiar, B., & Muñoz-Valle, J.F., 2009, 'A Functional Ser413/Ser413 PAI-2 Polymorphism Is Associated With Susceptibility and Damage Index Score in Systemic Lupus Erythematosus', *Clinical and Applied Thrombosis/Hemostasis*, 15: 233-238.
261. Vazquez-Del Mercado, M., Garcia-Cobian, T.A., Munoz Valle, J.F., Torres-Carrillo, N., Martin-Marquez, B.T., Arana-Argaez, V.E., Best-Aguilera, C.R., Martinez-Garcia, E.A., Petri, M.H., Nunez-Atahualpa, L., & Delgado-Rizo, V., 2007, 'Genotype Ser413/Ser of PAI-2 polymorphism Ser413/Cys is associated with anti-phospholipid syndrome and systemic lupus erythematosus in a familial case: comparison with healthy controls', *Scandinavian Journal of Rheumatology*, 36: 206-210.
262. Zhao, A., Yang, Z., Sun, R., Grinchuk, V., Netzel-Arnett, S., Anglin, I.E., Driesbaugh, K.H., Notari, L., Bohl, J.A., Madden, K.B., Urban, J.F., Jr., Antalis, T.M., & Shea-Donohue, T., 2013, 'SerpinB2 is critical to Th2 immunity against enteric nematode infection', *The Journal of Immunology*, 190: 5779-5787.
263. Schroder, W.A., Gardner, J., Le, T.T., Duke, M., Burke, M.L., Jones, M.K., McManus, D.P., & Suhrbier, A., 2010, 'SerpinB2 deficiency modulates Th1Th2 responses after schistosome infection', *Parasite Immunology*, 32: 764-768.
264. Shea-Donohue, T., Zhao, A., & Antalis, T.M., 2014, 'SerpinB2 mediated regulation of macrophage function during enteric infection', *Gut Microbes*, 5: 254-8.
265. Stringer, B., Udofa, E.A., & Antalis, T.M., 2012, 'Regulation of the Human Plasminogen Activator Inhibitor Type 2 Gene: COOPERATION OF AN UPSTREAM SILENCER AND TRANSACTIVATOR', *Journal of Biological Chemistry*, 287: 10579-10589.

266. Monney, L., Sabatos, C.A., Gaglia, J.L., Ryu, A., Waldner, H., Chernova, T., Manning, S., Greenfield, E.A., Coyle, A.J., Sobel, R.A., Freeman, G.J., & Kuchroo, V.K., 2002, 'Th1-specific cell surface protein Tim-3 regulates macrophage activation and severity of an autoimmune disease', *Nature*, 415: 536-41.
267. Sanchez-Fueyo, A., Tian, J., Picarella, D., Domenig, C., Zheng, X.X., Sabatos, C.A., Manlongat, N., Bender, O., Kamradt, T., Kuchroo, V.K., Gutierrez-Ramos, J.C., Coyle, A.J., & Strom, T.B., 2003, 'Tim-3 inhibits T helper type 1-mediated auto- and alloimmune responses and promotes immunological tolerance', *Nature Immunology*, 4: 1093-1101.
268. O'Neill, L.A.J., Kishton, R.J., & Rathmell, J., 2016, 'A guide to immunometabolism for immunologists', *Nature Reviews Immunology*, 16: 553-565.
269. Onguru, D., Liang, Y., Griffith, Q., Nikolajczyk, B., Mwinzi, P., & Ganley-Leal, L., 2011, 'Human schistosomiasis is associated with endotoxemia and Toll-like receptor 2- and 4-bearing B cells', *The American Journal of Tropical Medicine and Hygiene*, 84: 321-324.
270. Akira, S. & Takeda, K., 2004, 'Toll-like receptor signalling', *Nature Reviews Immunology*, 4: 499-511.
271. Pålsson-McDermott, E.M. & O'Neill, L.A.J., 2004, 'Signal transduction by the lipopolysaccharide receptor, Toll-like receptor-4', *Immunology*, 113: 153-162.
272. Mosser, D.M. & Zhang, X., 2008, 'Activation of Murine Macrophages', *Current protocols in immunology / edited by John E. Coligan ... [et al.]*, 14: 14.2.
273. Rex, J., Albrecht, U., Ehlting, C., Thomas, M., Zanger, U.M., Sawodny, O., Häussinger, D., Ederer, M., Feuer, R., & Bode, J.G., 2016, 'Model-Based Characterization of Inflammatory Gene Expression Patterns of Activated Macrophages', *PLoS Computational Biology*, 12: e1005018.
274. Yang, I.V., Jiang, W., Rutledge, H.R., Lackford, B., Warg, L.A., De Arras, L., Alper, S., Schwartz, D.A., & Pisetsky, D.S., 2011, 'Identification of novel innate immune genes by transcriptional profiling of macrophages stimulated with TLR ligands', *Molecular Immunology*, 48: 1886-1895.
275. Das, A., Chai, J.C., Yang, C.S., Lee, Y.S., Das, N.D., Jung, K.H., & Chai, Y.G., 2015, 'Dual transcriptome sequencing reveals resistance of TLR4 ligand-activated bone marrow-derived macrophages to inflammation mediated by the BET inhibitor JQ1', *Scientific Reports*, 5: 16932.
276. Nilsson, R., Bajic, V.B., Suzuki, H., di Bernardo, D., Bjorkegren, J., Katayama, S., Reid, J.F., Sweet, M.J., Gariboldi, M., Carninci, P., Hayashizaki, Y., Hume, D.A., Tegner, J., & Ravasi, T., 2006, 'Transcriptional network dynamics in macrophage activation', *Genomics*, 88: 133-42.
277. Schultz, J.R., Tu, H., Luk, A., Repa, J.J., Medina, J.C., Li, L., Schwendner, S., Wang, S., Thoolen, M., Mangelsdorf, D.J., Lustig, K.D., & Shan, B., 2000, 'Role of LXRs in control of lipogenesis', *Genes and Development*, 14: 2831-2838.
278. Wojcicka, G., Jamroz-Wisniewska, A., Horoszewicz, K., & Beltowski, J., 2007, 'Liver X receptors (LXRs). Part I: structure, function, regulation of activity, and role in lipid metabolism', *Postepy Hig Med Dosw (Online)*, 61: 736-759.
279. Pascual-Garcia, M. & Valledor, A.F., 2012, 'Biological roles of liver X receptors in immune cells', *Archivum Immunologiae et Therapia Experimentalis (Warsz)*, 60: 235-249.
280. Ghisletti, S., Huang, W., Ogawa, S., Pascual, G., Lin, M., Willson, T.M., Rosenfeld, M.G., & Glass, C.K., 2007, 'Parallel SUMOylation-dependent pathways mediate gene- and signal-specific transrepression by LXRs and PPARγ', *Molecular cell*, 25: 57-70.
281. Joseph, S.B., Castrillo, A., Laffitte, B.A., Mangelsdorf, D.J., & Tontonoz, P., 2003, 'Reciprocal regulation of inflammation and lipid metabolism by liver X receptors', *Nature Medicine*, 9: 213-219.
282. Joseph, S.B., Bradley, M.N., Castrillo, A., Bruhn, K.W., Mak, P.A., Pei, L., Hogenesch, J., O'Connell R, M., Cheng, G., Saez, E., Miller, J.F., & Tontonoz, P., 2004, 'LXR-

dependent gene expression is important for macrophage survival and the innate immune response′, *Cell*, 119: 299-309.
283. Park, M.C., Kwon, Y.J., Chung, S.J., Park, Y.B., & Lee, S.K., 2010, 'Liver X receptor agonist prevents the evolution of collagen-induced arthritis in mice′, *Rheumatology (Oxford)*, 49: 882-90.
284. Hindinger, C., Hinton, D.R., Kirwin, S.J., Atkinson, R.D., Burnett, M.E., Bergmann, C.C., & Stohlman, S.A., 2006, 'Liver X receptor activation decreases the severity of experimental autoimmune encephalomyelitis′, *Journal of Neuroscience Research*, 84: 1225-1234.
285. Steffensen, K.R., Jakobsson, T., & Gustafsson, J., 2013, 'Targeting liver X receptors in inflammation′, *Expert Opinion on Therapeutic Targets*, 17: 977-990.
286. Chawla, A., 2010, 'Control of macrophage activation and function by PPARs′, *Circulation Research*, 106: 1559-1569.
287. Gross, B., Pawlak, M., Lefebvre, P., & Staels, B., 2017, 'PPARs in obesity-induced T2DM, dyslipidaemia and NAFLD′, *Nature Reviews Endocrinology*, 13: 36-49.
288. Hevener, A.L., Olefsky, J.M., Reichart, D., Nguyen, M.T., Bandyopadyhay, G., Leung, H.Y., Watt, M.J., Benner, C., Febbraio, M.A., Nguyen, A.K., Folian, B., Subramaniam, S., Gonzalez, F.J., Glass, C.K., & Ricote, M., 2007, 'Macrophage PPAR gamma is required for normal skeletal muscle and hepatic insulin sensitivity and full antidiabetic effects of thiazolidinediones′, *The Journal of Clinical Investigation*, 117: 1658-1669.
289. Yang, Y., Lovett-Racke, A.E., & Racke, M.K., 2010, 'Regulation of Immune Responses and Autoimmune Encephalomyelitis by PPARs′, *PPAR Research*, 2010: 11.
290. Ogawa, S., Lozach, J., Benner, C., Pascual, G., Tangirala, R.K., Westin, S., Hoffmann, A., Subramaniam, S., David, M., Rosenfeld, M.G., & Glass, C.K., 2005, 'Molecular determinants of crosstalk between nuclear receptors and toll-like receptors′, *Cell*, 122: 707-21.
291. Lu, Y., Yeh, W., & Ohashi, P.S., 2008, 'LPS/TLR4 signal transduction pathway′, *Cytokine*, 42: 145-151.
292. Johnson, A.C., Li, X., & Pearlman, E., 2008, 'MyD88 functions as a negative regulator of TLR3/TRIF-induced corneal inflammation by inhibiting activation of c-Jun N-terminal kinase′, *The Journal of Biological Chemistry*, 283: 3988-3996.
293. Zhao, W., Wang, L., Zhang, M., Wang, P., Zhang, L., Yuan, C., Qi, J., Qiao, Y., Kuo, P.C., & Gao, C., 2011, 'Peroxisome proliferator-activated receptor gamma negatively regulates IFN-beta production in Toll-like receptor (TLR) 3- and TLR4-stimulated macrophages by preventing interferon regulatory factor 3 binding to the IFN-beta promoter′, *The Journal of Biological Chemistry*, 286: 5519-5528.
294. Dasu, M.R., Park, S., Devaraj, S., & Jialal, I., 2009, 'Pioglitazone inhibits Toll-like receptor expression and activity in human monocytes and db/db mice′, *Endocrinology*, 150: 3457-64.
295. Alleva, D.G., Johnson, E.B., Lio, F.M., Boehme, S.A., Conlon, P.J., & Crowe, P.D., 2002, 'Regulation of murine macrophage proinflammatory and anti-inflammatory cytokines by ligands for peroxisome proliferator-activated receptor-gamma: counter-regulatory activity by IFN-gamma′, *Journal of Leukocyte Biology*, 71: 677-685.
296. Paukkeri, E., Leppänen, T., Lindholm, M., Yam, M.F., Asmawi, M.Z., Kolmonen, A., Aulaskari, P.H., & Moilanen, E., 2013, 'Anti-inflammatory properties of a dual PPARgamma/alpha agonist muraglitazar in in vitro and in vivo models′, *Arthritis Research & Therapy*, 15: R51-R51.
297. Paukkeri, E., Pekurinen, A., & Moilanen, E., 2015, 'Peroxisome proliferator-activated receptor α and γ agonists differently regulate classical and alternative macrophage activation′, *Immunometabolism*, 2: 1-11.
298. Charbonnier, L. & Le Moine, A., *Rapamycin as Immunosuppressant in Murine Transplantation Model*, in *mTOR: Methods and Protocols*, T. Weichhart, Editor. 2012, Humana Press: Totowa, NJ. p. 435-445.
299. Esposito, M., Ruffini, F., Bellone, M., Gagliani, N., Battaglia, M., Martino, G., & Furlan, R., 2010, 'Rapamycin inhibits relapsing experimental autoimmune

encephalomyelitis by both effector and regulatory T cells modulation′, *Journal of Neuroimmunology*, 220: 52-63.
300. Padgett, L.E., Broniowska, K.A., Hansen, P.A., Corbett, J.A., & Tse, H.M., 2013, 'The role of reactive oxygen species and proinflammatory cytokines in type 1 diabetes pathogenesis′, *Annals of the New York Academy of Sciences*, 1281: 16-35.
301. Wang, J., Ren, Z., Xu, Y., Xiao, S., Meydani, S.N., & Wu, D., 2012, 'Epigallocatechin-3-gallate ameliorates experimental autoimmune encephalomyelitis by altering balance among CD4+ T-cell subsets′, *The American Journal of Pathology*, 180: 221-234.
302. Xuzhu, G., Komai-Koma, M., Leung, B.P., Howe, H.S., McSharry, C., McInnes, I.B., & Xu, D., 2012, 'Resveratrol modulates murine collagen-induced arthritis by inhibiting Th17 and B-cell function′, *Annals of the Rheumatic Diseases*, 71: 129-135.
303. Delmastro, M.M. & Piganelli, J.D., 2011, 'Oxidative stress and redox modulation potential in type 1 diabetes′, *Clinical and Developmental Immunology*, 2011: 593863.
304. Delmastro, M.M., Styche, A.J., Trucco, M.M., Workman, C.J., Vignali, D.A., & Piganelli, J.D., 2012, 'Modulation of redox balance leaves murine diabetogenic TH1 T cells "LAG-3-ing" behind′, *Diabetes*, 61: 1760-1768.
305. Delmastro-Greenwood, M.M., Votyakova, T., Goetzman, E., Marre, M.L., Previte, D.M., Tovmasyan, A., Batinic-Haberle, I., Trucco, M.M., & Piganelli, J.D., 2013, 'Mn porphyrin regulation of aerobic glycolysis: implications on the activation of diabetogenic immune cells′, *Antioxidants and Redox Signaling*, 19: 1902-1915.
306. Bermudez, V., Finol, F., Parra, N., Parra, M., Perez, A., Penaranda, L., Vilchez, D., Rojas, J., Arraiz, N., & Velasco, M., 2010, 'PPAR-gamma agonists and their role in type 2 diabetes mellitus management′, *American Journal of Therapeutics*, 17: 274-283.
307. Chen, X., Matthews, J., Zhou, L., Pelton, P., Liang, Y., Xu, J., Yang, M., Cryan, E., Rybczynski, P., & Demarest, K., 2008, 'Improvement of dyslipidemia, insulin sensitivity, and energy balance by a peroxisome proliferator-activated receptor alpha agonist′, *Metabolism*, 57: 1516-1525.
308. Lima, E., Lima, M.M.D., Marques, C.D.L., Duarte, A.L.B.P., Pita, I., & Pita, M.G., 2013, 'Peroxisome proliferator-activated receptor agonists (PPARs): a promising prospect in the treatment of psoriasis and psoriatic arthritis′, *Anais Brasileiros de Dermatologia*, 88: 1029-1035.
309. Annese, V., Rogai, F., Settesoldi, A., & Bagnoli, S., 2012, 'PPARγ in Inflammatory Bowel Disease′, *PPAR Research*, 2012: 9.
310. Choo, J., Lee, Y., Yan, X., Noh, T.H., Kim, S.J., Son, S., Pothoulakis, C., Moon, H.R., Jung, J.H., & Im, E., 2015, 'A Novel Peroxisome Proliferator-activated Receptor (PPAR)γ Agonist 2-Hydroxyethyl 5-chloro-4,5-didehydrojasmonate Exerts Anti-Inflammatory Effects in Colitis′, *Journal of Biological Chemistry*, 290: 25609-25619.
311. Shirinsky, I.V. & Shirinsky, V.S., 2011, 'Targeting Nuclear Hormone Receptors: PPARα Agonists as Potential Disease-Modifying Drugs for Rheumatoid Arthritis′, *International Journal of Rheumatology*, 2011: 937843.
312. Ormseth, M.J., Oeser, A.M., Cunningham, A., Bian, A., Shintani, A., Solus, J., Tanner, S., & Stein, C.M., 2013, 'Peroxisome proliferator-activated receptor gamma agonist effect on rheumatoid arthritis: a randomized controlled trial′, *Arthritis Research and Therapy*, 15: R110.
313. Beales, P.E., Liddi, R., Giorgini, A.E., Signore, A., Procaccini, E., Batchelor, K., & Pozzilli, P., 1998, 'Troglitazone prevents insulin dependent diabetes in the non-obese diabetic mouse′, *European Journal of Pharmacology*, 357: 221-225.
314. Beales, P.E. & Pozzilli, P., 2002, 'Thiazolidinediones for the prevention of diabetes in the non-obese diabetic (NOD) mouse: implications for human type 1 diabetes′, *Diabetes/Metabolism Research and Reviews*, 18: 114-117.
315. Evans-Molina, C., Robbins, R.D., Kono, T., Tersey, S.A., Vestermark, G.L., Nunemaker, C.S., Garmey, J.C., Deering, T.G., Keller, S.R., Maier, B., & Mirmira, R.G., 2009, 'Peroxisome proliferator-activated receptor gamma activation restores islet function in diabetic mice through reduction of endoplasmic reticulum stress and maintenance of euchromatin structure′, *Molecular and Cell Biology*, 29: 2053-2067.

316. Augstein, P., Dunger, A., Heinke, P., Wachlin, G., Berg, S., Hehmke, B., & Salzsieder, E., 2003, 'Prevention of autoimmune diabetes in NOD mice by troglitazone is associated with modulation of ICAM-1 expression on pancreatic islet cells and IFN-gamma expression in splenic T cells', *Biochemical and Biophysical Research Communications*, 304: 378-384.
317. Maganti, A.V., Tersey, S.A., Syed, F., Nelson, J.B., Colvin, S.C., Maier, B., & Mirmira, R.G., 2016, 'Peroxisome Proliferator-activated Receptor-gamma Activation Augments the beta-Cell Unfolded Protein Response and Rescues Early Glycemic Deterioration and beta Cell Death in Non-obese Diabetic Mice', *The Journal of Biological Chemistry*, 291: 22524-22533.
318. Niino, M., Iwabuchi, K., Kikuchi, S., Ato, M., Morohashi, T., Ogata, A., Tashiro, K., & Onoé, K., 2001, 'Amelioration of experimental autoimmune encephalomyelitis in C57BL/6 mice by an agonist of peroxisome proliferator-activated receptor-γ', *Journal of Neuroimmunology*, 116: 40-48.
319. Diab, A., Deng, C., Smith, J.D., Hussain, R.Z., Phanavanh, B., Lovett-Racke, A.E., Drew, P.D., & Racke, M., K., 2002, 'Peroxisome Proliferator-Activated Receptor-γ Agonist 15-Deoxy-Δ12,14,12,14-Prostaglandin J2 Ameliorates Experimental Autoimmune Encephalomyelitis', *The Journal of Immunology*, 168: 2508-2515.
320. Diab, A., Hussain, R.Z., Lovett-Racke, A.E., Chavis, J.A., Drew, P.D., & Racke, M.K., 2004, 'Ligands for the peroxisome proliferator-activated receptor-gamma and the retinoid X receptor exert additive anti-inflammatory effects on experimental autoimmune encephalomyelitis', *Journal of Neuroimmunology*, 148: 116-126.
321. Feinstein, D.L., Galea, E., Gavrilyuk, V., Brosnan, C.F., Whitacre, C.C., Dumitrescu-Ozimek, L., Landreth, G.E., Pershadsingh, H.A., Weinberg, G., & Heneka, M.T., 2002, 'Peroxisome proliferator-activated receptor-gamma agonists prevent experimental autoimmune encephalomyelitis', *Annals of Neurology*, 51: 694-702.
322. Iruretagoyena, M.I., Sepulveda, S.E., Lezana, J.P., Hermoso, M., Bronfman, M., Gutierrez, M.A., Jacobelli, S.H., & Kalergis, A.M., 2006, 'Inhibition of nuclear factor-kappa B enhances the capacity of immature dendritic cells to induce antigen-specific tolerance in experimental autoimmune encephalomyelitis', *Journal of Pharmacology and Experimental Therapeutics*, 318: 59-67.
323. Bhat, R., Bhansali, A., Bhadada, S., & Sialy, R., 2007, 'Effect of pioglitazone therapy in lean type 1 diabetes mellitus', *Diabetes Research and Clinical Practice*, 78: 349-354.
324. Kawano, Y., Irie, J., Nakatani, H., & Yamada, S., 2009, 'Pioglitazone might prevent the progression of slowly progressive type 1 diabetes', *Internal Medicine Journal*, 48: 1037-1039.
325. Zdravkovic, V., Hamilton, J.K., Daneman, D., & Cummings, E.A., 2006, 'Pioglitazone as adjunctive therapy in adolescents with type 1 diabetes', *Journal of Pediatrics*, 149: 845-849.
326. Kaiser, C.C., Shukla, D.K., Stebbins, G.T., Skias, D.D., Jeffery, D.R., Stefoski, D., Katsamakis, G., & Feinstein, D.L., 2009, 'A pilot test of pioglitazone as an add-on in patients with relapsing remitting multiple sclerosis', *Journal of Neuroimmunology*, 211: 124-130.
327. Klotz, L., Schmidt, S., Heun, R., Klockgether, T., & Kolsch, H., 2009, 'Association of the PPARgamma gene polymorphism Pro12Ala with delayed onset of multiple sclerosis', *Neuroscience Letters*, 449: 81-83.
328. Dinca, A., Chien, W.M., & Chin, M.T., 2016, 'Intracellular Delivery of Proteins with Cell-Penetrating Peptides for Therapeutic Uses in Human Disease', *International Journal of Molecular Sciences*, 17: 263.
329. Matsson, P. & Bergström, C.A.S., 2015, 'Computational modeling to predict the functions and impact of drug transporters', *In Silico Pharmacology*, 3: 8.
330. Milletti, F., 2012, 'Cell-penetrating peptides: classes, origin, and current landscape', *Drug Discovery Today*, 17: 850-860.

331. Guo, Z., Peng, H., Kang, J., & Sun, D., 2016, 'Cell-penetrating peptides: Possible transduction mechanisms and therapeutic applications', *Biomedical Reports*, 4: 528-534.
332. Henriques, S.T., Costa, J., & Castanho, M.A., 2005, 'Translocation of beta-galactosidase mediated by the cell-penetrating peptide pep-1 into lipid vesicles and human HeLa cells is driven by membrane electrostatic potential', *Biochemistry*, 44: 10189-98.
333. Deshayes, S., Heitz, A., Morris, M.C., Charnet, P., Divita, G., & Heitz, F., 2004, 'Insight into the mechanism of internalization of the cell-penetrating carrier peptide Pep-1 through conformational analysis', *Biochemistry*, 43: 1449-57.
334. Richard, J.P., Melikov, K., Vives, E., Ramos, C., Verbeure, B., Gait, M.J., Chernomordik, L.V., & Lebleu, B., 2003, 'Cell-penetrating peptides. A reevaluation of the mechanism of cellular uptake', *The Journal of Biological Chemistry*, 278: 585-590.
335. Duchardt, F., Fotin-Mleczek, M., Schwarz, H., Fischer, R., & Brock, R., 2007, 'A comprehensive model for the cellular uptake of cationic cell-penetrating peptides', *Traffic*, 8: 848-66.
336. LifeTechnologies, 2012, 'Alexa Fluor® Succinimidyl Esters (NHS esters)', 1-6.
337. Sun, J., Furio, L., Mecheri, R., van der Does, A.M., Lundeberg, E., Saveanu, L., Chen, Y., van Endert, P., Agerberth, B., & Diana, J., 2015, 'Pancreatic beta-Cells Limit Autoimmune Diabetes via an Immunoregulatory Antimicrobial Peptide Expressed under the Influence of the Gut Microbiota', *Immunity*, 43: 304-17.
338. Kleiner, G., Marcuzzi, A., Zanin, V., Monasta, L., & Zauli, G., 2013, 'Cytokine Levels in the Serum of Healthy Subjects', *Mediators of Inflammation*, 2013: 6.
339. Monastero, R.N. & Pentyala, S., 2017, 'Cytokines as Biomarkers and Their Respective Clinical Cutoff Levels', *International Journal of Inflammation*, 2017: 11.
340. Green, M., Ishino, M., & Loewenstein, P.M., 1989, 'Mutational analysis of HIV-1 Tat minimal domain peptides: Identification of *trans*-dominant mutants that suppress HIV-LTR-driven gene expression', *Cell*, 58: 215-223.
341. Calogera, M.S., 2016, 'Lysosomes, Lysosomal Storage Diseases, and Inflammation', *Journal of Inborn Errors of Metabolism and Screening*, 4: 2326409816650465.
342. Sakhrani, N.M. & Padh, H., 2013, 'Organelle targeting: third level of drug targeting', *Drug Design, Development and Therapy*, 7: 585-599.
343. Lim, S., Koo, J., & Choi, J., 2016, 'Use of Cell-Penetrating Peptides in Dendritic Cell-Based Vaccination', *Immune Network*, 16: 33-43.
344. Van Belle, T.L., Coppieters, K.T., & Von Herrath, M.G., 2011, 'Type 1 Diabetes: Etiology, Immunology, and Therapeutic Strategies', *Physiological Reviews*, 91: 79-118.
345. Diana, J. & Lehuen, A., 2014, 'Macrophages and β-cells are responsible for CXCR2-mediated neutrophil infiltration of the pancreas during autoimmune diabetes', *EMBO Molecular Medicine*, 6: 1090-1104.
346. In't Veld, P., 2014, 'Insulitis in human type 1 diabetes: a comparison between patients and animal models', *Seminars in Immunopathology*, 36: 569-579.
347. Tettey, P., Simpson, S., Taylor, B.V., & van der Mei, I.A.F., 2015, 'The co-occurrence of multiple sclerosis and type 1 diabetes: Shared aetiologic features and clinical implication for MS aetiology', *Journal of the Neurological Sciences*, 348: 126-131.
348. Navegantes, K.C., de Souza Gomes, R., Pereira, P.A.T., Czaikoski, P.G., Azevedo, C.H.M., & Monteiro, M.C., 2017, 'Immune modulation of some autoimmune diseases: the critical role of macrophages and neutrophils in the innate and adaptive immunity', *Journal of Translational Medicine*, 15: 36.
349. Nathan, C., 2006, 'Neutrophils and immunity: challenges and opportunities', *Nature Reviews. Immunology*, 6: 173-182.
350. Nordenfelt, P. & Tapper, H., 2011, 'Phagosome dynamics during phagocytosis by neutrophils', *Journal of Leukocyte Biology*, 90: 271-284.

351. Mantovani, A., Cassatella, M.A., Costantini, C., & Jaillon, S., 2011, 'Neutrophils in the activation and regulation of innate and adaptive immunity', *Nature Reviews. Immunology*, 11: 519-531.
352. Cloutier, A., Guindi, C., Larivee, P., Dubois, C.M., Amrani, A., & McDonald, P.P., 2009, 'Inflammatory cytokine production by human neutrophils involves C/EBP transcription factors', *Journal of Immunology*, 182: 563-571.
353. Kasama, T., Miwa, Y., Isozaki, T., Odai, T., Adachi, M., & Kunkel, S.L., 2005, 'Neutrophil-derived cytokines: potential therapeutic targets in inflammation', *Current Drug Targets. Inflammation and Allergy*, 4: 273-279.
354. Condliffe, A.M., Chilvers, E.R., Haslett, C., & Dransfield, I., 1996, 'Priming differentially regulates neutrophil adhesion molecule expression/function', *Immunology*, 89: 105-111.
355. Hallett, M.B. & Lloyds, D., 1995, 'Neutrophil priming: the cellular signals that say 'amber' but not 'green'', *Immunology Today*, 16: 264-268.
356. Dale, D.C., Boxer, L., & Liles, W.C., 2008, 'The phagocytes: neutrophils and monocytes', *Blood*, 112: 935-45.
357. Tanaka, M. & Miyake, Y., 2007, 'Apoptotic cell clearance and autoimmune disorder', *Current Medicinal Chemistry*, 14: 2892-2897.
358. Gomes, N.E., Brunialti, M.K., Mendes, M.E., Freudenberg, M., Galanos, C., & Salomao, R., 2010, 'Lipopolysaccharide-induced expression of cell surface receptors and cell activation of neutrophils and monocytes in whole human blood', *Brazilian Journal of Medical and Biological Research*, 43: 853-858.
359. Soler-Rodriguez, A.M., Zhang, H., Lichenstein, H.S., Qureshi, N., Niesel, D.W., Crowe, S.E., Peterson, J.W., & Klimpel, G.R., 2000, 'Neutrophil Activation by Bacterial Lipoprotein Versus Lipopolysaccharide: Differential Requirements for Serum and CD14', *The Journal of Immunology*, 164: 2674-2683.
360. Lieberman, M.M., Sachanandani, D.M., & Pinney, C.A., 1996, 'Comparative study of neutrophil activation by chemiluminescence and flow cytometry', *Clinical and Diagnostic Laboratory Immunology*, 3: 654-662.
361. Geffner, J.R., Fontan, P.A., Sordelli, D.O., & Isturiz, M.A., 1991, 'Neutrophil erythrotoxicity induced by phorbol myristate acetate: mechanisms involved in neutrophil activation', *Journal of Leukocyte Biology*, 49: 352-359.
362. Jersmann, H.P., Rathjen, D.A., & Ferrante, A., 1998, 'Enhancement of lipopolysaccharide-induced neutrophil oxygen radical production by tumor necrosis factor alpha', *Infection and Immunity*, 66: 1744-1747.
363. Gordon, S., 2016, 'Phagocytosis: An Immunobiologic Process', *Immunity*, 44: 463-75.
364. Citro, A., Valle, A., Cantarelli, E., Mercalli, A., Pellegrini, S., Liberati, D., Daffonchio, L., Kastsiuchenka, O., Ruffini, P.A., Battaglia, M., Allegretti, M., & Piemonti, L., 2015, 'CXCR1/2 inhibition blocks and reverses type 1 diabetes in mice', *Diabetes*, 64: 1329-40.
365. Wojkowska, D.W., Szpakowski, P., Ksiazek-Winiarek, D., Leszczynski, M., & Glabinski, A., 2014, 'Interactions between Neutrophils, Th17 Cells, and Chemokines during the Initiation of Experimental Model of Multiple Sclerosis', *Mediators of Inflammation*, 2014: 8.
366. Carlson, T., Kroenke, M., Rao, P., Lane, T.E., & Segal, B., 2008, 'The Th17–ELR(+) CXC chemokine pathway is essential for the development of central nervous system autoimmune disease', *The Journal of Experimental Medicine*, 205: 811-823.
367. Kishida, K., Kohyama, M., Kurashima, Y., Kogure, Y., Wang, J., Hirayasu, K., Suenaga, T., Kiyono, H., Kunisawa, J., & Arase, H., 2015, 'Negative regulation of DSS-induced experimental colitis by PILRalpha', *International Immunology*, 27: 307-314.
368. Bento, A.F., Leite, D.F., Claudino, R.F., Hara, D.B., Leal, P.C., & Calixto, J.B., 2008, 'The selective nonpeptide CXCR2 antagonist SB225002 ameliorates acute experimental colitis in mice', *Journal of Leukocyte Biology*, 84: 1213-1221.

369. Rahat, M.A., Coffelt, S.B., Granot, Z., Muthana, M., & Amedei, A., 2016, 'Macrophages and Neutrophils: Regulation of the Inflammatory Microenvironment in Autoimmunity and Cancer', *Mediators of Inflammation*, 2016: 3.
370. Huang, S.C., Everts, B., Ivanova, Y., O'Sullivan, D., Nascimento, M., Smith, A.M., Beatty, W., Love-Gregory, L., Lam, W.Y., O'Neill, C.M., Yan, C., Du, H., Abumrad, N.A., Urban, J.F., Jr., Artyomov, M.N., Pearce, E.L., & Pearce, E.J., 2014, 'Cell-intrinsic lysosomal lipolysis is essential for alternative activation of macrophages', *Nature Immunology*, 15: 846-855.
371. Mahajan, S., Dkhar, H.K., Chandra, V., Dave, S., Nanduri, R., Janmeja, A.K., Agrewala, J.N., & Gupta, P., 2012, 'Mycobacterium tuberculosis modulates macrophage lipid-sensing nuclear receptors PPARgamma and TR4 for survival', *The Journal of Immunology*, 188: 5593-5603.
372. Jiang, M., Jerome, W.G., & Hayward, S.W., 2010, 'Autophagy in nuclear receptor PPARgamma-deficient mouse prostatic carcinogenesis', *Autophagy*, 6: 175-6.
373. Jiang, M., Fernandez, S., Jerome, W.G., He, Y., Yu, X., Cai, H., Boone, B., Yi, Y., Magnuson, M.A., Roy-Burman, P., Matusik, R.J., Shappell, S.B., & Hayward, S.W., 2010, 'Disruption of PPARγ signaling results in mouse prostatic intraepithelial neoplasia involving active autophagy', *Cell death and differentiation*, 17: 469-481.
374. Yang, X., Zhang, W., Chen, Y., Li, Y., Sun, L., Liu, Y., Liu, M., Yu, M., Li, X., Han, J., & Duan, Y., 2016, 'Activation of Peroxisome Proliferator-activated Receptor gamma (PPARgamma) and CD36 Protein Expression: THE DUAL PATHOPHYSIOLOGICAL ROLES OF PROGESTERONE', *The Journal of Biological Chemistry*, 291: 15108-15118.
375. Rios, F.J., Jancar, S., Melo, I.B., Ketelhuth, D.F., & Gidlund, M., 2008, 'Role of PPAR-gamma in the modulation of CD36 and FcgammaRII induced by LDL with low and high degrees of oxidation during the differentiation of the monocytic THP-1 cell line', *Cellular Physiology and Biochemistry*, 22: 549-556.
376. Bujold, K., Rhainds, D., Jossart, C., Febbraio, M., Marleau, S., & Ong, H., 2009, 'CD36-mediated cholesterol efflux is associated with PPARgamma activation via a MAPK-dependent COX-2 pathway in macrophages', *Cardiovasccular Research*, 83: 457-464.
377. Liu, Y., Steinbusch, L.K.M., Nabben, M., Kapsokalyvas, D., van Zandvoort, M., Schönleitner, P., Antoons, G., Simons, P.J., Coumans, W.A., Geomini, A., Chanda, D., Glatz, J.F.C., Neumann, D., & Luiken, J.J.F.P., 2017, 'Palmitate-Induced Vacuolar-Type H+-ATPase Inhibition Feeds Forward into Insulin Resistance and Contractile Dysfunction', *Diabetes*, 66: 1521-1534.
378. Urban, B.C., Ferguson, D.J.P., Pain, A., Willcox, N., Plebanski, M., Austyn, J.M., & Roberts, D.J., 1999, 'Plasmodium falciparum-infected erythrocytes modulate the maturation of dendritic cells', *Nature*, 400: 73-77.
379. Urban, B.C., Willcox, N., & Roberts, D.J., 2001, 'A role for CD36 in the regulation of dendritic cell function', *Proceedings of the National Academy of Sciences*, 98: 8750-8755.
380. Marx, N., Bourcier, T., Sukhova, G.K., Libby, P., & Plutzky, J., 1999, 'PPARgamma activation in human endothelial cells increases plasminogen activator inhibitor type-1 expression: PPARgamma as a potential mediator in vascular disease', *Arteriosclerosis, Thrombosis, and Vascular Biology*, 19: 546-551.
381. Imbalzano, E., Quartuccio, S., Di Salvo, E., Crea, T., Casciaro, M., & Gangemi, S., 2017, 'Association between HMGB1 and asthma: a literature review', *Clinical and Molecular Allergy : CMA*, 15: 12.
382. Park, S. & Lee, Y., 2010, 'Interleukin-17 regulation: an attractive therapeutic approach for asthma', *Respiratory Research*, 11: 78-78.
383. Honda, K., Marquillies, P., Capron, M., & Dombrowicz, D., 2004, 'Peroxisome proliferator-activated receptor gamma is expressed in airways and inhibits features of airway remodeling in a mouse asthma model', *Journal of Allergy and Clinical Immunology*, 113: 882-888.

384. El-Naa, M.M., El-Refaei, M.F., Nasif, W.A., Abduljawad, S.H., El-Brairy, A.I., & El-Readi, M.Z., 2015, 'In-vivo antioxidant and anti-inflammatory activity of rosiglitazone, a peroxisome proliferator-activated receptor-gamma (PPAR-gamma) agonists in animal model of bronchial asthma', *Journal of Pharmacy and Pharmacology*, 67: 1421-1430.
385. Richards, D.B., Bareille, P., Lindo, E.L., Quinn, D., & Farrow, S.N., 2010, 'Treatment with a peroxisomal proliferator activated receptor gamma agonist has a modest effect in the allergen challenge model in asthma: A randomised controlled trial', *Respiratory Medicine*, 104: 668-674.
386. Anderson, J.R., Mortimer, K., Pang, L., Smith, K.M., Bailey, H., Hodgson, D.B., Shaw, D.E., Knox, A.J., & Harrison, T.W., 2016, 'Evaluation of the PPAR-γ Agonist Pioglitazone in Mild Asthma: A Double-Blind Randomized Controlled Trial', *PLoS ONE*, 11: e0160257.

Appendix

BMC Immunology

Selection of reliable reference genes for the normalisation of gene expression levels following time course LPS-stimulation of murine bone marrow derived macrophages

--Manuscript Draft--

Manuscript Number:	IMNO-D-17-00002R2
Full Title:	Selection of reliable reference genes for the normalisation of gene expression levels following time course LPS-stimulation of murine bone marrow derived macrophages
Article Type:	Methodology article
Section/Category:	Innate immunity
Funding Information:	National Health and Medical Research Council (1087341) — Dr Sheila Donnelly Diabetes Australia Research Trust — AProf Bronwyn A O'Brien
Abstract:	Background: Macrophages are key players in the initiation, perpetuation and regulation of both innate and adaptive immune responses. They largely perform these roles through modulation of the expression of genes, especially those encoding cytokines. Murine bone marrow derived macrophages (BMDMs) are commonly used as a model macrophage population for the study of immune responses to pro-inflammatory stimuli, notably lipopolysaccharide (LPS), which may be pertinent to the human situation. Evaluation of the temporal responses of these stimulated macrophages is widely conducted via the measurement of gene expression levels by RT-qPCR. While providing a robust and sensitive measure of gene expression levels, RT-qPCR relies on the normalisation of gene expression data to a stably expressed reference gene. Generally, a normalisation gene(s) is selected from a list of "traditional" reference genes without validation of expression stability under the specific experimental conditions of the study. Results: Here, we examined the stability of eight commonly used reference genes, and assessed each for their stability of expression during the peak (6h) and resolution (24h) phases of the BMDM response to LPS. Further, we identified two additional genes, which have not previously been described as reference genes, and have validated the stability of their expression levels during the same phases of the inflammatory response. Importantly, we demonstrate that certain "traditional" reference genes are in fact regulated by LPS exposure, and, therefore, are not reliable candidates as their inclusion may compromise the accuracy of data interpretation. Testament to this, we show that the normalisation of gene expression data using an unstable reference gene greatly affects the experimental data, and, therefore, the ultimate biological conclusions. Conclusion: This study reaffirms the importance of validating reference gene stability for individual experimental conditions. Given that gene expression levels in LPS stimulated macrophages is routinely used to infer biological phenomena that are of relevance to human conditions, verification of reference gene stability is crucial.
Corresponding Author:	Sheila Donnelly University of Technology Sydney AUSTRALIA
Corresponding Author Secondary Information:	
Corresponding Author's Institution:	University of Technology Sydney
Corresponding Author's Secondary Institution:	
First Author:	Akane Tanaka
First Author Secondary Information:	
Order of Authors:	Akane Tanaka Joyce To

	Bronwyn A O'Brien
	Sheila Donnelly
	Maria E Lund
Order of Authors Secondary Information:	
Response to Reviewers:	All editorial revisions have been completed as requested

Selection of reliable reference genes for the normalisation of gene expression levels following time course LPS stimulation of murine bone marrow derived macrophages.

Akane Tanaka[1], Joyce To[1], Bronwyn O'Brien[1,2], Sheila Donnelly[1], Maria Lund[1*].

[1]The School of Life Sciences, University of Technology Sydney, New South Wales, Australia; [2]The Centre for Health Technologies, University of Technology Sydney, New South Wales, Australia

*Correspondence: Maria.Lund@uts.edu.au

Email addresses for authors:

Akane.Tanaka@uts.edu.au

Joyce.To@uts.edu.au

Bronwyn.Obrien@uts.edu.au

Sheila.Donnelly@uts.edu.au

Abstract

Background: Macrophages are key players in the initiation, perpetuation and regulation of both innate and adaptive immune responses. They largely perform these roles through modulation of the expression of genes, especially those encoding cytokines. Murine bone marrow derived macrophages (BMDMs) are commonly used as a model macrophage population for the study of immune responses to pro-inflammatory stimuli, notably lipopolysaccharide (LPS), which may be pertinent to the human situation. Evaluation of the temporal responses of LPS stimulated macrophages is widely conducted via the measurement of gene expression levels by RT-qPCR. While providing a robust and sensitive measure of gene expression levels, RT-qPCR relies on the normalisation of gene expression data to a stably expressed reference gene. Generally, a normalisation gene(s) is selected from a list of "traditional" reference genes without validation of expression stability under the specific experimental conditions of the study. In the absence of such validation, and given that many studies use only a single reference gene, the reliability of data is questionable.

Results: The stability of expression levels of eight commonly used reference genes was assessed during the peak (6h) and resolution (24h) phases of the BMDM response to LPS. Further, this study identified two additional genes, which have not previously been described as reference genes, and the stability of their expression levels during the same phases of the inflammatory response were validated. Importantly, this study demonstrates that certain "traditional" reference genes are in fact regulated by LPS exposure, and, therefore, are not reliable candidates as their inclusion may compromise the accuracy of data interpretation. Testament to this, this study shows that the normalisation of gene expression data using an unstable reference gene greatly affects the experimental data obtained, and, therefore, the ultimate biological conclusions drawn.

Conclusion: This study reaffirms the importance of validating reference gene stability for individual experimental conditions. Given that gene expression levels in LPS stimulated

macrophages is routinely used to infer biological phenomena that are of relevance to human conditions, verification of reference gene expression stability is crucial.

Keywords: macrophage, lipopolysaccharide, pro-inflammatory responses, RT-qPCR, reference gene

Background

Macrophages play a significant role in the initiation and perpetuation of innate and adaptive immune responses. In this role, they perform multiple functions, including the uptake, processing and presentation of antigen, microbial killing, phagocytosis of apoptotic cells, and the secretion of cytokines, chemokines and chemical mediators [1]. The expression and secretion of immune modulators imparts the macrophage the ability to orchestrate immune responses, skewing them toward the pro-inflammatory, anti-inflammatory or regulatory arms of immunity. While pro-inflammatory responses are crucial to the elimination of pathogens, they are also central to the pathogenesis of autoimmune (for example type 1 diabetes, multiple sclerosis and rheumatoid arthritis) and pro-inflammatory (for example sepsis) diseases. Accordingly, much research has focused on understanding the responses of macrophages to pro-inflammatory conditions. These investigations often use murine bone marrow derived macrophages (BMDM), as a model mammalian macrophage system [2-4]. This is because BMDMs exhibit phenotypic and functional homogeneity and closely resemble ex *vivo* primary cells, thereby making them the preferable model, as opposed to other sources of primary macrophages or cell lines. Immortalised cell lines differ significantly in phenotype/function to primary murine macrophages. Primary resident macrophages of the peritoneum or lung are not naïve, and, therefore, differ phenotypically/functionally according to their previous immune experiences. Moreover, these cells are obtained in lower numbers, as compared to yields derived from bone marrow.

The pro-inflammatory response of macrophages is commonly investigated using lipopolysaccharide (LPS; a major component of bacterial membranes), as a biologically relevant inducer of inflammation [5-7]. The progression of this pro-inflammatory response in macrophages

has been well characterised, with an initial induction phase of inflammation at 2h following LPS exposure, a peak inflammatory phase at 6h, and, finally, a resolution phase at 24h post-stimulation [8-10]. The analysis of gene expression levels by RT-qPCR is often employed to study this pro-inflammatory response [11-13]. As a powerful tool, RT-qPCR is a rapid and sensitive technique with potential for high throughput, which allows the detection and quantitation of low abundance mRNA [14]. Despite these advantages, the accuracy and reliability of RT-qPCR data interpretation is dependent upon factors intrinsic to the preparation steps prior to RT-qPCR analysis, including RNA quality and quantity and reverse transcriptase (RT) efficiency. Indeed, it is crucial that the quantity of RNA input to the RT reaction be normalised. However, while necessary, this is not sufficient for direct comparisons of RT-qPCR data. A reference/normalisation gene(s), whose expression level is not regulated by the specific experimental conditions, is routinely included in RT-qPCR for all samples, thereby enabling normalisation of expression levels of the gene of interest (GOI) data [15,16]. It is recommended that for each set of experimental conditions, the optimal reference gene(s) be determined [15]. However, in reality, few studies validate this important optimisation parameter. Rather, "traditional" reference genes, such as glyceraldehyde 3-phosphate dehydrogenase (*Gapdh*) or β-2 microglobulin (*B2m*), that are presumed to be stable in their expression levels, are generally selected as reference genes, despite the fact that they may not be expressed at consistent levels under the specific experimental conditions being studied. Normalisation of target gene expression levels to those of a reference gene which is, itself, regulated by the experimental conditions, likely affects measurements of comparative gene expression levels, thereby compromising data interpretation and biological conclusions made [17-19]. Thus, it is crucial that for any given experimental condition, one or more consistently expressed reference genes are identified and used [15].

To date, no optimal reference gene (or combination of reference genes) has been identified and validated for the normalisation of gene expression levels between control and LPS stimulated BMDMs over the time course of the pro-inflammatory response. Thus, the current study aimed to

identify the most stably expressed reference genes during the peak (6h) and resolution (24h) phases of inflammation. A list of eight genes that have been used commonly for the normalisation of gene expression levels in BMDMs was initially investigated. From microarray analyses of untreated and LPS treated BMDMs at 6h and 24h post-LPS stimulation, three additional candidate reference genes, whose expression remained unchanged under these experimental conditions, were added to the list of commonly used reference genes. Thus, the expression levels of a total of 11 candidate reference genes were compared at each time point following LPS stimulation, and the optimal reference gene, or combination of reference genes, for each phase of the pro-inflammatory response was identified using NormFinder [20], GeNorm [21] and BestKeeper [22] softwares.

This study is the first to identify and validate *Hnrnpab* and *Stx5a*, as optimal reference genes for the normalisation of gene expression data during the peak and resolution phases, respectively, of the BMDM response to LPS. Moreover, this study demonstrates the consistency in expression levels of both *Hnrnpab* and *Stx5a* for peritoneal and RAW 264.7 macrophages stimulated with LPS. Importantly, the expression levels of these genes are more stable than those of *Gapdh* and *Actinb*, which are both commonly regarded as reference genes in the assessment of macrophage inflammatory responses. These observations demonstrate the importance of assessing the stability of reference genes for every experimental condition prior to normalisation of gene expression.

Results

The range of C_t values for candidate reference genes differs according to the time point post-LPS stimulation

The aim of the current study was to identify the optimal reference gene, or combination of reference genes, for the normalisation of gene expression data in the commonly studied LPS stimulation model using BMDMs. We first identified a list of eight genes routinely used for the normalisation of gene expression data from experiments using BMDMs in general [23-25] or LPS stimulated BMDMs [26-35]. These candidate genes were *Actinb, B2m, Gapdh, Gusb, Hmbs, Hprt, Ppia*

(cyclophilin A), and *Rpl13a*. We then identified candidate reference genes from a microarray data set comparing gene expression levels between control and LPS stimulated BMDMs at 6h and 24h post-exposure to LPS (Supplementary Table 1 and Supplementary Table 2, respectively). We selected three candidate reference genes whose expression remained unchanged between control and LPS-stimulated cells at both 6h and 24h, including chromatid cohesion factor homolog (*Mau2*; a gene involved in cell cycle), heterogenous nuclear ribonucleoprotein A/B (*Hnrnpab*; involved in mRNA processing) and Syntaxin 5a (*Stx5a*; a gene involved in autophagy; [36]). Thus, a total of eleven candidate reference genes were tested for the stability of their expression levels. The range of C_t values for untreated and LPS treated BMDMs at each time point, for each gene tested, are described in Figure 1. The level of expression of genes differed, with some being highly expressed, for example, *Actinb* (mean (standard deviation [SD]): 6h control; 18.34(0.18)), while others were expressed at much lower levels, for example, *Hmbs* (mean (SD): 6h control; 27.73(0.81)).

The variance in expression levels of candidate reference genes, as indicated by the range of C_t values and SD, differed within a single treatment group. For example, within the control group at 6h, the lowest variance in C_t values, as indicated by the lowest SD, was *Actinb* (SD=0.18; Figure 1A). The highest variance within the untreated group was for *Mau2* (SD=1.06; Figure 1A). Interestingly, in some cases, genes differed in their expression variability, dependent upon the time point following LPS stimulation. For example, in the control group, at 6h, the variance in C_t values between replicates recorded for the gene *Rpl13a* was larger (range(SD) = 26.15-27.96(0.91)) than the variance observed for *Rpl13a* at 24h post-LPS stimulation (range(SD) = 25.86-26.17(0.17)).

The most stable reference gene differs according to the stage of inflammation.

In order to identify the most consistently expressed reference gene candidate at each time point, the C_t values were inputted into GeNorm, NormFinder and BestKeeper programs. The analysis provided by NormFinder assigns a stability ranking to candidate reference genes using an algorithm which takes into account intra- and inter-variability (i.e. the variability in expression levels within

and between the treatment groups, respectively) [20]. GeNorm determines the expression stability of a gene using a stepwise exclusion of the least stably expressed gene, generating an M value for each reference gene, and M values are then ranked. The Bestkeeper software assigns a ranking to each candidate reference gene based on the SD between samples. The rankings provided by each software for samples at 6h and 24h after LPS or vehicle exposure are described in Figure 2A and B, respectively. There was broad agreement between the three programs regarding the two most and least consistently expressed reference genes between control and LPS stimulated groups at 6h. At this time point, according to NormFinder and GeNorm, the most stable reference genes were *Hnrnpab* and *Stx5a*. Similarly, BestKeeper ranked *Hnrnpab* and *Stx5a* in the top four most stably expressed genes, at second and fourth, respectively. Application of all three softwares indicated that the two least stable genes were *Gusb* and *Hmbs*.

After 24h LPS stimulation, there was less consensus among the softwares regarding the most reliable reference gene(s). NormFinder and BestKeeper were in agreement, ranking *Stx5a* and *Hnrnpab* as the two most stably expressed genes. GeNorm, however, identified *Hmbs* and *Rpl13a* as the most appropriate combination of genes for normalisation. In comparison, NormFinder and BestKeeper ranked *Hmbs* and *Rpl13a* seventh and eighth in stability, respectively. This discrepancy is likely due to the difference in the mathematical algorithms used to rank genes by NormFinder and BestKeeper, as compared to GeNorm. GeNorm assumes that two reference genes are not co-regulated. If they are co-regulated, they would score artificially high on the GeNorm ranking scale [37]. Indeed, the C_t values recorded for *Hmbs* and *Rpl13a* are both regulated in the same direction, in the LPS treated group, as compared to controls, that is, expression of each gene is lower in the LPS treated group, as compared to the controls, evident as a significantly higher C_t value (mean(SD); *Hmbs*: control: 28.7(0.2), LPS: 29.3(0.1), p=0.0084; *Rpl13a*: control: 26.0(0.2), LPS: 26.6(0.1), p=0.0078; Figure 1B). The least stable reference genes identified consistently between the three softwares were *Gusb* and *B2m*.

To validate these findings, an independent experiment was performed, and the expression of the most and least stable reference genes, as identified by NormFinder software, was analysed by RT-qPCR. In agreement with the findings described above, there was no difference in C_t values observed for *Hnrnpab*, between the control and LPS treated samples, at 6h (Figure 2C). In the above-mentioned analysis, *Gusb* was identified as the most unstable reference gene under these particular experimental conditions, and was clearly regulated by LPS exposure at 6h. In agreement with these findings, the C_t values observed for *Gusb* were significantly higher following LPS exposure at 6h ($p=0.0304$), indicating that LPS down-regulated *Gusb* gene expression levels. After 24h exposure to LPS, *Stx5a* was identified as the most stably expressed gene between control and treated cells. This was validated in the independent experiment, with no difference seen in C_t values between the two treatments (Figure 2D). In agreement with the above-mentioned analysis, C_t values observed for *B2m* were significantly lower in the LPS treated BMDMs, as compared to controls ($p=0.0034$), indicating that LPS up-regulated *B2m* expression at this time point.

To investigate the applicability of both *Hnrnpab* and *Stx5a* as reference genes in differently sourced macrophages, we compared the expression levels of six of the 11 candidate genes (three of the most stable and three of the least stable) in murine peritoneal macrophages and in the RAW 264.7 murine macrophage cell line. For all genes the C_t values were recorded for control and LPS stimulated (10ng/ml) cells at 6h (Figure 3A-D) and 24h (Figure 3E-H). Consistent with the stability of genes in LPS stimulated BMDMs, there was no difference in C_t values observed for *Hnrnpab*, between the control and LPS treated cohorts, at 6h. In addition, *Stx5a* was again identified as the most stably expressed gene between control and treated cells 24h after LPS treatment, with no difference seen in C_t values between the two treatments. This additional study therefore validates *Hnrnpab* and *Stx5a* as suitable reference genes in these multiple sources of macrophages and at multiple time points.

The choice of reference genes for data normalisation can affect biological conclusions.

To demonstrate the impact and importance of selecting the most stable reference gene(s) for data normalisation, we analysed the relative expression of three genes whose increased expression levels characterise the pro-inflammatory response in BMDMs. The expression of IL-1β and TNF (both pro-inflammatory cytokines) and NOS2 (inducible nitric oxide synthase, an enzyme produced during the pro-inflammatory response) were assessed by RT-qPCR, and then normalised using the most and least stable reference genes, as identified by NormFinder software. At 6h post-LPS stimulation, the fold change in expression levels of TNF was significantly higher in the LPS treatment group when gene expression data was normalised to the least stable reference gene, *Gusb* (mean±SD: 883±193), as compared to when normalisation was performed using the most stable reference gene, *Hnrnpab* (mean±SD: 165±12; p=0.0208; Figure 4A). When normalised to the traditional choice of housekeeping gene, *Gapdh*, the fold change in expression of TNF was similar (mean±SD: 123±19) to that seen when *Hnrnpab* was used for normalisation, which is consistent with its top stability ranking by BestKeeper software analysis. In contrast, using *Actinb*, which was ranked poorly by all 3 analytical programs, reduced the change in TNF gene expression by 3-fold (mean±SD: 44±2). Similarly, following 24h exposure to LPS, the fold change in expression levels of TNF in the LPS-treated group was significantly different when normalised to the most inconsistent reference gene, *B2m* (mean±SD: 2±0), as compared to normalisation using the most consistent reference gene, *Stx5a* (mean±SD: 13±1; p<0.0001; Figure 4B). At this 24h time point, *Gapdh* and *Actinb* were both ranked midway between *B2m* and *Stx5a* with respect to stability, and in agreement with this finding, when they were used as reference genes the fold change in expression of TNF was significantly less than that obtained using *Stx5a* as the reference gene (mean±SD: 9.7±0.4 and 9.2±0.3). Similarly, normalisation using an inconsistently expressed reference gene also altered the measurements of fold change in gene expression for IL-1β and NOS2 at each time point (Figure 4A, B).

Collectively, this data clearly demonstrates that normalisation of gene expression data using an inconsistently expressed reference gene can alter the magnitude of fold changes in expression,

which may impact upon the interpretation of the biological significance of the study. The two-fold change in gene expression of TNF observed at 24h after LPS stimulation when data was normalised to *B2m* expression levels may be interpreted as not a biologically significant increase above control. However, when data was normalised to *Stx5a*, there was a significant increase in TNF gene expression levels above control. Importantly, this increase in expression at the mRNA level was corroborated at the protein level as amounts of secreted TNF at 24h post-LPS stimulation were significantly higher than control samples (mean±SD: 2821±152 pg/ml, as compared to 34±1 pg/ml, respectively; $p<0.0001$; Figure 4C). Consequently, in this example, normalisation to an inconsistent reference gene resulted in an underestimation of the magnitude of the pro-inflammatory response. These data demonstrate that the selection of consistently expressed reference genes, under the experimental parameters chosen, is crucial for the accurate interpretation of data, and, ultimately, to the elucidation of biological responses.

Discussion

Murine BMDMs are well established as a model primary macrophage population for the study of the inflammatory response. Commonly, LPS is used as a pro-inflammatory stimulus to induce gene expression in BMDMs, to investigate this pro-inflammatory response. Given the efficiency, sensitivity and robustness of RT-qPCR, this technique is commonly employed to measure gene expression levels in the study of the macrophage inflammatory response. The use of RT-qPCR necessitates normalisation of gene expression data to a reference gene, which is stably expressed under the experimental conditions used. In fact, normalisation of GOI data to a reference gene whose expression is regulated by the experimental condition can lead to erroneous results, and therefore incorrect conclusions [17-19]. Thus, the current study aimed to identify the optimal reference genes for normalisation of gene expression data for experiments using BMDMs stimulated with LPS over the course of the inflammatory response, specifically the peak (6h) and resolution (24h) phases. The data presented herein demonstrates that the expression levels of

"traditional" reference genes may vary significantly in this cell model under pro-inflammatory conditions. Moreover, we demonstrate that the normalisation of GOI data using genes that are regulated by the experimental conditions can have a significant impact on the interpretation of RT-qPCR data and, ultimately, the validity of conclusions drawn.

A review of the literature identified eight candidate reference genes that have been used for the normalisation of gene expression data for BMDMs. We set out to evaluate the stability of these genes, and to identify any additional reliable reference genes. Microarray analyses of LPS stimulated BMDMs at 6h and 24h identified three candidate reference genes, whose expression remained unchanged between control and LPS treated cells. Two of the reference genes identified from the microarray analysis, *Hnrnpab* and *Stx5a*, were ranked as the most stable reference genes for normalisation of gene expression data, at both 6h and 24h. It should be noted that several commonly used reference genes, although not ranked in first or second position, were ranked in the top five for stability, and would, therefore, still be considered suitable for the normalisation of gene expression data. For example, at 6h, *Rpl13a, Hprt* and *Gapdh* ranked third, fourth and fifth, respectively, according to NormFinder analysis. At 24h, *Actinb* and *Ppia* were ranked third and fifth, respectively. Importantly, the current study identified several genes that should be excluded as reference genes under these particular experimental conditions, including *Hmbs* and *Gusb* after 6h of BMDM exposure to LPS, and *Gusb* and *B2m* after 24h LPS exposure. These genes were ranked lowest for stability by all three programs, and, therefore, their expression levels were clearly regulated by LPS exposure. The current study also indicates that *B2m* and *Actinb* are unsuitable candidates for normalisation of expression data at 6h post-LPS stimulation, as their expression levels are modulated by LPS exposure, and, accordingly, these genes were ranked in the lowest five for stability by all three programs.

Despite the publication of the MIQE (Minimum Information for Publication of Quantitative. Real-Time PCR Experiments) guidelines [15], incorrect presumptions that "traditional" reference genes are stably expressed, without reported validation under specific experimental conditions, are

widespread among gene expression studies [38]. The stability of traditional references genes, such as *Gapdh* and *Actinb*, has previously been called into question [39-41]. In agreement, the current study further highlights the pitfalls of using such an approach for the selection of reference genes for data normalisation. The commonly used reference gene, *Actinb*, although stably expressed at 24h post-LPS stimulation (ranked third and fourth, by NormFinder and BestKeeper, respectively), was found to be one of the most highly regulated genes when cells were exposed to LPS for 6h (ranked in the lowest four by all three programs). Similarly, levels of *Hprt* gene expression at 6h post LPS-treatment were stable, however, at 24h, expression levels were down-regulated by exposure to LPS. These results demonstrate that reference gene expression levels are modulated by their cellular conditions, and highlight the requirement that all genes must be tested for expression stability under the specific experimental conditions being studied.

The impact of normalising expression data using unstable reference genes has been demonstrated in several previous publications [17-19]. The current study demonstrates the importance of normalisation using a reference gene that is stably expressed under the experimental conditions of inducing a pro-inflammatory response over time. The data demonstrated that normalisation using a reference gene that was not stably expressed falsely diminished the magnitude of the inflammatory response measured. In fact, the relative level of TNF gene expression (~2 fold increase) calculated by normalisation to an inappropriate reference gene 24h after LPS treatment indicated an almost complete absence of the pro-inflammatory response to LPS. This result was in stark contrast to the actual higher levels of secreted TNF, and TNF at the level of gene expression when data was normalised to a stable reference gene, following LPS exposure at 24h as compared to controls. Gene expression of TNF is highly regulated by LPS exposure (~13-fold increase at 24h). Thus, caution must be exercised when normalising gene expression data for a GOI that is less highly regulated (i.e. a gene that exhibits smaller changes in expression levels attributed to the experimental conditions). Smaller changes in gene expression would be more likely to be masked by normalisation to an inappropriate reference gene.

This study has demonstrated that it is crucial to determine the stability of reference genes under the specific experimental conditions employed. This is perhaps of paramount importance when studying the responses of cell types, such as macrophages, which are highly responsive to even subtle changes in the inflammatory milieu of their environment. We suggest a potential approach for the identification of stable reference genes for studying new experimental conditions. Initially, a review of the literature should be undertaken to identify several reference gene candidates. Next, if published array data is available, this can be used to identify genes whose expression levels remain unchanged under experimental conditions. Next, the stability of several candidate reference genes should be determined under experimental conditions by RT-qPCR. Finally, two or more programs should be used to identify the most stable reference gene. However helpful these programs may be in identifying the most stably expressed gene, it is still important to confirm the stability of the chosen genes by examining C_t values. For example, we have shown that, at 24h, GeNorm identified a combination of genes as most stable, that were in fact regulated by LPS exposure, presumably because the algorithm used by GeNorm to rank stability assumes there is not co-regulation of the candidate reference genes.

Conclusions

The current study identified the most stably expressed genes for use in the normalisation of gene expression data during the course of the pro-inflammatory response of primary murine macrophages to LPS. The two most stably expressed genes were identified from microarray analyses of BMDMs exposed to LPS, and, here, make their debut as reference genes. The data presented also confirms the stability of other reference genes used previously in the literature for normalisation of gene expression data in this inflammatory BMDM model. Importantly, we have identified several "traditional" reference genes that are often assumed to be stable, whose expression levels are, in fact, strongly regulated during the BMDM inflammatory response to LPS. We recommend that these genes not be used for the normalisation of gene expression data in this model, due to the

likelihood of erroneous results, and the potential for invalid experimental conclusions to be drawn. This also highlights the need for experimental validation of reference gene stability under specific experimental conditions, and we have outlined a potential approach for identifying stable reference genes.

Methods

Differentiation and stimulation of macrophages

Bone marrow derived macrophages (BMDMs) were differentiated from the bone marrow of 6-8 week old female Balb/c mice (ARC, Perth, Australia), as previously described (Zhang et al. 2008). All procedures were in accordance with the guidelines of the UTS Animal Care and Ethics Committee (Protocol number: 2012-080). Briefly, bone marrow was flushed from freshly isolated femurs and tibias with RPMI 1640 (Life Technologies). Cells were collected by centrifugation (300xg, 5 min), and resuspended at a density of $2x10^6$ cells/ml in BMDM media (RPM1 1640, supplemented with 10% v/v heat inactivated, certified low endotoxin, foetal calf serum (Life Technologies, catalogue number 10082147), beta-mercaptoethanol (715nM), penicillin/streptomycin (1% v/v, Life Technologies) and macrophage colony-stimulating factor (M-CSF, 50ng/ml, eBioscience). Cells ($2x10^7$ cells in 10ml media) were then plated into sterile 90mm petri dishes (Techno Plas, catalogue number S90001G). Cells were differentiated for 6 days, with the addition of 10ml media at Day 3. At Day 6, media and non-adherent cells were removed, remaining non-adherent cells were rinsed away with 10ml sterile saline (Baxter Healthcare), and then 10ml fresh BMDM media was added. Cells were detached by gently scraping into media and collected by centrifugation (300xg, 5 min). The purity of the BMDM population was determined at day 6 by staining for CD11b by flow cytometry. The purity of the BMDM population was always greater than 98% $CD11b^+$ (data not shown).

Peritoneal lavages were collected from 6-8 week old female Balb/c mice. Macrophages were isolated from peritoneal exudate cells (PECs) by adherence to plastic in serum-free media.

BMDMs, peritoneal and RAW264.7 macrophages, were seeded at 2 x 10^6 cells in 2ml of media in 6 well tissue culture plates and allowed to adhere for 1.5h before stimulation with LPS (from *E. Coli*, 0111.B4; Sigma Aldrich) at a concentration of 10ng/ml. Cells were incubated with LPS for 6h or 24h at 37˚C/5%CO_2.

Isolation of RNA

Supernatants were removed from cell samples, and wells were rinsed twice with sterile saline. RNA was isolated from cell samples using the Isolate II RNA mini kit (Bioline, Australia). Genomic DNA (gDNA) was removed by treatment with DNase I (Sigma Aldrich), according to the manufacturer's instructions. The absence of contaminating gDNA was demonstrated by the absence of a product in wells using "no RT" control samples, which included all components of the cDNA synthesis reaction, except reverse transcriptase. The quality of RNA was assessed by spectrophotometry (NanoDrop One/One^c, Thermofisher Scientific). Ratios for all samples are reported in Supplementary Table 3.

cDNA synthesis

For the synthesis of cDNA, 500ng RNA was used with the Superscript First Strand Synthesis Kit (Thermofisher Scientific), primed with random hexamers, according to the manufacturer's instructions. The resultant cDNA was stored at -20˚C until RT-qPCR, when it was diluted 1/10 in RNAse/DNAse free water.

RT-qPCR

RT-qPCR was performed using the QuantStudioFlex 12K instrument (Applied Biosystems). Taqman gene expression assays listed in Table 1 were used according to the manufacturer's instructions, with cDNA (5ng) in technical triplicates. The PCR program was as follows: UNG activation (50˚C, 2 min), UNG inactivation (95˚C, 10 min), followed by 40 cycles of denaturation

(95˚C, 15 sec) and annealing/extension (60˚C, 1 min). The mean C_t values were calculated from technical triplicates. For the calculation of fold change in expression, the $\Delta\Delta C_t$ method was used [43]. For samples with C_t values that were greater than 35 was considered a negative, however for the purpose of calculating a fold change, these samples were assigned a C_t value of 35. The mean ΔC_t value of the control (untreated) samples was calculated, and individual ΔC_t values were calculated for experimental replicates within the LPS treated samples, using the formula: $\Delta C_t = C_t$ target gene – C_t reference gene. The $\Delta\Delta C_t$ value for each LPS treated sample was calculated as the ΔC_t LPS sample – mean ΔC_t control samples. This was then transformed into a fold change value for each LPS sample using the calculation $2^{-\Delta\Delta Ct}$.

Table 1. Taqman gene expression assays.

Gene		Assay ID	Dye
Actinb	β-actin	Mm00607939_s1	FAM-MGB
B2m	β-2-microglobulin	Mm00437762_m1	FAM-MGB
Gapdh	Glyceraldehyde-3-phosphate dehydrogenase	Mm99999915_g1	FAM-MGB
Gusb	β-glucuronidase	Mm01197698_m1	FAM-MGB
Hmbs	Hydroxymethylbilane synthase	Mm01143545_m1	FAM-MGB
Hnrnpab	Heterogeneous Nuclear Ribonucleoprotein A/B	Mm01288699_m1	FAM-MGB
Hprt	Hypoxanthine-guanine phosphoribosyltransferase	Mm00446968_m1	FAM-MGB
Mau2	MAU2 Sister Chromatid Cohesion Factor	Mm00512415_m1	FAM-MGB
Ppia	Peptidylprolyl Isomerase A	Mm02342430_g1	FAM-MGB
Rpl13a	Ribosomal protein L13a	Mm01612987_g1	FAM-MGB
Stx5a	Syntaxin 5a	Mm00502335_m1	FAM-MGB

Gene expression microarray analysis

BMDMs were treated with vehicle or LPS, for 6h and 24h, and then RNA was isolated using Trizol reagent (Life Technologies) and the Qiagen Rneasy Plus Mini Kit (Qiagen). The aqueous phase of the Trizol preparation was obtained, according to the manufacturer's instructions, and was applied to the gDNA-eliminating column of the RNeasy Plus Mini Kit, and then RNA was isolated according to the instructions of the manufacturer (Qiagen). RNA was submitted to the Ramaciotti Centre for Genomics (UNSW, Australia) for gene expression microarray analyses using the

Affymetrix Mouse Gene 2.1ST array. Array data were analysed using Partek Genomics Suite (Partek Inc. USA). Data files were grouped according to treatment (control or LPS) and individual gene lists for 6h and 24h LPS stimulation were generated by one way ANOVA comparison of the two groups, with a fold change cut off of -1.4<fold change<1.4 (Supplementary Tables 2 and 3, respectively). Then, the two lists (6h and 24h) were combined, and a list of genes that were common to both lists was generated, and three candidate reference genes were then selected.

Measurement of TNF in supernatants

Levels of secreted TNF in the supernatants were quantified by ELISA (BD Pharmingen), according to the manufacturer's instructions.

Statistical analyses

The softwares GeNorm [21], NormFinder [20] and BestKeeper [22] were used according to the instructions supplied. This required that raw C_t values were transformed to different input formats for GeNorm and NormFinder analyses. For analysis using BestKeeper software, raw C_t values were inputted. For the statistical comparison of two groups, an unpaired, two-tailed t test was used in GraphPad Prism 7 software (GraphPad). P values indicated in the figure legends.

Abbreviations

BMDM, Bone marrow derived macrophages; GOI, gene of interest; LPS, lipopolysaccharide; MIQE, minimum information for publication of quantitative real-time PCR experiments; NOS2, nitric oxide synthase; PEC, peritoneal exudate cells; RT, reverse transcriptase; SD, standard deviation.

Declarations

Ethics approval and consent to participate.

All experiments were performed in accordance with UTS Animal Care and Ethics Committee guidelines and the study was specifically approved under protocol 2012-080.

Consent for publication.

Not applicable.

Availability of data and materials.

The datasets during and/or analysed during the current study are available from the corresponding author upon request.

Competing interests.

The authors declare that they have no competing interests.

Funding

The findings of this study were funded in part by a National Health & Medical Research (NHMRC) project grant (1087341) and in part by a Diabetes Australia Research Trust (DART) general grant. AT receives a UTS post-graduate scholarship.

Author's contributions

AT designed and performed experiments, analysed experimental data and wrote the manuscript. ML and JT analysed experimental data and wrote the manuscript. SD and BOB provided discussion and edited the manuscript. All authors have read and approved the final version of this manuscript.

Acknowledgements

We thank Dr Nham Tran for helpful discussions. We thank Susel Loli Quinteros for technical assistance.

References

1. Murray PJ, Wynn TA. Protective and pathogenic functions of macrophage subsets. Nat Rev Immunol 2011; 11:723-737.
2. Fei F, Lee KM, McCarry BE, Bowdish DME. Age-associated metabolic dysregulation in bone marrow-derived macrophages stimulated with lipopolysaccharide. Sci Rep. 2016; 6: 22637.
3. Németh B, Doczi J, Csete D, Kacso G, Ravasz D, Adams D, Kiss G, Nagy AM, Horvath G, Tretter L, et al. Abolition of mitochondrial substrate-level phosphorylation by itaconic acid produced by LPS-induced Irg1 expression in cells of murine macrophage lineage. FASEB J. 2016; 1:286-300
4. Zhang X, Li N, Shao H, Meng Y, Wang L, Wu Q, Yao Y, Li J, Bian J, Zhang Y, Deng X. Methane limit LPS-induced NF-κB/MAPKs signal in macrophages and suppress immune response in mice by enhancing PI3K/AKT/GSK-3β-mediated IL-10 expression. Sci Rep. 2016;6:29359
5. Fang H, Pengal RA, Cao X, Ganesan LP, Wewers MD, Marsh CB, Tridandapani S. Lipopolysaccharide-induced macrophage inflammatory response is regulated by SHIP. J Immunol. 2004;173(1):360-6
6. Groeneweg M, Kanters E, Vergouwe MN, Duerink H, Kraal G, Hofker MH, de Winther MP. Lipopolysaccharide-induced gene expression in murine macrophages is enhanced by prior exposure to oxLDL. J Lipid Res. 2006;47(10):2259-67.
7. Mills EL, Kelly B, Logan A, Costa AS, Varma M, Bryant CE, Tourlomousis P, Däbritz JH, Gottlieb E, Latorre I, et al. Succinate Dehydrogenase Supports Metabolic Repurposing of Mitochondria to Drive Inflammatory Macrophages. Cell. 2016;167(2):457-470
8. Gilchrist M, Thorsson V, Li B, Rust AG, Korb M, Roach JC, Kennedy K, Hai T, Bolouri H, Aderem A. Systems biology approaches identify ATF3 as a negative regulator of Toll-like receptor 4. Nature. 2006;441(7090):173-8.

9. Nilsson R, Bajic VB, Suzuki H, di Bernardo D, Björkegren J, Katayama S, Reid JF, Sweet MJ, Gariboldi M, Carninci P, et al. Transcriptional network dynamics in macrophage activation. Genomics. 2006;88(2):133-42.

10. Schroder K, Irvine KM, Taylor MS, Bokil NJ, Le Cao KA, Masterman KA, Labzin LI, Semple CA, Kapetanovic R, et al. Conservation and divergence in Toll-like receptor 4-regulated gene expression in primary human versus mouse macrophages. Proc Natl Acad Sci U S A. 2012;109(16):E944-53.

11. Hammaker D, Boyle DL, Topolewski K, Firestein GS. Differential regulation of anti-inflammatory genes by p38 MAP kinase and MAP kinase kinase 6. J Inflamm (Lond). 2014;11:14

12. Schott J, Reitter S, Philipp J, Haneke K, Schäfer H, Stoecklin G. Translational regulation of specific mRNAs controls feedback inhibition and survival during macrophage activation. PLoS Genet. 2014;10(6):e1004368.

13. Sienerth AR, Scheuermann C, Galmiche A, Rapp UR, Becker M. Polycomb group protein Bmi1 negatively regulates IL-10 expression in activated macrophages. Immunol Cell Biol. 2011;89(7):812-6

14. Bustin SA. Absolute quantification of mRNA using real-time reverse transcription polymerase chain reaction assays.J Mol Endocrinol. 2000;25(2):169-93.

15. Bustin SA, Benes V, Garson JA, Hellemans J, Huggett J, Kubista M, Mueller R, Nolan T, Pfaffl MW, Shipley GL, et al. The MIQE guidelines: minimum information for publication of quantitative real-time PCR experiments. Clin Chem. 2009;55(4):611-22

16. Huggett J, Dheda K, Bustin S, Zumla A. Real-time RT-PCR normalisation; strategies and considerations. Genes Immun. 2005;6(4):279-84

17. Maess MB, Sendelbach S, Lorkowski S. Selection of reliable reference genes during THP-1 monocyte differentiation into macrophages. BMC Mol Biol. 2010;11:90.

18. Ren S, Zhang F, Li C, Jia C, Li S, Xi H, Zhang H, Yang L, Wang Y. Selection of housekeeping genes for use in quantitative reverse transcription PCR assays on the murine cornea. Mol Vis. 2010;16:1076-86.

19. Willems E, Mateizel I, Kemp C, Cauffman G, Sermon K, Leyns L.Selection of reference genes in mouse embryos and in differentiating human and mouse ES cells. Int J Dev Biol. 2006;50(7):627-35.

20. Andersen CL, Jensen JL, Ørntoft TF. Normalization of real-time quantitative reverse transcription-PCR data: a model-based variance estimation approach to identify genes suited for normalization, applied to bladder and colon cancer data sets. Cancer Res. 2004;64(15):5245-50.

21. Vandesompele J, De Preter K, Pattyn F, Poppe B, Van Roy N, De Paepe A, Speleman F. Accurate normalization of real-time quantitative RT-PCR data by geometric averaging of multiple internal control genes. Genome Biol. 2002;3(7):RESEARCH0034.

22. Pfaffl MW, Tichopad A, Prgomet C, Neuvians TP. Determination of stable housekeeping genes, differentially regulated target genes and sample integrity: BestKeeper--Excel-based tool using pair-wise correlations. Biotechnol Lett. 2004;26(6):509-15.

23. Bao Z, Chen R, Zhang P, Lu S, Chen X, Yao Y, Jin X, Sun Y, Zhou J.A potential target gene for the host-directed therapy of mycobacterial infection in murine macrophages. Int J Mol Med. 2016;38(3):823-33

24. Carlson BA, Yoo MH, Sano Y, Sengupta A, Kim JY, Irons R, Gladyshev VN, Hatfield DL, Park JM. Selenoproteins regulate macrophage invasiveness and extracellular matrix-related gene expression. BMC Immunol. 2009;10:57

25. Stephens AS, Stephens SR, Morrison NA. Internal control genes for quantitative RT-PCR expression analysis in mouse osteoblasts, osteoclasts and macrophages. BMC Res Notes. 2011;4:410

26. Aung HT, Schroder K, Himes SR, Brion K, van Zuylen W, Trieu A, Suzuki H, Hayashizaki Y, Hume DA, Sweet MJ et al. LPS regulates proinflammatory gene expression in macrophages by altering histone deacetylase expression. FASEB J. 2006;20(9):1315-27.

27. Björkbacka H, Fitzgerald KA, Huet F, Li X, Gregory JA, Lee MA, Ordija CM, Dowley NE, Golenbock DT, Freeman MW. The induction of macrophage gene expression by LPS predominantly utilizes Myd88-independent signaling cascades. Physiol Genomics. 2004;19(3):319-30

28. Cai L, Wang Z, Meyer JM, Ji A, van der Westhuyzen DR. Macrophage SR-BI regulates LPS-induced pro-inflammatory signaling in mice and isolated macrophages. J Lipid Res. 2012;53(8):1472-81

29. Cardwell LN, Weaver BK. IL-10 inhibits LPS-induced expression of miR-147 in murine macrophages. Adv Biol Chem 2014.

30. Deng H, Maitra U, Morris M, Li L. Molecular mechanism responsible for the priming of macrophage activation. J Biol Chem. 201;288(6):3897-906

31. Dillow A, Cardwell L, Smith T, Groppe B, Peterson B, Sickman M, Weaver B. Temporal Transcriptional Regulation of IL-10-Induced Anti-Inflammatory Genes in LPS-Triggered Macrophages. *Open Jnl Immunol*. 2014; 4: 96-116.

32. Maher K, Jerič Kokelj B, Butinar M, Mikhaylov G, Manček-Keber M, Stoka V, Vasiljeva O, Turk B, Grigoryev SA, Kopitar-Jerala N. A role for stefin B (cystatin B) in inflammation and endotoxemia. J Biol Chem. 2014;289(46):31736-50.

33. Sester DP, Trieu A, Brion K, Schroder K, Ravasi T, Robinson JA, McDonald RC, Ripoll V, Wells CA, Suzuki H, et al. LPS regulates a set of genes in primary murine macrophages by antagonising CSF-1 action. Immunobiology. 2005;210(2-4):97-107.

34. Wang C, Yu X, Cao Q, Wang Y, Zheng G, Tan TK, Zhao H, Zhao Y, Wang Y, Harris DCh. Characterization of murine macrophages from bone marrow, spleen and peritoneum. BMC Immunol. 2013;14:6

35. Wang Y, Shaked I, Stanford SM, Zhou W, Curtsinger JM, Mikulski Z, Shaheen ZR, Cheng G, Sawatzke K, Campbell AM, et al. The autoimmunity-associated gene PTPN22 potentiates toll-like receptor-driven, type 1 interferon-dependent immunity. Immunity. 2013;39(1):111-22.

36. Frank B, Marcu A, de Oliveira Almeida Petersen AL, Weber H, Stigloher C, Mottram JC, Scholz CJ, Schurigt U. Autophagic digestion of Leishmania major by host macrophages is associated with differential expression of BNIP3, CTSE, and the miRNAs miR-101c, miR-129, and miR-210. Parasit Vectors. 2015;8:404.

37. Ragni E, Viganò M, Rebulla P, Giordano R, Lazzari L. What is beyond a qRT-PCR study on mesenchymal stem cell differentiation properties: how to choose the most reliable housekeeping genes. J Cell Mol Med. 2013 ;17(1):168-80

38. Taylor SC, Mrkusich EM. The state of RT-quantitative PCR: firsthand observations of implementation of minimum information for the publication of quantitative real-time PCR experiments (MIQE). J Mol Microbiol Biotechnol. 2014;24(1):46-52

39. Barber RD, Harmer DW, Coleman RA, Clark BJ. GAPDH as a housekeeping gene: analysis of GAPDH mRNA expression in a panel of 72 human tissues. Physiol Genomics. 2005;21(3):389-95.

40. Jacob F, Guertler R, Naim S, Nixdorf S, Fedier A, Hacker NF, Heinzelmann-Schwarz V. Careful selection of reference genes is required for reliable performance of RT-qPCR in human normal and cancer cell lines. PLoS One. 2013;8(3):e59180.

41. Schmittgen TD, Zakrajsek BA. Effect of experimental treatment on housekeeping gene expression: validation by real-time, quantitative RT-PCR. J Biochem Biophys Methods. 2000;46(1-2):69-81.

42. Zhang X, Goncalves R, Mosser DM. The isolation and characterization of murine macrophages.Curr Protoc Immunol. 2008;Chapter 14:Unit 14.1

43. Livak KJ, Schmittgen TD. Analysis of relative gene expression data using real-time quantitative PCR and the 2(-Delta Delta C(T)) Method. Methods. 2001;25(4):402-8.

Additional Files

Supplementary Tables 1 and 2. Gene expression in murine macrophages treated with LPS. Microarray analysis of gene expression in macrophages treated with LPS for 6 hours (Table 1) and 24 hours (Table 2).

Supplementary Table 3. Assessment of RNA quality. Spectrophotometry analysis of the quality of RNA used in all qRT-PCRs

Figure Legends

Figure 1. Ranges of C_t values of the 11 pre-selected reference genes in control and LPS stimulated BMDMs at 6h and 24h. C_t values were recorded for control and LPS stimulated (10ng/ml) BMDMs at A. 6h and B. 24h. Plotted as boxes are the range of Ct values, with the included horizontal line identifying the mean, of triplicate biological replicates. The unfilled boxes represent control BMDMs, and the grey filled boxes represent LPS stimulated BMDMs.

Figure 2. Stability ranking of reference genes in control and LPS stimulated BMDMs at 6h and 24h by Normfinder, GeNorm and BestKeeper softwares. C_t values were recorded for control and LPS stimulated (10ng/ml) BMDMs at 6h and 24h. C_t values were transformed as instructed and applied to each reference gene analysis software. The tables above show the ranking of most to least stably expressed reference genes between control and LPS stimulated cells, from top to bottom, as identified by Normfinder, GeNorm and BestKeeper softwares, at A. 6h and B. 24h. The most and least stable reference genes were identified by NormFinder from an initial data set at 6h and 24h. The stability in expression levels of these selected genes were then analysed in an independent experiment by RT-qPCR and C_t values are shown at 6h (C) and 24h (D). The error bars represent means ± SD. The significance values were calculated by comparison of control and LPS treated samples as a group, at each time point. *$p<0.05$, **$p<0.01$.

Figure 3. Stability ranking of select reference genes in LPS treated RAW 264.7 cells and peritoneal macrophages at 6h and 24h. C_t values were recorded for control and LPS (10ng/ml) stimulated RAW 264.7 cells and peritoneal macrophages at 6h (A-D) and 24h (E-H). C_t values were transformed as instructed and applied to the 3 reference gene analysis softwares. The tables above show the ranking of most to least stably expressed reference genes between control and LPS stimulated cells in (A, E). RAW264.7 cells and (B, G) peritoneal macrophages, from top to bottom, as identified by Normfinder, GeNorm and BestKeeper softwares. The C_t values are plotted for LPS stimulated (C, F). RAW 264.7 cells and (D, H) peritoneal macrophages. The error bars represent means ± SDs. The significance values were calculated by comparison of control and treated samples as a group, at each time point. *p<0.05, **p<0.01, ***p<0.001, ****p<0.0001.

Figure 4. Fold change in TNF, IL-1β and NOS2 gene expression levels at 6h and 24h as calculated using different reference genes. Fold change in expression of TNF (top row), IL-1β (middle row) and NOS2 (bottom row) in the LPS treated group, as compared to the control group, at A. 6h and B. 24h, was calculated using the $\Delta\Delta C_t$ method, as described in the methods section. For normalisation, the most (*Hnrnpap, Stx5a*) and least consistently expressed reference genes (*Gusb, B2m*), as identified by Normfinder software analysis, and the traditional choice of *Actinb* and *Gapdh* were used for the calculation of ΔC_t. C. The release of TNF from control and LPS stimulated BMDM was measured by ELISA at 6h and 24h of LPS exposure. Bars represent the mean ± SD. *p≤0.05, **p ≤ 0.01, ***p≤ 0.001, ****p≤ 0.0001.

Figure 1

Click here to download Figure Figure 1 word.docx

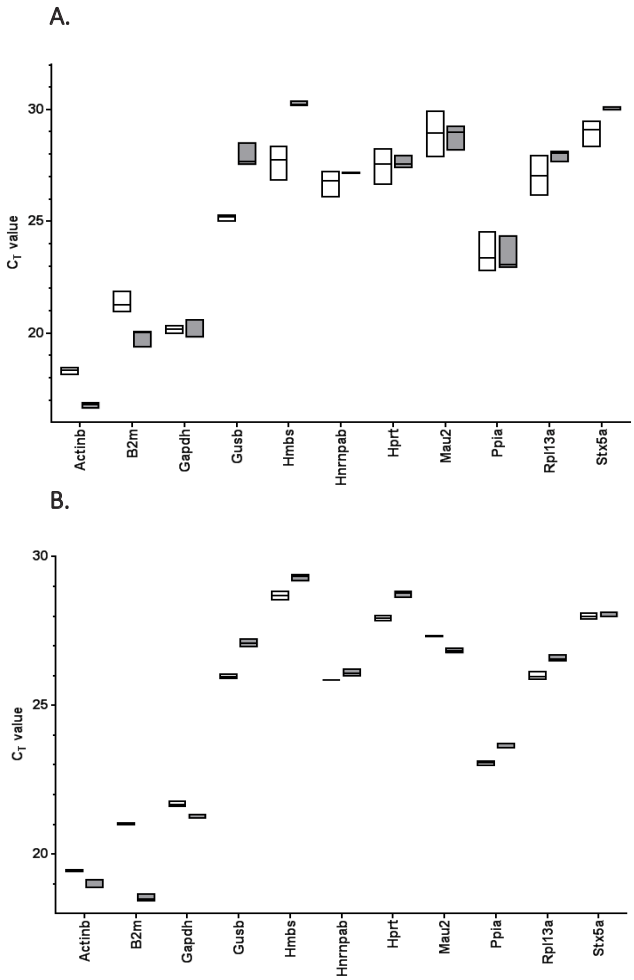

Figure 2

A.

Normfinder	GeNorm	BestKeeper
Hnrnpab	Hnrnpab | Stx5a	Gapdh
Stx5a	Rpl13a	Hnrnpab
Rpl13a	Mau2	Hprt
Hprt	Ppia	Stx5a
Gapdh	Hprt	Mau2
Mau2	Gapdh	Rpl13a
Ppia	Actinb	B2m
Actin b	B2m	Ppia
B2m	Gusb	Actinb
Hmbs	Hmbs	Hmbs
Gusb		Gusb

B.

Normfinder	GeNorm	BestKeeper
Stx5a	Hmbs | Rpl13a	Stx5a
Hnrnpab	Ppia	Hnrnpab
Actinb	Hprt	Gapdh
Mau2	Hnrnpab	Actinb
Ppia	Stx5a	Mau2
Gapdh	Gapdh	Ppia
Rpl13a	Actinb	Hmbs
Hmbs	Mau2	Rpl13a
Hprt	Gusb	Hprt
Gusb	B2m	Gusb
B2m		B2m

C.

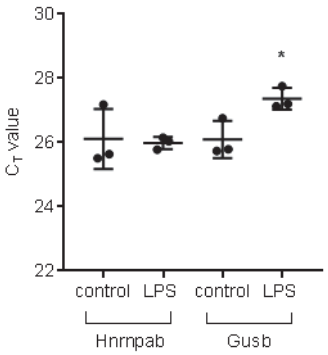

D.

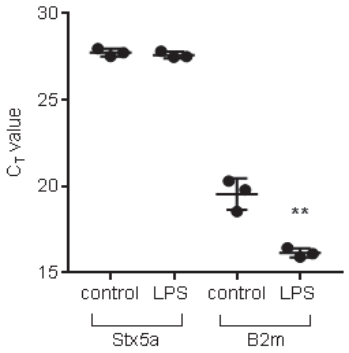

Figure 3

A

Normfinder	GeNorm	BestKeeper
Hnrnpab	Stx5a	Gapdh
Stx5a	Hnrnpab	Stx5a
Gapdh	Gapdh	Hnrnpab
Gusb	Gusb	Gusb
Hmbs	Hmbs	B2m
B2m	B2m	Hmbs

C

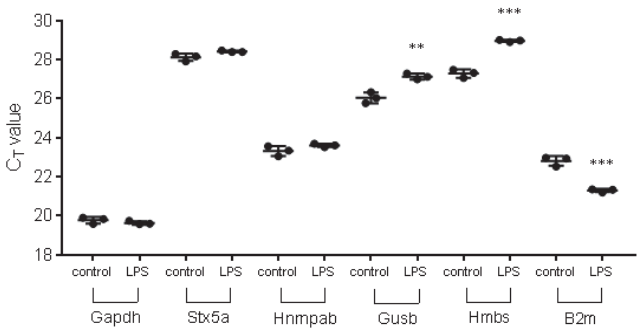

B

Normfinder	GeNorm	BestKeeper
Hmbs	Hmbs	Stx5a
Stx5a	Stx5a	Hmbs
Hnrnpab	Hnrnpab	Hnrnpab
Gapdh	Gapdh	Gapdh
B2m	B2m	B2m
Gusb	Gusb	Gusb

D

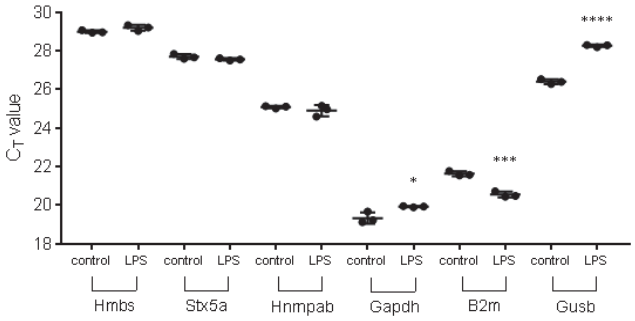

E

Normfinder	GeNorm	BestKeeper
Stx5a	Stx5a	Stx5a
Gusb	Gusb	Gapdh
Gapdh	Gapdh	Gusb
Hmbs	Hmbs	Hmbs
Hnrnpab	Hnrnpab	Hnrnpab
B2m	B2m	B2m

F

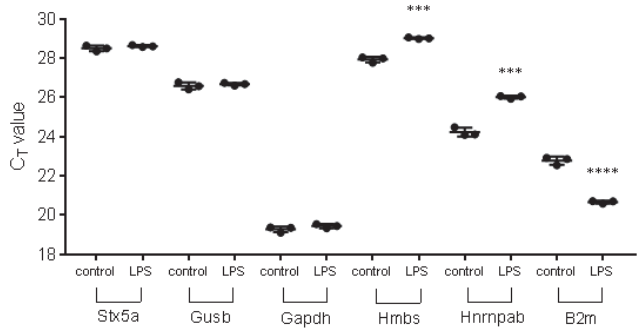

G

Normfinder	GeNorm	BestKeeper
Gapdh	Gapdh	Stx5a
Stx5a	Hnrnpab	Gapdh
Hnrnpab	Hmbs	Hnrnpab
Hmbs	Stx5a	Hmbs
Gusb	Gusb	Gusb
B2m	B2m	B2m

H

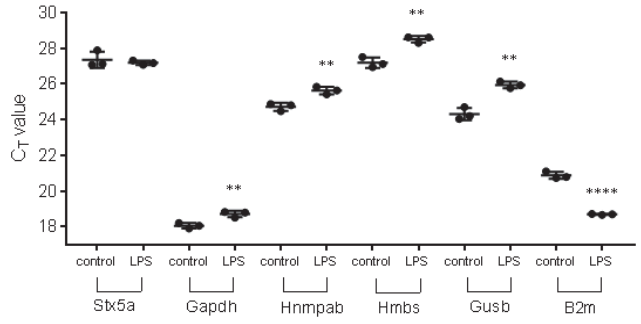

Figure 4

Click here to download Figure FINAL-IMNO-D-17-00002-Resubmission - Figure 4 word.docx

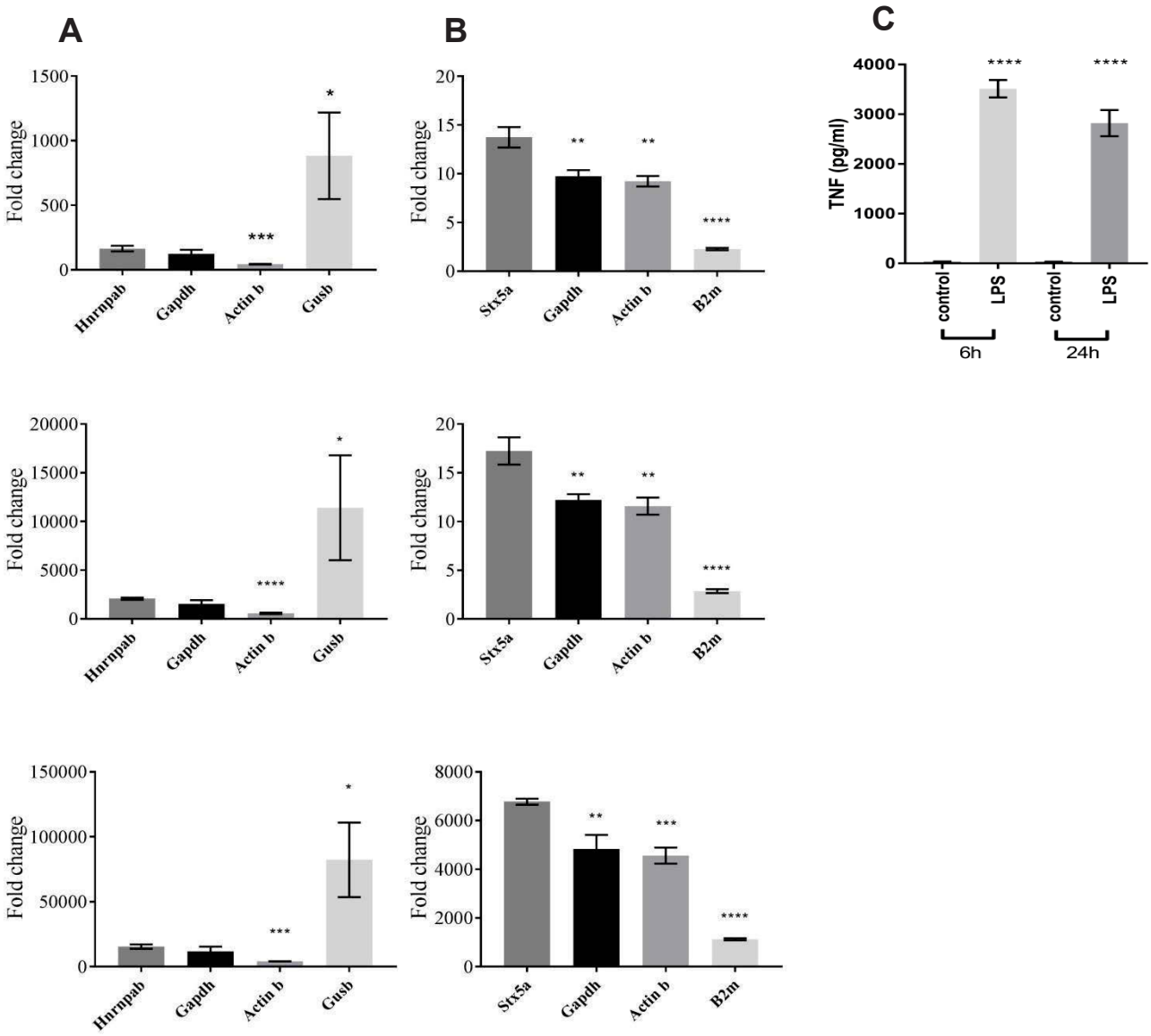

Supplementary Tables 1 and 2

Click here to access/download

Supplementary Material

Supplementary Table 1 and 2.xlsx

Supplementary Table 3